

Medische Bibliotheek  
2004 E.U.R. 61

# **Evaluation of Acoustic Noise in Magnetic Resonance Imaging**


Adriaan Moelker

ISBN 90-9018210-1

Lay-out: A.W. Zwamborn

Cover: A.W. Zwamborn

Illustrations: A. Moelker

Printed by Ridderprint B.V.  Ridderkerk

© 2004, A. Moelker

© 2001 Chapter 2, 2002 Chapter 3, 2003 Chapter 4, by the Radiological Society of North America

© 2003 Chapter 5, 2003 Chapter 7, 2004 Chapter 9, by John Wiley & Sons, Ltd

© 2003 Chapter 6, by Springer-Verlag GmbH

# **Evaluation of Acoustic Noise in Magnetic Resonance Imaging**

## **Evaluatie van geluid bij magnetische resonantie beeldvorming**

PROEFSCHRIFT

ter verkrijging van de graad van doctor  
aan de Erasmus Universiteit Rotterdam  
op gezag van de Rector Magnificus

Prof.dr. S.W.J. Lamberts

volgens besluit van het College voor Promoties.

De openbare verdediging zal plaatsvinden op  
woensdag 30 juni 2004 om 15:45 uur

door

Adriaan Moelker  
geboren te Leiden

## PROMOTIECOMMISSIE

Promotor: Prof.dr. P.M.T. Pattynama

Overige leden: Prof.dr. G.P. Krestin  
Prof.dr. L. Feenstra  
Prof.dr.ir. J.W. Verheij

Financial support by the department of Radiology, Erasmus MC - University Medical Center Rotterdam, for the publication of this thesis is gratefully acknowledged.

Aan mijn ouders  
voor *Christel*



# Contents

Chapter 1	Introduction	9
Chapter 2	Acoustic noise and related safety considerations in MR imaging environments <i>Published as a part of the RSNA Special Cross-Specialty Categorical Course in Diagnostic Radiology: Practical MR Safety Considerations for Physicians, Physicists, and Technologists. 2001;123-137.</i>	11
Chapter 3	Interventional MR imaging at 1.5 T: quantification of sound exposure <i>Radiology 2002;224:889-895.</i>	25
Chapter 4	Verbal communication in MR environments: effect of MR system acoustic noise on speech understanding <i>Accepted by Radiology.</i>	33
Chapter 5	Acoustic noise concerns in functional magnetic resonance imaging <i>Human Brain Mapping 2003;20:123-141.</i>	41
Chapter 6	Relationship between magnetic field strength and magnetic-resonance-related acoustic noise levels <i>MAGMA 2003;16:52-55.</i>	59
Chapter 7	Efficacy of passive acoustic screening: implications for the design of imager and MR suite <i>Journal of Magnetic Resonance Imaging 2003;17:270-275.</i>	63
Chapter 8	Importance of bone conducted sound transmission on patient hearing in the MR scanner <i>Submitted to Investigative Radiology.</i>	69
Chapter 9	Real-time modulation of acoustic gradient noise in interventional MR imaging <i>Concepts in Magnetic Resonance Part B (Magnetic Resonance Engineering) 2004;20B:34-39.</i>	77
Chapter 10	Summary and Prospects	83
	Samenvatting en Perspectief	87
	Dankwoord	91
	List of Publications	93
	Curriculum Vitae	95





# Chapter 1

## Introduction

Non-invasive visualization of human organs is of principal importance to modern medicine. Magnetic Resonance Imaging, MRI, as such, represents a modality for obtaining diagnostic images. The technique has extensive potential for further developments and is powerful in monitoring many diseases in the human body. Imaging with magnetic resonance (MR) is an invaluable aid in health-care, from screening and detection, diagnosis and treatment, up to follow up of diseases. The physical phenomenon of nuclear magnetic resonance has first been demonstrated by Felix Bloch and Edward Mills Purcell in 1946. Bloch et al. developed what was termed nuclear induction and Purcell et al. developed their nuclear MR absorption method, both accomplished independently and without knowledge of each other's work (1, 2). In the early 1970s, the possibility to create a two-dimensional image by introducing magnetic gradients in the magnetic field was discovered and based on the idea of back-projection, similar to that used in computed-tomography (3). In 1975, Richard Ernst proposed MRI using slice, phase and frequency encoding and image formation by Fourier Transform (4). This technique is the basis of current MRI techniques. Peter Mansfield has recently been rewarded for the Nobel Prize in Physics at the Karolinska Institute in Stockholm in 2003 for being the inventor of an extremely fast pulse sequence echo-planar-imaging, EPI (5). Echo planar imaging is an MRI technique which is capable of producing tomographic images rapidly. As time progressed, multiple variations of this acquisition strategy have been devised to produce images with high resolution at video rates. These techniques record an entire image in milliseconds and a requisite is therefore in the construction of dedicated gradient coils and power amplifiers that allow fast switching while maintaining high gradient fields. Current clinical MR imagers are equipped with 40 mT/m gradient strengths that can build up in

less than 300 microseconds. Novel pulse sequences such as hybrid pulse sequences (6) or pulse sequences with gradient dependent full magnetization recovery (7,8) have now emerged providing rapid image formation but typically require extremely high performance gradients.

A drawback of excessive gradient pulses is the acoustic noise produced during the process of image acquisition. This is the primary subject of this dissertation. Acoustic noise is generated when gradients are switched and results from subsequent changes in Lorentz forces in the gradient coil conductor. MR imagers can produce sound levels that are beyond the pain level. **Chapter 2** gives an overview of the problems associated with MR-related acoustic noise. Theoretical and practical aspects of sound measurements in the MR environment are discussed. Next, the quantitative and qualitative characteristics are described and the current status on methods for sound reduction and MR-related health issues are discussed. In **Chapter 3**, the medico-legal issue of chronic exposure to MR noise as experienced by health workers is presented. The results of sound level measurements that were performed are discussed with regard to the current guidelines in the United States and Europe. From a practical point of view, adequate speech understanding is a prerequisite in a number of circumstances such as MR guided interventional procedures and in functional MRI (fMRI). Therefore, **Chapter 4** describes the investigation on the negative effects that MR-related acoustic noise has on verbal communication between patients and/or interventionalists in the MR suite. In **Chapter 5**, an extensive overview is provided on the current knowledge on the effects of confounding acoustic MR noise in fMRI experiments. The principles and effectiveness of various imaging methods that reduce these confounding effects in fMRI are

reviewed.

At higher magnetic field strengths, the acoustic noise produced is expected to be increasingly high. This was the objective of investigation as described in **Chapter 6**, in which the static magnetic field of an MR system was ramped from 0.5 to 2.0 Tesla and concurrent acoustic measurements were performed.

The sound level of acoustic noise in MRI scanners is commonly reduced by the use of hearing protection such as earplugs and headphones. Alternatively, the sound levels can be reduced by blocking the source pathways of MR noise to both the patient and the interventionalist, i.e. from the imager's shrouds and in-room reflections. In **Chapter 7**, we studied these pathways for their relevance to the sound exposure by patient and interventionalist. Furthermore, passive hearing protection is confined to sounds conducted through air, but leaves the transmission of sounds through the subject's body unaffected. The efficacy of hearing protection decreases when the level of airconducted sounds becomes softer than those conducted through the subject's body. In **Chapter 8**, the question to find an answer to was therefore whether sound conduction through the body is different in an MR imager from that in a calibrated sound environment. Finally, **Chapter 9** investigates the applicability of a previously described principle of silent pulse sequences in an interventional MR setting.

## References

1. Bloch F, Hansen WW, Packard M. Nuclear induction. *Phys Rev* 1946; 69:127.
2. Purcell EM, Torrey HC, Round RV. Resonance absorption by nuclear magnetic moments in a solid. *Phys Rev* 1946; 69:37-38.
3. Lauterbur PG. Image formation by induced local interactions: examples employing nuclear magnetic resonance. *Nature* 1973;242:190-191.
4. Kumar A, Welti D, Ernst RR. NMR Fourier zeugmatography. *J. Magn. Reson* 1975; 18:69-83.

5. Mansfield P. Multi-planar image formation using NMR spin-echos. *J. Phys. C* 1977; 10:L55-L58.
6. McKinnon GC. Ultrafast interleaved gradient-echo-planar imaging on a standard scanner. *Magn Reson Med* 1993; 30:609-616.
7. Nitz WR. Fast and ultrafast non-echo-planar MR imaging techniques. *Eur Radiol* 2002; 12:2866-2882.
8. Nitz WR. MR imaging: acronyms and clinical applications. *Eur Radiol* 1999; 9:979-997.

Adriaan Moelker, MD  
Piotr A. Wielopolski, PhD  
Peter M. T. Pattynama, MD

Published as a part of the  
RSNA Special Cross-Specialty  
Categorical Course in Diagnostic  
Radiology:  
Practical MR Safety Considerations  
for Physicians, Physicists, and  
Technologists  
2001; pages 123-137

#### Abbreviations:

GRE = gradient-recalled echo  
 $L(A)_{eq}$  = equivalent-continuous A-weighted SPL  
 $L(A)_{eq,8h}$  = equivalent-continuous A-weighted daily (8-hour) noise exposure  
 $L(L)_{eq}$  = equivalent-continuous linear SPL  
 $dB(A)_{eq}$  = continuous-equivalent A-weighted SPL  
 $dB(L)_{eq}$  = continuous-equivalent linear SPL  
 $db(A)_p$  = peak A-weighted SPL  
 $dB(L)_p$  = peak linear SPL (all expressed in decibels)  
SPL = sound pressure level  
EP = echo-planar imaging  
FGRE = fast GRE  
FGRET = hybrid of EP and FSPGR imaging with real-time possibilities  
FISP = fast imaging with steady-state precession (synonym for GRASS)  
FLASH = fast low-angle shot  
FSE = fast SE  
FSPGR = fast spoiled gradient-recalled acquisition in the steady state  
GRASS = gradient-recalled acquisition in the steady state  
MP-RAGE = magnetization-prepared rapid gradient echo (synonym for 3D FSPGR)  
RARE = rapid acquisition with relaxation enhancement (synonym for FSE)  
SE = spin echo  
SNAP = synonym for FSPGR spiral = spiral k-space imaging  
SSFSE = single-shot FSE (EXPRESS = synonym for SSFSE)  
t-FLASH = turbo FLASH  
IR = inversion recovery

<sup>1</sup>From the Department of Radiology, Erasmus University Medical Center Rotterdam, 40 Dr Molewaterplein, 3015 GD Rotterdam, the Netherlands (e-mail: a.moelker@erasmusmc.nl).

© RSNA, 2001

## Acoustic Noise and Related Safety Considerations in MR Imaging Environments<sup>1</sup>

Acoustic noise is inextricably related to magnetic resonance (MR) imaging and has long been recognized as an important issue for patients being examined with MR imaging. In 1988, Brummett et al. (1) were the first, to our knowledge, to report the presence of temporary hearing disability in 43% of their imaged patients, and numerous studies on sound pressure levels (SPLs) in MR imaging have been published since then (2,3). Initially, acoustic noise was considered not to cause permanent hearing damage because SPLs were well within safety guidelines (2-4). Advances in MR imaging technology, however, have pushed the generated acoustic noise up toward hazardous levels at which permanent hearing loss may occur. In addition, the focus of interest in MR-related noise has broadened, as the advent of interventional MR imaging may have created an occupational hazard for interventional radiologists working near the MR magnet bore (5).

Aside from potential hearing loss, which is the predominant risk affecting long-term health, acoustic noise poses additional problems for patients and health workers. MR-related acoustic noise may interfere with verbal communication and is often annoying; periodic and high-frequency noises tend to be unpleasant and cause stress (6,7). Acoustic noise may induce or enhance preexisting anxiety, particularly in elderly, pediatric, and psychiatric patients (8,9).

In functional MR imaging, a technique used to detect metabolic changes in brain tissue, acoustic noise may spoil the stimulus-to-noise ratios. Such disturbances have been demonstrated in various brain regions, including auditory, motor, and visual cortices (10-13). Brain activation studies for language functions are partic-

ularly disturbed by imager noise because the noise-induced hearing threshold shifts are distributed over frequencies important to speech (14).

Recently, it has been suggested that acoustic-magnetic coupling (i.e. transmission of acoustic energy to the MR cryogen) may be a relevant issue. This acoustic-magnetic coupling might induce substantial fluctuations in the main magnetic field and impair MR image quality (15), but whether it truly degrades MR image quality, and to what extent, has not yet been established.

This chapter provides an overview of considerations relevant to acoustic noise in the MR environment. Subjects include the MR-related aspects of sound level measurements, the production of noise and its quantitative and qualitative characteristics, methods for sound reduction, MR-related health issues, and practical considerations and recommendations.

#### Audiology: Theory and Practice

Sound is the human perception of fluctuations in air pressure within a certain frequency range (20 Hz to 20 kHz (16)). The loudness of sound can be quantified by the root-mean-squared instantaneous acoustic pressure over a time period ( $P_1$ ). More relevant in audiology, however, is the linear SPL expressed in decibels ( $dB(L)$ ), which is the logarithm of the ratio of  $P_1$  to the international standardized reference sound pressure ( $P_0$ ) of 20  $\mu$ Pa (17):

$$SPL = 10 \cdot \log(p_1 / p_0)^2 \quad (1)$$

or in terms of power  $I_1$  standardized to  $I_0$  ( $1 \cdot 10^{-12}$  W) by  $SPL = 10 \cdot \log(I_1 / I_0)$ . The reference pressure is the hearing threshold at 1.000 Hz for young healthy people. This gives a range of amplitudes in human hearing from

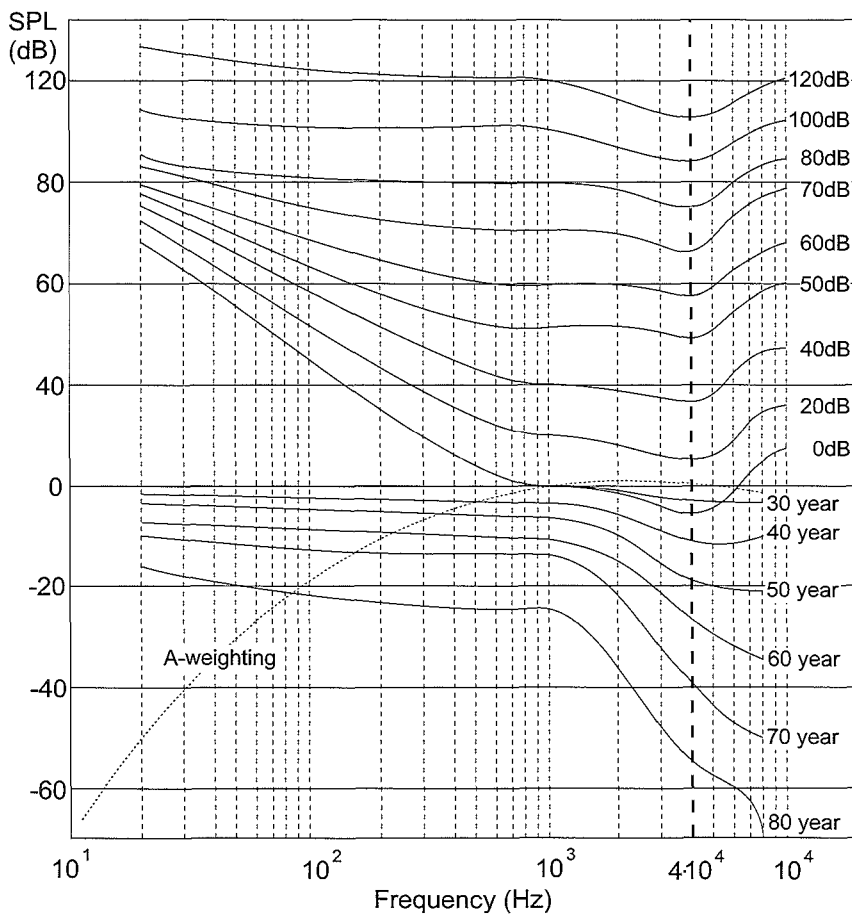


Figure 1. Upper curves indicate frequency dependence of human hearing at different amplitudes (decibels). Lower curves indicate decrease in hearing threshold with age in men. Dotted curve shows A-weighted filter.

0 dB, the reference minimum, to 120 dB, the pain threshold.

The human ear is not uniformly sensitive to the audible frequencies. This is accounted for by adding an A-weighted filter to the linear (unfiltered) SPL, which adjusts for the acoustic response of the human hearing. To estimate the hearing damage caused by occupational sound exposure, the time-averaged A-weighted sound level  $L(A)_{eq}$  is the preferred measure (18,19). The A-weighted filter is derived from the hearing threshold curve of young healthy people (Fig 1). The maximum sensitivity of the human ear to sound is at about 4 kHz for all SPLs (Fig 1). Therefore, hearing loss will primarily be at this 4-kHz frequency, followed by dissemination into neighboring frequencies, which are all relevant to speech (500-2,000 Hz (14,20)). Sounds can be classified as continuous or intermittent (defined as SPLs  $\leq$  background SPLs at least two times per measurement) and as steady, fluctuating (duration  $> 1$  second at  $> 3$  dB

above background SPL), or impulsive (duration  $< 1$  second and  $> 10$  dB above background SPL for  $< 250$  msec) (17).

### Measuring Sound Levels in the MR Imaging Environment

Sound measurements for assessing noise exposures should ideally comply with appropriate professional standards such as American National Standards Institute Standard S12.19-1996 or International Organization for Standardization (ISO) Standard 1999:1990. These standards are generally considered a prerequisite for occupational noise exposure standards (21) and encompass all relevant factors of the experimental setup, including positioning and orientation of the microphone, settings of the sound-level meter, and usage of tripods and extension cables (17). When one wishes to make comparative measurements (e.g., when comparing SPLs of two MR sequences), accurate comparison requires equality of environmental and experimental conditions.

Many of the situations described subsequently may be circumvented by placing the measurement equipment at a safe distance from the MR imager (22,23).

Most digital sound-level analyzers will smooth instantaneous SPLs by applying time-averaging over 1,000-, 125-, or 35-msec intervals, that is, at slow, fast, or impulse settings, respectively. In addition, the sound-level analyzers generally provide the magnitude of the peak SPL (i.e., the highest SPL, based on a  $< 50$ - $\mu$ sec time weighting) encountered during the measurement period (18). The recorded time-averaged SPLs are averaged over the duration of the measurement period, resulting in a continuous-equivalent SPL. Most investigators report A-weighted continuous-equivalent SPLs ( $L(A)_{eq}$ ) (6,24-28) measured with a fast time constant and 125-msec time averaging (3,12,22-24,27,28). The measurement period should be long enough to cover all marked variations in SPL (17) and thus should exceed at least one repetition time (TR). For imaging sequences with long silences (intermittent noise) (e.g., in respiratory-gated sequences), conventional analog sound-level meters cannot approximate  $L(A)_{eq}$  and digital equipment is therefore preferred (17,22, 23).

The physical properties of the main magnetic field are of concern when one is dealing with ferromagnetic equipment (29). Most sound-level meters, extension cables, and microphones usually contain some nickel and stainless steel, which makes the devices attractable and vulnerable to the static magnetic field (30,31). As is well known, ferromagnetic objects can gain disastrous speeds during attraction and may even become projectiles (29). The MR imaging main magnet field, radio-frequency (RF) system, and gradient system may induce measurement artifacts caused by electromagnetic coupling between fluctuating electromagnetic fields and the microphone and extension cables (32).

Although some investigators have applied copper shielding to the microphone (4,26), most experiments involving sound measurements have circumvented the problem by using

prepolarized condenser microphones (3,22,23,27,28,32,33). Such microphones do not contain a coil structure, which is susceptible to oscillating electromagnetic fields, but rather rely on capacitory changes induced by airborne pressure fluctuations of sound (30). It has been shown that the accuracy of the condenser microphone is not influenced by the gradient and RF systems (3,15,24-26,28,32) (although one study demonstrated a small decrease in SPL with the RF system switched off (25)). This was demonstrated either by switching off the RF system (3,26,32), by varying the flip angle of a gradient-echo-based sequence (24,28), or by covering the microphone with dense putty, thereby blocking environmental noise, unlike the electromagnetic fields (15,25,28,32,34). Interference of the static magnetic field with the sensitivity of the microphone has been ruled out by making noise measurements at different angles of the microphone to the main magnetic field (3,24,25,28) and by conducting a reference sound via a tube to the microphone, located both in the magnet isocenter and in the console room (32). Changes in sensitivity because of the main magnetic field have been shown to be irrelevant, which is also true for ferromagnetic condenser microphones (3,25,28,30,31,33,34).

In the design of the measurement setup, the characteristics of the MR imaging room and the MR imaging sound should be considered (32). For sound measurements, the acoustic environment can be either a free-field or a diffuse-field environment (a diffuse-field environment is characterized by sound coming from any direction, which increases the SPL less than 3 dB while halving the distance to the sound source). An MR imaging suite is generally considered a diffuse environment because of the presence of reflective hard walls (27,32). Because the frequency distribution of MR noise is well below 10 kHz (6,7,12,15,23,25,27,28,32,33,35), sound wave diffraction around the microphone is negligible (30). Therefore, both free-field microphones (which correct for diffractions) and diffuse-field microphones can be used in the MR imaging environment.

## Sound Generation in the MR Imaging Environment

### *Primary Source of Acoustic Noise*

The interaction between the static main magnetic field ( $B_0$ ) and the fluctuating currents in gradient coils is the most important source of acoustic noise in MR imaging (36). Oscillating currents passing through the gradient coils and through unscreened connecting wires (37) induce Lorentz forces acting on their wires (37-42). The Lorentz forces are proportional to both  $B_0$  and the gradient current (with a maximum when the gradient current is normal to  $B_0$ ) (32,37-41). When the magnetic field strength is doubled, Lorentz forces are expected to quadruple, if the gradient strength increases approximately proportionally to  $B_0$  to reduce regression of image quality by chemical shift and susceptibility artifacts (43). The fluctuating Lorentz forces at the wires induce vibrational waves in the surrounding structures and, finally, an acoustic wave is launched in the air (37,38,41).

The x- and y-gradient coils, which are usually the read-out and phase-encoding gradients in transverse imaging, are most dominant in sound production (15,33,35,44). The z-gradient coil consists of two single looped coils with opposite currents; Lorentz forces of the z-gradient coil tend to cancel out (net result is zero), resulting in only limited sound generation (44). The contribution of section-selective and presaturating gradients is minor compared with the readout and phase-encoding gradients (32).

Most imaging sequences are periodic, producing a fundamental frequency  $f$ , as the reciprocal of the period, and its harmonics (i.e., frequencies that are multiples of the fundamental frequency with a whole integer) (28,32,43). For conventional spin-echo and gradient-echo sequences, the fundamental frequency and its first harmonics are of low frequencies and hardly audible to human hearing (43). In these sequences, most gradient noise is attributed to the higher-order harmonics (7). The fundamental frequency and harmonics are deducible from the frequency domain of a single period of the gradient current by means of Fourier transform (Fig 2) (43). The faster imaging se-

quences with shorter data acquisition, requiring higher currents with steeper slew rates at shorter duration, result in the appearance of higher frequencies and amplitudes. Hedeem and Edelstein (34) found small dissimilarities between the amplitudes in the frequency spectrum of measured noise and the Fourier-transformed gradient current spectra. These differences were assigned to the natural frequencies (i.e., mechanical resonances) of the supporting structures and a low-frequency offset of ambient noise. Therefore, a transfer function was measured that described the evolution of the initial current amplitudes of the coils to the amplitudes of sound in air (Fig 3) (34,40). Using that transfer function, Hedeem and Edelstein (34) were able to predict the SPL of a clinical fast spin-echo sequence within 0.4 dB, although errors appeared at higher frequencies in the frequency domain.

### *Secondary Sources of Acoustic Noise*

Resonances are thought to be due to bending modes the coil encasings, called Chladni resonances, and volume resonances in air (40). The occurrence of resonances depends on interaction between the frequency spectrum of the exciting gradient current and the characteristics of the encasing structures of the coils, that is, their dimensions and the propagation velocity of waves (28,37,40). Therefore, the contribution of resonances to the noise profiles and their frequency spectra will depend on the type of imager (27,35). Cho et al. (35) showed different resonances in a 2-T research imager, exhibiting a small frequency distribution, compared with a commercial 1.5-T echo-planar imager, exhibiting a complex frequency distribution (35). Wu et al. (15) analyzed acoustic and magnetic fluctuations of the gradient coil system of a 4-T MR imager. Various modes of gradient current impulses were applied to the gradient coils to generate the frequency response function. In both x- and y-gradient coils, distinct resonance peaks were found at about 430 and 950 Hz, probably representing the mechanical resonances of the gradient coil structures. The z-gradient coil showed peak amplitudes at about 1.170 and 1.310 Hz, reflecting



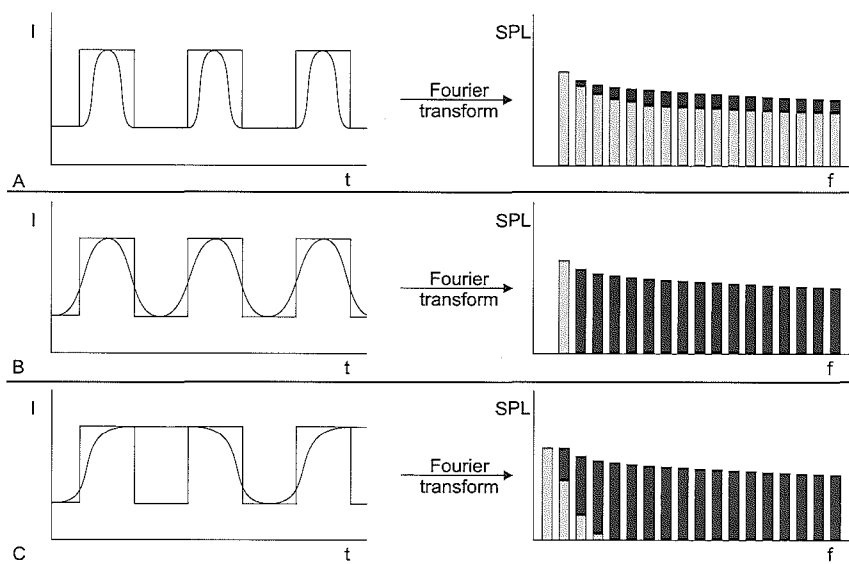


**Figure 2.** Frequency analysis of gradient currents by means of Fourier transform. Note decrease in amplitude at higher frequencies with decreasing slews rate. The three panels demonstrate the principles of silent gradient designing (see text).

a design dissimilar from that of the x- and y-gradient coils (45).

Recently, Ravicz et al. (32) demonstrated a slow decay of imager noise within 300-500 msec, presumably caused by resonating structures and reverberation of the MR imaging suite itself (28). That noise reentrance from the suite into the magnet bore may be a real phenomenon was further elucidated by an experiment in which the entrance and exit of the MR magnet bore were blocked, resulting in a reduction in SPL of 12 dB(L) (unit for linear SPL) in the magnet isocenter (32).

#### Other Sources of Acoustic Noise

Other less important sources of MR-related noise are baseline noise levels and RF hearing. Baseline noise levels represent the sound levels of in-room air-conditioning and ventilation systems and the MR-cooling cryogen (ambient noise). The SPL of ambient noise is usually negligible because its SPL is more than 10 dB lower than that generated by the MR imager (15,17,24,28,32,34). RF hearing, originating from thermoelastic

expansion of endolymph in the inner ear, may induce hearing sensations, probably without any harmful health effects (36). The magnitude of RF hearing relative to total sound perception in MR imaging is likely to be small.

### Characteristics of MR-related Acoustic Noise

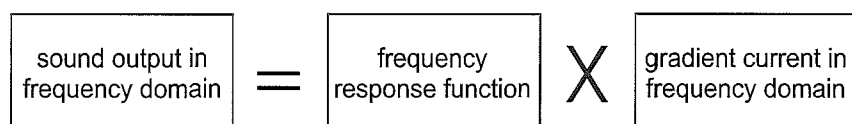
#### Quantitative Characteristics

Table 1 provides an overview of reported linear SPLs (in dB(L)) and A-weighted SPLs (in dB(A)) of various pulse sequences. In most experiments, the  $L(A)_{eq}$  values have been recorded (3,4,7,22-28,32,46,47). An analysis of the peak and continuous-equivalent SPLs in Table 1 shows that peak SPLs are more than 10 dB higher than the continuous-equivalent  $L(A)_{eq}$  for all pulse sequences, indicating that the MR imager noise includes substantial impulse noise. For SPLs of less than 140 dB(A),  $L(A)_{eq}$  is considered a reliable predictor of noise-induced hearing loss for all types of noise (i.e., both continuous and impulse noise) (21). The fast time weighting generally used in MR-re-

lated noise measurements, however, reduces the influence of impulses on the continuous-equivalent SPL by smoothing the impulsive instantaneous SPLs and thereby slightly underestimates the actual  $L(A)_{eq}$  (by <5 dB). Thus, the reported SPLs tend to underestimate the true acoustic noise in the MR environment.

It has been shown that the continuous-equivalent SPLs of pulse sequences are highly repeatable, provided that the MR imagers, environments, and pulse sequences are identical (32). The discrepancies in SPLs in Table 1 may therefore be due to differences in imaging parameters, the MR environment, and, in particular, the mechanical properties of the supporting structures of the MR imager (24,27). Some investigators have used worst-case pulse sequences to standardize acoustic measurements in the MR environment by selecting minimum values of imaging parameters that are inversely proportional to SPL (4,24,26). It has been suggested that peak levels should be unaffected by differences in measurement methods and may be preferable when comparisons have to be made between, for example, MR imagers or imaging protocols (32). Additionally, discrepancies may be caused by the presence of a phantom in the magnet bore during noise measurements (24-26,32). It has been found that SPLs were about 3 dB higher whenever a person was inside the magnet bore; the investigators suggested that in-phase reflections inside the magnet bore might cause pressure doubling and a subsequent increase in SPL (34). On the other hand, in our own experience, the presence of a person in the magnet bore reduced SPLs by 2.7 dB(A) on average when measurements were made with the microphone beside the MR imager (5).

Previous reports found a relationship between SPL and field strength, gradient strength, and slew rates (23,25,27,33,46), but these associations may be inter-related because higher fieldstrength systems require higher performance gradients (24). Recently, Price et al. (24) demonstrated an increase in SPL of 1.8 dB(A) caused by an increase in field strength alone, by comparing similar MR systems at 1.0 and 1.5 T. This in-



**Figure 3.** Frequency spectrum output is calculated by multiplying the frequency response function and the gradient current in frequency domain.

**TABLE 1**  
**Rounded A-weighted and Linear Continuous-Equivalent and Peak Levels for Common Imaging Protocols Performed in Different MR Systems**

Reference	B <sub>0</sub> (T)*	Pulse Sequence †	SPL			
			dB(A) <sub>eq</sub>	dB(L) <sub>eq</sub>	dB(A) <sub>p</sub>	dB(L) <sub>p</sub>
Hurwitz et al (3)	3.5	GRE	93	103	NA	NA
	0.5	GRE	85	84	NA	NA
	1.0	GRE	82	90	NA	NA
	1.5	GRE	84-91	94-100	NA	NA
Shellock et al (26)	1.5	SE	90	98	NA	NA
		FSE	90	97	NA	NA
		GRASS	92	99	NA	NA
		FSPGR	90-103	99-106	NA	NA
McJury et al (22)	1.5	SE	97-99	107-110	99-101	NA
		FLASH	92-103	104-115	94-105	NA
		MP-RAGE (3D)	106	116	NA	NA
McJury (23)	1.0 (10,15)	SE	90-97	98-106	NA	NA
		FSE	96-100	103-107	NA	NA
		FLASH	88-97	97-103	NA	NA
		FLASH (3D)	96-98	101-106	NA	NA
Cho et al (35)	1.5	SE	NA	98	NA	NA
		GRE	NA	104	NA	NA
		EP	NA	103	NA	NA
	2.0	SE	NA	98	NA	NA
		GRE	NA	102	NA	NA
		SE	NA	98	NA	NA
Counter et al (25)	0.5 (10)	SE	80	88-88	90-91	98
		FSE	81	87	93	98
		SPGR	67	80	78	83
	1.0 (17)	SE	90-110	94-105	101-112	104-117
		FSE	96	99	108	112
		GRE	83-105	91-106	102-113	91-106
		GRE (3D)	103	105	111	115
		FISP (3D)	97	100	109	111
	1.5 (10)	SE	91-108	101-115	103-108	106-115
		FSE	103	106	105	107
		GRE	90-91	96-97	101-103	105-106
		FLASH	103-108	110-113	105-109	112-114
		MP-RAGE (3D)	108	112	109	113
Shellock et al (4)	1.5	FSE (3D)	97-107	NA	NA	NA
		EP	101-114	NA	NA	NA
Prieto et al (47)	3.0	EP	NA	105-128	NA	125-140
Prieto (46)	1.5	EP	105-117	NA	NA	117-130
	3.0	EP	114-133	NA	NA	126-139
Miyati et al (27)	0.5-1.5 (8-19)	EP	94	NA	NA	109
Foster et al (28)	3.0	EP	123-132	122-131	131-140	130-139
Ravicz et al (32)	1.5 (25)	SE	NA	NA	NA	123
	3.0 (34)	SE	NA	NA	NA	138
Counter et al (33)	4.7	RARE	113-118	112-118	125-130	124-129
		SNAP	113	113	128	127
Price et al (7)	1.5	FGRE	98	NA	NA	NA
		FGRE (3D)	107	NA	NA	NA
		EXPRESS	100	NA	NA	NA
		EP	97-98	NA	NA	NA
Price et al (24)	1.0	t-FLASH	88-95	NA	NA	NA
Moelker et al (5)	1.5 (40)	FSE	92-101	92-100	NA	114-118
		SSFSE	97	97	NA	116
		FSPGR	104-110	104-109	NA	119-122
		FGRET	99-110	99-109	NA	117-121
		Spiral	103-104	102-103	NA	120-121

Note. -Levels were measured in the magnet bore. Data are listed in order of publication date, with minimum and maximum SPLs given for identical sequences. NA = not available.

\*Parenthetical numbers indicate gradient strength, in milli-Teslas per meter.

crease is only half of the calculated value of 3.5 dB (assuming a log-relationship, i.e., a 6-dB increase when the magnetic field is doubled).

Most intense sound levels are probably generated during echo-

planar imaging, particularly with high fieldstrength systems (Table 1) (28, 46,47). In mid fieldstrength MR systems, however, SPLs of echo-planar and non-echo-planar pulse sequences are of similar magnitude

(4,7,27). Some investigators have demonstrated slight increases in SPL during three-dimensional imaging (7,22,23, 25), which may be due to the secondary phase-encoding gradient along the third dimension applied simultaneously with

the readout and primary phase-encoding gradients (36).

#### Qualitative Characteristics

As already mentioned, pulse sequences are periodic, producing an acoustic fundamental frequency and harmonics determined by the driving gradient current. The degree of periodicity is dependent on both the pulse sequence and the imaging parameters (25). Several investigators have reported the frequency content of noise during MR imaging (Table 2). Frequencies with maximum energy (i.e., those with maximum SPL) tend to be higher in later studies. This frequency shift is attributed to faster imaging techniques and steeper slew rates of the tested MR imagers. In 1989, Hurwitz et al. (3) found most energy concentrated at low frequencies around 250 Hz, whereas a decade later, Foster et al. (28) demonstrated a fundamental frequency at 1.9 kHz and higher-order harmonics toward 9.6 kHz during echo-planar imaging. Recently, we tested a fast gradient-recalled echo train sequence (FGRET), a hybrid pulse sequence of echo-planar and gradient-echo imaging, fully exploiting the slew rate ( $150 \text{ Tm}^{-1}\cdot\text{sec}^{-1}$ ) and gradient amplitude ( $40 \text{ mT}\cdot\text{m}^{-1}$ ) of the 1.5-T MR system. The fundamental frequency was concentrated around 3-4 kHz, while most other fast imaging sequences showed frequencies between 1 and 2 kHz (5). The shift toward higher frequencies of MR-generated noise with newer MR hardware and software may have implications for acoustic noise exposure because human hearing is most sensitive at these higher frequencies around 4 kHz. The efficiency of both passive and active noise-reduction strategies is also dependent on this frequency; at higher frequencies, passive hearing protection has better attenuation, but active hearing protection is less effective (35).

The A-weighted and linear SPLs of ambient noise are shown in Table 3. The frequency distribution of ambient noise is around 100-500 Hz, to which the human ear is relatively insensitive (5,27,32,35). Consequently, the A-weighted SPL is 10-30 dB lower than the linear SPL. Generally, ambient SPLs are negligible compared with levels

**TABLE 2**  
Frequency Distributions and Peak Frequencies

Reference	Pulse Sequence	SPL Peak (Hz)	Frequency Range (kHz)
Hurwitz et al (3)	GRE	125-250	60-300 Hz
McJury (23)	NA	250	NA
Cho et al (35)	SE	NA	≤ 2.5
	EP	NA	≤ 4.0
	GRE	NA	≤ 4.0
	IR	Multiple peaks	≤ 4.0
	SE*	NA	≤ 1.0
	GRE*	NA	≤ 1.0
	Counter et al (25)	SE†	70, 300, 550
	SE‡	60, 90, 180, 280, 300, 490, 600, 700	≤ 1.5
	SE§	100, 700	≤ 0.7
	FGRE †	500	≤ 0.6
	FGRE ‡	800	≤ 1.5
	FGRE §	200-500, 1,300	NA
	IR	50-100	≤ 0.7
	MP-RAGE§	100, 200, 300, 400, 500, 600	NA
Miyati et al (27)	EP	2,000	1-4
Ravicz et al (32)	EP"	1,000, 2,000	NA
	EP#	1,400, 2,800	NA
Poster et al (28)	EP	1,923, 3,800, 5,800, 7,700, 9,600	NA

Note.—Data are listed in order of publication date, NA = not available;

\* Research imager at 2.0 T

† Field strength, 1.5 T; gradient strength, 10 mT/m (GE Medical Systems, Milwaukee, Ws)

‡ Field strength, 1.0 T; gradient strength, 17 mT/m (Siemens, Erlangen, Germany)

§ Field strength, 1.5 T; gradient strength, 10 mT/m (Siemens)

" Gradient strength, 25 mT/m (Siemens)

# Gradient strength, 34 mT/m

recorded during actual imaging, but they could be important for calculating stimulus-to-noise ratios in functional MR imaging (28).

#### Relation between Noise and Imaging Parameters

Imaging parameters are expected to exert their influence on acoustic noise production by affecting the strength, slew rate, pulse rate, and/or duration of gradient coil activation (Table 4) (33).

Most quantitative experiments have demonstrated distinct increases in SPL when the TR is decreased (3,24,25,32,47). The image acquisition time is covered by a series of TRs, each with an equal number of gradient pulses. Doubling the TR should result in halving the number of gradient pulses per unit of time (i.e., the amount of acoustic energy per unit of time) and therefore reduces SPL by 3 dB (equal energy rule; see subsequent text). Data of Prie-

to et al. (47) and recent experiments by Ravicz et al. (32) have confirmed this relationship. Additional encoding steps within the TR (e.g., during multisection imaging) would increase the SPL. The equal energy rule applies likewise because doubling the number of sections adds 3 dB (32).

The echo time (TE) changes the timing of the gradient pulses within the TR and should theoretically not influence the SPL. Previously, an inverse influence of TE on SPL has been suggested, but this suggestion was based on an observation that combined simultaneous lengthening of both TR and TE (3). It has recently been shown that there is generally no relation between SPL and TE, although there may be a small increase in SPL with minimal TE due to slight changes in the waveform of the readout gradient (24, 32).

The field of view is inversely pro-



**TABLE 3**  
**Ambient Noise Levels**

Reference	Noise Level	
	dB(A) <sub>eq</sub>	dB(L) <sub>eq</sub>
Hurwitz et al (3)	53-63	NA
Shellock et al (26)	63	NA
McJury et al (22)	51	NA
McJury (23)	53	NA
Cho et al (35)	NA	80
Shellock et al (4)	66-78	NA
Miyati et al (27)	63	NA
Foster et al (28)	45-63	76
Moelker et al (5)	52	69

Note.-The difference between A-weighted and linear levels is caused by the low frequency ambient noise.  
NA = not available.

portional to the gradient strength of either readout or phase-encoding gradient. The relationship between field of view and SPL has been shown in several studies (23,24,47). A similar pattern could be expected for the section thickness because the section-select gradient strength determines the section thickness (inversely proportional). In terms of sound production, however, the section-select gradient is less important than the readout and phase-encoding gradients and therefore plays a minor part in the total SPL (24,32,47). Former reports have suggested more effect of section thickness on SPL (3,22,23,25,33), probably because of the larger section-select gradient amplitude relative to readout and phase-encoding gradient amplitudes. Moreover, the section-select gradient may use the more dominant x- or y-gradient coil (in terms of noise production) for section orientations other than transversal, thereby increasing its influence on SPL.

Previous studies (including our own) have failed to demonstrate substantial influence of section orientation on SPL (3,22,24,32). In contrast, Prieto et al. (47) found reductions in SPL (5-10 dB) with less noise production for sagittal and/or coronal imaging compared with transverse imaging (47).

**Methods for Noise Reduction in MR Imaging**

*Noise Reduction at the Source: Gradient Coil Design*

Increasing the mass of the coils will increase their inertia and stiffness to Lorentz forces and limit their movement and noise production. This method is limited because it increases the weight of the MR imager (39). An alternative solution, other than massive coil design, makes use of the so-called Lorentz force balancing (37-42).

**TABLE 4**  
**Influence of TR, TE, Field of View, Section Thickness, and Imaging Plane on Sound Level**

Reference	TR	TE	Field of View	Section Thickness	Imaging Plane
Hurwitz et al (3)	+	+	NA	+	-
McJury et al (22)	NA	NA	NA	+	-
McJury (23)	NA	NA	+	+	NA
Counter et al (25)	+	NA	NA	+	NA
Prieto et al (47)	+	NA	+	-	+
Ravicz et al (32)	+	-	NA	-	-
Counter et al (33)	NA	NA	NA	+	NA
Price et al (24)	+	-	+	-	NA
Moelker et al (5)	+	-	+	-	NA

Note.-Data are ordered according to date of publication. In all cases, the relationship is inverse; + = related, - = not related, NA = not available.

The principle of quiet gradient coils is active canceling of Lorentz forces acting on the coil support. One can achieve force balancing, or force canceling, by mechanically coupling the primary coil to a secondary screening coil over the entire area or at strategic points and applying a 180° phase-shifted current to the secondary coil (Fig 4) (37,38). As a result, the induced opposite mechanical forces on the gradient structure will null and cancel, provided that both currents have identical amplitudes and the main magnetic field is homogeneous and normal to the coil support (36).

Theoretically, a completely noncompressive coil support would then prevent noise generation entirely (37,38,40). Because all materials have some viscoelasticity, however, residual movement of the coils will produce acoustical waves with velocity  $v$  (Fig 5, A). Phase errors, which interfere with the cancellation process, should be avoided for optimal acoustic screening. Such phase errors result from short wavelengths ( $\lambda$ ) in relation to large dimensions of the supporting materials (40). Using coil supports with

intrinsically higher  $v$  results in larger  $\lambda$  because they are related by  $v=\lambda f$  and, therefore, reduces the occurrence of phase errors (Fig 5, B) (37). Moreover, reducing coil support dimensions will cause phase errors to occur at higher current frequencies (Fig 5, C) (40). Experiments using solid polystyrene potting with moderately high velocity

demonstrated noise attenuation at particularly low frequencies of 40 dB at 100 Hz, decreasing to 0 dB at 3.5 kHz (37,38).

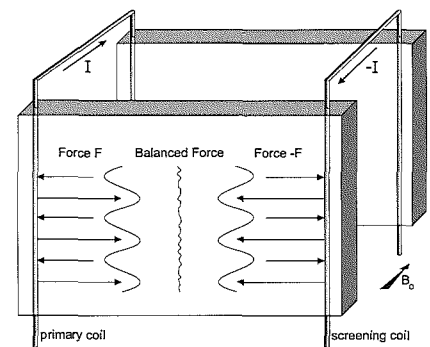


**Figure 4.** Principle of Lorentz force balancing. Opposite currents ( $I$  and  $-I$ ) through mechanically coupled coils induce opposite Lorentz forces ( $F$  and  $-F$ ), which cancel out and thereby reduce noise production.

A consideration in Lorentz force balancing is the decreased efficiency of the gradient strength. Gradient strength is considerably reduced by the opposite gradient field of the screening coil. Increasing gradient currents could compensate for this reduction but at the expense of increasing noise generation.

Recently, a new arrangement of quiet gradient coils has been described, which improved the gradient efficiency (41). The basic idea was a reduction of screening coil area, and thus the magnetic field, to limit interference with the primary gradient field (Fig 6). Tests were done with epoxy glass-reinforced supports with a propagation velocity of  $2.5 \cdot 10^3$  m·sec<sup>-1</sup>. Data showed an average noise attenuation of about 35 dB at 3.26 kHz and 3.0-T (41).

As mentioned, the x- and y-gradient coils are the most dominant sound-producing coils. Cho et al. (35,44) replaced the x- and y-gradient pulsings with a mechanically hand-rotating direct-current (DC) gradient coil (35, 44). As in computed tomography, acquired projection data were reconstructed by means of projection reconstruction, although the conventional MR Fourier technique could also be used. With the rotating DC gradient, the SPL of a spin-echo sequence was at least 20 dB less. Images showed good quality but with a slight tilting in the z-direction. The tilting was due to the simultaneous presence of both the DC gradient and the selection gradient (z-gradient) and resulted in a volume loss of 18% at the image periphery. In addition, section selection was restricted to axial planes but might be overcome by multisection or three-dimensional imaging. Moreover, the use of a rotating coil may be considered a potential safety hazard (48).

#### Noise Reduction at the Source: Passive Methods

As mentioned, the mechanical properties of coil support are relevant in noise production during MR imaging. Reduction of noise propagation could be achieved by decoupling the gradient supports from their surroundings (floating) and mounting them to the floor (32). Recently, quiet MR systems that use vacuum-enclosed gradient systems in addition to insulators have become commercially available (24).

Various dampening materials have been examined, including sand and silicon surrounding a phantom; sand proved to be an adequate barrier to sound, especially at frequencies ranging from 0 to 2 kHz (49). Foster et al. (28) ap-

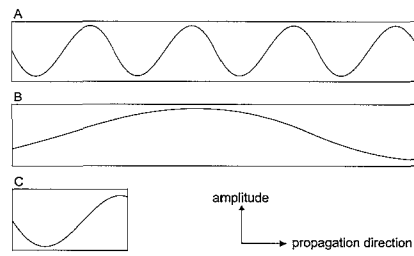


**Figure 5.** Reduction of phase errors with either higher velocity or small dimensions of supportive materials. A, Basic situation. B, Increased velocity. C, Reduced material dimensions.

plied polyvinyl chloride acoustic foam positioned between the gradient coils and shimming coils. Measurements at the isocenter showed noise reduction of

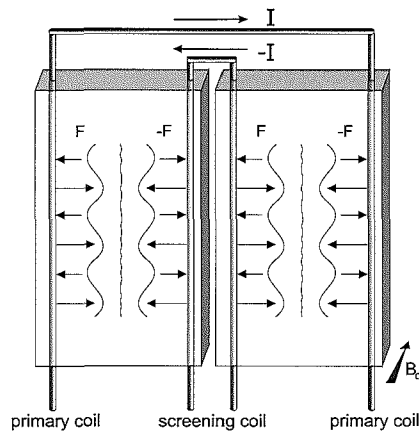


**Figure 6.** New approach to Lorentz force balancing. Screening coil (inner loop) is small, to minimize magnetic field disturbance of the primary winding (outer loop).  $F$  and  $-F$  = opposite Lorentz forces,  $I$  and  $-I$  = opposite currents.

about 10 dB during echo-planar imaging. Foam lining the entrance and exit of the magnet bore did not further reduce noise. Ravicz et al. (32), however, blocked the entrance and exit with foam, resulting in 12-dB peak SPL reduction in noise reentering the magnet bore. Applying sound-absorbing material to the wall of the MR suite has been suggested, although the relationship between SPL and room geometric structure is not fully established (27).

#### Noise Reduction at the Source: Gradient Current Design

In the area of silent pulse sequences, relatively little work has been done. Because acoustic noise is predominantly caused by high-order

harmonics, avoidance of these high frequencies would reduce SPLs considerably. Hennel et al. (43) formulated three rules for redesigning pulse sequences to eliminate these harmonics. These principles, demonstrated in Figure 2, included the application of (a) sinusoidal gradient slopes for band limiting of the frequencies, (b) maximum slope durations for more efficient band limiting, and (c) minimizing the number of slopes by merging pulses whenever possible to lower the fundamental frequency.

Both spin-echo and gradient-echo sequences showed noise attenuation up to 40 dBA, mainly comprising low frequencies (<500 Hz), with acceptable image quality. Noise levels of a silent fast spin-echo sequence (TE = 140 msec) were 23 dBA less than those of a standard fast spin-echo sequence with identical imaging parameters (48). The signal-to-noise ratio, gray-scale distribution, and resolution were equal, although the silent sequence showed slight ghosting due to increased flow sensitivity (43,48). Because no notable reduction could be obtained when the TE was less than 20 msec, the silent sequence rules were not suitable for more rapid sequences (50). Additionally, gradient amplitudes should increase to maintain gradient efficiency, thereby counteracting the efficiency of noise reduction by pulse sequence redesign. The principles of silent sequence design have recently been revised, encompassing prevention of readout gradient plateaus and extension of variable phase encoding to the readout for further narrowing the acoustic bandwidth and improving the gradient amplitude (50). Both fast gradient-echo and fast spin-echo sequences with short TE showed noise reductions of about 30-40 dBA. Additionally, all gradients of the last acquisition could be desloped (51). The findings of Wu et al. (15) have suggested that appropriate choice of gradient current plateau duration might minimize specific frequency components of noise spectra. At the resonance frequency of an x-gradient, periodic decreases of up to 39 dB were observed, when the gradient current width was changed. It was not clear whether these SPL changes were due to enhancement

or cancelling of resonances.

In the field of functional MR imaging, ultrafast imaging is a prerequisite for identifying stimulus-induced activation in brain tissue. Because MR imager noise for echo-planar-based sequences confounds brain activation studies (10-13,52), ultrafast silent sequences have been developed. The generic silent sequence for functional MR imaging, burst imaging, applies a burst of low-flip-angle RF pulses with DC readout and phase-encoding gradients instead of pulsing gradients (53). Jakob et al. (54) acoustically assessed a single-shot burst-imaging-based imaging technique that created images with only 12 gradient ramps, with a 105-msec acquisition time and a matrix of 48 x 64. Peak SPLs at a distance of 2 meter ranged from 52 to 55 dB(A), about 40 dBA less than those for a comparable echo-planar imaging sequence (54,55). In a similar experiment, less noise reduction was reported (15 dB), probably because of shorter acquisition times and steeper slew rates (53). Burst imaging has other attractive properties besides low noise production, such as low demands on gradient strength, small power deposition with low-flip-angle pulses, and suitability for systems without hardware for echo-planar imaging (53). Its major drawbacks are inadequate signal-to-noise ratio because of low flip angles, limitations in available resolution, and increased motion sensitivity (54).

#### *Passive Noise Cancellation*

A simple and economical approach to noise abatement is the use of earplugs and/or earmuffs (36,56). Characteristically, such devices attenuate proportionally with the frequency of noise (57). A widely used commercial foam earplug provides noise attenuation of 20 dB at 0.5 kHz and 30 dB at frequencies of more than 1 kHz (57,58). Earmuffs show an equal reduction pattern but with less reduction at frequencies less than 1 kHz (59).

For both passive and active hearing aids, efficacy is restricted to air-conducted sound waves. Conse-

quently, demonstrated values for particular combinations of preventive hearing aids will not necessarily equal the actual gradient-induced SPLs heard by the subjects because bone-conducted noise comprises the minimum SPL (28,32,59); earplugs and earmuffs combined reduce noise by only 40-56 dB (28,57). Bone-conducted noise is reduced by about 10 dB with the use of insulating foam mattresses on the MR table (36) and by up to 25 dB with a foam-filled helmet enclosing the subject's head (32,57).

It has been suggested that passive hearing protection aids may interfere with communication, particularly with the understanding of speech (1,3,60). Passive hearing protection, however, actually improves speech intelligibility for persons with normal hearing during acoustic environmental noise (61), but it decreases speech intelligibility for hearing-impaired subjects (59). A promising development is hearing protection aids with nonlinear acoustic filters that may allow better communication while still providing adequate protection from acoustic noise.

Other issues of concern, particularly to earmuffs, are discomfort, moderate compliance, and variations in individual fitting (20,36,56,58). Counseling and basic instructions should be provided; however, this does not influence the behavior of people (wearing hearing protection, etc) because of, for example, the discomfort of such protective devices (62).

#### *Active Noise Cancellation*

Recent advances in digital signal processing technology have given rebirth to the old idea of active noise control (ANC), that is, the reduction of an undesirable sound by superposition of a sound that is exactly the inverse of the original sound. The ANC system is constructed with either feedback or feedforward mechanisms (60,63).

A feedback ANC strategy, as used in many commercial headsets, encompasses an error microphone for capturing residual noise in the zone of

silence, a processing unit for generating the canceling signal, and an output speaker (Fig 7 A). Such a feedback system integrated in the existing audio system of the MR suite has been tested. With antinnoise introduced during both spin-echo and gradient-echo sequences, acoustic noise was reduced by 11.1 dB on average for frequencies less than 500 Hz (6). Implementation of self-adapting neural networks into the ANC processing unit for further error minimization demonstrated extended noise extinction to about 20 dB with a 4-kHz cut-off frequency (63). Although this system needed less than 1 second to adapt itself to a new environment, added speech was clearly preserved, probably because of its stochastic nature, but the effect of speech on the performance of the ANC system was not further analyzed.

A feedforward ANC system encompasses a reference sensor located at the noise source and injects the cancellation signal into the noise propagation path (Fig 7B) (63). With a combination of feedback and feedforward algorithms provided by additional error and reference microphones, noise reduction averaged 15 dB over the frequency range of 100-350 Hz during spin-echo and gradient-echo sequences (60).

Which type of ANC to use in MR imaging is not clear. The advantage of a feedback ANC strategy is in its spatial independence, because the error signal is received at the location of interest. Instability problems may arise because of time delays in wave propagation and signal processing (32) and because the residual signal is random and not correlated with the sound source (63).

In the feedforward ANC strategy, the reference signal is highly correlated with the original signal, but instability may also occur because of canceling signals reentering the reference microphone (36). As gradient acoustic noise is highly repeatable and predictable (32), generation of antinnoise in feedforward cancellation with inverted copies of previously measured noise or with calculation by the transfer func-

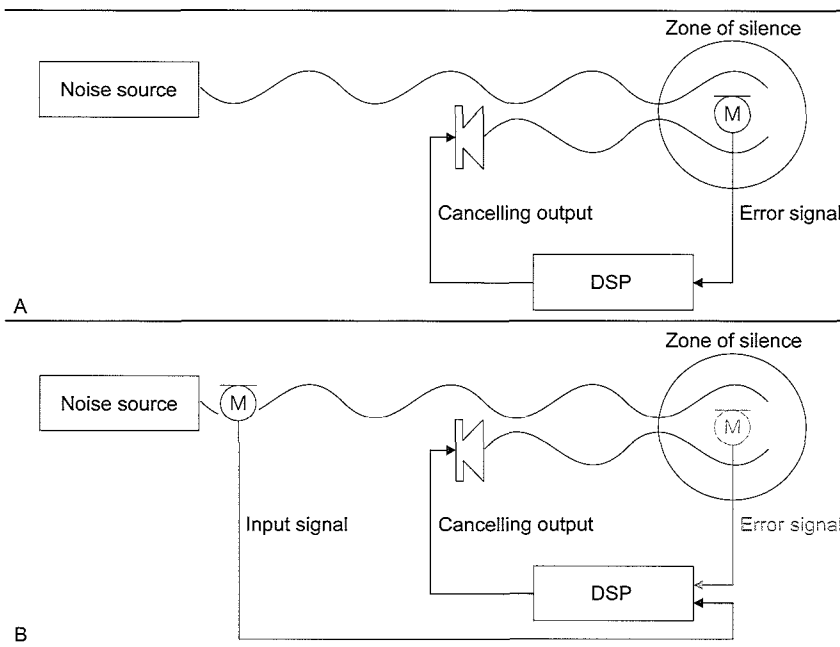


**Figure 7.** Demonstration of feedback (panel *A*) and feedforward (panel *B*) antinoise control (ANC) strategies. Note the additional (gray) error microphone for combined feedforward and feedback ANC in panel *B*. *DSP*= digital signal processing unit, *M* = microphone.

**TABLE 5**  
**Median Permanent Noise-induced Threshold Shifts in Hearing Levels across Averaged Audiometric Test Frequencies of 1-4 kHz**

$L(A)_{eq8h}$ (dB)	Exposure Time (y)				Typical SPLs
	10	20	30	40	
60	0	0	0	0	Normal conversation
85	2	3	3	4	Automobile
90	5	7	8	8	Motorcycle at 10 m
95	11	14	16	17	Subway (inside)
100	18	23	26	29	Diesel truck at 10 m

Note. Data extracted from reference 19.

tion mentioned has potential.

ANC is best suited for low frequency noise (<1 kHz) because sufficient noise suppression is achieved with the control noise and the zone of silence separated by no more than one-tenth of the acoustic wavelength (64). Above 1 kHz, however, ANC seems less effective. The wavelength is small compared with the dimensions of the human body, resulting in unexpected phase and amplitude variations in imager noise (32) and, therefore, accidental superposition with injected antinoise.

The application of ANC in MR imaging is controversial because the trend toward faster imaging techniques pushes up the generated frequencies. Fortunately, earplugs and earmuffs adequately

ly attenuate noise at frequencies above 1 kHz. Combining ANC with either earplugs or earmuffs has proved to be beneficial, with a subjective 10-dB reduction at 250 Hz, but there was no additional benefit of ANC when earplugs and earmuffs were combined (59). The effect on speech of combining ANC with passive aids is unclear, but evidence suggests that ANC improves intelligibility by 10% (61).

#### Health issues and noise exposure in the MR environment

The risk of hearing loss caused by chronic noise exposure, slowly and imperceptibly developing over several years, is well documented in the literature (16,20,65,66). Chronic exposure to noise at levels of more than 80 dB(A)

results in permanent hearing loss in 85% of the exposed healthy population (3,21,27). Moreover, acoustic noise may produce hearing problems at lower SPLs in susceptible subjects, for example, those who take certain drugs (aminoglycosides, cisplatin) (67). The SPL and duration of exposure are the predominant physical factors in determining the deleterious effects of noise on hearing (Table 5) (36). The main rationale for preventing hearing loss is to preserve hearing for speech intelligibility (20,65,66,68).

#### Calculation of Safe Noise Dosage

To estimate hearing impairment and risks of hearing handicap (Table 5), the A-weighted SPL normalized to a nominal 8-hour working day ( $L(A)_{eq8h}$ ) is used (19,21,68,69). In the MR environment, interruptions and changes in SPL are common, and calculations should therefore indicate the daily exposure of both operator and patient (Fig 8). The normalized daily noise exposure for a single event (e.g., an image acquisition) with measured continuous-equivalent sound level  $L(A)_m$  and exposure duration  $T_m$  in hours (or minutes) is calculated as follows:

$$L(A)_{eq8h} = L(A)_m - 10 \cdot \log\left(\frac{T_r}{T_m}\right) \quad (2)$$

where  $T_r$  is 8 hours (or 480 minutes) (17,19,28). Combining multiple events (e.g., image acquisitions with different pulse sequences) to obtain a total daily continuous-equivalent sound level  $L(A)_c$  is possible with the following equation:

$$L(A)_c = 10 \times \log\left(\sum_{i=1}^n 10^{0.1 \times L(A)_{eq8h,i}}\right) \quad (3)$$

where  $L(A)_{eq8h,i}$  equals  $n$  number  $L(A)_{eq8h}$  as calculated in Equation (2). Figure 8 shows a representative example of an interventional procedure with estimated SPLs of real-time and anatomic imaging.

During anatomic imaging, increasing TR decreases SPL, whereas the sound exposure level equals as the total imaging time increases proportionally with TR. On the other hand, during real-time imaging, increasing TR simultaneously decreases SPL and noise exposure, although at the expense of the image refresh rate.

## Guidelines and Legislation to Safe Noise

Based on the 8-hours working day (5 days per week), safety guidelines have been established for industry workers to limit the noise exposure. The guidelines applied in different countries and different employment sectors, however, disagree on the maximum daily occupational sound exposure level and the so-called trading rule (28). The trading rule holds that increasing the SPL with a certain trade-off value halves the permitted exposure time. According to European Community guidelines, maximum  $L(A)_{eq8h}$  should not exceed 90 dB without hearing protection (69). A 3-dB trade-off value applies, and the permitted exposure duration is halved with every 3-dB increase in SPL (also called the equal energy rule). By contrast, in the United States, the Occupational Safety and Health Administration has recommended an  $L(A)_{eq8h}$  of 90 dB(A) with a 5-dB exchange rate (68), although the National Institute for Occupational Safety and Health (NIOSH) advises a maximum  $L(A)_{eq8h}$  of 85 dB(A) with a 3-dB exchange rate. Many different U.S. employment sectors have adopted the more prudent NIOSH guidelines (21).

Applying the NIOSH guidelines to the example of Figure 8, an interventional radiologist exceeds the maximum exposure level in less than half a procedure, whereas a patient exceeds maximum exposure within 10 minutes (without hearing protection). Notably, the risk for the operator is in the accumulation of occupational noise exposure during long-standing and repetitive procedures over a period of years (Table 5). Nonoccupational patient exposure is of relatively short duration, and there are no explicit recommendations for safety (36).

Hearing protective equipment must be provided to employees exposed to  $L(A)_{eq8h}$  of more than 85 dB in both European Community countries and the United States. In several European countries,  $L(A)_{eq8h}$  is set even lower, at 80 dB. The use of appropriate attenuation equipment is mandatory for  $L(A)_{eq8h}$  of more than 90 dB, as mentioned previously, and should reduce the sound dosage to acceptable levels (68,69).

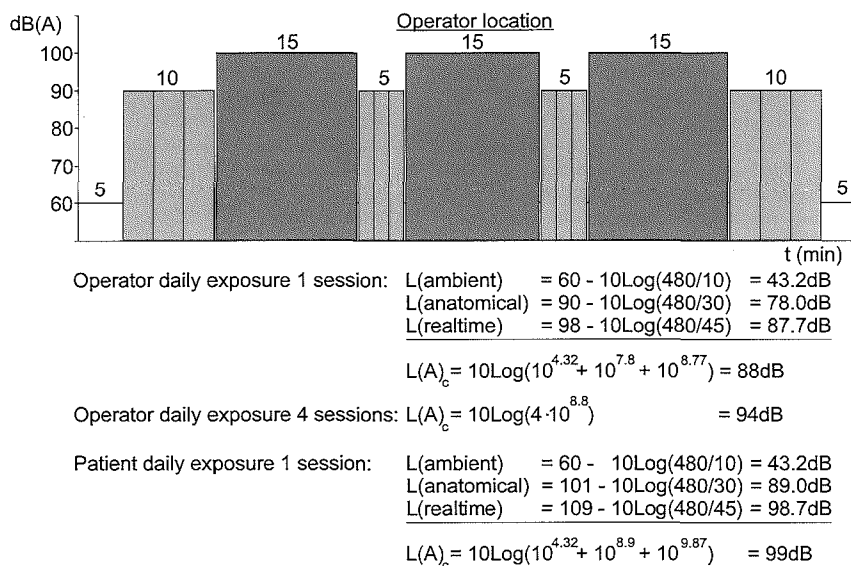


**Figure 8.** Example of an interventional procedure. SPLs at the operator location (1.70 m high, 80 cm from magnet bore) are estimated at 98 dB(A) and 90 dB(A), respectively, for real-time and anatomic imaging. Ambient noise is at 60 dB(A). SPL at the magnet bore is estimated to be 11 dB higher. For the operator, daily exposure is calculated for one and for four sessions, with Equations (2) and (3).  $T_r = 480$  minutes (8 hours). Values are unpublished data.

## Practical considerations and recommendations

The following are practical considerations and recommendations:

1. Noise exposure should be recognized as a relevant occupational problem because of increasing SPLs and frequencies in the MR environment.
2. Noise and frequency assessment in the MR environment require special attention to measurement methods and equipment, preferably according to guidelines from the American National Standards Institute and the ISO.
3. The continuous evolution of MR equipment, particularly its increasing sound levels and higher frequencies, increases noise exposure and thus the need for adequate reduction methods.
4. The relationship between imaging parameters and frequency may be important in noise-reduction strategies, for example, in optimizing the duration of gradient pulses or prevention of resonances.
5. New insights into the design of both gradient coils and gradient pulse sequences are encouraging developments in noise reduction and should be explored further.
6. Passive noise reduction (earplugs, earmuffs) becomes more efficient with the higher-frequency noise gen-

erated by fast MR imaging sequences.

7. ANC systems have moderate efficiency at lower frequencies when used in combination with passive hearing protection. Moreover, such systems are technically matured, and substantial improvement is therefore not expected.

8. Interventional radiologists and other health workers should be aware of the cumulative nature of the occupational noise hazard. Hearing protective devices are recommended to reduce the high SPL to safe levels ( $L(A)_{eq8h} < 80\text{dB}$ ).

9. Active audiologic screening at regular intervals may be considered for interventionalists working in interventional MR imaging.

## References

1. Brummett RE, Talbot JM, Charuhas P. Potential hearing loss resulting from MR imaging. *Radiology* 1988; 169:539-540.
2. Langkowski JH, Thiele F, Maas R, Kooijman H. Messungen zur geräuschbelastung in der MR-tomographie bei 1,5 Tesla. *Rofo Fortschr Geb Rontgenstr Neuen Bildgeb Verfahr* 1989; 151:483-486.
3. Hurwitz R, Lane SR, Bell RA, Brant-Zawadzki MN. Acoustic analysis of gradient-coil noise in MR imaging. *Radiology* 1989; 173:545-548.
4. Shellock FG, Ziarati M, Atkinson D, Chen DY. Determination of gradient magnetic field-induced acoustic noise associated

- with the use of echo planar and three-dimensional, fast spin echo techniques. *J Magn Reson Imaging* 1998; 8:1154-1157
5. Moelker A, Vogel M, Ouhlous M, Lethimonnier F, Pattynama PMT. Operator exposure to acoustic noise in interventional MRI (abstr). In: Proceedings of the Ninth Meeting of the International Society for Magnetic Resonance in Medicine. Berkeley, Calif: International Society for Magnetic Resonance in Medicine, 2001; p2180.
  6. Goldman AM, Gossman WE, Friedlander PC. Reduction of sound levels with antinose in MR imaging. *Radiology* 1989; 173:549-550.
  7. Price DL, De Wilde JP, Papadaki AM, Curran JS, Kitney RI. Frequency analysis of MRI acoustic noise (abstr). In: Proceedings of the Eighth Meeting of the International Society for Magnetic Resonance in Medicine. Berkeley, Calif: International Society for Magnetic Resonance in Medicine, 2000; p2008.
  8. Quirk ME, Letendre AJ, Ciottone RA, Lingley JF. Evaluation of three psychological interventions to reduce anxiety during MR imaging. *Radiology* 1989; 173:759-762.
  9. Quirk ME, Letendre AJ, Ciottone RA, Lingley JF. Anxiety in patients undergoing MR imaging. *Radiology* 1989; 170:463-166.
  10. Elliott MR, Bowtell RW, Morris PG. The effect of scanner sound in visual, motor, and auditory functional MRI. *Magn Reson Med* 1999; 41:1230-1235.
  11. Talavage TM, Edmister WB, Ledden PJ, Weisskoff RM. Quantitative assessment of auditory cortex responses induced by imager acoustic noise. *Hum Brain Mapp* 1999; 7:79-88.
  12. Hall DA, Summerfield AQ, Goncalves MS, Foster JR, Palmer AR, Bowtell RW. Time-course of the auditory BOLD response to scanner noise. *Magn Reson Med* 2000; 43: 601-606.
  13. Cho ZH, Chung SC, Lim DW, Wong EK. Effects of the acoustic noise of the gradient systems on fMRI: a study on auditory, motor, and visual cortices. *Magn Reson Med* 1998; 39:331-335.
  14. Ulmer JL, Biswal BB, Mark LP, et al. Acoustic echoplanar scanner noise and pure tone hearing thresholds: the effects of sequence repetition times and acoustic noise rates. *J Comput Assist Tomogr* 1998; 22:480-486.
  15. Wu Y, Chronik BA, Bowen C, Mechefske CK, Rutt BK. Gradient-induced acoustic and magnetic field fluctuations in a 4T whole-body MR imager. *Magn Reson Med* 2000; 44: 532-536.
  16. National Institute for Occupational Safety and Health. Criteria for a recommended Standard: Occupational noise exposure. Publication no. 73-11001. Cincinnati, Ohio: National Institute for Occupational Safety and Health, 1973.
  17. Acoustical Society of America. American National Standard S1.13-1995: measurement of sound pressure levels in air. Melville, NY: Acoustical Society of America, 1995.
  18. Acoustical Society of America. American National Standard S3.28-1986: methods for the evaluation of the potential effect on human hearing of sounds with peak A-weighted sound pressure levels above 120 decibels and peak C-weighted sound pressure levels below 140 decibels. Melville, NY: Acoustical Society of America, 1986.
  19. Acoustical Society of America. American National Standard S3.44-1996: determination of Occupational noise exposure and estimation of noise-induced hearing impairment. Melville, NY: Acoustical Society of America, 1996.
  20. Brookhouser PE. Prevention of noise-induced hearing loss. *Prev Med* 1994; 23:665-669.
  21. National Institute for Occupational Safety and Health. Criteria for a recommended Standard: Occupational noise exposure-revised criteria 1998. Publication no. 98-126. Cincinnati, Ohio: National Institute for Occupational Safety and Health, 1998.
  22. McJury M, Blug A, Joerger C, Condon B, Wyper D. Short communication: acoustic noise levels during magnetic resonance imaging scanning at 1.5 T. *Br J Radiol* 1994; 67:413-415.
  23. McJury MJ. Acoustic noise levels generated during high field MR imaging. *Clin Radiol* 1995; 50:331-334.
  24. Price DL, De Wilde JP, Papadaki AM, Curran JS, Kitney RI. Investigation of acoustic noise on 15 MRI scanners from 0.2 T to 3 T. *J Magn Reson Imaging* 2001; 13:288-293.
  25. Counter SA, Olofsson A, Grahn HF, Borg E. MRI acoustic noise: sound pressure and frequency analysis. *J Magn Reson Imaging* 1997; 7:606-611.
  26. Shellock FG, Morisoli SM, Ziarati M. Measurement of acoustic noise during MR imaging: evaluation of six "worstcase" pulse sequences. *Radiology* 1994; 191:91-93.
  27. Miyati T, Banno T, Fujita H, et al. Acoustic noise analysis in echo planar imaging: multicenter trial and comparison with other pulse sequences. *IEEE Trans Med Imaging* 1999; 18:733-736.
  28. Foster JR, Hall DA, Summerfield AQ, Palmer AR, Bowtell RW. Sound-level measurements and calculations of safe noise dosage during EPI at 3 T. *J Magn Reson Imaging* 2000; 12:157-163.
  29. Kanal E, Shellock FG, Talagala L. Safety considerations in MR imaging. *Radiology* 1990; 176:593-606.
  30. Brüel & Kjaer. Condenser microphone cart-ridges: types 4133-4181. Product data. Naerum, Denmark: Brüel & Kjaer.
  31. Knowles Electronics. EK series: data sheet. Available at: [www.knowlesinc.com/KNelec/KNmic/html/ek.htm](http://www.knowlesinc.com/KNelec/KNmic/html/ek.htm). Accessed August 30, 2001.
  32. Ravicz ME, Melcher JR, Kiang NY. Acoustic noise during functional magnetic resonance imaging. *J Acoust Soc Am* 2000; 108:1683-1696.
  33. Counter SA, Olofsson A, Borg E, Bjelke B, Haggstrom A, Grahn HF. Analysis of magnetic resonance imaging acoustic noise generated by a 4.7 T experimental system. *Acta Otolaryngol* 2000; 120:739-743.
  34. Hedeem RA, Edelstein WA. Characterization and prediction of gradient acoustic noise in MR imagers. *Magn Reson Med* 1997; 37:7-10.
  35. Cho ZH, Park SH, Kim JH, et al. Analysis of acoustic noise in MRI. *Magn Reson Imaging* 1997; 15:815-822.
  36. McJury M, Shellock FG. Auditory noise associated with MR procedures: a review. *J Magn Reson Imaging* 2000; 12:37-45.
  37. Mansfield P, Chapman BL, Bowtell R, Glover P, Coxon R, Harvey PR. Active acoustic screening: reduction of noise in gradient coils by Lorentz force balancing. *Magn Reson Med* 1995; 33:276-281.
  38. Mansfield P, Glover P, Bowtell R. Active rapid acoustic screening: design principles for quiet gradient coils in MRI. *Meas Sci Technol* 1994; 5:1021-1025.
  39. Mansfield P, Chapman BL. Quiet gradient coils: active acoustically and magnetically screened distributed transverse gradient designs. *Meas Sci Technol* 1995; 6:349-353.
  40. Mansfield P, Glover PM, Beaumont J. Sound generation in gradient coil structures for MRI. *Magn Reson Med* 1998; 39:539-550.
  41. Mansfield P, Hayward B. Principles of active acoustic control in gradient coil design. *MAGMA* 2000; 10:147-151.
  42. Chapman BLW, Mansfield P. Quiet gradient coils: active acoustically and magnetically screened distributed transverse gradient designs. *Meas Sci Technol* 1995; 6:349-354.
  43. Hennel F, Girard F, Loenneker T. "Silent" MRI with soft gradient pulses. *Magn Reson Med* 1999; 42:6-10.
  44. Cho ZH, Chung ST, Chung JY, et al. A new silent magnetic resonance imaging using a rotating DC gradient. *Magn Reson Med* 1998; 39:317-321.
  45. Bowtell R, Peters A. Analytic approach to the design of transverse gradient coils with co-axial return paths. *Magn Reson Med* 1999; 41:600-608.
  46. Prieto TE. Acoustic noise levels in head gradient coils during EPI as a function of frequency encoding direction (abstr). In: Proceedings of the Seventh Meeting of the International Society for Magnetic Resonance in Medicine. Berkeley, Calif: International Society for Magnetic Resonance in Medicine, 1999; p105.
  47. Prieto TE, Bennet K, Weyers D. Acoustic noise levels in a head gradient coil during echo planar imaging at 3T (abstr). In: Proceedings of the Sixth Meeting of the International Society for Magnetic Resonance in Medicine. Berkeley, Calif: International Society for Magnetic Resonance in Medicine, 1998; p750.
  48. Girard F, Marcar VL, Hennel F, Martin E. Anatomic MR images obtained with silent sequences. *Radiology* 2000; 216:900-902.
  49. Monroe JW, Holtman R, Holtman K, Schmalbrock P, Clymer BD. Evaluation of various materials for acoustic noise attenuation in MRI (abstr). In: Proceedings

- of the Seventh Meeting of the International Society for Magnetic Resonance in Medicine. Berkeley, Calif: International Society for Magnetic Resonance in Medicine, 1999; p101.
50. Hennel F. Acoustic optimisation of rapid MRI (abstr). In: Proceedings of the Eighth Meeting of the International Society for Magnetic Resonance in Medicine. Berkeley, Calif: International Society for Magnetic Resonance in Medicine, 2000; p2010.
  51. Zhou Y, Ma J. Acoustic noise reduction in MRI by selective gradient derating (abstr). In: Proceedings of the Eighth Meeting of the International Society for Magnetic Resonance in Medicine. Berkeley, Calif: International Society for Magnetic Resonance in Medicine, 2000; p2009.
  52. Yang Y, Engelen A, Engelen W, Xu S, Stern E, Silbersweig DA. A silent event-related functional MRI technique for brain activation studies without interference of scanner acoustic noise. *Magn Reson Med* 2000; 43:185-190.
  53. Cremillieux Y, Wheeler-Kingshott CA, Briguet A, Doran SJ. STEAM-Burst: a single-shot, multi-slice imaging sequence without rapid gradient switching. *Magn Reson Med* 1997; 38:645-652.
  54. Jakob PM, Schlaug G, Griswold M, et al. Functional burst imaging. *Magn Reson Med* 1998; 40:614-621.
  55. Lovblad KO, Thomas R, Jakob PM, et al. Silent functional magnetic resonance imaging demonstrates focal activation in rapid eye movement sleep. *Neurology* 1999; 53:2193-2195.
  56. Dancer A, Grateau P, Cabanis A, et al. Effectiveness of ear-plugs in high-intensity impulse noise. *J Acoust Soc Am* 1992; 91:1677-1689.
  57. Ravicz ME, Melcher JR. Isolating the auditory system from acoustic noise during functional magnetic resonance imaging: examination of noise conduction through the ear canal, head, and body. *J Acoust Soc Am* 2001; 109:216-231.
  58. Berger EH, Franks JR, Behar A, et al. Development of a new Standard laboratory protocol for estimating the field attenuation of hearing protection devices. III. The validity of using subject-fit data. *J Acoust Soc Am* 1998; 103:665-672.
  59. Abel SH, Spencer DL. Speech understanding in noise with earplugs and muffs in combination. *Appl Acoust* 1999; 57:61-68.
  60. McJury M, Stewart RW, Crawford D, Toma E. The use of active noise control (ANC) to reduce acoustic noise generated during MRI scanning: some initial results. *Magn Reson Imaging* 1997; 15:319-322.
  61. Abel SM, Spencer DL. Active noise reduction versus conventional hearing protection: relative benefits for normal-hearing and impaired listeners. *Scand Audiol* 1997; 26: 155-167.
  62. Rabinowitz PM. Noise-induced hearing loss. *Am Fam Phys* 2000; 61:2749-2756, 2759-2760.
  63. Chen CK, Chiueh TD, Chen JH. Active cancellation system of acoustic noise in MR imaging. *IEEE Trans Biomed Eng* 1999; 46:186-191.
  64. Baumgart F, Kaulisch T, Tempelmann C, et al. Electrodynamical headphones and woofers for application in magnetic resonance imaging scanners. *Med Phys* 1998; 25: 2068-2070.
  65. Rosler G. Progression of hearing loss caused by occupational noise. *Scand Audiol* 1994; 23:13-37.
  66. Prince MM, Stayner LT, Smith RJ, Gilbert SJ. A re-examination of risk estimates from the NIOSH Occupational Noise and Hearing Survey (ONHS). *J Acoust Soc Am* 1997; 101: 950-963.
  67. Laurell G, Engstrom B. The combined effect of cisplatin and furosemide on hearing function in guinea pigs. *Hear Res* 1989; 38:19-26.
  68. Occupational Safety and Health Administration. Occupational noise exposure (occupational health and environmental control). FR-1910.95.61 Federal Register 9227 (1996).
  69. Council of European Communities. Council Directive 86/188/EEC of 12 May 1986 on the protection of workers from the risks related to exposure to noise at work. Available at: [europa.eu.int/eur-lex/en/lif/dat/1986/en\\_386L0188.html](http://europa.eu.int/eur-lex/en/lif/dat/1986/en_386L0188.html). Accessed September 20, 2001.
  70. Nitz WR. MR imaging: acronyms and clinical applications. *Eur Radiol* 1999; 9:979-997.





Adriaan Moelker, MD  
Ronald A. J. J. Maas, PhD  
Franck Lethimonnier, PhD  
Peter M. T. Pattynama, MD

### Index terms:

Magnetic resonance (MR),  
biological effects  
Magnetic resonance (MR),  
quality assurance  
Magnetic resonance (MR),  
safety  
Magnetic resonance (MR),  
technology  
Radiology and radiologists

Published online before print  
10.1148/radiol.2243010978  
Radiology 2002; 224:889–895

### Abbreviations:

GRE = gradient-recalled echo  
 $L(A)_{eq}$  = equivalent-continuous A-weighted SPL  
 $L(A)_{eq^{8h}}$  = equivalent-continuous A-weighted daily (8-hour) noise exposure  
 $L(L)_{eq}$  = equivalent-continuous linear SPL  
SPL = sound pressure level

From the Departments of Radiology (A.M., F.L., P.M.T.P.) and Audiophysics (R.A.J.J.M.), Erasmus University Medical Center Rotterdam, 50 Dr Molewaterplein, P.O. Box 1738, Rotterdam 3000 DR, the Netherlands.

Received May 29, 2001; revision requested July 20; final revision received February 6, 2002; accepted March 19.

Address correspondence to A.M. (e-mail: a.moelker@erasmusmc.nl).

### Author contributions:

Guarantors of integrity of entire study, all authors; study concepts and design, all authors; literature research, A.M., F.L.; experimental studies, A.M., R.A.J.J.M., F.L.; data acquisition, A.M.; data analysis / interpretation, A.M., R.A.J.J.M., F.L.; statistical analysis, A.M., F.L.; manuscript preparation, A.M.; manuscript definition of intellectual content, editing, revision / review, and final version approval, all authors.

© RSNA, 2002

# Interventional MR Imaging at 1.5 T: Quantification of Sound Exposure

Sound pressure levels (SPLs) during interventional magnetic resonance (MR) imaging may create an occupational hazard for the interventional radiologist (i.e., the potential risk of hearing impairment). Therefore, A-weighted and linear continuous-equivalent SPLs were measured at the entrance of a 1.5-T MR imager during cardiovascular and real-time pulse sequences. The SPLs ranged from 81.5 to 99.3 dB (A-weighted scale), and frequencies were from 1 to 3 kHz. SPLs for the interventional radiologist exceeded a safe SPL of 80 dB (A-weighted scale) for all sequences; therefore, hearing protection is recommended.

© RSNA, 2002

Acoustic noise has long been recognized as an important issue in magnetic resonance (MR) imaging because of the potential risk of induced hearing impairment (1–11). The recent advent of interventional MR imaging has potentially created an occupational hazard for radiologists, that is, the acoustic burden on the interventional radiologist who works near the MR magnet bore. The risk for the interventional radiologist is in the accumulation of noise exposure during long and repetitive interventional MR procedures. The risk that hearing loss will develop slowly and imperceptibly over several years as a result of chronic noise exposure at levels less than pain is well documented in the literature (12,13).

Previous emphasis in discussions about the acoustic noise of MR imaging has been on patient exposure during MR imaging. Because of this emphasis, most published noise measurements represent the acoustic noi-

se levels in the isocenter of the magnet bore. Only a few investigators have reported the sound pressure levels (SPLs) at the entrance of the magnet bore (4,8), which are more relevant to assess the acoustic burden on the interventional radiologist. Furthermore, no data are available for the acoustic noise of newer real-time sequences used in interventional MR imaging. The high-performance gradients and fast gradient switching necessary for real-time MR imaging are likely to cause greater acoustic noise levels (3,6,10,14). In addition, there is a growing tendency for use of the higher magnetic field strength of 1.5 T (15,16), with correspondingly increased acoustic noise levels.

The purposes of our study were (a) to quantify the SPLs of the imaging sequences that are relevant for interventional MR imaging at 1.5 T for the interventional radiologist and (b) to determine the patient's acoustic exposure in interventional MR procedures.

### Materials and Methods

Data were obtained with a 1.5-T cardiovascular MR imager (Signa CV/i, with LX 8.4 software; GE Medical Systems, Milwaukee, Wis) with gradients of 40 mT·m<sup>-1</sup>, slew rate of 150 T·m<sup>-1</sup>·sec<sup>-1</sup>, and rise time of 268 μsec, with use of an integrated quadrature-driven transceiver and a radio-frequency body coil. This cardiovascular MR system allows fast imaging with high signal-to-noise ratios suitable for real-time imaging. Fast pulse sequences with rapid data collection and calculation are required to achieve adequate image refresh rates that allow visualization of the anatomy depicted and devices used during an interventional MR proce-

ture; the sequences result in an on-the-fly adaptation of the image formation.

Noise measurements were made with a 1/2-inch (1.27-cm) prepolarized free-field condenser microphone (type 4189; Brüel & Kjær, Nærum, Denmark) mounted on a tripod, with a 10-m extension cable (AO-0442; Brüel & Kjær) connected to a type 1 digital sound level analyzer (Investigator 2260; Brüel & Kjær) with oscilloscope (PM-3218; Philips) located in the adjacent MR control room. All SPLs were measured during 50 seconds and recorded on both linear and A-weighted scales. The linear SPL, which is expressed in decibels, is the logarithm of the ratio of  $P_1$  (measured in micropascals) to the international standardized reference sound pressure ( $P_0$ ) of 20  $\mu$ Pa:

$$\text{SPL} = 10 \cdot \log \left( \frac{P_1}{P_0} \right)^2 \quad (1)$$

The human ear is not uniformly sensitive to the audible frequencies (decrease of sensitivity to less than 1 and more than 6 kHz). This decreased sensitivity is accounted for by adding an A-weighted filter to the linear (unfiltered) SPL; the filter adjusts for the acoustic response of human hearing. In addition, the peak SPLs (the highest instantaneous sound pressure level in less than 50  $\mu$ sec,  $L(L)_p$ ) and the frequency distributions on 1/3-octave bands (i.e., doublings of 16, 20, and 25 Hz) to 12 kHz were recorded on a linear scale. The time weighting (i.e., the time to average the instantaneous fluctuations in sound pressure) was 125 msec (3,10). To estimate hearing damage due to occupational sound exposure, the equivalent continuous A-weighted SPL,  $L(A)_{eq}$ , is the preferred measure; it reflects the overall (time-averaged) SPL during the 50-second measurement period. The sound profiles were monitored with an oscilloscope for impulse noise (which is characterized by a sharp increase and rapid decay of SPL in less than 1 second that is more than 10 dB above background SPL in less than 250 msec) (17).

In a pilot experiment, tests were conducted to optimize the experimental set-up for the acoustic measurements (18). The initial SPL measurements showed that the MR imaging

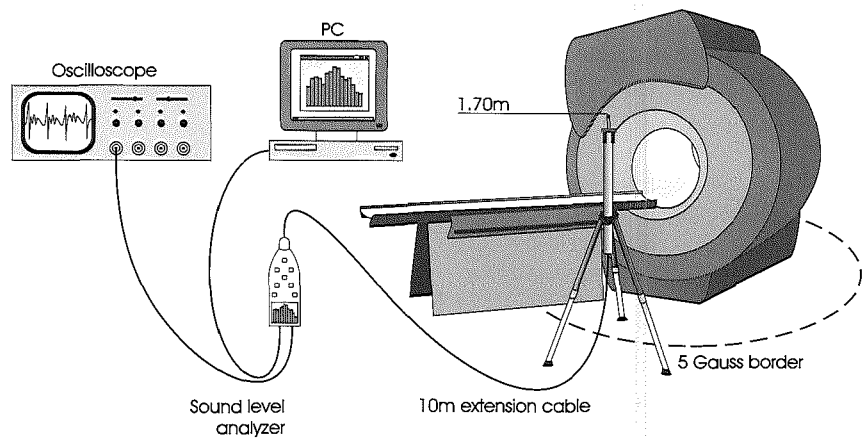


Figure 1. Experimental set-up of noise measurements. PC = personal computer.

suite, with its flat and hard surfaces (in acoustic terms) a diffuse field (i.e., the SPL increased less than 3 dB when the distance to the sound source was halved). This finding led us to position the microphone vertically in the experimental set-up (in compliance with American National Standard protocol S1.13-1995 of the Acoustical Society of America) (3,4,17). Because the frequency distribution was well below 20 kHz in our pilot experiment, sound wave diffraction around the microphone was negligible. Therefore, a free-field microphone, which corrects for diffraction in free-field measurements, could be used in the diffuse-field MR imaging suite.

Findings in previous reports have shown that, despite the presence of some amount of ferromagnetic material (mostly nickel), the accuracy of the microphone is not influenced by gradients and the radiofrequency system (3,4,6,10,19,20). We also ruled out possible interference of the static 1.5-T magnetic field by the sensitivity of the microphone by coupling a reference sound to the microphone with a fixed wave propagation path (2-m-long plastic tube). Insertion of the microphone into the magnet isocenter resulted in SPLs equal to those measured in the MR control room. The sound level meter calibration was checked, with 94 dB at 1 kHz, at regular intervals throughout the experiments.

To quantify the operator exposure, the microphone was placed 0.8 m from the MR imager (at the 5-G line from the magnet bore) at a height of

1.70 m, which is a plausible location for the ear of the interventional radiologist (Fig 1). These measurements were performed without a person in the magnet bore. To measure patient exposure to noise, the microphone was positioned inside the magnet bore at the isocenter.

The MR imaging sequences to be tested for acoustic noise were chosen on the basis of their relevance to cardiovascular interventional MR imaging: single-shot fast spin echo, fast spoiled gradient-recalled echo (GRE), time-of-flight fast spoiled GRE, fast GRE echo train (a hybrid echo-planar fast spoiled GRE sequence [21]), and spiral trajectory k-space sampling.

Of these sequences, the fast spoiled GRE and fast GRE echo train sequences seem especially suitable for real-time interventional MR imaging. Relevant imaging parameters, including repetition time (n=74 measurements), echo time (n=32 measurements), flip angle (n=84 measurements), field of view (n=83 measurements), section thickness (n=81 measurements), matrix size (n=50 measurements), and plane of imaging (n=41 measurements), were varied over a wide range for each of the sequences tested. The influence of imaging parameters recorded both inside and outside the magnet bore was evaluated with median values and quartiles of the differences between the recorded SPL and the mean SPL for each sequence. The influence of a person inside the magnet bore on the noise level, with respect to the operator, was assessed at the 5-G line by using different sequences (n=42 measurements), mainly GRE, both

**TABLE 1**  
**Typical Imaging Protocols with SPLs Measured at the 5-G Border and Magnet Isocenter**

Sequence	Imaging Parameters							5-G Border			Isocenter		
	Repetition Time (msec)	Echo Time (msec)	Echo Train Length	Field of View	Matrix	Section (mm)	No. of Sections per Second	$L(A)_{eq}$	$L(L)_{eq}$	$L(L)_p$	$L(A)_{eq}$	$L(L)_{eq}$	$L(L)_p$
	Ambient	NA	NA	NA	NA	NA	NA	NA	52.3	69.1	82.0	63.8	84.5
Fast spin echo	200	14	8	25	256 x 256	10	0.15	88.4	88.1	101.8	98.8	98.1	117.5
	1.040	14	8	25	256 x 256	10	0.03	81.5	81.3	101.7	92.1	92.3	115.4
	200	14	8	40	256 x 256	10	0.15	88.4	87.9	101.9	100.1	99.5	118.1
	560	14	20	25	256 x 256	10	0.12	87.9	87.5	102.5	98.7	98.3	114.2
	200	14	8	25	256 x 128	10	0.31	88.2	87.8	102.3	100.5	99.8	118.0
Single-shot fast spin echo		42	NA	25	256 x 256	10	0.31	86.6	86.1	102.6	97.4	97.0	116.3
Fast spoiled GRE	4.4	1.3	NA	25	256 x 96	4	2.41	96.6	96.3	108.4	109.2	108.1	118.9
	4.4	1.3	NA	40	256 x 96	4	2.41	90.5	90.4	101.8	104.4	104.4	118.6
	4.6	1.3	NA	25	256 x 192	4	1.19	98.1	97.8	109.3	110.4	109.4	121.9
	4.4	1.3	NA	25	256 x 96	8	2.41	96.8	96.5	106.6	108.5	107.4	118.7
Three-dimensional time of flight	5.3	1.0	NA	25	256 x 192	4	0.97	96.2	96.2	107.9	106.2	105.3	118.9
Fast GRE echo train	10.2	1.9	4	25	256 x 256	8	1.10	99.3	99.0	110.0	109.7	108.6	121.1
	9.6	1.7	4	40	256 x 256	8	1.16	93.4	92.9	106.3	105.9	105.1	120.3
	12.0	3.1	4	30	256 x 256	2	0.98	96.1	96.4	107.1	105.2	104.4	118.7
	17.0	1.7	8	30	256 x 256	8	1.25	95.1	95.1	107.3	104.2	103.5	117.6
	40.0	1.8	4	30	256 x 256	8	0.36	90.0	90.1	102.9	99.3	98.7	116.6
Spiral trajectory k-space sampling	22	2.3	NA	25	2.048 / 20*	6	2.22	94.9	95.2	107.3	103.1	102.4	121.0
	20	2.2	NA	25	2.048 / 20*	8	2.21	94.9	95.2	107.4	103.0	102.4	121.0
	22	2.5	NA	25	2.048 / 10*	6	3.60	94.3	94.4	105.4	103.7	103.2	120.4

Note. NA = not applicable.  $L(L)_p$  = highest instantaneous SPL in less than 50  $\mu$ sec.  
 \* Number of data collection points per spiral per number of spirals in k space.

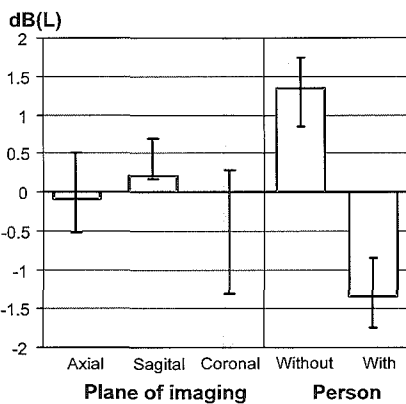


**Figure 2.** Bar graphs of the plane of imaging ( $n = 41$  measurements) and the presence of a person ( $n = 44$  measurements) depict median (height of box) and 25th and 75th quartiles of the differences between measured SPLs and their mean SPL for each sequence. Different planes of imaging had identical SPLs. The presence of a person inside the magnet bore caused a decrease in SPL of about 3 dB.

with and without a person in the magnet bore. The recordings with a volunteer in the bore were not performed during routine procedures. We obtained informed consent from each volunteer. We consulted the chairman of our institutional review board, and he concluded that board approval was not required for the volunteer study. In addition, baseline noise levels in

the MR suite were recorded that represented the sound level of the in-room air-conditioning and ventilation systems and the MR cooling cryogen (ambient noise). Ambient noise was negligible during the measurements of the imaging sequences because the resulting SPLs were then much higher than 10 dB (17).

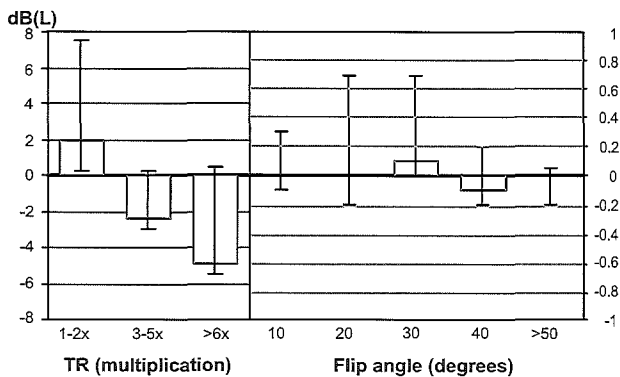
**Results**

Table 1 lists the equivalent-continuous and peak SPLs on linear and A-weighted scales. Of these measures,  $L(A)_{eq}$  is considered a reliable predictor of noise-induced hearing loss for all types of noise (i.e., continuous and impulse noise) (22). The ambient noise in the MR imaging suite at rest (measured at the 5-G line) was remarkably high, with equivalent continuous linear SPL,  $L(L)_{eq}$ , of 69.1 dB. Because the main frequency of the ventilation system was at about 100 Hz, however, the more relevant  $L(A)_{eq}$  was considerably lower (52.3 dB). These results are similar to previously reported values (3,5,23).

The  $L(A)_{eq}$  values depended on the sequence (Table 1) and ranged from 81.5 to 99.3 dB (A-weighted scale) at

the 5-gauss line. The fast sequences, fast spoiled GRE and fast GRE echo train, had  $L(A)_{eq}$  values as high as 98.1 and 99.3 dB (A-weighted scale), respectively. The peak SPLs were greater than 100 dB for all sequences (range 101.7-110.0 dB [linear scale]). On average, the noise exposure to the patient was 11 dB greater than that to the interventional radiologist. The presence of a person inside the magnet caused a noticeable decrease in SPL for the operator of 2.7 dB (Fig 2). In audio physics, 3 dB is generally taken as the transition between irrelevant and relevant differences.

On the basis of our analysis, it appears that in all sequences tested, the main parameter influencing the SPL was repetition time. With all other variables unchanged, a doubling or quadrupling of repetition time resulted in a decrease in SPL of about 3 and 6 dB, respectively (Fig 3). The fast spin-echo sequence (200/14.3 [repetition time msec/echo time msec]) generated 88.1 dB (linear scale), while the same sequence with 1.040/14.3 produced 81.3 dB (Table 1). On the other hand, changing the echo time (Fig 4), flip angle (Fig 3), section thickness (Fig 5), and matrix



**Figure 3.** Bar graphs of multiplications of repetition time (*TR* multiplications) ( $n = 74$  measurements) and flip angle ( $n = 84$  measurements) depict median (height of box) and 25th and 75th quartiles of the differences between measured linear SPLs and their mean SPL for each sequence. SPL decreased with increasing repetition time. The flip angle did not influence the SPL.

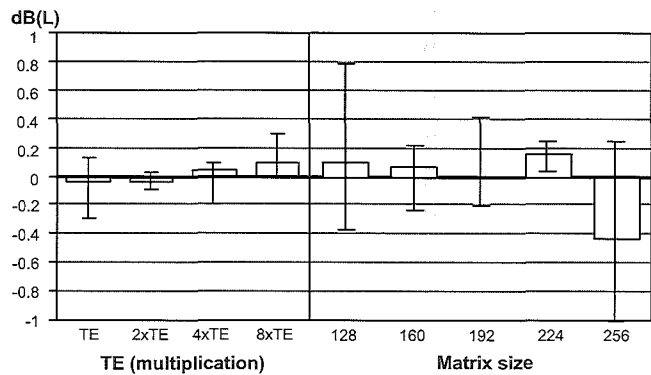


**Figure 4.** Bar graphs of multiplications of echo time (*TE* multiplications) ( $n = 32$  measurements) and matrix size (in pixels) ( $n = 50$  measurements) depict median (height of box) and 25th and 75th quartiles of the differences between measured SPLs and their mean SPL for each sequence. Neither echo time nor matrix size influence SPL.

(Fig 4) had no noticeable effect on SPL. On average, an increase in the field of view resulted in a small reduction in SPL of less than 1 dB (Fig 5). For sequences with very short repetition time ( $<15$  msec), as in fast spoiled GRE and fast GRE echo train, the SPL decreased remarkably when the field of view was enlarged (Table 1); an increase in repetition time resulted in a reduced influence of the field of view on the measured SPL. Variation of the orientation and positioning of the imaging plane seemed not to have an influence on SPL: axial, sagittal, and coronal planes had identical SPLs (Fig 2), as did imaging planes that were translated in cranial or caudal direction along the *z*-axis (not shown).

All but one sequence had a frequency distribution ranging from 1 to 3 kHz, with a distinctive peak around the 2-kHz octave band when measured inside the MR imager. The exception was the fast GRE echo train sequence, which had frequencies ranging from 2 to 5 kHz (Fig 6). The higher frequencies in the fast GRE echo train sequence are probably caused by the increased slew rates of the gradients (14). A comparison of measurements inside the magnet bore and at the 5-gauss line showed attenuation of frequencies higher than 2 kHz. Therefore, in the frequency distribution, maximum SPLs were between 800 and 1.600 Hz at the 5-gauss line. Because these frequencies are precisely within the frequency range that is important for speech (0.5–2.0 kHz) (9), hearing loss due to gradient noise exposure will primarily affect

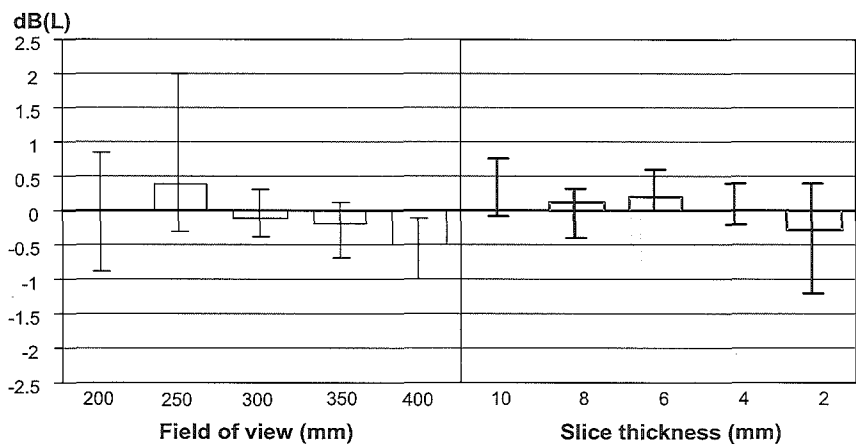


**Figure 5.** Bar graphs of field of view ( $n = 83$  measurements) and section thickness ( $n = 81$  measurements) depict median (height of box) and 25th and 75th quartiles of the differences between measured linear SPLs and their mean SPL for each sequence. The field of view and section thickness did not influence the SPL, although a decreasing trend in SPL with increasing field of view was seen.

the frequencies that are used in speech, followed by dissemination into neighbouring frequencies. Moreover, speech-to-noise ratios will drastically decrease during the interventional procedure and reduce the intelligibility of speech.

Analysis of the noise profile with an oscilloscope did not reveal impulse features but rather a quite complex disordered profile (not shown). This profile probably reflects the resonances generated in the coil supports (23).

### Discussion

Our measurements show that the acoustic burden on the interventional radiologist is of great magnitude.  $L(A)_{eq}$  values as high as 99 dB (A-weighted scale) were common with the MR imaging sequences likely to be used for real-time imaging

during interventions (fast GRE echo train and fast spoiled GRE). These values were measured at approximately 80 cm from the magnet bore entrance, but they will be higher whenever the operator works more closely to the patient in the magnet during the actual intervention. The results also show a small effect of a 2.7-dB reduction in SPL when a person is lying inside the magnet; this reduction is probably caused by attenuation of frequencies above 2 kHz (not shown). In previous experiments, authors found that, when measured inside the magnet bore, the SPLs are about 3 dB higher whenever a person was inside the magnet; a tentative explanation given by these authors is that in-phase reflections inside the magnet bore could cause a doubling of pressure and a subsequent increase in SPL (19).

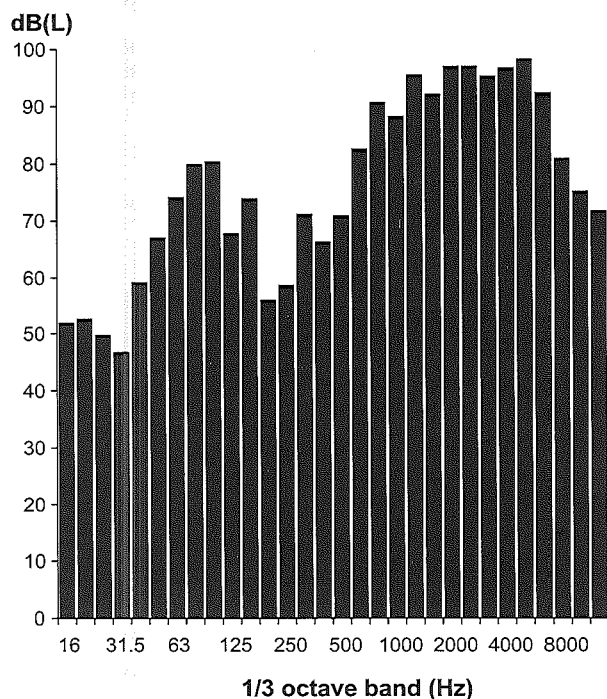


**Figure 6.** Frequency spectrum in 1/3-octave bands of a fast GRE echo train sequence (isocenter). High SPLs with frequencies between 1.000 and 5.000 Hz exceed ambient noise levels (y-axis) with frequencies around 100 Hz.

In additional analyses, the effects of various MR parameters on the acoustic noise were assessed. It appeared that repetition time was most relevant in this respect. The image acquisition time is covered by a series of repetition times, each with an equal number of gradient pulses. Therefore, as is expected, a doubling or quadrupling of the number of encoding steps per unit time (i.e., the amount of acoustic energy per unit time) caused by shortening repetition time, resulted in about a 3- and 6-dB increase in SPL, respectively. The field of view proved to be less important in this respect. The field of view is inversely proportional to the gradient strength of either the readout or phase-encoding gradient. However, the relationship between field of view and SPL resulted in a small audiotologically irrelevant (<1-dB) decrease in SPL, especially with the fast GRE echo train and fast spoiled GRE sequences.

In contrast to findings in previous reports (3), our results did not show an effect of changing echo time. An inverse influence of echo time on SPL has been suggested, but this suggestion was based on an observation of combined simultaneous lengthening

**TABLE 2**  
The 3-dB Trading Rule for Maximum  $L(A)_{eq8h}$

SPL	Exposure Time	Common Sound with Comparable SPL
90	8 h	Motorcycle at 10 m
93	4 h	
96	2 h	Subway (inside)
99	1 h	
102	30 min	Diesel truck at 10 m
105	15 min	
108	7 min	Power mower at 1 m

of both repetition time and echo time (3). However, the echo time changes the timing of the gradient pulses within repetition time and should theoretically not influence the SPL. In terms of sound production, the section-select gradient is less important than are the readout and phase-encoding gradients; therefore, section thickness plays a minor role in the total loudness of generated noise. Authors of previous reports, however, suggest that section thickness has more effect on SPL (3,5,6), probably owing to the larger section-select gradient amplitude relative to readout and phase-encoding gradient amplitudes.

Our results did not show an effect of changing the flip angle, which could be expected because radio-frequency pulses are short in contrast to the length of encoding gradients. In pulse sequences with multiple radio-frequency pulses (e.g., burst imaging), the flip angle may influence SPL to a greater extent.

Permanent hearing loss may occur as a result of chronic exposure to noise at levels greater than 80 dB (A-weighted scale) (22). Safety guidelines have been established for industry workers to limit the maximum (daily) noise exposure, on the basis of an 8-hour working day for 5 days a week (Appendix). The main rationale for these safety guidelines is to preserve hearing for speech discrimination (12,13,24).

According to the European Community guidelines, the maximum equivalent continuous A-weighted daily (8-hours) noise exposure,  $L(A)_{eq8h}$ , should not exceed 90 dB without hearing protection (25). The SPLs for all but one sequence were well above this permissible noise pressure level. A so-called 3-dB trading rule (or equal-energy rule) applies: an increase in SPL of 3 dB will halve the permitted exposure time (Table 2). Thus, noise exposure at 102 dB (A weighted scale) during an interventional MR procedure is permitted for only 30 minutes a day. In the United States, the Occupational Safety and Health Administration, or OSHA, has recommended an  $L(A)_{eq8h}$  value of 90 dB with a 5-dB exchange rate (24), although the National Institute for Occupational Safety and Health, or NIOSH, advises maximum  $L(A)_{eq8h}$  of 85 dB (A-weighted scale) with a 3-dB exchange rate (22).

Many different nongovernmental U.S. employment sectors have adopted the more prudent NIOSH guidelines. In European Community countries and the United States, hearing-protection equipment should be provided to employees exposed to  $L(A)_{eq8h}$  of greater than 85 dB (A-weighted scale). (In several European countries,  $L(A)_{eq8h}$  is set even lower, at 80 dB.) The use of such equipment is mandatory for  $L(A)_{eq8h}$  of greater than 90 dB (A-weighted scale) (1,11,24). Good hearing protection for SPLs as high as 110 dB

(A-weighted scale) can be achieved by using universal passive earplugs, custom molded earplugs, or earmuffs. Universal passive earplugs have increased attenuation for frequencies above 1 kHz (5,7), with a 35-dB decrease in air-conducted SPLs at a relevant frequency component of around 2 kHz for interventional MR imaging (10). The combination of passive earplugs and earmuffs could achieve greater than 40-dB sound attenuation for frequencies below 2 kHz (26). An issue that has been raised with passive hearing-protection aids is possible interference with communication (1,3, 11). As has been recently shown, however, passive hearing protection actually improves speech intelligibility for people with normal hearing in acoustic environmental noise (26). In contrast, passive hearing protection has a negative effect on speech intelligibility for hearing-impaired listeners (27). Hearing-protection aids, which encompass nonlinear acoustic filters or built-in noise reduction systems, may allow better communication while still providing adequate protection from acoustic noise. However, selective filtering or suppression may be complicated by similar frequency distributions of both speech and gradient noise. A 10-30-dB reduction in SPLs has been achieved with active noise reduction systems in MR imaging (2,7,28).

Ultimately, noise reduction should be achieved at the source (i.e., the design of the MR gradient system and supports) (7,10,20). Recently, more quiet MR systems have become commercially available with vacuum-enclosed gradient systems in addition to insulators (Excelart, Toshiba, Tochi-gi, Japan; Signa Twinspeed, GE Medical Systems). Vacuum enclosures provide greater than 15-dB noise reduction (for the Excelart system) (29). Additional noise reduction by means of vacuum enclosure may be restricted, however, by the requirement for an adequate gradient cooling system. The application of passive noise-reducing materials is also limited because it counterbalances the dimensions of the magnet bore.

There is a growing trend for use of MR systems with high field strength for interventional MR procedures. Such systems provide better homoge-

neity and stability of the main magnetic field, higher signal-to-noise ratios and resolution, and faster imaging (15,16). However, many interventional procedures are currently preformed with less than 1.0-T MR imagers. Therefore, our results may not be directly applied to interventional MR imaging at lower field strengths. Some conclusions, however, can be derived with cautious extrapolation of our results because there is a logarithmic relationship between field strength and SPL (29). Similar sequences at 1.5 and 0.7 T, for example, will generally differ by 6 dB (less noise at 0.7 T).

In conclusion, interventional MR imaging at 1.5 T is noisy and may be a likely cause of hearing loss for the interventional radiologist if no hearing protection is used during procedures. SPLs outside the magnet bore exceed the safety limits for chronic noise exposure during interventional MR imaging, from both the scientific (12,13) and judicial perspectives that are valid in the European Community (25) and United States (24). Interventional radiologists should be aware of this occupational hazard. They should use adequate hearing protection such as earplugs and earmuffs, because noise-induced hearing loss is virtually totally preventable by avoiding excessive SPLs. Likewise, hearing-protection equipment should be provided to the patient undergoing the interventional MR procedure. As with industrial workers, we believe interventional radiologists who are to perform interventional MR procedures on a regular basis should undergo baseline audiography. Active audiologic screening of interventional radiologists who perform interventional MR imaging at regular recurrent intervals may be considered.

### Appendix

This appendix provides details about the concept of cumulative operator exposure during an interventional MR procedure. To estimate hearing impairment and risk of hearing handicap as a result of exposure to noise, the noise exposure level is normalized to a nominal 8-hours working day,  $L(A)_{eq8h}$ , which can be calculated from SPL measurements and exposure time. Calculations of the daily

**TABLE A1**  
Median Permanent Noise-induced Threshold Shifts in Hearing Levels across Averaged Audiometric Test Frequencies of 1-4 kHz

$L(A)_{eq8h}$ (dB)	Exposure Time (years)			
	10	20	30	40
85	2	3	3	4
90	5	7	8	8
95	11	14	16	17
100	18	23	26	29

cumulative exposure are possible for interruptions and changes in SPL with use of the following functions (10,17,30).

$$L(A)_{eq8h} = L(A)_m - 10 \log \left( \frac{T_r}{T_m} \right) \quad (2)$$

is used to calculate daily noise exposure for one equivalent-continuous sound level  $L(A)_m$ , where  $T_r$  is 28,800 seconds (8 hours) and  $T_m$  is the duration of noise exposure in seconds.

$$L(A)_c = 10 \log \left( \sum_{i=1}^n 10^{0.1 \cdot L(A)_{eq8h,i}} \right) \quad (3)$$

is used to obtain a combined daily noise exposure  $L(A)_c$ , in which  $L(A)_{eq8h,i}$  equals n number of equivalent-continuous daily sound exposures,  $L(A)_{eq8h}$ .  $L(A)_c$  is used to estimate the risk of hearing loss (Table A1) and should not exceed 90 dB (A-weighted scale). The equal-energy rule can be deduced from reciprocal use of Equation (2): the halving of exposure time  $T_m$  results in a 3-dB ( $10 \cdot \log 2$ ) decrease in SPL.

### References

1. Brummett RE, Talbot JM, Charuhas P. Potential hearing loss resulting from MR imaging. *Radiology* 1988; 169:539-540.
2. Goldman AM, Gossman WE, Friedlander PC. Reduction of sound levels with antinose in MR imaging. *Radiology* 1989; 173:549-550.
3. Hurwitz R, Lane SR, Bell RA, Brant-Zawadzki MN. Acoustic analysis of gradient-coil noise in MR imaging. *Radiology* 1989; 173:545-548.
4. Shellock FG, Morisoli SM, Ziarati M. Measurement of acoustic noise during MR imaging: evaluation of six "worst-case" pulse sequences. *Radiology* 1994; 191:91-93.
5. McJury MJ. Acoustic noise levels generated during high field MR imaging. *Clin Radiol* 1995; 50:331-334.
6. Counter SA, Olofsson A, Grahn HF, Borg E. MRI acoustic noise: sound pressure and frequency analysis. *J Magn Reson Imaging* 1997; 7:606-611.

7. McJury M, Stewart RW, Crawford D, Toma E. The use of active noise control (ANC) to reduce acoustic noise generated during MRI scanning: some initial results. *Magn Reson Imaging* 1997; 15:319-322.
8. Shellock FG, Ziarati M, Atkinson D, Chen DY. Determination of gradient magnetic field-induced acoustic noise associated with the use of echo planar and threedimensional, fast spin echo techniques. *J Magn Reson Imaging* 1998; 8:1154-1157.
9. Ulmer JL, Biswal BB, Mark LP, et al. Acoustic echoplanar scanner noise and pure tone hearing thresholds: the effects of sequence repetition times and acoustic noise rates. *J Comput Assist Tomogr* 1998; 22:480-486.
10. Foster JR, Hall DA, Summerfield AQ, Palmer AR, Bowtell RW. Sound-level measurements and calculations of safe noise dosage during EPI at 3 T. *J Magn Reson Imaging* 2000; 12:157-163.
11. McJury M, Shellock FG. Auditory noise associated with MR procedures: a review. *J Magn Reson Imaging* 2000; 12:37-45.
12. Rosler G. Progression of hearing loss caused by occupational noise. *Scand Audiol* 1994; 23:13-37.
13. Prince MM, Stayner LT, Smith RJ, Gilbert SJ. A re-examination of risk estimates from the NIOSH Occupational Noise and Hearing Survey (ONHS). *J Acoust Soc Am* 1997; 101:950-963.
14. Hennel F, Girard F, Loenneker T. "Silent" MRI with soft gradient pulses. *Magn Reson Med* 1999; 42:6-10.
15. Hall WA, Liu H, Martin AJ, Pozza CH, Maxwell RE, Truwit CL. Safety, efficacy, and functionality of high-field strength interventional magnetic resonance imaging for neurosurgery. *Neurosurgery* 2000; 46:632-641.
16. Ladd ME, Quick HH, Debatin JF. Interventional MRA and intravascular imaging. *J Magn Reson Imaging* 2000; 12:534-546.
17. American National Standard S1.13-1995. Measurement of sound pressure levels in air. Melville, NY: Acoustical Society of America, 1995.
18. Moelker A, Vogel M, Ouhlous M, Lethimonnier F, Pattynama P. Operator exposure to acoustic noise in interventional MRI (abstr). In: Proceedings of the Ninth Meeting of the International Society for Magnetic Resonance in Medicine. Berkeley, Calif: International Society for Magnetic Resonance in Medicine, 2001; p2180.
19. Hedeem RA, Edelstein WA. Characterization and prediction of gradient acoustic noise in MR imagers. *Magn Reson Med* 1997; 37:7-10.
20. Wu Y, Chronik BA, Bowen C, Mechefske CK, Rutt BK. Gradient-induced acoustic and magnetic field fluctuations in a 4T whole-body MR imager. *Magn Reson Med* 2000; 44:532-536.
21. McKinnon GC. Ultrafast interleaved gradient-echo-planar imaging on a standard scanner. *Magn Reson Med* 1993; 30:609-616.
22. National Institute for Occupational Safety and Health (NIOSH). Criteria for a recommended standard, occupational noise exposure, revised criteria 1998. Publication No. 98-126. Washington, DC: U.S. Department of Health and Human Services, 1998.
23. Cho ZH, Park SH, Kim JH, et al. Analysis of acoustic noise in MRI. *Magn Reson Imaging* 1997; 15:815-822.
24. Occupational Safety and Health Administration (OSHA) FR-1910.95, 61 Federal Regulations 9227. Occupational noise exposure (Occupational Health and Environmental Control). Washington, DC: U.S. Department of Labor, Occupational Safety and Health Administration, 1996.
25. The Council of European Communities. Council Directive of 12 May 1986 on the protection of workers from the risks related to exposure to noise at work 1986; 86/188/EEC.
26. Abel SH, Spencer DL. Speech understanding in noise with earplugs and muffs in combination. *Appl Acoust* 1999; 57:61-68.
27. Abel SM, Spencer DL. Active noise reduction versus conventional hearing protection: relative benefits for normal-hearing and impaired listeners. *Scand Audiol* 1997; 26:155-167.
28. Chen CK, Chiueh TD, Chen JH. Active cancellation system of acoustic noise in MR imaging. *IEEE Trans Biomed Eng* 1999; 46:186-191.
29. Price DL, De Wilde JP, Papadaki AM, Curran JS, Kitney RI. Investigation of acoustic noise on 15 MRI scanners from 0.2 T to 3 T. *J Magn Reson Imaging* 2001; 13:288-293.
30. American National Standard S3.44-1996. Determination of occupational noise exposure and estimation of noise-induced hearing impairment. Melville, NY: Acoustical Society of America, 1996.





## Chapter 4

Adriaan Moelker, MD  
Ronald A.J.J. Maas, PhD  
Peter M.T. Pattynama, MD

### Index terms:

Magnetic resonance (MR),  
biological effects  
Magnetic resonance (MR),  
functional imaging  
Magnetic resonance (MR),  
guidance  
Magnetic resonance (MR),  
safety

Published online before print  
10.1148/radiol.2321030955

### Abbreviations:

FGRET = fast gradient-recalled echo  
train  
FSPGR = fast spoiled gradient-recalled  
echo  
STNR = speech-to-noise ratio

From the Departments of Radiology  
(A.M., P.M.T.P.) and Audiophysics  
(R.A.J.J.M.),  
Erasmus Medical Center Rotterdam,  
50 Dr. Molewaterplein, P.O. Box 1738,  
3000 DR Rotterdam, The Netherlands

Received June 18, 2003; revision  
requested August 13; final revision  
received November 4; accepted  
November 20

Address correspondence to A.M.  
(e-mail: a.moelker@erasmusmc.nl)

### Author contributions:

Guarantors of integrity of entire study,  
A.M., R.A.J.J.M., P.M.T.P.; study  
concepts and design, A.M., R.A.J.J.M.,  
P.M.T.P.; literature research, A.M.,  
R.A.J.J.M.; experimental studies, A.M.;  
data acquisition, A.M.; data analysis /  
interpretation, A.M., R.A.J.J.M.;  
statistical analysis, A.M.; manuscript  
preparation, definition of intellectual  
content, editing, revision/review, and  
final version approval, A.M., R.A.J.J.M.,  
P.M.T.P.

© RSNA, 2004

# Verbal Communication in MR Environments: Effect of MR System Acoustic Noise on Speech Understanding

**Purpose:** To assess the masking effect of magnetic resonance (MR)-related acoustic noise on speech understanding and the effect of passive hearing protection on speech understanding.

**Materials and methods:** Acoustic recordings were made at 1.5 Tesla at patient and operator (interventionalist in the MR suite) locations for relevant pulse sequences. In an audiologic laboratory, speech-to-noise ratios (STNRs) were determined, defined as the difference between the absolute sound pressure levels of MR noise and speech. The recorded noise of the MR sequences was played simultaneously with recorded sentences at various intensities, and 15 healthy volunteers (seven women, eight men; median age, 27 year) repeated these sentences as accurately as possible. The STNR that corresponded with a 50% correct repetition was used as measure for speech intelligibility. In addition, the effect of passive hearing protection on speech intelligibility was tested using an earplug model.

**Results:** Overall, speech understanding was reduced more at operator than at patient location. Most problematic were FGRET and spiral-k sequences. As the absolute sound pressure level of these was approximately 100dB(A) at patient location, the vocal effort needed to attain 50% intelligibility was shouting (>77dB(A)). At operator location, less effort was required because of the lower sound pressure levels of the MR noise. Fast spoiled gradient-recalled echo and echo-planar imaging sequences showed relatively favorable results with raised voice at operator location and loud speaking at patient location. Hearing protection slightly improved STNR.

**Conclusions:** At 1.5 Tesla, the level of MR noise requires that large vocal effort is used, at the operator and especially at the patient location. Depending on the specific MR sequence used, loud speaking or shouting is needed to achieve adequate bidirectional communication with the patient. The wearing of earplugs improves speech intelligibility.

© RSNA, 2004

Acoustic noise generated during magnetic resonance (MR) is an unwanted side effect (1) that may, it has been suggested, negatively affect verbal communication between patient and operator (the interventionalist in the MR suite) and between multiple operators (2). From a practical point of view, adequate speech understanding is a prerequisite in a number of circumstances. Firstly, speech intelligibility between operators is essential for MR-guided interventional procedures, particularly in potentially dangerous situations. Second, in functional MR imaging of the auditory brain, both the instruction and presentation of verbal stimuli to subjects require clear speech intelligibility (3). In addition, in audiologic experiments, the subject's verbal responses to language tasks should be accurately perceived by the operator (4). To our knowledge, the effects of MR acoustic noise in speech intelligibility in functional and interventional MR imaging have not yet been investigated.

Various techniques of acoustic noise reduction have been proposed and implemented in the MR environment with the goal of improving speech understanding (5). These techniques are used in an attempt to reduce MR acoustic noise while minimally affecting or enhancing speech understanding (6). One such technique is passive hearing protection (e.g., by means of earplugs or earmuffs), which substantially reduces acoustic noise levels (5). Only few investigators emphasized that passive hearing devices might be favorable for speech intelligibility in noisy environments (7,8). This assumption, to our knowledge, has also never been validated in the MR environment.

Thus, the purpose of our study was to assess the masking effect of MR-related acoustic noise and the effect of passive hearing protection on speech understanding.

## Materials and Methods

### Study design

In audiology, the measure commonly applied for speech intelligibility is the speech reception threshold, which is the speech-to-noise ratio (STNR) that corresponds with a 50% correct response of subjects to speech in noisy conditions (9). The speech reception threshold is a robust and validated measure of speech intelligibility and makes use of a large set of sentence material (9). In this study, the STNR was defined as the difference between the absolute sound pressure levels (the continuous sound pressure level expressed in decibels with an A-weighted scale [10]) of speech and masking MR noise; the STNR in white noise is typically -5 dB for listeners with normal hearing ability. A lower STNR (larger negative value) corresponds with better speech understanding. The speech level required for 50% intelligibility can be found by iteratively adjusting the level of speech (which is masked by fixed MR noise) and can be qualitatively classified in terms of normal, raised, loud or shouting voice (Table 1) (11). The MR imaging sequences tested were chosen on the basis of their potential relevance to vascular, interventional and functional MR ima-

**TABLE 1**  
Overall Sound Level of Speech at Each Vocal Effort at 1 meter Distance

Vocal Effort	SPL (dB)*
Normal	57
Raised	63
Loud	71
Shouted	77

Note.— Adapted, with permission, from reference 11. SPL = sound pressure level. \* A-weighted scale.

ging. Speech intelligibility was quantified for MR acoustic noise recorded both at the operator's location next to the MR system, and the patient's location. In addition, we assessed the effect of passive hearing protection on speech reception thresholds during MR imaging by using an earplug model.

### Volunteers and Speech Reception Threshold measurements

Our analysis was based on measurements obtained in 15 native Dutch-speaking volunteers (seven women, eight men; median age, 27 year) without hearing impairment. Although our institutional review board did not require its approval, informed consent was obtained from all participants. The acoustic exposures were well below daily permissible limits (12). Before the experiments were performed, a baseline audiogram (Clinical Audiometer OB822, Madsen Electronics, Bloomington, MN) was obtained in all subjects to exclude hearing impairment (13). In all the subjects, the minimum hearing levels of the pure-tone audiogram did not exceed 20 dB, at octave frequencies from 125 to 8,000 Hz; thus hearing levels were normal in all subjects.

As all subjects were native Dutch speakers, the measurements for speech reception threshold were obtained by using Dutch test sentences (14) that have previously been validated for phonetic balance (15,16). These sentences are short and redundant to enhance their intelligibility against distortions or interfering sounds to listeners with normal and impaired hearing (15). None of the subjects had heard or read the sentences before, and each sentence was presented only once to

each subject to avoid memory effects. In addition, the listeners participated in a brief speech reception threshold training session to reduce learning effects of speech intelligibility in noise.

In the adaptive procedure of measuring the speech reception threshold (9), pre-recorded MR noise was played out simultaneously with the test sentences through loudspeakers (Lab-501; Westra Electronic, Wertingen, Germany) in an anechoic environment (Industrial Acoustic Company, Bronx, NY) (15). The listeners were seated perpendicularly to a loudspeaker that reproduced the MR noise and facing another loudspeaker that provided the test sentences (13). This arrangement was considered a plausible representation of an interventional MR imaging procedure. After a sentence was presented, the subject responded by repeating it as accurate as possible. The first sentence (from a list of 13) was initially presented at such low STNR that it was unlikely to be intelligible to the subject. This sentence was then presented repeatedly, at increasing sound level (in 4-dB steps), until the listener could reproduce the sentence correctly. This method provided a quick convergence to the 50% speech intelligibility threshold. The remaining 12 sentences were presented only once, at a sound speech level that depended on the subject's response to the previous sentence (i.e., the level was 2 dB higher after an incorrect response and 2 dB lower after correct repetition of the complete sentence). By averaging the STNR values for the last 10 sentences, a 50% sentence intelligibility threshold was obtained and initialization effects were eliminated. Because little deviation of STNRs between sentence lists has been reported previously (9,15), an average of three sentence lists was taken as a speech reception threshold value for that particular condition.

A computer equipped with Matlab (R13; The MathWorks, Novi, Mich) performed STNR adjustments with custom-written software and delivered the MR noise and sentences to the active loudspeaker systems. The speech reception threshold meas-

**TABLE 2**  
Parameters and Acoustic Characteristics for Each Pulse Sequence

Sequence	Imaging parameters			Operator		Patient		Qualitative Description	Passive Attenuation (dB)*
	Repetition Time (msec)	Echo Time (msec)	Matrix	SPL (dB)	Peak Frequency (Hz)	SPL (dB)	Peak Frequency (Hz)		
FGRET	9	1.7	128x128	93	1.132	NA	NA	Harmonics of 125 Hz	27
	40	1.7	128x128	87	1.158	100 †	2.094	Harmonics of 25 Hz	26 (31)
FSPGR	4.4	2.0	256x192	93	908	NA	NA	Harmonics of 227 Hz	25
	35	2.0	256x192	84	1.164	93	994	Harmonics of 30 Hz	25 (28)
Spiral-k	18	2.8	2048x8	97	784	NA	NA	Harmonics of 55 Hz	24
	36	2.8	2048x8	94	1.170	100 ‡	2.069	Harmonics of 28 Hz	24 (27)
Fast spin echo	40	17	256x256	87	774	97	1.000	Harmonics of 25 Hz	25 (27)
Echo-planar	240	30	128x128	NA	NA	100	2.740	Tonal 500, 1,640, 2,740 Hz	(30)

Note.—NA = not applicable; Operator = tested at operator location; Patient = tested at patient location; SPL = sound pressure level, measured in decibels on an A-weighted scale.  
 \* Attenuation caused by filtering that simulates passive hearing protection. Data obtained at operator location; data in parentheses obtained at patient location.  
 † repetition time increased to 50 msec (for safety).  
 ‡ repetition time increased to 45 msec (for safety).

urements were automatically logged and stored for analyses.

*MR equipment and acoustic noise measurements*

The acoustic data were obtained with a 1.5-T cardiovascular MR scanner (Signa CV/i, GE Medical Systems, Milwaukee, Wis) operating under LX8.4 software with gradients of up to 40mTm<sup>-1</sup> slew rates of 150Tm<sup>-1</sup>s<sup>-1</sup>, by using an integrated quadrature-driven transceiver radio-frequency body coil. The pulse sequences tested were as follows: echo-planar, fast spoiled gradient recalled echo (FSPGR), fast gradient-recalled echo train (FGRET, hybrid echo-planar and FSPGR sequence), spiral trajectory k-space, and conventional fast spin-echo imaging.

FSPGR, FGRET, and spiral-k sequences are especially suitable for real-time imaging and were therefore considered most relevant to interventional MR imaging (17). Echo-planar is the most extensively employed pulse sequence in functional MR imaging and was therefore not assessed at the operator location (18). The acoustic characteristics for all pulse sequences are given in table 2. The imaging parameters, in particular the repetition time, were chosen to test pulse sequences as worst-case for clinical imaging (19). The bandwidth was similar for all pulse sequences tested (100-125 kHz), with the exception of the fast spin-echo sequence (62 kHz). For safety reasons, however, all pulse sequences, especially those recorded

in the magnet bore, were limited to a maximum sound intensity of approximately 100 dB (A-weighted scale) (20) by omitting pulse sequences with extremely short repetition time or by increasing repetition time slightly (FGRET and spiral k-space).

The sound levels of the imaging pulse sequences and their acoustic waveforms were recorded by using a digital sound analyzer (Investigator 2260; Brüel & Kjær, Nærum, Denmark) connected to a computer that was equipped with a sound card (Audio DSP24; Hoontech, Bucheon City, Korea) (21). To quantify the speech intelligibility at the operator position, the acoustic recordings were made with a microphone (type 4189; Brüel & Kjær) placed at a distance of 0.8 meter from the MR imaging entrance and at a height of 1.70 meter, close to the MR imaging table, which is a plausible location for the ear of the interventional radiologist. Also, similar recordings were made with the microphone positioned inside the magnet bore (at the isocenter), deployed for quantifying speech intelligibility at the location of the patient's ear.

*Calibration and analysis*

The digital sound analyzer was calibrated with a sound calibrator (type 4231; Brüel & Kjær) at regular intervals and showed an accuracy of better than 0.1 dB. The sound card setup for recording the acoustic MR noise was calibrated by matching sound card and sound analyzer at all

relevant frequencies. The sound pressure level calibration for delivered speech and MR noise in the anechoic room was performed as follows: in the MR suite, the continuous-equivalent sound level and waveform of an FGRET pulse sequence were recorded with the sound analyzer at the operator location. Next, the waveform was replayed in the anechoic room while the sound intensity was adjusted to its original level as measured in the MR environment. The sound pressure levels of all other pulse sequences were registered in the same experimental setting and could be easily compared to this reference level and calibrated accordingly.

Since human hearing is less sensitive to frequencies below 1 kHz, a so-called A-weighted filter was applied to both speech and MR noise waveforms (expressed as decibels with an A-weighted scale) before calculating the STNR (22). Also, a level threshold method was required for suppression of the silent periods in the speech signals and MR noise (23). This was done by filtering the waveforms with a low-pass filter (47 Hz) to obtain an intensity envelope of speech and MR noise. The resultant waveform was thresholded (14 dB below its root-mean-square value) to eliminate the silent periods and its resulting sound pressure level was finally used for determining the actual STNR (23).

In the speech reception threshold procedure, speech was presented at levels ranging from approximately 50

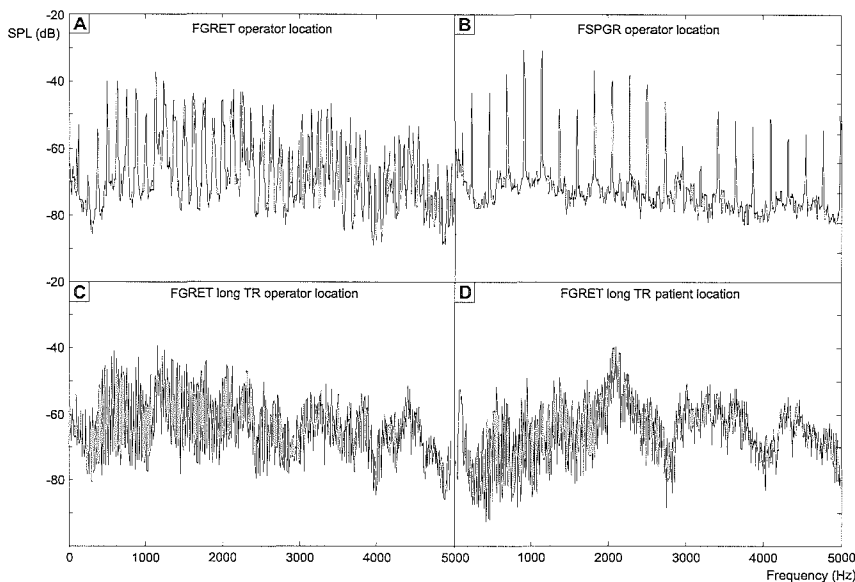


**Figure 1.** Acoustic noise spectra of FGRET and FSPGR at operator location with short repetition time (A,B) and of FGRET at operator location and patient location with long repetition time (C,D). In A and B, the harmonics are clearly distinguishable, whereas in C and D, the harmonics are too closely spaced, giving rise to a broadband noise spectrum. Note the peak frequency at approximately 2 kHz in D. FFT-size: 4.096 points; filter: Hamming (15). SPL = sound pressure level.

to 90 dB (A-weighted scale), depending on the required speech reception threshold and the absolute sound pressure level of the pulse sequence investigated. In other words: the speech level ranged from a normal conversational level to extremely loud shouting. With increasing vocal effort, however, the frequency spectrum of speech changes; the level of frequencies around 2 kHz is relatively raised (11). This was simulated by digitally filtering the sentences in the frequency domain before presentation, in accordance with internationally standardized values (11).

#### Passive hearing protection

In addition to the 12 different experiment conditions already described (Table 2), additional speech reception threshold measurements were obtained in all 15 subjects by using digital filtering of speech and MR noise that represented the wearing of passive hearing protection. Toward this end, the insertion loss of earplugs as inserted by untrained users was adapted from a recent publication (24). The insertion loss of earplugs is comparable with that of earmuffs, which are more frequently used in functional MR imaging (5). The rationale for using digital filtering rather than real passive hearing protection is the rela-

tively large difference between auditory attenuation with earplugs in subjects who have been taught proper insertion and that in untrained subjects (24). Recall that the computed STNR equals the difference between the sound levels of MR noise and speech (i.e., the difference between the sound levels measured in the MR environment). The presented speech level is the unfiltered speech level produced by, for example, the operator. The STNR, based on sound pressure levels of MR noise and speech after the filtering procedure, represent the performance of the subject's hearing rather than the required speech level during MR imaging.

#### Statistical analysis

Measured values for speech intelligibility at the operator and patient locations (as an average, as well as for each type of filtering) were compared and tested for statistically significant differences by using pulse sequences with imaging parameters that were similar for operator and patient locations (FSPGR, FGRET, spiral k-space and fast spin-echo with long repetition time) (14). Also, for the filtered and unfiltered measurement conditions, the speech intelligibility (as an average and for each recording location) was tested for statistically

significant differences. Toward this end, Student t-tests were performed by using a statistical software package (SPSS version 11.0 for Windows; SPSS, Chicago, Ill). A P-value of .05 (with CIs) was considered to denote a statistically significant difference.

## Results

### Characteristics of MR acoustic noise

The acoustic noise levels in the isocenter of the MR imager were, on average, 10 dB higher than those measured at the entrance of the MR system; this is consistent with previously reported values (25). For all sequences except FGRET and FSPGR with short repetition time, the MR noise had a broadband frequency distribution that peaked between 1 and 3 kHz (Fig 1). This was a result of the typically low fundamental frequency (equal to the inverse of repetition time) and the associated higher harmonics that were, consequently, closely spaced in the frequency domain. As the fundamental frequency for FGRET and FSPGR with short repetition time was relatively high, these pulse sequences showed distinct frequency components (Fig 1). Also, the frequency distribution of the pulse sequences differed with respect to the location at which they were recorded; high frequencies (up to 3 kHz) were recorded at the isocenter of the imager, while lower frequencies (up to 1 kHz) were recorded near the imager. As an example, FGRET noise peaked at 1.158 Hz whenever recorded besides the MR imager, whereas for a similar pulse sequence recorded in the magnet bore, the most intense frequencies were near 2 kHz (Fig 1C,D).

Passive hearing protection greatly reduced MR noise (Table 3), by on average 25 dB at the operator location, and showed better reduction for imaging sequences recorded at the isocenter (noise reduced by 29 dB). This was evidently a result of the low-pass characteristics of passive filtering in concurrence with higher frequencies generated in the magnet bore (7).

**TABLE 3**  
**Mean STNR Values Required for 50% Speech Intelligibility (Speech Reception Threshold)**

Sequence	Repetition Time (msec)	Operator Location		Patient Location	
		Unfiltered STNR (dB)	Filtered STNR (dB)	Unfiltered STNR (dB)	Filtered STNR (dB)
FGRET	9	-11.8 (81.2)	-16.6 (76.4)	NA	NA
	40	-14.1 (72.9)	-13.5 (73.5)	-23.3 (76.7)*	-28.0 (72.0)*
FSPGR	4.4	-20.3 (72.7)	-24.6 (68.4)	NA	NA
	35	-20.9 (63.1)	-18.9 (65.1)	-16.9 (76.1)	-18.5 (74.5)
Spiral-k space	18	-16.2 (80.8)	-20.3 (76.7)	NA	NA
	36	-19.1 (74.9)	-21.0 (73.0)	-19.6 (80.4)†	-23.0 (77.0)†
Fast spin echo	40	-18.5 (68.5)	-18.9 (68.1)	-16.6 (80.4)	-19.4 (77.6)
Echo planar	240	NA	NA	-26.3 (73.7)	-29.6 (70.4)

Note.— A lower STNR (larger negative number) indicates a better level of speech intelligibility. Filtered STNR indicates results with passive hearing protection. Data in parentheses are mean speech levels, measured in decibels on A-weighted scale. NA = not applicable.

\* repetition time increased to 50 msec (for safety).

† repetition time increased to 45 msec (for safety).

#### *Speech intelligibility at operator location*

Table 3 shows both the speech reception thresholds and sound pressure levels of the speech. Of the pulse sequences recorded at the operator location, the most problematic were FGRET, with a STNR of -11.8 dB, and spiral k-space sequences, with and STNR of -16.2 dB. FSPGR and fast spin-echo showed more favorable results, with speech reception thresholds ranging from -20.3 to -20.9 dB STNR and -18.5 dB STNR, respectively. As the absolute sound levels of FGRET and spiral k-space sequences were up to 97 dB (A-weighted scale), the 50 % intelligibility threshold required speech levels that ranged from 72.9 to 81.2 dB (A-weighted scale). In other words, the vocal effort with which one needed to speak to attain 50% intelligibility was loud speaking, which escalated to extremely loud shout during imaging with worst-case imaging parameters (short repetition time). On the other hand, both the advantageous speech reception threshold and low absolute sound pressure levels of fast spin-echo and FSPGR allowed for ambient communication with only mildly raised vocal effort.

#### *Speech intelligibility at patient location*

It can be appreciated from Table 3 that the speech reception threshold results determined at patient location were opposite to those found at operator location: FGRET and spiral

k-space were most favorable (-23.3 and -19.6 dB STNR, respectively), whereas FSPGR and fast spin-echo substantially reduced speech understanding (-16.9 and -16.6 dB STNR, respectively). In terms of vocal effort, the absolute speech levels ranged from 73.7 to 80.4 dB (A-weighted scale), corresponding to loud speaking and shouting. Despite the intense masking level of echo-planar imaging (100 dB [A-weighted scale]), the speech level required for 50% intelligibility was only 73.7 dB on the A-weighted scale (loud speaking). Note that these pulse sequences did not represent worst-case scenarios, as they were restricted to a maximum sound pressure level for safety reasons. Speech levels would have been higher if worst-case imaging parameters were used.

For similar pulse sequences, speech understanding proved significantly better at the isocenter of the imager with regard to the speech reception threshold (2.5 dB  $\Delta$ STNR) on average, Table 4), but more advantageous at operator location with regard to the absolute speech levels (-7.0 dB  $\Delta$ STNR) on average, Table 4).

#### *Effect of passive hearing protection on speech intelligibility*

The effect of passive hearing protection on speech understanding with MR noise was assessed by using sound filters that simulated the effect of earplugs. Table 4 shows the improvement in speech reception threshold with hearing protection at

operator and patient locations for similar imaging conditions. The average increase was 1.5 dB, which was predominantly attributed to pulse sequences recorded in the imager bore. Although the speech reception threshold did increase considerably at operator location with earplug simulation, this finding was exclusive to worst-case pulse sequences (high sound pressure level,  $\Delta$ STNR of 4.4 dB). At relatively low sound pressure levels, passive hearing protection had only insignificant adverse effects on intelligibility (-0.2 dB  $\Delta$ STNR, filtered minus unfiltered STNR averaged for FSPGR, spiral k-space, FGRET and fast spin-echo sequences). The beneficial effect of passive (low-pass) protection on intelligibility could be partially explained by the different frequency distributions of speech and MR noise. In particular, at the isocenter, the higher frequencies in the MR noise resulted in greater sound attenuation in comparison with that of spoken sentences. Consequently, computing of the subjective STNRs (i.e., as perceived by the listener after filtering) almost completely compensated for the improvement in STNR (-0.2 dB  $\Delta$ STNR). In contrast, at operator location, earplug filtering proved substantially beneficial with worst-case pulse sequences (subjective improvement 3.4 dB  $\Delta$ STNR, filtered minus unfiltered STNR averaged for FSPGR, spiral k-space, and FGRET sequences), but intelligibility deteriorated during pulse sequences with long repetition time (-2.2 dB  $\Delta$ STNR, filtered minus unfiltered STNR averaged for FSPGR, spiral k-space, and FGRET sequences).

#### **Discussion**

Our measurements show that depending on the specific MR imaging sequence used, speech understanding is greatly reduced at both operator and patient locations at 1.5 T. Speech levels of up to 80 dB (A-weighted scale) were common with use of the MR imaging sequences most likely to be used for interventional MR imaging (FGRET, spiral k-space, and FSPGR). In other words, 50% speech understanding can

**TABLE 4**  
Average Differences in STNR and Sound Pressure Level for Parameters Tested with Similar Pulse Sequences

Parameter	Difference	
	$\Delta$ STNR	$\Delta$ SPL
Patient versus operator		
Overall	2.5 (2.0-3.1)	7.0 (6.4-7.5)
Unfiltered	0.8*	8.6
Filtered	4.0	5.5
Filtered versus unfiltered		
Averaged	1.5 (1.2-1.9)	1.5 (1.2-1.9)
Patient location	3.1	3.1
Operator location	-0.1*	-0.1*
Operator location high SPL	4.4	4.4
Operator location low SPL	-0.2*	-0.2*

Note.— Data in parentheses are 95% CIs. SPL = sound pressure level. STNR = measured in decibels; sound pressure level measured in decibels on an A-weighted scale.

\* Difference not significant ( $P > .05$ )

be attained on the condition that the voice level is raised to extremely loud or shouting levels. Although speech levels could be as low as 63.1 dB (A-weighted scale), especially for the less demanding pulse sequences, and seem to approach conversational levels (11), the real intelligibility level in clinical practice is expected to be worse and should be placed in proper context.

First, the experiment setup was designed so that the interfering MR noise was presented towards the listener's right ear. Such an arrangement improves speech intelligibility by 10 dB compared with that at binaural presentation, during which MR noise is decreased due to head shadow (decrease of 3 dB) and differences in arrival time of MR noise and speech (decrease of 7 dB) (13,26), and so speech levels at the patient location were underestimated. Second, the standard speech reception threshold at 50% intelligibility is too low for adequate verbal communication (16,27,28). A more relevant measure of communication in a noisy environment is the range of STNRs for which intelligibility is about 80% (27). Fortunately, near the 50% speech reception threshold, a 1-dB increase in STNR results in a 20% higher intelligibility score (9,26,29). This implies that, for satisfying communication, the speech level should be raised by 1 to 2 dB. Finally, our data represent speech levels as measured at the subject's ear; in the actual MR environment, however, the spatial distance between speaker and

listener would have to be compensated for by further raising of the speaker's voice.

Speech reception thresholds differed considerably between the various imaging sequences and recording locations, ranging from -11.8 to -26.3 dB STNR. One tentative explanation is in the dissimilarities of the frequency spectra of these sequences. In conventional audiometry, the test for speech reception threshold is conducted with modified white masking noise that has a frequency spectrum similar to that of normal speech (15). Speech is consequently masked at its greatest extent with a speech reception threshold of about -5 dB (15). Analogously, we can appreciate, for example, that FSPGR noise masks speech only at specific frequencies (-20.3 dB STNR), whereas FGRET has a broadband masking profile that resembles that of speech (-11.8 dB STNR). In addition, the absolute sound pressure levels of the MR noise might have influenced speech intelligibility. Although it is widely believed that the speech reception threshold depends only on the STNR whenever the absolute noise level is less than 120 dB (A-weighted scale) (26), some level-dependent effect has recently been described by Van Wijngaarden and Steeneken (30). A theoretical reason was that auditory masking at high levels is different from masking at low levels (less masking) (8,30). Remarkably, this relation was stronger for low-frequency noise (so-called upward

spread of masking), in accordance with our finding that this level-dependent effect was present particularly at the operator location (30).

Disturbances in speech understanding are critical in potentially dangerous situations such as the MR environment. It is evident that clear bidirectional speech understanding between cooperating operators is essential during interventional procedures, low sound levels are required. Most MR systems have a pause capability, but this halts the image acquisition. Interventional procedures do not continuously require full system capabilities; this allows for intervals with less demanding gradient pulses during imaging. To this end, we recently developed a tool, to be located in the MR room, that hooks up with the imager interface and remotely lowers the gradient performance (and acoustic noise level) without ceasing imaging (31). Furthermore, verbal communication is critical in emergent situations (related to the MR procedure or MR hardware), and the exchange of information regarding the type and extent of the emergent condition must be adequate. MR-related acoustic noise may, therefore, pose an occupational hazard, particularly to interventionalists. An emergency button is generally present, but should be used with care, especially in super-conductive systems, because it initiates quenching. In the United States, the Occupational Safety and Health Administration of the department of Labor has advised that industrial environments with high ambient noise levels must be equipped with a dedicated voice alarm system (32). The power of such a system should be at least 15 dB above the speech reception threshold, but a range of 15-25 dB is more desirable. This equals a speech level of approximately 105 dB (A-weighted scale) in the MR environment.

Echo-planer is the most widely used pulse sequence in functional MR imaging (18). Although the lowest speech intelligibility scores were noted for echo-planar imaging (-29.6 dB STNR), the intense sound levels generated during the imaging process may interfere with functional MR



imaging examinations (33). This is problematic in studies of the auditory system, specifically in studies in which speech perception is being investigated (4). Furthermore, results in some reports have demonstrated that the MR noise impairs the mapping of brain functions by evoking undesirable blood oxygen level-dependent, or BOLD, signals (34,35). Fortunately, unilateral communication is sufficient during most auditory functional MR imaging examinations that include an auditory component, because responses by subjects are often not required or are expressed through non-verbal communication (e.g., by pressing a button) (4). This allows for the application of abundant acoustic noise insulators (e.g., earplugs, earmuffs, cushions) with concurrent delivery of speech signals either via the audio system with compensation for the passive attenuation (5) or via pneumatic headsets with integrated probe tubes. The latter reduce MR noise levels without comprising speech levels.

A limitation of our study might be in the magnetic field strength of the MR system used. Many interventional procedures are currently performed at less than 1.0 T, and the absolute speech levels measured for our 1.5 T MR system may not be directly applicable to systems with lower field strengths (36). Also, there is a growing trend toward use of MR systems with field strengths greater than 1.5 T in functional MR imaging. Such systems provide better homogeneity and stability of the main magnetic field, higher signal-to-noise ratios and spatial resolution, and faster imaging (37). As a relative measure, however, the STNR values are likely to be similar at field strengths lower and higher than 1.5 T, because speech intelligibility is only slightly dependent on the sound pressure level of the masking MR imager noise. Absolute speech levels can therefore be calculated by taking the absolute sound levels of the particular MR system into account. In addition, conclusions about absolute sound levels may be derived from cautious extrapolation of MR sound levels based on the logarithmic relationship between magnetic field

strength and sound pressure level (38).

In contrast to what is generally believed (1), we found a positive and distinct gain in speech intelligibility with use of simulated earplugs for MR noise. This advantageous effect was negligible or even negative at low MR noise levels. On the other hand, a typical attenuation of -27 dB with passive hearing protection is known to largely reduce the MR-related risks of hearing damage (by approximately  $10^3$  times) (25,39). We deem this risk reduction more relevant than the minor adverse effect on speech intelligibility and, therefore, recommend the usage of earplugs.

A final consideration is the possibility of combined use of passive and active noise reduction, in which additional sounds interfere with the MR noise according the superposition principle (6). From the noise reduction perspective, this is beneficial, as active noise reduction is best suited for low-frequency noise (<1 kHz) (8), whereas passive devices progressively attenuate noise at frequencies above 1 kHz (5). The effect of combining active noise reduction with passive aids for speech understanding is unclear, but evidence suggests a small improvement in intelligibility for subjects with normal hearing (8). A more viable concept, not currently applied in MR imaging, may be in the capture of the voice with a highly directional microphone located close to the speaker's mouth, the amplification of the sound, and the projection of the sound through headphones or a loudspeaker. Such a setup would be expected to result in a better STNR and, potentially, better speech understanding.

#### References

1. McJury M, Shellock FG. Auditory noise associated with MR procedures: a review. *J Magn Reson Imaging* 2000; 12:37-45.
2. Edelstein WA, Hedeen RA, Mallozzi RP, El-Hamamsy SA, Ackermann RA, Havens TJ. Making MRI quieter. *Magn Reson Imaging* 2002; 20:155-163.
3. Shah NJ, Steinhoff S, Mirzazade S, et al. The effect of sequence repeat time on auditory cortex stimulation during phonetic discrimination. *Neuroimage* 2000; 12:100-108.
4. Mohr CM, King WM, Freeman AJ, Briggs RW, Leonard CM. Influence of speech

stimuli intensity on the activation of auditory cortex investigated with functional magnetic resonance imaging. *J Acoust Soc Am* 1999; 105:2738-2745.

5. Ravicz ME, Melcher JR. Isolating the auditory system from acoustic noise during functional magnetic resonance imaging: examination of noise conduction through the ear canal, head, and body. *J Acoust Soc Am* 2001; 109:216-231.
6. Chen CK, Chiueh TD, Chen JH. Active cancellation system of acoustic noise in MR imaging. *IEEE Trans Biomed Eng* 1999; 46:186-191.
7. Abel SM, Spencer DL. Speech understanding in noise with earplugs and muffs in combination. *Appl Acoust* 1999; 57:61-68.
8. Abel SM, Spencer DL. Active noise reduction versus conventional hearing protection. Relative benefits for normal-hearing and impaired listeners. *Scand Audiol* 1997; 26:155-167.
9. Plomp R, Mimpen AM. Improving the reliability of testing the speech reception threshold for sentences. *Audiology* 1979; 18:43-52.
10. American National Standard S1.13-1995: Measurement of sound pressure levels in air. Melville, NY: Acoustical Society of America, 1995.
11. American National Standard S3.79-1993: American national standard methods for the calculation of the speech intelligibility index. Melville, NY: Acoustical Society of America, 1993.
12. National Institute for Occupational Safety and Health (NIOSH). Criteria for a recommended standard: occupational noise exposure - revised criteria, 1998. Publication No. 98-126. Washington, DC: U.S. Department of Health and Human Services, 1998.
13. Festen JM, Plomp R. Speech-reception threshold in noise with one and two hearing aids. *J Acoust Soc Am* 1986; 79:465-471.
14. Van Wijngaarden SJ, Steeneken HJ, Houtgast T. Quantifying the intelligibility of speech in noise for non-native listeners. *J Acoust Soc Am* 2002; 111:1906-1916.
15. Versfeld NJ, Daalder L, Festen JM, Houtgast T. Method for the selection of sentence materials for efficient measurement of the speech reception threshold. *J Acoust Soc Am* 2000; 107:1671-1684.
16. Van Wijngaarden SJ, Steeneken HJ, Houtgast T. Quantifying the intelligibility of speech in noise for non-native talkers. *J Acoust Soc Am* 2002; 112:3004-3013.
17. Moelker A, Vogel MW, Pattynama PM. Efficacy of passive acoustic screening: implications for the design of imager and MR-suite. *J Magn Reson Imaging* 2003; 17:270-275.
18. Parrish T. Functional MR imaging. *Magn Reson Imaging Clin N Am* 1999; 7:765-782.
19. Shellock FG, Morisoli SM, Ziarati M. Measurement of acoustic noise during MR imaging: evaluation of six "worst-case" pulse sequences. *Radiology* 1994; 191:91-93.
20. Guidance for the submission of premarket notifications for magnetic resonance

- diagnostic devices. Washington, DC: U.S. Department of Health and Human Services, Food and Drug Administration, Center for Devices and Radiological Health, 1998.
21. Counter SA, Olofsson A, Borg E, Bjelke B, Haggstrom A, Grahn HF. Analysis of magnetic resonance imaging acoustic noise generated by a 4.7 T experimental system. *Acta Otolaryngol* 2000; 120:739-743.
  22. American National Standard S3.44-1996: Determination of occupational noise exposure and estimation of noise-induced hearing impairment. Melville, NY: Acoustical Society of America, 1996.
  23. Steeneken HJM, Houtgast T. Basics of the STI measuring method. In: Van Wijngaarden SJ, ed. Past, present and future of the Speech Transmission Index. Soesterberg, the Netherlands: TNO Human Factors, 2002; 13-43.
  24. Toivonen M, Paakkonen R, Savolainen S, Lehtomaki K. Noise attenuation and proper insertion of earplugs into ear canals. *Ann Occup Hyg* 2002; 46:527-530.
  25. Moelker A, Maas RA, Lethimonnier F, Pattynama PM. Interventional MR Imaging at 1.5 T: Quantification of Sound Exposure. *Radiology* 2002; 224:889-895.
  26. Plomp R. A signal-to-noise ratio model for the speech-reception threshold of the hearing impaired. *J Speech Hear Res* 1986; 29:146-154.
  27. Brand T, Kollmeier B. Efficient adaptive procedures for threshold and concurrent slope estimates for psychophysics and speech intelligibility tests. *J Acoust Soc Am* 2002; 111:2801-2810.
  28. Saunders GH, Cienkowski KM. A test to measure subjective and objective speech intelligibility. *J Am Acad Audiol* 2002; 13:38-49.
  29. Plomp R, Mimpfen AM. Speech-reception threshold for sentences as a function of age and noise level. *J Acoust Soc Am* 1979; 66:1333-1342.
  30. Van Wijngaarden SJ, Steeneken HJM. Objective prediction of speech intelligibility at high ambient noise levels using the speech transmission index. Presented at the 6th European conference on speech communication and technology (Eurospeech 1999), Budapest, Hungary, 1999.
  31. Moelker A, Vogel MW, Pattynama PM. Real-Time Modulation of Acoustic Gradient Noise in Interventional MR Imaging. *Concepts in Magnetic Resonance Part B, Vol. 20B(1)* 2004;34-39.
  32. Occupational Safety and Health Administration (OSHA) CFR-1910.165, Federal Regulations. Employee alarm systems (Occupational Safety and Health Standards). Washington, DC: U.S. Department of Labor, Occupational Safety and Health Administration, 1981.
  33. Amaro E, Jr., Williams SC, Shergill SS, et al. Acoustic noise and functional magnetic resonance imaging: Current strategies and future prospects. *J Magn Reson Imaging* 2002; 16:497-510.
  34. Bandettini PA, Jesmanowicz A, Van Kylen J, Birm RM, Hyde JS. Functional MRI of brain activation induced by scanner acoustic noise. *Magn Reson Med* 1998; 39:410-416.
  35. Cho ZH, Chung SC, Lim DW, Wong EK. Effects of the acoustic noise of the gradient systems on fMRI: a study on auditory, motor, and visual cortices. *Magn Reson Med* 1998; 39:331-335.
  36. Bartels LW, Bakker CJ. Endovascular interventional magnetic resonance imaging. *Phys Med Biol* 2003; 48:R37-64.
  37. Campeau NG, Huston J, 3rd, Bernstein MA, Lin C, Gibbs GF. Magnetic resonance angiography at 3.0 Tesla: initial clinical experience. *Top Magn Reson Imaging* 2001; 12:183-204.
  38. Moelker A, Wielopolski PA, Pattynama PM. Relationship between magnetic field strength and magnetic-resonance-related acoustic noise levels. *Magma* 2003; 16:52-55.
  39. Foster JR, Hall DA, Summerfield AQ, Palmer AR, Bowtell RW. Sound-level measurements and calculations of safe noise dosage during EPI at 3 T. *J Magn Reson Imaging* 2000; 12:157-163.



## Chapter 5

# Acoustic Noise Concerns in Functional Magnetic Resonance Imaging

Adriaan Moelker\* and Peter M.T. Pattynama

*Department of Radiology, Erasmus Medical Center Rotterdam, Rotterdam, The Netherlands*

---

**Abstract:** Magnetic resonance (MR) acoustic scanner noise may negatively affect the performance of functional magnetic resonance imaging (fMRI), a problem that worsens at the higher field strengths proposed to enhance fMRI. We present an overview of the current knowledge on the effects of confounding acoustic MR noise in fMRI experiments. The principles and effectiveness of various methods to reduce acoustic noise in fMRI are discussed, practical considerations are addressed and recommendations are made.

*Hum. Brain Mapp. 20:123-141, 2003. © 2003 Wiley-Liss, Inc.*

**Keywords:** MRI; fMRI; EPI; acoustic noise; SPL; acoustic noise reduction

---

### INTRODUCTION

Within the last decade, functional magnetic resonance imaging (fMRI) has evolved into a widely used technique for functional brain imaging [Belliveau et al., 1991] that provides valuable insights into sensory, motor, and cognitive brain processing [Cacace et al., 2000]. Briefly, fMRI is based on quantifying the increase in regional cerebral blood flow as a response to activation of brain regions [Ogawa et al., 1993], which can be made visible by proportionate changes in the blood oxygen level dependent (BOLD) MR contrast [Ogawa et al., 1990]. The MR signal changes are generally small, in the range of 5-7% at 1.5 T [Bernal and Altman, 2001], and careful composition of stimuli and tasks for evoking brain activation and their presentation in complex paradigms is essential for inducing distinct BOLD responses. The statistical inferences to be drawn (relating stimulus presentation to BOLD response) are, therefore, vulnerable to various sources of errors [Josephs et al., 1999].

An important confounding factor caused by the MR imager itself is acoustic noise [Cacace et al., 2000; Cho et al., 1997]. Intense sound levels are generated during imaging that may interfere with the mapping of brain functions [Cho et al., 1997]. A particular problem in the auditory system is that the MR-generated acoustic noise evokes undesirable BOLD signals [Shah et al., 1999]. In other brain regions, acoustic noise may spoil fMRI experiments, primarily by way of other mechanisms such as distraction [Cho et al., 1998].

The acoustic issue in fMRI is likely to expand with increasing use of high performance MR systems, most of them at 1.5 T, that are suitable for demanding echo planar imaging (EPI) with high spatial resolution [de Zwart et al., 2002]. Moreover, the current trend to higher field strength systems of >7 T for human fMRI [Yacoub et al., 2001a], illustrated by the recent FDA approval for clinical fMRI at 4.0 T [Campeau et al., 2001], makes the acoustic problem even more important, as acoustic noise levels increase with the magnetic field strength [Moelker et al., 2003a].

This study presents a systematic overview of the various aspects of MR-related acoustic noise with regard to fMRI experiments: (1) a description of the multiple sources of acoustic noise in the MR environment, (2) the mechanisms and (3) extent of the interference with regard to both the stimulus and cortical activation, (4) methods for sound reduction that are currently used or are under investigation, and (5) practical considerations and recommendations to minimize the effects of MR-generated acoustic noise on functional brain mapping.

---

\*Correspondence to: Dr. Adriaan Moelker, Erasmus Medical Center Rotterdam, Department of Radiology, Dr. Molewaterplein 50, PO Box 1738, 3000 DR Rotterdam, The Netherlands.

E-mail: a.moelker@erasmusmc.nl

Received for publication 2 June 2003; Accepted 31 July 2003

DOI 10.1002/hbm.10134

---

## SOUND GENERATION IN THE MR ENVIRONMENT

There are multiple different sources of acoustic noise in the MR imager. In descending order of relative contribution to the overall sound pressure level (SPL), these are: (1) the gradient currents, (2) eddy currents, (3) radio frequency (RF) and slice-selection pulses and, as a non-imaging related entity, (4) ambient or background noise.

### Gradient Currents

The interactions between the fluctuating readout and phase encoding currents in the gradient coils and the main static magnetic field of the MR scanner evoke Lorentz forces that act on the gradient coils and their connecting wires [Edelstein et al., 2002; Mansfield et al., 1994, 1995, 1998; Mansfield and Haywood, 2000]. As a result, the coils and wires buckle and bend inducing compressional waves in the surrounding gradient supports. Subsequently, these acoustical waves are conducted toward the peripheral structures of the MR system, such as the main magnet, and launched into air as acoustic sound. The Lorentz forces increase linearly with the magnetic field strength and the applied gradient current [Mansfield et al., 1998]. Noise levels, therefore, also increase with both stronger magnetic field strengths and gradient currents [Moelker et al., 2003a; Price et al., 2001]. During EPI, the most extensively employed pulse sequence in fMRI [Parrish, 1999], equivalent-continuous SPLs range from 90-117 dB at 1.5 T and from 105-133 dB at 3.0 T. Peak levels are even higher: up to 130 and 140 dB at 1.5 T and 3 T, respectively [Cho et al., 1997; Foster et al., 2000; Miyati et al., 1999, 2001; Moelker et al., 2003a; Price et al., 2000; Prieto et al., 1998, 1999; Shellock et al., 1998].

The frequency distribution of the gradient sounds is relevant to the confounding effects of acoustic noise on fMRI and the efficacy of noise reduction techniques (see below). The range of frequencies that are present in the imager noise is dictated by both the spectral shape of the gradient current (or pulse sequence) and the mechanical construction of the MR imager [Hedeen and Edelstein, 1997]. Pulse sequences are periodic with a fundamental frequency (reciprocal of the period) and harmonics, the latter being multiples of the fundamental frequency. The fundamental frequency can be extracted from the gradient current by means of a Fourier transform [Hedeen and Edelstein, 1997; Hennel et al., 1999; Ravicz et al., 2000]. In EPI the fast succession of alternating readout and phase encoding gradient currents results in the appearance of a relatively high, audible, fundamental frequency of (in one reported instance) 1.9 kHz with softer but still audible harmonics at 3.8, 5.8, 7.7, and 9.6 kHz [Foster et al., 2000]. Most MR imagers do not generate these pure tones in isolation, rather a complex, broadband acoustic noise spectrum [Ravicz et al., 2000]. This is because of a modulation of the acoustic noise by MR system-specific structural resonances in the gradient coils and supportive mate-

rials, and by additional volume resonances in the system and MR room [Bowtell and Peters, 1999; Cho et al., 1997; Mansfield et al., 1998; Miyati et al., 1999, 2001; Moelker et al., 2003b; Ravicz and Melcher, 2001]. The entire transition from gradient current to acoustic noise, including these resonances, is referred to as the “frequency response function” [Hedeen and Edelstein, 1997].

### Eddy Currents

The large fluctuating electromagnetic gradient fields in the MR system induce eddy currents in the electrically conducting parts of the imager [Hedeen et al., 2001]. The eddy currents themselves give rise to additional mechanical movements, in particular in the warm (inner) magnet bore, the RF coil and the RF shield [Edelstein et al., 2002; Katsunuma et al., 2002]. In single-shot EPI, eddy current leakage seems to cause an acoustic noise that is soft (> 3 dB less) compared to that produced by the gradient coils [Edelstein et al., 2002]. This is in contrast with gradient echo based pulse sequences in which avoiding eddy current induced noise might reduce the sound intensity by as much as 10 dB [Edelstein et al., 2002].

### RF and Slice Selection Pulses

RF and slice selection pulses represent a third, small source of noise in fMRI. Slice selection currents are in fact similar to the readout and phase encoding currents, but as slice selection is generally done simultaneously with RF excitation, both are discussed here. In single-shot EPI acquisitions the incidence of these pulses is low when playing out the imaging sequence. As a result, the time-averaged acoustic noise level of RF and slice-selective pulses is small compared to gradient noise (for RF alone at least 5 dB less) [Edelstein et al., 2002]. This may be different in spin echo and purely RF-based pulse sequences that encompass multiple RF excitations per image acquisition [Counter et al., 1997]. However, these pulse sequences are less frequently used in fMRI studies. In a fast spin echo sequence, for example, RF produced only slightly less sound compared to the gradient currents (2 dB) [Edelstein et al., 2002].

### Ambient Noise

The in-room air-conditioning, the MR ventilation system, and the cryogen pumping in (most) MR systems are perceptible sources of acoustic noise in the MR environment not related to the imaging procedure. These background noises are of low magnitude with intensities ranging from 45-71 dB on an A-weighted scale. The frequencies are < 100 Hz (environmental equipment) and range from 100 to 500 Hz (cryogen cooling installation) [Cho et al., 1997; Counter et al., 1997; Foster et al., 2000; Hurwitz et al., 1989; Loenneker et al., 2001; McJury et al., 1994; McJury, 1995; Miyati et al., 1999, 2001; Moelker et al., 2003b; Oesterle et al., 2001; Ravicz et al., 2000; Shellock et al., 1994]. During conventional MR imaging, ambient

noises are usually negligible because their sound intensity is much lower than those generated by the gradient coils [American National Standard S1.13-1995; Miyati et al., 2001]. One can assume, however, that ambient noise may have a (small) negative effect on fMRI experiments (to our knowledge, there are no publications on this subject). First, ambient noise levels are relatively low, but still clearly audible in the absence of gradient noise. Therefore, general assumption that the absence of image acquisition sounds equals a period of silence in which stimuli can be presented uninterrupted and uncontaminated [Belin et al., 1999] is not valid. Second, low frequencies in the range of ambient noise are likely to induce activation in a larger area of the auditory cortex compared to higher frequencies (with otherwise identical sound intensity) [Bilecen et al., 1998a]. This has been tentatively explained by the increased sensitivity of the auditory system to higher frequencies.

It should be mentioned that, although the equivalent continuous SPL has been predominantly used as a measure for assessing the effects of acoustic scanner noise in fMRI [Cho et al., 1998; Elliott et al., 1999; Shah et al., 1999, 2000; Talavage et al., 1999; Ulmer et al., 1998a], it is probably the peak sound pressure level that is the more appropriate measure. Peak levels do not take into account the silent periods that occur during the functional experiment. Consequently, peak levels better represent the sound intensity when the acoustic noise generation is primarily condensed in the image acquisition window (between concurrent fMRI acquisitions) [Brechmann et al., 2002; Jakob et al., 1998].

### PATHWAYS OF ACOUSTIC NOISE INTERFERENCE WITH FMRI EXPERIMENTS

MR-related acoustic noise may interfere with functional MR acquisitions both through direct and indirect pathways. Direct interference occurs because the acoustic noise in itself induces an increase in regional cerebral blood flow, interacting with the BOLD response of the brain activation of interest. Indirect interference implies that acoustic noise may affect the perception and processing of the stimulus of interest by a distracting effect. This section discusses these mechanisms of interference (summarized in Table I), followed by mechanisms that are specific for fMRI experiments of the auditory, motor, and visual senses.

#### Direct Confounding

##### General mechanisms

MR-related acoustic noise induces a BOLD response in the auditory cortex. It has been shown that, similar to other auditory stimuli [Di Salle et al., 2001; Hall et al., 1999], acoustic noise induces a hemodynamic response within 2 to 3 seconds after the onset of acoustic noise [Talavage et al., 1998a, 1999] that peaks after 3 to 8 seconds (hemodynamic delay) [Bandettini et al., 1998; Belin

et al., 1999; Edmister et al., 1999; Hall et al., 1999, 2000a; Le et al., 2001] and returns to baseline in > 8 sec [Hall et al., 1999, 2000a; Le et al., 2001; Robson et al., 1998]. The variation in the hemodynamic response is due to the fMRI methodology used to identify these response times [Bandettini and Cox, 2000; Hall et al., 1999] and also due to intersubject variability. A BOLD response induced by the scanner sounds in areas other than the auditory cortex is, to our knowledge, unknown. Acoustic confounding in these cortices is primarily thought to occur through indirect effects.

TABLE I. Mechanisms of acoustic noise interference

Mechanism	Characteristics
<b>Direct confounding</b>	
Intra-acquisition response	Activation by scanner noise within same volume acquisition; primarily interfering with auditory fMRI
Inter-acquisition response	Activation by scanner noise of preceding volume acquisition; primarily interfering with auditory fMRI
<b>Indirect confounding</b>	
Attention	Increased activation in attention-related cortical areas
Distraction	Decreased activation in cortical areas by (inter-modal) distraction
Habituation	Slowly developing adaptational loss of attention; might be advantageous in noisy environments
Motion artifacts	Not substantially related to scanner noise
Masking	Overlap of spectral components of scanner noise and auditory stimuli; confined to auditory fMRI
Stapedial muscle reflex	Changes in cochlear perception of auditory stimuli (intensity and frequency); confined to auditory fMRI
Temporary hearing loss	Changes in cochlear perception auditory stimuli (intensity and frequency); confined to auditory fMRI

The adverse hemodynamic response to acoustic scanner noise results in an elevation of the BOLD response to be measured, in particular the baseline level (OFF condition) [Hall et al., 1999]. Thus, the dynamic range (ON vs. OFF condition) of the BOLD response decreases (also called clipping [Bandettini and Cox, 2000]), making the stimulus-induced cortical activation more difficult to detect statistically [Edmister et al., 1999; Hall et al., 1999, 2000a; Robson et al., 1998; Talavage et al., 1999; Yang et al., 2000]. The hemodynamic responses to MR-related acoustic noise and stimulus induced brain activation do not add up linearly [Talavage et al., 1998b]; this implies that a simple subtraction is not possible [Bandettini et al., 1998; Edmister et al., 1999; Hall et al., 1999; Mazard et al., 2002; Robson et al., 1998]. It is assumed that BOLD responses do not add up linearly because of saturation,

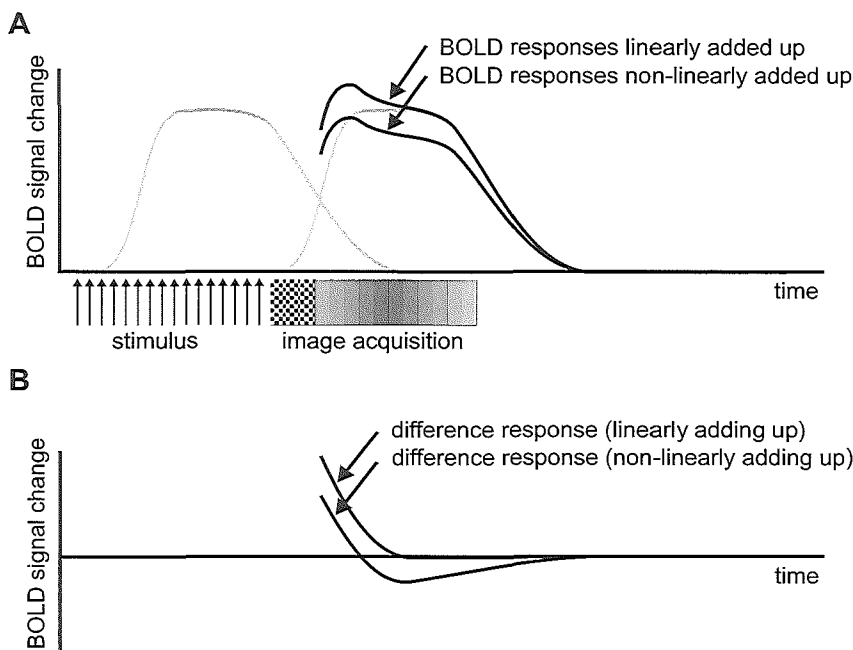


**Figure 1.** BOLD-to-stimulus response (left grey curve) and BOLD-to-scanner-noise response (right grey curve) do not linearly add up because of saturation of the BOLD-response (A). Therefore, simple subtraction of baseline (BOLD response without preceding stimulation) results in a net negative response (B). The checked boxes are dummy image acquisitions to allow longitudinal magnetization to reach steady state.

illustrated by a reduced BOLD response to acoustic scanner noise when preceded by another acoustic stimulation (Fig. 1) [Di Salle et al., 2001]. Furthermore, it has been suggested that imager noise influences the spatial distribution of the stimulus-induced fMRI responses in auditory cortex [Edmister et al., 1999]. Through what mechanism and to what extent has not yet been investigated.

Based on the BOLD response time course of the scanner noise in the fMRI experiment, two mechanisms of acoustic confounding in fMRI can be distinguished, i.e., intra-acquisition and inter-acquisition responses (black areas in Fig. 2A and 2B, respectively). The intra-acquisition response refers to an imager noise-induced BOLD response that interferes with the functional data to be acquired later on within the same multislice (or volume) acquisition [Talavage et al., 1998]. As the BOLD response starts 2 sec after onset of noise, the intra-acquisition response occurs when the image acquisition window is > 2 sec. The inter-acquisition response, on the other hand, is generated when the acoustic noise BOLD response persists during the next volume acquisition [Talavage et al., 1998a]. The parameter determining whether the inter-acquisition response applies is the time between two successive slices or volume acquisitions, i.e., the sequence repetition time (TR) minus the acquisition window [Shah et al., 2000]. For short acquisition times, therefore, the inter-acquisition response occurs when the TR is shorter than the time required for the BOLD response to return to baseline level (Fig. 2B).

### Direct confounding in auditory cortex

The auditory cortex encompasses primary, secondary and adjacent regions. The primary auditory cortex is a relatively small (1–4 cm<sup>3</sup>) region bilaterally located on the superior temporal gyrus (Heschl's gyrus), including Brodmann's area BA41 (Fig. 3). This auditory field is

characterized by a strong connection with the peripheral auditory system. Sounds elicit robust responses in the primary auditory cortex reflecting both the intensity and tonotopy of the sound as perceived by the cochlea [Ehret, 1997]. The adverse effects of imager noise are most apparent in the primary auditory cortex and have been described in detail elsewhere [Bandettini et al., 1998; Bilecen et al., 1998a; Cho et al., 1998; Elliott et al., 1999; Hall et al., 1999, 2000a; Jakob et al., 1998; Loenneker et al., 2001; Shah et al., 1999; Talavage et al., 1999; Ulmer et al., 1998b]. The secondary auditory cortex is the surrounding area and includes among others BA22 (including Wernicke's area) and BA42. This region is relevant in early auditory processing intimately involved in phonological and nonword auditory decoding and attention-related enhancement of responses [Shapleske et al., 1999]. Cortical activation of the secondary auditory cortex by imager noise is less conclusive than for the primary region. This is due to both ambiguous activation below significant threshold levels [Talavage et al., 1999] and omitted classification of the auditory cortex into primary and secondary cortex in some studies [Bilecen et al., 1998a; Cho et al., 1998; Elliott et al., 1999]. Only one investigation failed in the attempt to identify activation in the secondary auditory cortex using MR noise [Bandettini et al., 1998]. Recent investigations have demonstrated activation (changes) in the middle temporal gyrus and superior temporal sulcus, pertaining to the secondary auditory cortex [Jakob et al., 1998; Loenneker et al., 2001; Ulmer et al., 1998b], and the associated auditory cortices [Hall et al., 1999, 2000a; Mazard et al., 2002; Shah et al., 1999]. The BOLD signal changes in both primary and secondary auditory cortex vary considerably ranging from 0.32–9%. This large variability probably reflects differences in the MR noise duration (prolonged stimulation causes stronger activation) [Robson et al., 1998] and intensity (the more intense the MR noise, the greater the signal changes) [Brechmann et

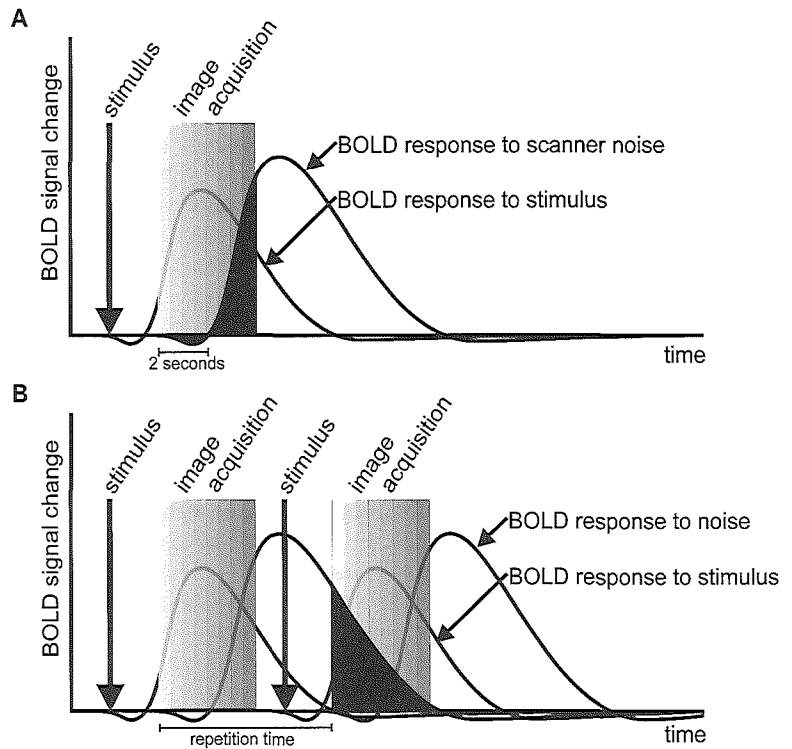


**Figure 2.**

BOLD-to-stimulus responses confounded by intra-acquisition response (A) and inter-acquisition response (B) to acoustic scanner noise (black areas). The intra-acquisition occurs when the volume acquisition takes >2 sec; the inter-acquisition response occurs when the time between the volume acquisitions is shorter than the time the BOLD response (to scanner noise) takes to return to baseline.

al., 2002; Hall et al., 2001; Jancke et al., 1998].

It has been hypothesized that the dissemination of the acoustic noise-induced activation into the secondary regions is a response to the complex periodic properties of scanner noise, similar to those present in conversational speech [Belin et al., 1999; Mazard et al., 2002; Ulmer et al., 1998a]. As human speech is predominantly processed in the left hemisphere [Binder et al., 1997], it is not surprising that imager noise activation favors the left over the right secondary auditory cortex [Bilecen et al., 1998b; Ulmer et al., 1998b].

Recent studies found small negative BOLD responses in visual and motor cortices [Hu et al., 1997], i.e., within the initial 2-3 sec after stimulus presentation [Yacoub et al., 1999]. This initial dip, caused by an oxygen depletion at microvascular level [Yacoub and Hu, 2001b], allows for imaging with higher spatial specificity suitable for cortical columnar functional imaging [Duong et al., 2000]. Unfor-

tunately, in auditory cortex the ensuing intra-acquisition response is likely to impede the exploration of this initial dip. Although an initial dip has been described recently by Bandettini and Cox [2000], this was explained by the negative overshoot of a previous time series.

## Indirect Confounding

### General mechanisms

Imager noise can also confound functional experiments through indirect pathways that are predominantly attention-related. Basically, attention is a mechanism enabling the processing of a stimulus or task of a specific sense (modality) [Woldorff et al., 1993]. Neuroregulative dysfunctions, such as schizophrenia, are known to exhibit disruptions in attention. Therefore, it has been hypothesized that psychiatric disorders are more vulnerable to indirect confounding by MR-generated noise [Mathiak et al., 2002]. Focusing attention on a specific modality implies that the perception and cortical response related to that modality are positively influenced and modulated [Berman and Colby, 2002]. On the other hand, involuntary loss of focus (distraction) and neglect may reduce the cortical response to the stimulus [Escera et al., 1998; Jancke et al., 1999]. Distracting stimuli might be perceived from either the same modality (intra-modal interaction), e.g., acoustic scanner noise in auditory fMRI or from other modalities (inter-modal interaction), e.g., scanner noise in visual fMRI [Mazard et al., 2002]. Accordingly, the changes in attention as a result of MR-related acoustic noise may lead to both an increase in activity in attention-related brain areas and to a drop in cortical activity in the brain areas of interest (distraction). The location of these effects can be appreciated at both cortical and

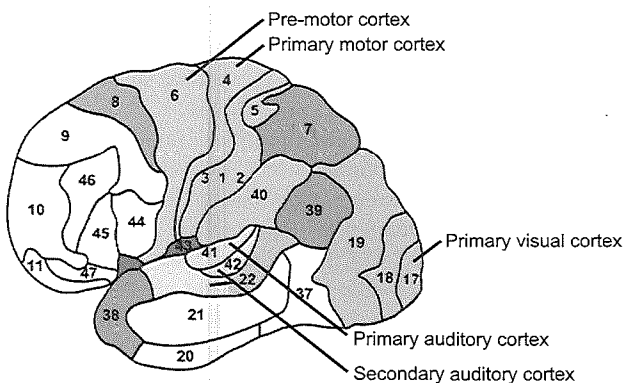


**Figure 3.**

Human cortex (lateral view) according to Brodmann's cytoarchitectural map.

---

subcortical levels [Maeder et al., 2001; Opitz et al., 2002].

It has been shown that the left auditory cortex (T1a, anterior part of Heschl's gyrus) is involved in foreground background decomposition, i.e., the capability of the auditory system to monitor targets in a background [Scheich et al., 1998]. This cortical area shows more activation in response to low intensity tones (36 dB) in a background of MR-related acoustic noise (40 dB) compared to louder tones (> 48 dB) [Brechmann et al., 2002]. This increased activation in T1a was assigned to the required attentional effort for detecting the softer sounds [Brechmann et al., 2002]. In an analogous experiment, increased activation has been demonstrated in the posterior part of the calcarine cortex during visual imagery tasks in noisy MR conditions (compared to less noisy conditions) [Mazard et al., 2002]. The activation in the calcarine cortex reflected the greater visual attentional load required for maintaining vivid images [Mazard et al., 2002]. In a similar manner, secondary motor areas, involved in motor activity planning, showed inconsistent activation among subjects that were exposed to loud MR imager noise. Again, activation has been attributed to attention responses in this area [Elliott et al., 1999].

Distraction by scanner noise may potentially modulate BOLD responses both intra- and inter-modally [Mazard et al., 2002]. Its modulations are in the same order of magnitude as the BOLD response of interest [Vouloumanos et al., 2001] but not in the time course of the BOLD response [Hall et al., 2000]. In a recent fMRI study, fMRI signal changes by visual stimulation decreased by approximately 50% in the presence of acoustic MR noise, attributed to exhaustion and a loss of attention [Cho et al., 1998; Loenneker et al., 2001]. By contrast, congruent, simultaneous stimulation in different modalities might enhance their cortical response [Calvert et al., 1999]. As an example, the presentation of speech employing both auditory and visual stimuli can amplify the cortical responses of both these senses [Calvert et al., 1999]. Difficult tasks require increased attentional efforts and may, therefore, be more affected by distracting scanner noise [Elliott et al., 1999]. Parallel to this, a close relationship has been demonstrated between the intensity of scanner noise and performance, reaction time and BOLD signal changes (experiments carried out for auditory cortex) [Edmister et al., 1999; Shah et al., 1999, 2000; Ulmer et al., 1998b].

Functional MRI studies are vulnerable to motion artifacts, because of the (generally) long experiment times and the small BOLD signal changes [Seto et al., 2001]. It has been hypothesized that motion artifacts are related to anxiety, and anxiety itself to acoustic scanner noise [Quirk et al., 1989]. Artifactual brain activations might, therefore, be temporally correlated with the stimulus but are in fact correlated with the imager noise [Sunaert and Yousry, 2001]. One study reported that anxiety was not significantly associated with motion artifacts, making the above hypothesis less likely [Dantendorfer et al., 1997]. This outcome has been supported by an fMRI experiment that found a similar incidence of motion artifacts in silent and loud acoustic scanner noise conditions [Elliott et al., 1999].

### ***Indirect confounding in auditory cortex***

Auditory fMRI may be further impaired by the (louder) imager noise due to its screening effects on stimuli [Scheich et al., 1998; Shah et al., 2000]. Extracting the stimuli in an obscuring acoustic background encompasses the interplay of the auditory system at both the cochlear (masking) and at the cortical levels (foreground background decomposition), discussed earlier. Cochlear masking, at the inner ear, is frequency selective whereby hearing thresholds peak around the masker frequency (Fig. 4) [Oxenham and Plack, 1998]. In auditory fMRI the competitive effect between stimulus and scanner noise depends on the overlap of the spectral components [Belin et al., 1999; Di Salle et al., 2001]. Recent experiments have suffered from acoustic scanner noise with frequencies from 800 to 1.200 Hz that largely hindered the perception of a 1.000 Hz pure tone stimulus [Le et al., 2001]. In contrast, stimulation with pure sinusoidal tones at 200 and 3.000 Hz were clearly perceived, as evidenced by large BOLD signal changes [Le et al., 2001].

Masking continues even after the MR scanner noise has stopped (forward masking) [Backes and van Dijk, 2002]. The reason for this is that the cochlear nerve fibers have a recuperation phase of up to 400 msec during which they show a reduced response to novel stimulation [Frisina, 2001]. The louder the background noise the longer this effect will last, and this phenomenon has been implied as the cause of highly variable BOLD responses (by a factor of 2) between different fMRI studies of otherwise similar set-up [Backes and van Dijk, 2002; Belin et al., 1999]. In cases where the hemodynamic response to scanner noise takes longer to subside than forward masking, however, forward masking is expected to be a trivial confounding factor.

Both cochlear and cortical processing are required for stimulus extraction in noisy environments. Their relative contributions depend on among others the physical properties of the presented auditory stimulus. There is an empirically found difference between pure tones and complex sounds in that the obscuring effects of pure tones occur at a cochlear level, whereas complex amplitude and frequency modulated stimuli have an effect at primarily a cortical level [Hari and Makela, 1988]. As a consequence, MR-related acoustic noise may have a different effect on fMRI processing of simple versus complex acoustic stimulation. To minimize concurrent processing at cortical and cochlear levels, pure tones can be used, e.g., as standard stimuli within the broad-band (complex) imager noise.

Acoustic scanner noise might further interfere with auditory fMRI by means of habituation. Habituation is an adaptational phenomenon of the auditory cortex, characterized by a reduced BOLD response after prolonged exposure of several minutes [Bandettini et al., 1998; Bernal and Altman, 2001; Pfliegerer et al., 2002]. The fMRI mapping of the tonotopic organization by Bilecen et al. [1998b] suffered from habituation effects in several of their subjects. During continuous scanner background noise, this effect might in fact be advantageous; the confounding effect of imager noise vanishes during the functional ex-

periment. For noncontinuous acoustic noise, as in sparse temporal sampling, this phenomenon is obviously less likely to occur.

Intense scanner noise may also potentially alter the sound levels and spectral characteristics of the presented auditory stimulus by inducing a stapedial muscle reflex [Hall et al., 2001]. This reflex, occurring when the sound intensity is  $> 80$  dB, lowers the perceived loudness for frequencies  $< 1$  kHz ( $-10$  to  $-20$  dB) and amplifies frequencies between 1-3 kHz [Counter and Borg, 1993; Pascal et al., 1998]. Whether the stapedial muscle reflex modulates stimuli in auditory fMRI, and to what extent this alters brain activation, has not yet been investigated.

A final confounding factor relevant to specifically auditory fMRI is in the temporary loss of hearing that ensues in the presence of intense MR noise [Brummett et al., 1988]. The extent of hearing loss is correlated with the scanner noise intensity with dominant effects in the frequency range of the acoustic noise [Ulmer et al., 1998a]. For example, an EPI pulse sequence with a TR of 1 second has been reported to induce a convex-shaped reduction of minimum hearing thresholds over the audible frequency range [Ulmer et al., 1998a]. This caused auditory stimuli, such as speech and syllables, to be perceived as relatively flat sounds.

### **Indirect confounding in visual and motor cortices**

MR scanner noise may also cause measurable artifacts in fMRI of non-auditory cortices, although the effects are less pronounced than in the auditory cortex. In this respect, few investigators have evaluated visual and motor cortices [Cho et al., 1998; Elliott et al., 1999; Loenneker et al., 2001; Ludwig et al., 1999; Mazard et al., 2002].

The visual cortex is located in the occipital lobe of the cerebrum (Fig. 3), encompassing the primary visual cortex (V1, BA17) receiving afferent bundles from the thalamus and projecting to the associated visual cortices (anterior temporal and the parietal lobes). Investigators mentioned decreases of up to 50% less significantly activated pixels in primary [Cho et al., 1998; Loenneker et al., 2001; Ludwig et al., 1999] and associated [Loenneker et al., 2001] visual cortex in imager noise backgrounds. Only one investigator did not observe signal changes in noisy compared to silent experiment conditions, which might have been caused by the relatively small sample size used [Elliott et al., 1999].

To our knowledge, only two investigators tested for imager noise interference with functional experiments of the human motor cortex [Cho et al., 1998; Elliott et al., 1999], which comprises primary motor cortex (BA4), premotor (BA6) and supplementary motor areas (Fig. 3) [Mattay and Weienberger, 1999]. In an experiment that made use of additional scanner noise, Cho et al. reported a 30% increase in the extent (number of activated pixels) of motor cortex activation [Cho et al., 1998]. The larger cortical activation was attributed to a facilitated processing of the motor stimulus by simultaneous acoustic stimulation [Burke et al., 2000; Cho et al., 1998]. In the experiments of Elliott et al. [1999], a higher variability among subjects

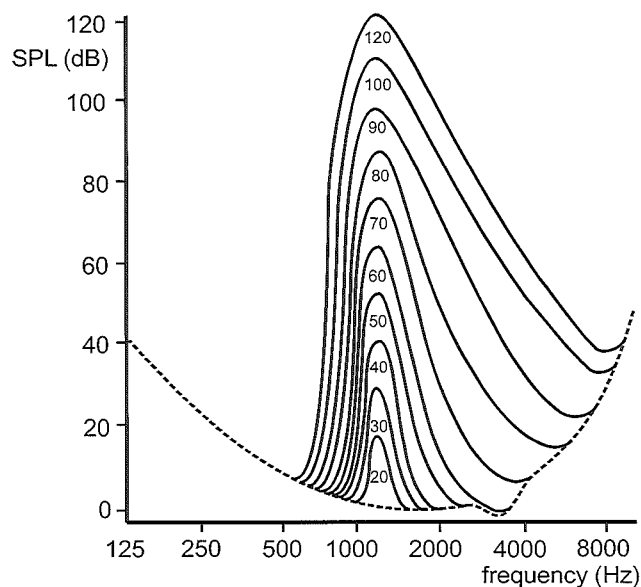


**Figure 4.**

Principle of cochlear masking by a pure sinusoidal tone at 1.2 kHz at various SPLs (shown within curves) demonstrating broad-band increments in minimum hearing thresholds with increasing pure tone intensities. Hearing thresholds are on a linear scale (vertical axis). The dotted line represents the sensitivity of human hearing over frequency (horizontal axis), being significantly reduced at lower and higher frequencies. Note the asymmetry (upward spread) of masking, i.e., higher frequencies are masked to a greater extent than lower frequencies.

in the supplementary motor areas was detected; an area that is involved in the planning of motor activities. Their findings indicated that MR-related acoustic noise predominantly effects through an indirect mechanism.

### **METHODS TO REDUCE ACOUSTIC IMAGER NOISE**

Various methods exist to lower the adverse effects of acoustic noise. First, the functional experiment paradigm can be optimized by taking into account the temporal characteristics of the cortical responses to both the MR noise and the stimulus. Such an acoustic artifact-free experiment is also referred to as a silent paradigm design. A second, more fundamental approach is the elimination of the actual sources of acoustic noise. This can be achieved by differently exciting the gradient system (silent pulse sequence design) and by engineering improvements in MR hardware. Finally, pragmatic methods of passive and active noise canceling can be used. Table II lists the various noise reduction techniques and their current status of application in fMRI.

#### **Silent Functional Paradigm Designs**

MR-related acoustic noise precludes a completely controlled functional environment and poses restrictions on the usable functional paradigm designs. The most widely used paradigm in fMRI is the conventional block design (Fig. 5A), composed of alternating ON and OFF conditions of each several tens of seconds [Parrish, 1999]. This simple design is sensitive to MR noise because of interfer-

**TABLE II. Noise reduction techniques in functional MRI**

Technique	Characteristics
<b>Functional paradigm design</b>	
Sparse temporal sampling	Avoiding inter-acquisition BOLD response to MR noise by increasing TR to > 7 sec
Clustered volume acquisition	Avoiding intra-acquisition BOLD response by clustering image acquisitions
Magnetization subtraction method	Subtraction of intra-acquisition response
<b>Silent pulse sequence design</b>	
Burst imaging	Train of RF pulses under constant phase and readout gradients; SPL reduction > 15 dB; scarce resolution and SNRs
Low-pass filtering gradient pulses	Avoiding higher harmonics in the acoustic noise spectrum; attenuation up to 40 dB; limited to slow sequences
Low-pass filtering with SIMEX pulses	Addition of SIMEX pulses for better volume coverage within same acquisition window; FLASH imaging at 43 dB
Low-pass filtering with SENSE	Addition of multiple array detectors for compensating smaller gradient current amplitudes and under sampling; reduction 14 dB(A)
Interleaved spiral-k imaging	Intrinsically low-pass filtered due to sinusoidal gradient currents; further reduction of acoustic noise at the expense of imaging time; BOLD contrast images acquired at 67 dB with good coverage
<b>MR-imager configuration changes</b>	
Increasing mass gradient system	Increases inertia and stiffness to mechanical vibrations
Mounting gradient system to floor	Reduction of acoustic vibrations; ~ 10 dB less during EPI
Vacuum enclosing gradient coils	Reduction of up to 10 dB during EPI at 1.5 Tesla; currently applied in Toshiba's Excelart and General Electric's Twinspeed
Insulation	Acoustic noise reduction up to 20 dB, particularly at higher frequencies
Lorentz force balancing	Canceling of opposite forces in coil assemblies; not implemented in commercial MR imagers; reductions of up to 35 dB
Eddy current reduction	Reduction of eddy currents in RF-coil and main magnet
Passive noise reduction	Passive absorption of acoustic noise by earplug, earmuff, helmet, vacuum cushions or total body encapsulation; subjective reductions up to 60 dB when combining earplug, earmuff and helmet
Active noise reduction	Destructive interposition of anti-noise; objective reductions up to 40 dB; subjective reduction 5 dB at 2 kHz; not commonly used in fMRI

ence along the inter- and intra-acquisition time scales and the simultaneous presentation of stimulus and scanner noise [Le et al., 2001]. A more careful construction of the functional paradigm can minimize the effects of scanner noise, as discussed below in more detail.

**Avoiding inter-acquisition interference**

Edmister et al. [1999] and Shah et al. [2000] have experimented with silent paradigms that eliminated the inter-acquisition interference making use of continuous music and speech-related sounds, respectively. By using long TRs, such that the next volume acquisition occurs only after the acoustic noise BOLD response has subsided, these investigators could completely avoid the inter-acquisition response (Fig. 5B). They independently found an optimal TR (which included an acquisition window of ~ 2 sec), in terms of magnitude and extent of activation, of at least 7 sec [Edmister et al., 1999; Shah et al., 2000]. The use of such long TRs is referred to as sparse temporal sampling [Hall et al., 1999].

From the imaging perspective, an advantage of sparse temporal sampling is in the complete recovery of the MR magnetization during the lengthy imaging intervals, resulting in better signal-to-noise ratios (SNR) in the next volume acquisition (increased T2\*-weighting) [Elliott et al., 1999; Hall et al., 1999]. This largely compensates for the

data reduction per unit time of the sparse temporal sampling technique [Hall et al., 2001]. Also, stimuli are presented and subject responses evaluated in virtual silence (except from ambient noise). This is particularly suitable in psycho-acoustic experiments, in which the relation between human perception of sound and its characteristics is under investigation [Belin et al., 1999]. An additional gain in the dynamic range of the BOLD response can be attained by taking advantage of the BOLD overshoot phase in the OFF condition [Bandettini et al., 2000; Hall et al., 1999]. This overshoot is a temporary negative level of the BOLD response before it returns to the baseline level. By acquiring the OFF condition during the overshoot phase, the signal difference between stimulus and non-stimulus conditions is optimally enhanced [Hall et al., 1999].

**Avoiding intra-acquisition interference**

As fMRI is moving toward whole brain imaging with larger brain coverage, thinner slices and better in-plane resolution, the intra-acquisition response becomes more relevant [Shah et al., 2000]. Intra-acquisition interference has been found to decrease when using very rapid volume acquisitions, such as clustered volume acquisitions (CVA) [Talavage et al., 1998a]. In CVA, a series of volumes is rapidly imaged making use of tailored RF pulses and rescaled gradient amplitudes for reducing cross-talk be-



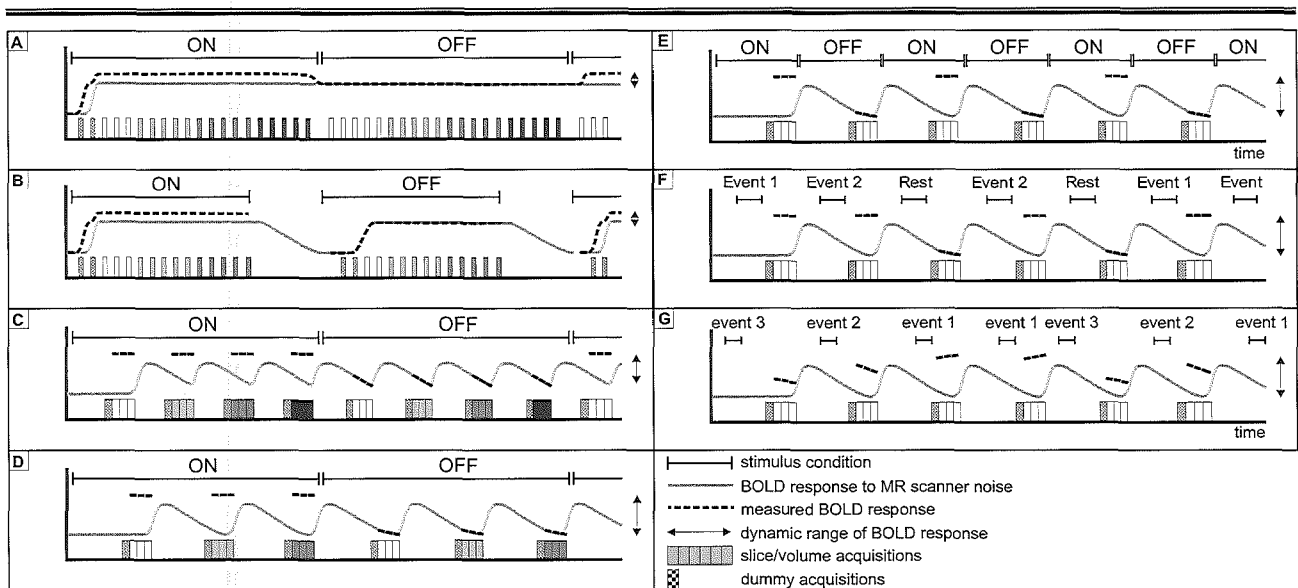


**Figure 5.**

Silent functional paradigms (B-G) vs. conventional block design (A), including event-related paradigms (E-G). Grey lines represent BOLD responses to scanner noise during imaging (white and grey scaled bars), and the dotted lines the measured BOLD response. **B:** The intra-acquisition response. **C:** BOLD responses are spoiled by MR scanner noise of preceding acquisitions (inter-acquisition response). Note that the acquisition time prolongs when avoiding the inter-acquisition response (not scaled). The size of the arrows indicates the dynamic range of that particular imaging paradigm (ON vs. OFF conditions) and is smallest in the conventional imaging paradigm. **G:** Stroboscopic event-related imaging paradigm illustrated by the random time shifts of the various events. Dummy acquisitions are taken and discarded to allow time for the longitudinal magnetization to reach steady state.

tween adjacent slices [Edmister et al., 1999]. Its temporal location within the functional paradigm ideally coincides with the peak of the BOLD response to the stimulus of interest (Fig. 5C) [Eden et al., 1999; Hall et al., 1999]. Because of intersubject variability of the BOLD response [Amaro et al., 2002], prolonged stimulation may be preferred to reach the plateau in most subjects. An optimal time span of a CVA acquisition of  $< 3$  sec has been empirically found making use of short CVA image acquisitions preceded with additional MR noise (readout pulses) [Talavage et al., 1999]. By contrast, a distributed volume acquisition (Fig. 5B), in which imaging was done equally throughout the TR period, resulted in remarkably lower, insignificant signal changes [Talavage et al., 1999]. Hence, a scanning time of a volume of  $< 2$  sec will completely avoid the intra-acquisition effects of the scanner noise within that volume (Fig. 5C) [Shah et al., 2000; Talavage et al., 1998a, 1999].

An advantage of the CVA method over the distributed volume acquisition method is the improvement of motion registration methods, because motion is relatively more likely to occur between rather than within CVA acquisitions [Edmister et al., 1999]. As a relative drawback, compressing the image acquisition to within 2 sec evidently restricts slice coverage. Also, the burst of imaging noise produces louder imager sounds (peak sound level) than when the imaging noise is distributed equally over the TR period.

Ideally, both the intra- and inter-acquisition responses to MR scanner noise are to be avoided. To this end, it is advised that the functional paradigm should comprise a combination of short CVA-like data acquisitions and sparse temporal sampling with long TR. This provides a virtually silent functional experiment (Fig. 5D, E), with the

quiet periods shifted to one end of TR and the whole imaging procedure to the other end. Currently, this combined functional paradigm design is most widely employed for silent auditory fMRI studies [e.g., Scheffler et al., 1998; Tanaka et al., 2000].

Another approach to quiet functional paradigm design that makes use of compensation for the intra-acquisition response rather than avoiding it is the magnetization subtraction method [Bandettini et al., 1998; Di Salle et al., 2001]. As depicted in Figure 6, the decay of the (plateau-ed) BOLD response to the stimulus can be corrected for the imager noise-induced BOLD response by a voxel wise subtraction. Magnetization subtraction proved successful in several experiments showing relatively large signal changes of up to 9% in the auditory cortex [Bandettini et al., 1998; Di Salle et al., 2001]. In contrast to sparse temporal sampling, this decay sampling procedure has a high temporal resolution suitable for detailed sampling of the decaying BOLD course [Di Salle et al., 2001]. This method assumes that the BOLD responses to both the stimulus of interest and the MR scanner noise add up in a linear manner [Di Salle et al., 2001]. Subsequently, subtraction might be justifiable when the longitudinal magnetization changes during initial imaging are equal in both ON and OFF conditions [Bandettini et al., 1998]. In one magnetization subtraction experiment, negative signal changes were measured that might have been caused by such nonlinearities [Di Salle et al., 2001]. With this and the above-mentioned studies in mind, the validity of the procedure is in our opinion debatable.

### **Event-related sparse temporal sampling**

A relative drawback of the above-described silent func-

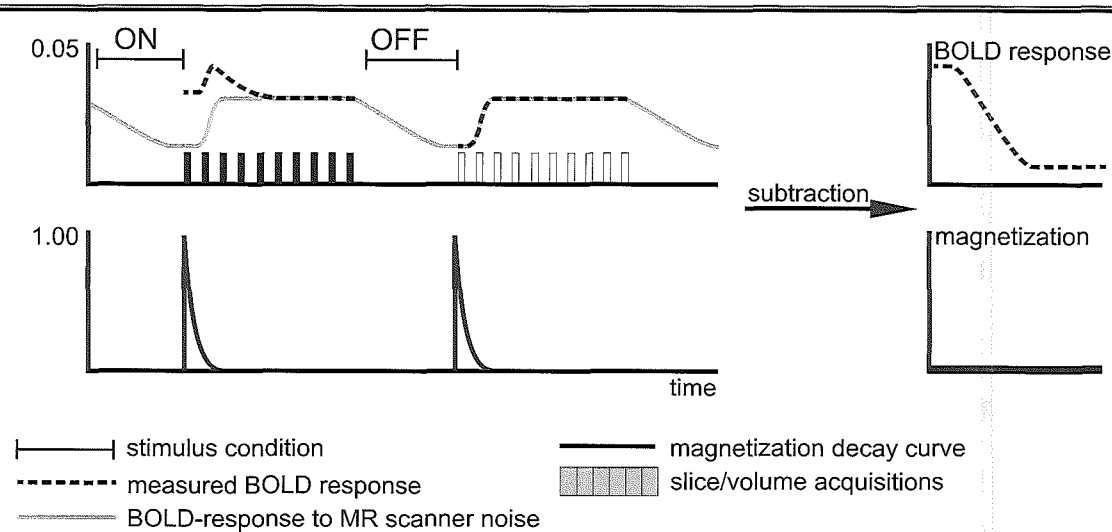


**Figure 6.**

Principle of the magnetization subtraction technique. The three main components that contribute to the functional acquisition, i.e., measured BOLD curve, the response to MR scanner noise (**upper panels**) and the longitudinal magnetization (**lower panels**) are depicted. The similar magnetization decay curves in both ON and OFF conditions are assumed to be similar allowing (voxel-wise) subtraction. Note that the scale of the BOLD-signals is small compared to the scale of the longitudinal magnetization.

tional paradigm designs is in their long duration (proportionate with the increase in TR). More rapid event-related based designs have therefore been proposed for silent paradigms [Belin et al., 1999; Yang et al., 2000]. Event-related functional experiment set-ups are characterized by short, discrete stimulation (Fig. 5E) of < 2 sec, rather than prolonged stimulation (Fig. 5A-D). Such short stimuli have been found to be enough to induce significant brain activation [Rosen et al., 1998]. General advantages of event-related paradigms are among others the randomization of stimulus presentations (trials), the application of different stimuli (Fig. 5F) and the post hoc sorting of data based on arbitrary parameters or stimuli [Cacace et al., 2000]. Analogous to this, event-related designs are less susceptible to image motion artifacts because the actual behavioral responses can be temporally resolved from the undisturbed important functional images [Birn et al., 1999].

In silent event-related fMRI, stimuli are basically presented in the scanner noise-free intervals (between volume acquisitions) and attempts are made to measure the BOLD response at its peak hemodynamic response [Le et al., 2001]. Despite the high inter-subject variability of the BOLD response in auditory cortex [Josephs et al., 1999], consistent results with silent event-related paradigms have been found. Using pure tone bursts of 900 msec, Yang et al. [2000] found a 54% increase (to 2.17%) in BOLD signal changes when comparing a silent event-related acquisition with a conventional event-related acquisition [Yang et al., 2000]. As another example, this method has been successfully employed in tonotopic mapping experiments of the auditory cortex [Engelien et al., 2002; Le et al., 2001]. Functional acquisitions with stimulus durations as short as 50 msec were only minimally hampered by the MR imager noise [Engelien et al., 2002].

The silent event-related technique may be further enhanced by randomly shifting the temporal location of stim-

uli within the scanner noise-free period (Fig. 5G) [Backes et al., 2002; Belin et al., 1999; Amaro et al., 2001]. With this so-called stroboscopic BOLD imaging, the temporal shifts of stimuli within the functional paradigm represent different trials that provide sampling of the complete BOLD response. Stroboscopic BOLD imaging is beneficial in terms of its temporal resolution (resolution equal to minimum time shift between trials) and reduced habituation effects [Belin et al., 1999]. As a potential drawback, BOLD responses from stimuli that were shifted to the end of TR might interfere with BOLD response of preceding (early) stimuli. This might be avoided by adapting TR congruent with the stimulus time shift that in addition benefits from shorter experiment durations. Subsequent differences in longitudinal magnetization should, however, be dealt with during image postprocessing [Talavage et al., 1999].

Several fMRI paradigm designs have been discussed with the aim to provide an acoustically controlled fMRI experiment with increases in signal amplitude and extent. It is obvious that the sparse temporal sampling technique increases the total imaging time compared to conventional block designs [Bilecen et al., 1998a,b; Hall et al., 1999, 2000a; Robson et al., 1998]. Parallel to this, longer TRs (>9 sec) may result in attention loss and subsequently lower BOLD responses [Shah et al., 2000] and are, therefore, better avoided. TRs of several seconds allow more time for the longitudinal magnetization to recover, which intrinsically results in larger relative signal changes [Amaro et al., 2002]. Several studies have reported recently the successful use of TRs of >9 sec [Formisano et al., 2002; Liebenthal et al., 2003]. Besides its extended experiment time, the sparse temporal sampling technique is also unsuitable to acquire a fine temporal resolution of the BOLD response [Belin et al., 1999; Hall et al., 1999]. Both the magnetization subtraction method and the stroboscopic event-related paradigms provide better temporal sampling

---

of the BOLD response. The magnetization subtraction technique demonstrated large signal changes compared to the sparse temporal sampling techniques (up to 9% using magnetization subtraction [Di Salle et al., 2001] vs. up to 2.2% using sparse temporal sampling [Hall et al., 1999]). Its validity is, however, in debate because of expected nonlinearities when adding up BOLD responses to the stimulus of interest and the imager noise. Also, the sampling of the BOLD response is partial, i.e., restricted to its plateau phase and return to baseline level. The stroboscopic event-related method is a promising technique in terms of its good temporal sampling of the BOLD response (signal changes reported up to 1.5%) [Backes et al., 2002]. Although the image acquisition time tends to increase as compared to sparse temporal sampling (because of the larger number of different trials with otherwise identical TR) adequate results with experiment times of only 10 min have been reported (temporal resolution of 2 sec) [Backes et al., 2002].

### Silent Pulse Sequence Design

As mentioned previously, the most dominant noise source in the MR environment originates from the gradient system. Modulating the motion behavior of the gradient system, i.e., by redesigning the pulse sequence, may therefore decrease scanner noise. Such silent pulse sequences can broadly be differentiated into (1) the sequences based on RF Burst imaging, and (2) those based on re-shaping the readout and phase encoding gradient currents.

#### **Burst imaging pulse sequences**

In the area of silent Burst imaging relatively little work has been done. Burst is the generic name given to a class of pulse sequences that employ multiple low flip-angle pulses under a constant readout and phase encoding gradient (and the subsequent refocusing of a set of echoes equal to the number of RF bursts) [Hennig and Hodapp, 1993]. This results in barely audible acoustic clicks due to the low number of gradient switching steps [Jakob et al., 1998]. Jakob et al. [1998] assessed a single-shot technique that showed well localized activity in visual and auditory cortex within only 12 gradient ramps in 105 msec. Peak sound levels at 2 meter distance from the MR system ranged from 52-55 dB(A) [Jakob et al., 1998]. From the imaging perspective, functional Burst imaging proved successful in sleep staging and in visual and auditory experiments with signal changes of up to 6% and 3%, respectively [Jakob et al., 1998; Lovblad et al., 1999]. Additional attractive properties besides its quietness include the geometric fidelity, small power deposition, low demands on gradient strength (high amplitudes but low switching rates) and, therefore, suitability for systems without EPI hardware [Cremillieux et al., 1997; Jakob et al., 1998]. Nevertheless, in our opinion, the major drawbacks limit further development of the Burst sequences in fMRI, which are: poor SNRs trading off with resolution, limited multislice capabilities (due to rapid T2\* signal loss) and

considerable motion sensitivity [Cremillieux et al., 1997; Jakob et al., 1998]. The application of Burst imaging is, therefore, primarily restricted to functional experiments in which absence of scanner noise throughout the entire examination is a prerequisite (as in sleep staging, although many successful studies have also been carried out with EPI).

#### **Silent pulse sequences based on redesigning gradient pulses**

The acoustic scanner noise spectrum primarily comprises a fundamental frequency and harmonics, both deducible from the gradient current spectrum by means of Fourier transform (Fig. 7) [Hedeen and Edelstein, 1997]. For relatively slow pulse sequences (fundamental frequency below 100 Hz), the higher order harmonics are predominantly audible. Avoidance of these by band-pass filtering the gradient current (pulse sequence design) would, therefore, result in a significant reduction of the loudness [Hennel et al., 1999]. Based on this, Hennel et al. [1999] formulated three principles for silent modeling of gradient pulses: (1) use sinusoidal gradient slopes, (2) maximize slope durations (that lowers the fundamental frequency), and (3) minimize the number of slopes by merging gradient pulses [Ludwig et al., 1999]. Applying these behavioral restrictions to both spin-echo and gradient-echo based pulse sequences has reduced noise production by up to 40 dB(A) with acceptable image quality [Girard et al., 2000; Hennel et al., 1999]. For faster pulse sequences such as FLASH (fast low angle shot gradient echo) and EPI, considerably less reduction could be obtained [Girard et al., 2000; Hennel et al., 1999]. The reason is that the fundamental frequency of these rapid imaging protocols shifts toward the audible range of human hearing, thereby making the harmonics relatively less influential in the acoustic domain [Hennel et al., 1999].

Recently, modifications of silent gradient pulse modeling have been proposed to allow for faster imaging while still preserving significant noise reduction [Hennel, 2000; 2001; Loenneker et al., 2001; Ludwig et al., 1999; Oesterle et al., 2001].

First, simultaneous multislice excitation (SIMEX) pulses have been implemented into a silent FLASH sequence providing larger volume coverage within the same image acquisition window [Loenneker et al., 2001; Ludwig et al., 1999]. SIMEX pulses are single multifrequency RF pulses composed of linearly combined carrier frequencies that selectively excite parallel slices [Loenneker et al., 2001]. While maintaining high SNR and spatial resolution, it was possible to measure up to eight slices simultaneously making use of one SIMEX pulse [Loenneker et al., 2001]. Successful stimulation of four parallel slices was appreciated in auditory and visual cortices with increased extent of cerebral activation in the silent pulse sequence condition (43.1 dB(A)) [Loenneker et al., 2001].

Another silent pulse sequence design has been proposed by de Zwart et al. [2002]. Sensitivity encoding (SENSE) with multi-element detector arrays was incorporated into a silent BOLD-contrast EPI pulse sequence,

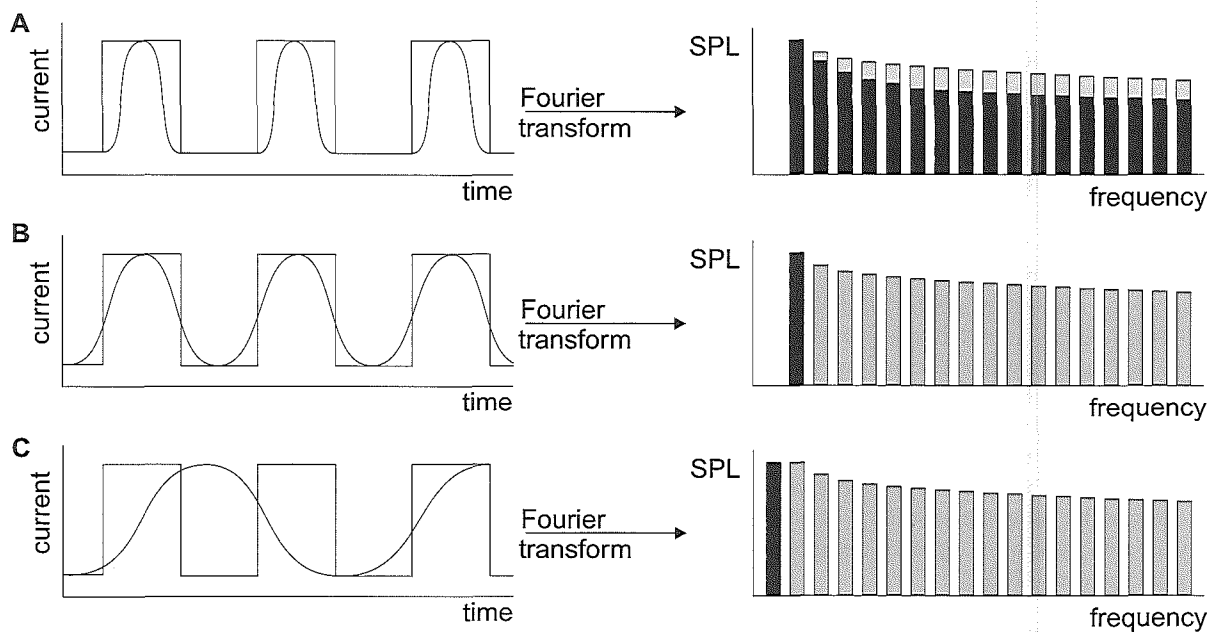


Figure 7.

Relationship between gradient current and acoustic noise frequency distribution (in bands) obtained for several sinusoidal pulses by means of Fourier transform (A, black bars). With flattening of the slew rate, higher order harmonics disappear from the acoustic spectrum. For a pure sinusoidal gradient current, the acoustic noise comprises one pure tone (B). Extending the gradient current over time causes the fundamental frequency to lower (C). Grey bars represent the frequency distribution of a rectangular gradient pulse.

which performed excellently from the acoustic perspective. With a two-fold undersampling and halving the gradient amplitude, the acoustic load subsided about 14 dB(A) on a 1.5 T imager. From the imaging perspective, image acquisition time, resolution and the quality of the functional maps were similar in both conventional and SENSE-prepared EPI sequences [de Zwart et al., 2002]. However, these findings might be task-dependent and not applicable to other imaging paradigms and pulse sequences [de Zwart et al., 2002].

A final way of improving the temporal resolution is by making use of interleaved spiral trajectory k-space imaging. Spiraled filling of k-space is more time-efficient than conventional filling, because almost 100% of the image acquisition window is spent on data collection [Oesterle et al., 1999]. Oesterle et al. [1999, 2001] adjusted a silent spiral-k BOLD contrast pulse sequence by slow ramp times and several spiral interleaves. They found that a minimum rise time of 6 msec (20 times below the hardware limit) and 64 interleaves (24.3 msec/interleave) with a slow return leading off to zero generated only 72 dB(A) at a Bruker 2 Tesla system [Oesterle et al., 2001]. Image contrast and SNR were slightly reduced compared to a conventional silent gradient echo sequence due to the long duration of the spiral readout ( $T_2^*$  signal loss). Slightly lower resolution was a result of the missing parts in the k-space corners. Despite that, volume coverage was four times better.

In summary, the current silent pulse sequences allow for fast BOLD contrast imaging suitable to measure the hemodynamic response in a relatively low noise environment. In particular the incorporation of parallel imaging techniques in spiral MR imaging, eventually combined with other techniques such as SIMEX pulses, might pro-

vide substantial advances in acoustic scanner noise reduction. With such an imaging protocol the sound intensity is expected to drop below 55 dB(A).

### MR Hardware Configuration Changes

Restricting the mobility of the gradient coil assembly is a time-honored engineering approach to make quieter MR scanners. This can be achieved by constructing heavier gradient coils and mountings, thereby effectively limiting their responsiveness to Lorentz forces [Katsunuma et al., 2002]. Mounting the gradient coils supports directly to the floor provides an additional reduction of about 10 dB during EPI imaging [Katsunuma et al., 2002]. These methods reached a maximum because of the currently used strong static magnetic fields and gradient strengths required for ultra-fast imaging techniques. Evidently, the acceptable total mass of the gradient system is limited [Mansfield et al., 1994, 1995]. An interesting MR hardware development is the incorporation of the gradient coils in vacuum enclosures that effectively interrupt airborne acoustic noise propagation (reduction ~10 dB) [Katsunuma et al., 2002]. For additional restriction of structure-borne noise, the gradient assembly is (acoustically) released from its mountings by means of rubber dampers [Katsunuma et al., 2002]. A research scanner with such a configuration provided acoustic noise reductions of up to 30 dB [Edelstein et al., 2002; Katsunuma et al., 2002]. So-called “quiet” MR-systems have become commercially available encompassing a vacuum enclosed gradient system in addition to insulators (Excelart, Toshiba Corporation, Tochigi, Japan, and Signa Twinspeed, General Electric, Milwaukee, WI) [Katsunuma et al., 2002; Price et al., 2001]. PVC-vinyl acoustic foam insula-

---

tors, positioned between the gradient coils and shimming coils, reduce acoustic noise levels by 10 dB during common EPI imaging at 3 T [Foster et al., 2000]. For similar pulse sequences, passive insulation with a fiberglass cylinder mounted directly on the inner warm bore provides approximately 20 dB noise reduction [Mechefske et al., 2002; Moelker et al., 2003b].

An alternative but still experimental solution makes use of the principle of Lorentz force balancing [Bowtell et al., 1995, 1999; Mansfield et al., 1994, 1995, 1998]. In a force balanced coil arrangement, opposite Lorentz forces can mechanically be coupled by embedding the coil in stiff, noncompressive enclosures [Mansfield et al., 1994]. As a result, the opposite forces in the gradient structure will null and cancel [McJury and Shellock, 2000]. Typical force balanced gradient coils have proven good noise attenuation of up to 40 dB at particularly low excitation frequencies of 100 Hz, unfortunately decreasing to 0 dB at 3.5 kHz [Mansfield et al., 1995; Mansfield et al., 1994]. The disappointing results were due to the natural resonance frequencies of the gradient structure that were overlapping the excitation frequencies [Mansfield et al., 1994]. In turn these resonances resulted in phase errors, thus providing less cancellation and even unintended boosting of acoustic amplitudes [Mansfield et al., 1994].

Two recent improvements in the acoustic screening principle should be mentioned. First, the resonance frequencies of the gradient set could be pushed up toward higher frequencies (minimizes phase errors) [Mansfield et al., 1998]. This can be accomplished by either reducing the dimensions of the gradient supports (Fig. 8) or by choosing stiffer materials [Mansfield et al., 1994, 1995, 1998]. Additional screening loops in the assembly may further cancel the resonances of the gradient structure (Fig. 8) [Mansfield et al., 1998]. For such coil arrangements cast in epoxy glass-reinforced material, average noise attenuation of about 35 dB at 3.26 kHz has been reported [Mansfield et al., 2000].

Other important scanner configuration changes are possible in the restriction of eddy currents in both the RF coil and main magnet [Katsunuma et al., 2002]. A typical low acoustic noise RF coil is equipped with thinner copper plates for less induction of eddy currents and independently mounted to the patient bore [Edelstein et al., 2002]. Similarly, eddy currents are sufficiently strong to cause substantial vibrations in the main magnet [Edelstein et al., 2002]; less noise is produced when making the shielding coils (secondary gradient coils) longer than the magnet [Katsunuma et al., 2002]. This construction effectively counteracts eddy current leakage into the main magnet [Katsunuma et al., 2002].

### Passive Noise Reduction

The most widely used approach to counter the effects of scanner noise in fMRI is the simple and economical application of earplugs and/or earmuffs [Dancer et al., 1992; McJury and Shellock, 2000]. Characteristically, these protective devices attenuate proportionally with the frequency [Ravicz et al., 2001]. For example, the exten-

sively used compressional E-A-R foam earplug (Aearo Company, Southbridge, UK) provides noise attenuation of 20 dB at 0.5 kHz and 30 dB at the frequencies >1 kHz [Berger et al., 1998; Ravicz et al., 2001]. Earmuffs show a similar reduction pattern, but with slightly less reduction at frequencies <1 kHz [Berger et al., 1998]. Obviously, the efficacy of passive acoustic screening is restricted to air-conductive hearing. With respect to the close contact of the subject with the mechanically vibrating MR table and imager, bone conduction emerges as a relevant issue in fMRI. Although air-conduction dominates in the absence of hearing protection, bone conduction through head and body become significant when wearing earplugs and earmuffs [Ravicz et al., 2001]. Therefore, combining earplug and earmuff results in a subjective attenuation of only 39-49 dB during EPI noise at >1.9 kHz. This is considerably less than an objective reduction, i.e., recordings made in the external ear canal that excludes bone-conducted noise, of over 60 dB [Foster et al., 2000; Ravicz et al., 2001].

Incorporation of a passive noise attenuating system into a head RF coil has been suggested as a measure to restrict bone-conduction [Talavage et al., 1999]. Ravicz et al. [2001] assessed the attenuation efficacy of combining earmuffs and earplugs with a helmet, and heavy barrier layers of foam composites. Subjective reductions were up to 60 dB with a residual acoustic load that was dominated by body conduction. More commonly used is the application of vacuum-pumped cushions (inside the head coil) filled with, e.g., sand [Monroe et al., 1999] and eventually in combination with earmuffs [Baumgart et al., 1998; Brechmann et al., 2002]. For complete acoustic screening, total encapsulation of the subject might be a viable option providing an additional reduction of 10 dB [McJury and Shellock, 2000].

An issue that has been raised with the use of passive hearing protectors is the possible interference with speech and syllable understanding relevant to auditory fMRI [Brummett et al., 1988; Chambers et al., 2001; Hurwitz et al., 1989; McJury et al., 1997]. Passive devices, however, improve rather than impair speech intelligibility for normal hearing persons in noisy environments [Abel and Spencer, 1997]. The effects of combining passive aids with active noise cancellation on speech are unclear, but evidence suggests that active noise cancellation improves intelligibility by about 10% [Abel and Spencer, 1997]. Another issue with passive noise cancelling devices is the non-uniform attenuation in the frequency domain. Specifically when performing tonotopic mapping studies of the auditory cortex, one should be aware of the frequency distortions of auditory stimuli. This issue might be circumvented by frequency-specific compensation of the stimuli in the audio system. Also, the integration of probe tubes in earplugs or earmuffs for pneumatic-driven sound delivery is helpful. With such devices, auditory stimuli can be conducted to the subject's auditory pathway relatively unattenuated, thereby not impeding stimulus perception. Other concerns with hearing protectors are discomfort and variations in individual fitting. Deep insertion of an earplug, for example, reduces low frequencies (<500 Hz) better than a "partially" inserted earplug [Berger et al.,

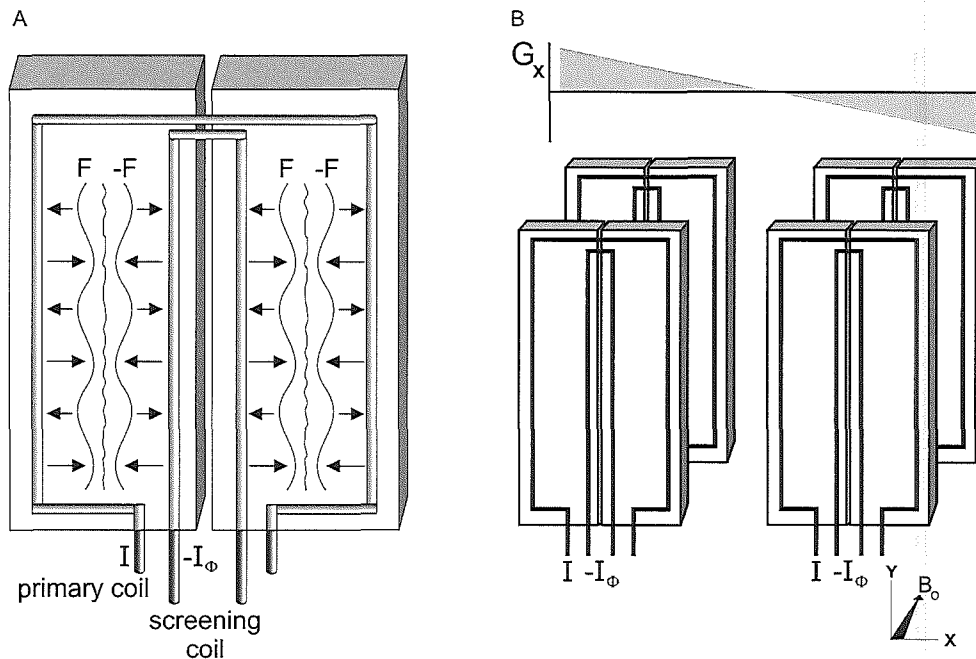


**Figure 8.**

**A:** Improved principle of acoustic screening by force balancing: small coil dimension and an additional screening coil. The amplitude and phase of the screening currents should be adjusted for optimal acoustic noise reduction. **B:** Four-sector gradient coil for generation of x-, y-, or z-gradient (x-gradient in this figure).  $F$ , Lorentz forces acting on gradient coil wires induced by the gradient current  $I$ .

1998; Dancer et al., 1992; McJury et al., 2000; Ravicz et al., 2001].

### Active Noise Cancellation

Additional noise reduction can be achieved by the incorporation of Active Noise Cancellation (ANC) techniques into passive hearing protectors. Active noise cancellation reduces acoustic noise by the introduction of a sound that is exactly the inverse of the original noise [Goldman et al., 1989]. An ANC system makes use of either feedback or feedforward mechanisms [Chen et al., 1999; McJury et al., 1997].

The feedback ANC strategy is used in many commercial headsets (although not yet commercially available for use in MRI) and encompasses an error microphone for capturing residual noise close to the subject's ear, and a processing unit that generates the anti-sound. Previously, moderate decreases in the perceived noise level (11.1 dB) during both spin-echo and gradient-echo pulse sequences have been measured for frequencies of <500 Hz [Goldman et al., 1989]. Implementation of self-adapting neural networks for further error minimization demonstrated extended noise extinction to about 20 dB while clearly preserving added speech [Chen et al., 1999]. A problem of feedback ANC in auditory fMRI is a result of the short distance between the error microphone and the subject's ear, causing cancellation of both the MR-related acoustic noise and, more importantly, acoustic stimuli [Chambers et al., 2001].

In feedforward ANC, the microphone is placed close

to the noise source and the anti-noise is injected into the noise propagation path [Chen et al., 1999]. Because the timings and amplitudes of the gradient noise during fMRI are very predictable [Edelstein et al., 2002], a feedforward strategy seems preferable to the feedback strategy [Ravicz et al., 2000]. Noise reductions of up to 40 dB for frequencies between 0.5 and 3 kHz have been reported [Chambers et al., 2001]. The subjective performance during EPI (that includes bone conduction) was substantially worse with reductions of only 12 and 5 dB at 0.6 and 1.9 kHz, respectively [Chambers et al., 2001].

A technique analogous to ANC is active structural acoustic control (ASAC) that might be a novel solution to the acoustic problem in fMRI. This method makes use of panels with vibro-acoustic sensors and active actuators that introduce anti-vibrations (similar to anti-noise but in materials other than air) [Berry, 2001]. Such active panels, combined with passive insulators, could theoretically replace the currently used inner and outer shroud materials of the MR imager, thereby providing SPL reductions over a large frequency range.

In summary, ANC is a promising technique that substantially lessens the imager noise levels, especially at lower frequencies <1 kHz. Considering the current trend toward faster imaging techniques with consequently more intense noise at higher frequencies, the application of ANC in fMRI may become less effective. Combining ANC with passive measures has proven beneficial in terms of the quality of sound (timbre), because of their complementary frequency characteristics [Abel and Spencer, 1999].

---

## CONCLUSIONS

MR-related acoustic noise has demonstrable effects on fMRI of the auditory cortex. Its interference with auditory functional experiments is primarily a result of direct cortical activation. With respect to the nonauditory cortices, the empirical data to date are limited and sometimes contradictory, therefore more experiments are necessary to better elucidate the effects of MR-related acoustic noise. The answer to this problem may be in the design of a silent functional paradigm that controls the (psycho-) acoustic interferences that play a role in the non-auditory cortices.

The current trend toward clinical fMRI and cognitive research makes the acoustic problem more relevant. In neurodegenerative diseases (e.g., Alzheimer's disease) and psychiatric diseases (e.g., schizophrenia), fixation and attention to stimuli is complicated [Mathiak et al., 2002]. In such patients, the confounding effects of MR-generated acoustic noise on functional data acquisitions are, therefore, likely to be of greater magnitude. In addition, fMRI plays an increasing role in planning of surgical procedures in the brain, i.e., by delineating diseased from normal tissue [Sunaert and Yousry, 2001]. Impaired statistical inferences from functional images due to artifactual absence of activation might potentially cause normal tissue to be considered diseased. Besides the trend toward clinical imaging, technical developments in magnetic resonance imaging considerably boost the acoustic noise levels and subsequently its effects in fMRI. Until now, most of the fMRI research has been carried out on 1.5 T systems, but the current need for higher field strengths and stronger gradients will lead to substantially more intense scanner noise that may counteract the efforts to reduce acoustic noise.

Various methods to reduce acoustic noise may help to provide artifact-free fMRI. The efficacy of these measures is, unfortunately, interdependent. For example, derating gradient currents through silent imaging designs lowers the frequency distribution of scanner noise, but thereby also confines the acoustic benefits of passive barrier materials (less reduction at lower frequencies). Consequently, the simultaneous application of both, results in less reduction of the sound intensity than one would expect based on the reduction that can be gained for each method separately. The use of earplugs or earmuffs is currently the most widely used approach to soften the MR-related acoustic noise to sufficiently low levels. From the hardware engineering perspective, successful advances in noise reduction are primarily in the application of vacuum enclosures with passive acoustic liners. These developments, specifically the hardware modifications, should allow for quieter MRI scanners that enable fast (conventional) fMRI unhampered by MR-related acoustic noise.

## REFERENCES

- Abel SM, Spencer DL (1999): Speech understanding in noise with earplugs and muffs in combination. *Appl Acoust* 57:61-68.
- Abel SM, Spencer DL (1997): Active noise reduction versus conventional hearing protection. Relative benefits for normal-hearing and impaired listeners. *Scand Audiol* 26:155-167.
- Amaro E, Brammer MJ, Cruz AC, Trezza PM, Leite CC, CerriGG (2001): Comparing silent event related fMRI to normal acquisitions. *Proceedings of the 87th Scientific Assembly and Annual Meeting, Chicago, IL*, p 137.
- Amaro E, Williams SC, Shergill SS, Fu CH, MacSweeney M, Picchioni MM, Brammer MJ, McGuire PK (2002): Acoustic noise and functional magnetic resonance imaging: Current strategies and future prospects. *J Magn Reson Imaging* 16:497-510.
- American National Standard (1995): Measurement of sound pressure levels in air. Melville, NY: Acoustical Society of America: S1.13-1995
- American National Standard S3.44-1996 (1996): Determination of occupational noise exposure and estimation of noise-induced hearing impairment. Melville, NY: Acoustical Society of America.
- Backes WH, van Dijk P (2002): Simultaneous sampling of event-related BOLD responses in auditory cortex and brainstem. *Magn Reson Med* 47:90-96.
- Bandettini PA, Cox RW (2000): Event-related fMRI contrast when using constant interstimulus interval: theory and experiment. *Magn Reson Med* 43:540-548.
- Bandettini PA, Jesmanowicz A, Van Kylen J, Birn RM, Hyde JS (1998): Functional MRI of brain activation induced by scanner acoustic noise. *Magn Reson Med* 39:410-416.
- Baumgart F, Kaulisch T, Tempelmann C, Gaschler-Markefski B, Tegeler C, Schindler F, Stiller D, Scheich H (1998): Electro-dynamic headphones and woofers for application in magnetic resonance imaging scanners. *Med Phys* 25:2068-2070.
- Belin P, Zatorre RJ, Hoge R, Evans AC, Pike B (1999): Event-related fMRI of the auditory cortex. *Neuroimage* 10:417-429.
- Belliveau JW, Kennedy DN, McKinstry RC, Buchbinder BR, Weisskoff RM, Cohen MS, Vevea JM, Brady TJ, Rosen BR (1991): Functional mapping of the human visual cortex by magnetic resonance imaging. *Science* 254:716-719.
- Berger EH, Franks JR, Behar A, Casali JG, Dixon-Ernst C, Kieper RW, Merry CJ, Mozo BT, Nixon CW, Ohlin D, Royster JD, Royster LH (1998): Development of a new standard laboratory protocol for estimating the field attenuation of hearing protection devices. Part III. The validity of using subject-fit data. *J Acoust Soc Am* 103:665-672.
- Berman RA, Colby CL (2002): Auditory and visual attention modulate motion processing in area MT+. *Cogn Brain Res* 14:64-74.
- Bernal B, Altman NR (2001): Auditory functional MR imaging. *Am J Roentgenol* 176:1009-1015.
- Berry A (2001): Advanced sensing strategies for the active control of vibration and structural radiation. *Noise Control Eng J* 49:54-65.
- Bilecen D, Radu EW, Scheffler K (1998a): The MR tomograph as a sound generator: fMRI tool for the investigation of the auditory cortex. *Magn Reson Med* 40:934-937.
- Bilecen D, Scheffler K, Schmid N, Tschopp K, Seelig J (1998b): Tonotopic organization of the human auditory cortex as detected by BOLD-fMRI. *Hear Res* 126:19-27.
- Binder JR, Frost JA, Hammel TA, Cox RW, Rao SM, Prieto T (1997): Human brain language areas identified by functional magnetic resonance imaging. *J Neurosci* 17:353-362.
- Birn RM, Bandettini PA, Cox RW, Shaker R (1999): Event related fMRI of tasks involving brief motion. *Hum Brain Mapp* 7:106-114.
- Bowtell R, Peters (1999): Analytic approach to the design of transverse gradient coils with co-axial return paths. *Magn Reson Med* 41:600-608.
- Bowtell RW, Mansfield P (1995): Quiet transverse gradient coils: Lorentz force balanced designs using geometrical similitude. *Magn Reson Med* 34:494-497.
- Brechmann A, Baumgart F, Scheich H (2002): Sound-level-dependent representation of frequency modulations in human auditory cortex: a low-noise fMRI study. *J Neurophysiol* 87:423-433.
- Brummett RE, Talbot JM, Charuhas P (1988): Potential hearing loss resulting from MR imaging. *Radiology* 169:539-540.
- Burke, M, Schwindt W, Ludwig U, Hennig J, Hoehn M (2000): Facilitation of electric forepaw stimulation-induced somatosensory activation in rats by additional acoustic stimulation: an fMRI investigation. *Magn Reson Med* 44:317-321.
- Cacace AT, Tasciyan T, Cousins JP (2000): Principles of functional magnetic resonance imaging: application to auditory neuroscience. *J Am Acad Audiol* 11:239-272.
- Calvert GA, Brammer MJ, Bullmore ET, Campbell R, Iversen SD, Da-



- vid AS (1999): Response amplification in sensory-specific cortices during cross modal binding. *Neuroreport* 10:2619-2623.
- Campeau NG, Huston J, Bernstein MA, Lin C, Gibbs GF (2001): Magnetic resonance angiography at 3.0 Tesla: initial clinical experience. *Top Magn Reson Imaging* 12:183-204.
- Chambers J, Akeroyd MA, Summerfield AQ, Palmer AR (2001): Active control of the volume acquisition noise in functional magnetic resonance imaging: method and psychoacoustical evaluation. *J Acoust Soc Am* 110:304-3054.
- Chen CK, Chiueh TD, Chen JH (1999): Active cancellation system of acoustic noise in MR imaging. *IEEE Trans Biomed Eng* 46:186-191.
- Cho ZH, Chung SC, Lim DW, Wong EK (1998): Effects of the acoustic noise of the gradient systems on fMRI: a study on auditory, motor, and visual cortices. *Magn Reson Med* 39:331-335.
- Cho ZH, Park SH, Kim JH, Chung SC, Chung ST, Chung JY, Moon CW, Yi JH, Sin CH, Wong EK (1997): Analysis of acoustic noise in MRI. *Magn Reson Imaging* 15:815-822.
- Counter SA, Borg E (1993): Acoustic middle ear muscle reflex protection against magnetic coil impulse noise. *Acta Otolaryngol* 113:483-488.
- Counter SA, Olofsson A, Grahn HF, Borg E (1997): MRI acoustic noise: sound pressure and frequency analysis. *J Magn Reson Imaging* 7:606-611.
- Cremillieux, Y, Wheeler-Kingshott CA, Briguet A, Doran SJ (1997): STEAM-Burst: a single-shot, multi-slice imaging sequence without rapid gradient switching. *Magn Reson Med* 38:645-652.
- Dancer A, Grateau P, Cabanis A, Barnabe G, Cagnin G, Vaillant T, Lafont D (1992): Effectiveness of earplugs in high-intensity impulse noise. *J Acoust Soc Am* 91:1677-1689.
- Dantendorfer K, Amering M, Bankier A, Helbich T, Prayer D, Youssefzadeh S, Alexandrowicz R, Imhof H, Katschnig H (1997): A study of the effects of patient anxiety, perceptions and equipment on motion artifacts in magnetic resonance imaging. *Magn Reson Imaging* 15:301-306.
- de Zwart JA, van Gelderen P, Kellman P, Duyn JH (2002): Reduction of gradient acoustic noise in MRI using SENSE-EPI. *Neuroimage* 16:1151-1155.
- Di Salle F, Formisano E, Seifritz E, Linden DE, Scheffler K, Saulino C, Tedeschi G, Zanella FE, Pepino A, Goebel R, Marciano E (2001): Functional fields in human auditory cortex revealed by time-resolved fMRI without interference of EPI noise. *Neuroimage* 13:328-338.
- Duong TQ, Kim DS, Ugurbil K, Kim SG (2000): Spatiotemporal dynamics of the BOLD fMRI signals: toward mapping submillimeter cortical columns using the early negative response. *Magn Reson Med* 44:231-242.
- Edelstein WA, Hedeon RA, Mallozzi RP, El-Hamamsy SA, Ackermann RA, Havens TJ (2002): Making MRI quieter. *Magn Reson Imaging* 20:155-163.
- Eden GF, Joseph JE, Brown HE, Brown CP, Zeffiro TA (1999): Utilizing hemodynamic delay and dispersion to detect fMRI signal change without auditory interference: the behavior interleaved gradients technique. *Magn Reson Med* 41:13-20.
- Edmister WB, Talavage TM, Ledden PJ, Weisskoff RM (1999): Improved auditory cortex imaging using clustered volume acquisitions. *Hum Brain Mapp* 7:89-97.
- Ehret G (1997): The auditory cortex. *J Comp Physiol [A]* 181:547-557.
- Elliott MR, Bowtell RW, Morris PG (1999): The effect of scanner sound in visual, motor, and auditory functional MRI. *Magn Reson Med* 41:1230-1235.
- Engelien A, Yang Y, Engelen W, Zonana J, Stern E, Silbersweig DA (2002): Physiological mapping of human auditory cortices with a silent event-related fMRI technique. *Neuroimage* 16:944-953.
- Escera C, Alho K, Winkler I, Naatanen R (1998): Neural mechanisms of involuntary attention to acoustic novelty and change. *J Cogn Neurosci* 10:590-604.
- Formisano E, Linden DE, Di Salle F, Trojano L, Esposito F, Sack AT, Grossi D, Zanella FE, Goebel R (2002): Tracking the mind's image in the brain I: time-resolved fMRI during visuospatial mental imagery. *Neuron* 35:185-194.
- Foster JR, Hall DA, Summerfield AQ, Palmer AR, Bowtell RW (2000): Sound-level measurements and calculations of safe noise dosage during EPI at 3 T. *J Magn Reson Imaging* 12:157-163.
- Frisina RD (2001): Subcortical neural coding mechanisms for auditory temporal processing. *Hear Res* 158:1-27.
- Girard F, Marcar VL, Hennel F, Martin E (2000): Anatomic MR images obtained with silent sequences. *Radiology* 216:900-902.
- Goldman AM, Gossman WE, Friedlander PC (1989): Reduction of sound levels with anti-noise in MR imaging. *Radiology* 173:549-550.
- Hall DA, Haggard MP, Akeroyd MA, Palmer RA, Summerfield AQ, Elliott MR, Gurney EM, Bowtell RW (1999): "Sparse" temporal sampling in auditory fMRI. *Hum Brain Mapp* 7:213-223.
- Hall DA, Haggard MP, Summerfield AQ, Akeroyd MA, Palmer AR, Bowtell RA (2001): Functional magnetic resonance imaging measurements of sound-level encoding in the absence of background scanner noise. *J Acoust Soc Am* 109:1559-1570.
- Hall DA, Summerfield AQ, Goncalves MS, Foster JR, Palmer AR, Bowtell RW (2000a): Time-course of the auditory BOLD response to scanner noise. *Magn Reson Med* 43:601-606.
- Hall WA, Liu H, Martin AJ, Pozza CH, Maxwell RE, Truwit CL (2000b): Safety, efficacy, and functionality of high-field strength interventional magnetic resonance imaging for neurosurgery. *Neurosurgery* 46:632-642.
- Hari R, Makela JP (1988): Modification of neuromagnetic responses of the human auditory cortex by masking sounds. *Exp Brain Res* 71:87-92.
- Hedeon RA, Mallozzi R, Edelstein WA, Havens T (2001): Vibroacoustic modeling of noise in magnetic resonance imagers. Proceedings of the 9th Annual Meeting of the International Society of Magnetic Resonance in Medicine, Glasgow, UK. p 1751.
- Hedeon RA, Edelstein WA (1997): Characterization and prediction of gradient acoustic noise in MR imagers. *Magn Reson Med* 37:7-10.
- Hennel F (2000): Acoustic optimisation of rapid MRI. Proceedings of the 8th Annual Meeting of the International Society of Magnetic Resonance in Medicine, Denver, CO. p 2010.
- Hennel F (2001): Fast spin echo and fast gradient echo MRI with low acoustic noise. *J Magn Reson Imaging* 13:960-966.
- Hennel F, Girard F, Loenneker T (1999): "Silent" MRI with soft gradient pulses. *Magn Reson Med* 42:6-10.
- Hennig J, Hodapp M (1993): Burst imaging. *MAGMA* 1:39-48.
- Hu X, Le TH, Ugurbil K (1997): Evaluation of the early response in fMRI in individual subjects using short stimulus duration. *Magn Reson Med* 37:877-884.
- Hurwitz R, Lane SR, Bell RA, Brant-Zawadzki MN (1989): Acoustic analysis of gradient-coil noise in MR imaging. *Radiology* 173: 545-548.
- Jakob PM, Schlaug G, Griswold M, Lovblad KO, Thomas R, Ives JR, Matheson JK, Edelman RR (1998): Functional burst imaging. *Magn Reson Med* 40:614-621.
- Jancke L, Mirzazade S, Shah NJ (1999): Attention modulates activity in the primary and the secondary auditory cortex: a functional magnetic resonance imaging study in human subjects. *Neurosci Lett* 266:125-128.
- Jancke L, Shah NJ, Posse S, Grosse-Ryukun M, Muller-Gartner HW (1998): Intensity coding of auditory stimuli: an fMRI study. *Neuropsychologia* 36:875-883.
- Josephs O, Henson RN (1999): Event-related functional magnetic resonance imaging: modelling, inference and optimization. *Philos Trans R Soc Lond B Biol Sci* 354:1215-1228.
- Katsunuma A, Takamori H, Sakakura Y, Hamamura Y, Ogo Y, Katayama R (2002): Quiet MRI with novel acoustic noise reduction. *MAGMA* 13:139-144.
- Le TH, Patel S, Roberts TP (2001): Functional MRI of human auditory cortex using block and event-related designs. *Magn Reson Med* 45:254-260.
- Liebenthal E, Binder JR, Piorowski RL, Remez RE (2003): Shortterm reorganization of auditory analysis induced by phonetic experience. *J Cogn Neurosci* 15:549-558.
- Loenneker T, Hennel F, Ludwig U, Hennig J (2001): Silent BOLD imaging. *MAGMA* 13:76-81.
- Lovblad KO, Thomas R, Jakob PM, Scammell T, Bassetti C, Griswold M, Ives J, Matheson J, Edelman RR, Warach S (1999): Silent functional magnetic resonance imaging demonstrates focal activation in rapid eye movement sleep. *Neurology* 53:2193-2195.
- Ludwig U, Loenneker T, Hennel F, Hennig J (1999): Getting rid of acoustic noise: functional MRI with silent simultaneous multislice excitation gradient-echo (SIMEX) sequences. Proceedings of the 7th Annual Meeting of the International Society of Magnetic Resonance in Medicine, Philadelphia, PA. p 1662.



- Maeder PP, Meuli RA, Adriani M, Bellmann A, Fornari E, Thiran JP, Pittet A, Clarke S (2001): Distinct pathways involved in sound recognition and localization: a human fMRI study. *Neuroimage* 14:802-816.
- Mansfield P, Chapman BL, Bowtell R, Glover P, Coxon R, Harvey PR (1995): Active acoustic screening: reduction of noise in gradient coils by Lorentz force balancing. *Magn Reson Med* 33:276-281.
- Mansfield P, Glover P, Bowtell R (1994): Active rapid acoustic screening: design principles for quiet gradient coils in MRI. *Meas Sci Technol* 5:1021-1025.
- Mansfield P, Glover PM, Beaumont J (1998): Sound generation in gradient coil structures for MRI. *Magn Reson Med* 39:539-550.
- Mansfield P, Haywood B (2000): Principles of active acoustic control in gradient coil design. *MAGMA* 10:147-151.
- Mathiak K, Rapp A, Kircher TT, Grodd W, Hertrich I, Weiskopf N, Lutzenberger W, Ackermann H (2002): Mismatch responses to randomized gradient switching noise as reflected by fMRI and whole-head magneto-encephalography. *Hum Brain Mapp* 16:190-195.
- Mattay VS, Weinberger DR (1999): Organization of the human motor system as studied by functional magnetic resonance imaging. *Eur J Radiol* 30:105-114.
- Mazard A, Mazoyer B, Etard O, Tzourio-Mazoyer N, Kosslyn SM, Mellet E (2002): Impact of fMRI acoustic noise on the functional anatomy of visual mental imagery. *J Cogn Neurosci* 14:172-186.
- McJury M, Blug A, Joerger C, Condon B, Wyper D (1994): Short communication: acoustic noise levels during magnetic resonance imaging scanning at 1.5 T. *Br J Radiol* 67:413-415.
- McJury M, Shellock FG (2000): Auditory noise associated with MR procedures: a review. *J Magn Reson Imaging* 12:37-45.
- McJury M, Stewart RW, Crawford D, Toma E (1997): The use of active noise control (ANC) to reduce acoustic noise generated during MRI scanning: some initial results. *Magn Reson Imaging* 15:319-322.
- McJury M (1995): Acoustic noise levels generated during high field MR imaging. *Clin Radiol* 50:331-334.
- Mechefske CK, Geris R, Gati JS, Rutt BK (2002): Acoustic noise reduction in a 4 T MRI scanner. *MAGMA* 13:172-176.
- Miyati T, Banno T, Fujita H, Mase M, Narita H, Imazawa M, Ohba S (1999): Acoustic noise analysis in echo planar imaging: multicenter trial and comparison with other pulse sequences. *IEEE Trans Med Imaging* 18:733-736.
- Miyati T, Banno T, Fujita H, Mase M, Narita H, Imazawa M, Sanada S, Koshida K, Kasuga T (2001): Characteristics of acoustic noise in echo-planar imaging. *Front Med Biol Eng* 10:345-356.
- Moelker A, Wielopolski PA, Pattynama PMT (2003a): Relationship between magnetic field strength and MR-related acoustic noise levels. *MAGMA* 16:52-55.
- Moelker A, Vogel MW, Pattynama PMT (2003b): Efficacy of passive acoustic screening in the MR-Environment: Implications for the design of imager and MR-suite. *J Magn Reson Imaging* 17:270-275.
- Monroe JW, Holtman R, Holtman K, Schmalbrock P, Clymer BD (1999): Evaluation of various materials for acoustic noise attenuation in MRI. Proceedings of the 7th Annual Meeting of the International Society of Magnetic Resonance in Medicine, Glasgow, UK. p 101.
- Oesterle C, Hennel F, Hennig J (2001): Quiet imaging with interleaved spiral read-out. *Magn Reson Imaging* 19:1333-1337.
- Oesterle C, Hennel F, Kraemer F, Hennig J (1999): Silent spiral imaging. *MAGMA* 8:S479.
- Ogawa S., Lee TM, Kay AR, Tank DW (1990): Brain magnetic resonance imaging with contrast dependent on blood oxygenation. *Proc Natl Acad Sci USA* 87:9868-9872.
- Ogawa S, Menon RS, Tank DW, Kim SG, Merkle H, Ellermann JM, Ugurbil K (1993): Functional brain mapping by blood oxygenation level-dependent contrast magnetic resonance imaging. A comparison of signal characteristics with a biophysical model. *Biophys J* 64:803-812.
- Opitz B, Rinne T, Mecklinger A, von Cramon DY, Schroger E (2002): Differential contribution of frontal and temporal cortices to auditory change detection: fMRI and ERP results. *Neuroimage* 15:167-174.
- Oxenham AJ, Plack CJ (1998): Suppression and the upward spread of masking. *J Acoust Soc Am* 104:3500-3510. Parrish T (1999): Functional MR imaging. *Magn Reson Imaging Clin N Am* 7:765-782.
- Pascal J, Bourgeade A, Lagier M, Legros C (1998): Linear and nonlinear model of the human middle ear. *J Acoust Soc Am* 104:1509-1516.
- Pfleiderer B, Michael N, Ostermann J, Soros P, Heindel W (2002): Visualization of auditory habituation by means of fMRI. Proceedings of the 10th Annual Meeting of the International Society of Magnetic Resonance in Medicine, Honolulu, HI. p 1470.
- Price DL, De Wilde JP, Papadaki AM, Curran JS, Kitney RI (2000): Frequency analysis of MRI acoustic noise. Proceedings of the 8th Annual Meeting of the International Society of Magnetic Resonance in Medicine, Denver, CO. p 2008.
- Price DL, De Wilde JP, Papadaki AM, Curran JS, Kitney RI (2001): Investigation of acoustic noise on 15 MRI scanners from 0.2 T to 3 T. *J Magn Reson Imaging* 13:288-293.
- Prieto TE (1999): Acoustic noise levels in head gradient coils during EPI as a function of frequency encoding direction. Proceedings of the 7th Annual Meeting of the International Society of Magnetic Resonance in Medicine, Philadelphia, PA. p 105.
- Prieto TE, Bennet K, Weyers D (1998): Acoustic noise levels in a head gradient coil during echo planar imaging at 3T. Proceedings of the 6th Annual Meeting of the International Society of Magnetic Resonance in Medicine, Sydney, Australia. p 750.
- Quirk ME, Letendre AJ, Ciottone RA, Lingley JF (1989): Anxiety in patients undergoing MR imaging. *Radiology* 170:463-466.
- Ravicz ME, Melcher JR (2001): Isolating the auditory system from acoustic noise during functional magnetic resonance imaging: examination of noise conduction through the ear canal, head, and body. *J Acoust Soc Am* 109:216-231.
- Ravicz ME, Melcher JR, Kiang NY (2000): Acoustic noise during functional magnetic resonance imaging. *J Acoust Soc Am* 108: 1683-1696.
- Robson MD, Dorosz JL, Gore JC (1998): Measurements of the temporal fMRI response of the human auditory cortex to trains of tones. *Neuroimage* 7:185-198.
- Rosen BR, Buckner RL, Dale AM (1998): Event-related functional MRI: past, present, and future. *Proc Natl Acad Sci USA* 95:773-780.
- Scheffler K, Bilecen D, Schmid N, Tschopp K, Seelig J (1998): Auditory cortical responses in hearing subjects and unilateral deaf patients as detected by functional magnetic resonance imaging. *Cereb Cortex* 8:156-163.
- Scheich H, Baumgart F, Gaschler-Markefski B, Tegeler C, Tempelmann C, Heinze HJ, Schindler F, Stiller D (1998): Functional magnetic resonance imaging of a human auditory cortex area involved in foreground-background decomposition. *Eur J Neurosci* 10:803-809.
- Seto E, Sela G, McIlroy WE, Black SE, Staines WR, Bronskill MJ, McIntosh AR, Graham SJ (2001): Quantifying head motion associated with motor tasks used in fMRI. *Neuroimage* 14:284-297.
- Shah NJ, Jancke L, Grosse-Ruyken ML, Muller-Gartner HW (1999): Influence of acoustic masking noise in fMRI of the auditory cortex during phonetic discrimination. *J Magn Reson Imaging* 9:19-25.
- Shah NJ, Steinhoff S, Mirzazade S, Zafiris O, Grosse-Ruyken ML, Jancke L, Zilles K (2000): The effect of sequence repeat time on auditory cortex stimulation during phonetic discrimination. *Neuroimage* 12:100-108.
- Shapleske J, Rossell SL, Woodruff PW, David AS (1999): The planum temporale: a systematic, quantitative review of its structural, functional and clinical significance. *Brain Res Rev* 29:26-49.
- Shellock FG, Morisoli SM, Ziarati M (1994): Measurement of acoustic noise during MR imaging: evaluation of six "worst-case" pulse sequences. *Radiology* 191:91-93.
- Shellock FG, Ziarati M, Atkinson D, Chen DY (1998): Determination of gradient magnetic field-induced acoustic noise associated with the use of echo planar and three-dimensional, fast spin echo techniques. *J Magn Reson Imaging* 8:1154-1157.
- Sunaert S, Yousry TA (2001): Clinical applications of functional magnetic resonance imaging. *Neuroimaging Clin N Am* 11:221-236.
- Talavage TM, Edmister WB, Ledden PJ, Weisskoff RM (1998a): Quantification of the impact of fMRI scanner noise on auditory cortex. Proceedings of the 6th Annual Meeting of the International Society of Magnetic Resonance in Medicine. p 1502.
- Talavage TM, Edmister WB (1998b): Saturation and nonlinear fMRI responses in auditory cortex. *Neuroimage* 7:S362.
- Talavage TM, Edmister WB, Ledden PJ, Weisskoff RM (1999): Quantitative assessment of auditory cortex responses induced by imager acoustic noise. *Hum Brain Mapp* 7:79-88.
- Tanaka H, Fujita N, Watanabe Y, Hirabuki N, Takahashi M, Oshiro Y, Nakamura H (2000): Effects of stimulus rate on the auditory cortex using fMRI with 'sparse' temporal sampling. *Neuroreport* 11:2045-

- 
- 2049.
- Ulmer JL, Biswal BB, Mark LP, Mathews VP, Prost RW, Millen SJ, Garman JN, Horzewski D (1998a): Acoustic echoplanar scanner noise and pure tone hearing thresholds: the effects of sequence repetition times and acoustic noise rates. *J Comput Assist Tomogr* 22:480-486.
- Ulmer JL, Biswal BB, Yetkin FZ, Mark LP, Mathews VP, Prost RW, LD Estkowski, McAuliffe TL, Haughton VM, Daniels DL (1998b): Cortical activation response to acoustic echo planar scanner noise. *J Comput Assist Tomogr* 22:111-119.
- Vouloumanos A, Kiehl KA, Werker JF, Liddle PF (2001): Detection of sounds in the auditory stream: event-related fMRI evidence for differential activation to speech and nonspeech. *J Cogn Neurosci* 13:994-1005.
- Woldorff MG, Gallen CC, Hampson SA, Hillyard SA, Pantev C, Sobel D, Bloom FE (1993): Modulation of early sensory processing in human auditory cortex during auditory selective attention. *Proc Natl Acad Sci USA* 90:8722-8726.
- Yacoub E, Hu X (2001b): Detection of the early decrease in fMRI signal in the motor area. *Magn Reson Med* 45:184-190.
- Yacoub E, Le TH, Ugurbil K, Hu X (1999): Further evaluation of the initial negative response in functional magnetic resonance imaging. *Magn Reson Med* 41:436-441.
- Yacoub E, Shmuel A, Pfeuffer J, Van De Moortele PF, Adriany G, Andersen P, Vaughan JT, Merkle H, Ugurbil K, Hu X (2001a): Imaging brain function in humans at 7 Tesla. *Magn Reson Med* 45:588-594.
- Yang Y, Engelien A, Engelien W, Xu S, Stern E, Silbersweig DA (2000): A silent event-related functional MRI technique for brain activation studies without interference of scanner acoustic noise. *Magn Reson Med* 43:185-190.

# Chapter 6

MAGMA (2003) 16:52-55  
DOI 10.1007/s10334-003-0005-9

RESEARCH ARTICLE

Adriaan Moelker  
Piotr A. Wielopolski  
Peter M. T. Pattynama

## Relationship between magnetic field strength and magnetic-resonance-related acoustic noise levels

Received: 29 July 2002  
Accepted: 20 September 2002  
Published online: 18 February 2003  
ESMRMB 2003

Correspondence to: A. Moelker  
Department of Radiology,  
Erasmus Medical Center Rotterdam, 50  
Dr. Molewaterplein,  
3000 DR Rotterdam, The Netherlands  
e-mail: a.moelker@erasmusmc.nl  
Tel.: +31-10-4088001  
Fax: +31-10-4089467

**Abstract** The need for better signal-to-noise ratios and resolution has pushed magnetic resonance imaging (MRI) towards high-field MR scanners for which only little data on MR-related acoustic noise production have been published. The purpose of this study was to validate the theoretical relationship of sound pressure level (SPL) and static magnetic field strength. This is relevant for allowing adequate comparisons of acoustic data of MR systems at various magnetic field strengths. Acoustic data were acquired during various pulse sequences at field strengths of 0.5, 1.0, 1.5 and 2.0 Tesla using the same MRI unit by means of a Helicon rampable magnet. Continuous-equivalent, time-averaged,

linear SPLs and 1/3-octave band frequencies were recorded. Ramping from 0.5 to 1.0 Tesla and from 1.0 to 2.0 Tesla resulted in an SPL increase of 5.7 and 5.2 dB(L), respectively, when averaged over the various pulse sequences. Most of the acoustic energy was in the 1-kHz frequency band, irrespective of magnetic field strength. The relation between field strength and SPL was slightly non-logarithmic, i.e. less increase at higher field strengths, presumably caused by the elastic properties of the gradient coil encasings.

**Keywords** Acoustic noise · Magnetic field strength · Sound pressure level

### Introduction

Acoustic noise production during magnetic resonance imaging (MRI) is a well-recognized issue of concern [1]. It has been demonstrated to cause, e.g. temporary shifts in hearing thresholds and disturbance of verbal communication [2, 3, 4]. Also, acoustic noise may affect image quality in functional MRI studies [5].

Various studies have reported on acoustic noise levels and on their relation to pulse sequences and imaging parameters for clinically used MR systems of up to 1.5 Tesla [2, 3, 6, 7, 8, 9, 10, 11]. However, the current trend in MRI is towards using high-field MR systems at which acoustic noise levels are thought to be elevated. Only a few studies, to our knowledge, report on noise levels for MR systems at 3 Tesla, restricted to echo planar imaging [12, 13]. However, for adequate comparison of the properties of MR-related acoustic noise, the influence of the magnetic field strength on acoustic noise should be known. Moreover, previous data on noise levels at lower

magnetic field strengths may still be valuable if the relationship is used for cautious extrapolation.

The relation between magnetic field strength and acoustic noise, which according to theory is logarithmic [14], has not been experimentally validated yet. This was the purpose of our study.

#### *Theoretical prediction of the relation between magnetic field strength and acoustic noise*

Acoustic noise is thought to be generated by bending of gradient coils induced by Lorentz forces ( $F$ ) acting on these coils during MRI. The magnitude of these forces acting on a wire element with length  $dl$  is described by Eq. 1 [14]:

$$F = B_0 \cdot Idl \quad (1)$$

where  $B_0$  is the magnetic field strength and  $I$  is the gradient current. The induced mechanical waves in the gradient-supporting structures are transferred into air, des-

**Table 1** Imaging parameters of the pulse sequences tested

Sequence	Imaging parameters				
	TR (ms)	FOV (mm)	Matrix	Slice thickness (mm)	Number of slices/s
FSE	22	300	256 x 256	4	0.48
FLASH	7	300	256 x 256	6	0.54
EPI	600	315	128 x 128	3	1.67
tFISP	3.1	160	115 x 128	5	0.85

cribed by an acoustic transfer function [15], resulting in airborne acoustic waves with pressure  $P$ . The linear sound pressure level (SPL), expressed in decibels (dB(L)), is the logarithm of the ratio of this pressure  $P$  to an international standardized reference sound pressure ( $P_0$ ) of 20 micropascals, described in Eq. 2 [16]:

$$SPL = 10 \cdot \log \left( \frac{P}{P_0} \right)^2 \quad (2)$$

Therefore, theoretically, doubling the magnetic field strength (or the gradient current likewise) will result in a doubling of the sound pressure, holding an increase of 6 dB(L).

## Materials and methods

Acoustic data were acquired using a Siemens Magnetom Vision magnetic resonance system (Erlangen, Germany) with a gradient hardware delivering a maximum of 25 mTesla/m gradients and with 85 Tesla/m/s slew rates (rise-time 300  $\mu$ s), and by using an integrated quadrature-driven transceiver body coil. A Helicon rampable magnet was ramped in successive steps of 0.5 Tesla from 0.5 to 2.0 Tesla. Acoustic data were recorded for various pulse sequences, i.e. fast spin-echo (FSE), fast low-angle shot (FLASH), echo-planar imaging (EPI) and true fast-imaging with steady state (tFISP). All imaging parameters in a given pulse sequence were kept equal at the different magnetic field strengths (Table 1) and were measured for all slice slab orientations (axial, sagittal and coronal). This made it possible to preserve the acoustic environment properties while the magnetic field strength was varied in isolation. In addition, the cold-head refrigerator system of this MR system is quiet compared to the cryogen pumping system used in most MR systems, resulting in low background or ambient noise levels.

We measured continuous-equivalent, i.e. time-averaged over a 20-s period, linear SPLs ( $L(L)_{eq}$  in dB(L)), and 1/3-octave band frequencies. The experimental set-up was in compliance with ANSI-protocol S1.13-1995 of the Acoustical Society of America [16, 17], i.e. a vertical positioning of the microphone, as the acoustic environment of the MR suite was thought to be diffuse [4]. Although possible interference of the MR environment with the measurement set-up has been shown to be negligible [4], recordings were made at 1.5 m from the imager bore in order to completely circumvent the magnetic field affecting the microphone (type 4189, Brüel and Kjaer, Naerum, Denmark). It is of note that the relative SPL changes at the various magnetic field strengths are not affected by the distance from the MR imager. The microphone was connected to the sound analyzer equipment (Investigator 2260, Brüel and Kjaer) using a 10-m extension cable (AO-0442, Brüel and Kjaer). Ambient acoustic noise was assumed to be negligible as its SPL was >10dB lower than the SPLs of the imaging pulse sequences during the actual experiments [16]. The experimental set-up was calibrated using

an appropriate sound level calibrator (pistonphone type 4231, Brüel and Kjaer). In a short pilot study, we tested the accuracy of the acoustic data elucidated by repeatedly measuring SPLs for an FSE pulse sequence at fixed magnetic field strength. As these showed variations <0.5 dB(L), all recordings were made once.

## Results

The continuous-equivalent linear SPL had an almost linear relationship with the magnetic field strength on average (Fig. 1). The relation was slightly non-logarithmic, with a smaller increase at higher field strength. Doubling magnetic field strength by ramping up from 0.5 to 1.0 Tesla and from 1.0 to 2.0 Tesla resulted in an average 5.7 and 5.2 dB(L) increase of SPL, respectively ( $p=0.27$ ). This trend was similar for all but one sequence, i.e. the tFISP sequence. Moreover, an increase of about 6 dB(L) for doubling the magnetic field strength was measured for all slice orientations (Fig. 2); the average SPLs for the coronal, sagittal and axial slice orientations at 1.5 Tesla were 92.5, 93.6 and 94.2 dB(L), respectively.

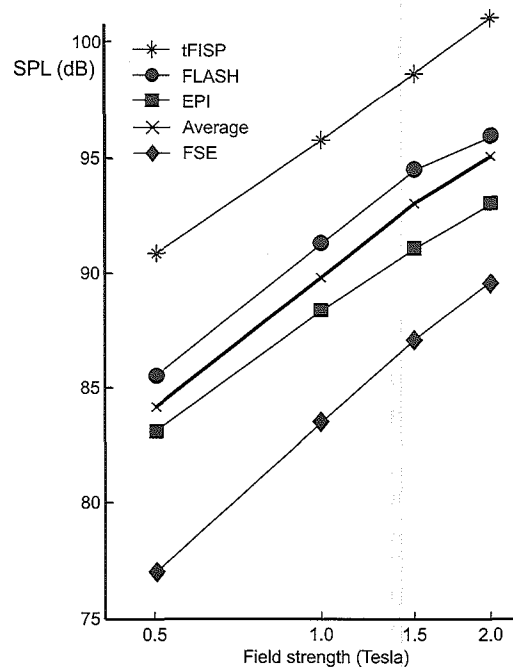


**Fig. 1** Linear continuous-equivalent sound pressure levels (SPLs) at different magnetic field strengths for all imaging sequences measured and their average (thick line). The average curve increases 5.7 dB and 5.2 dB for magnetic fields strength increments of 0.5–1.0 Tesla and 1.0–2.0 Tesla, respectively. Magnetic field strength logarithmically scaled.

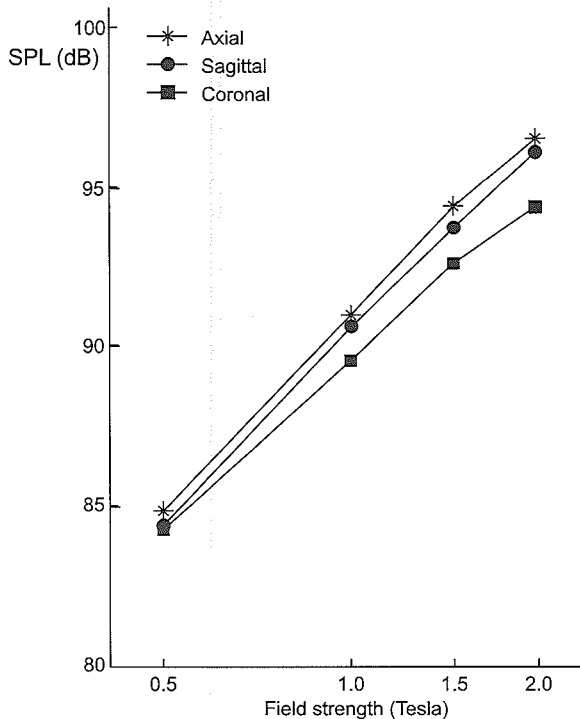


**Fig. 2** Continuous-equivalent linear SPLs for sagittal, coronal and axial imaging as measured for all pulse sequences on average at different magnetic field strengths. Magnetic field strength logarithmically scaled.

Most of the acoustic energy was in the 1-kHz band, which did not substantially change with the magnetic field strength (Fig. 3). Moreover, for all 1/3-octave band frequencies, the above-described trend for the continuous-equivalent SPLs applied. At 100 and 250 Hz, background acoustic noise SPLs were approximately equal to the SPLs of the actual MR sequences (about 40 and 50 dB(L), respectively), resulting seemingly in a lower increase of SPL with magnetic field strength.

## Discussion

In this study, the rampable magnet of our MRI scanner (Siemens Magnetom Vision with Helicon rampable magnet) allowed us to carefully preserve the acoustic environment while changing the magnetic field strength in isolation. This is relevant for measurements of acoustic noise, as it has been demonstrated previously that the type of imager dominates the overall acoustic noise levels [9, 18], that is, the influence of the magnetic field strength on SPL might not adequately be elucidated by comparing various MR systems. The results of our experiments were in good agreement with what theory predicts, i.e. an increase of 6 dB(L) when doubling the magnetic field strength. As this was similar for all imaging protocols tested, it is likely that the trend applies in general, i.e. regardless of the pulse sequence. The small but insignificant flattening of 0.5 dB(L) may tentatively be explained by restriction of extr-

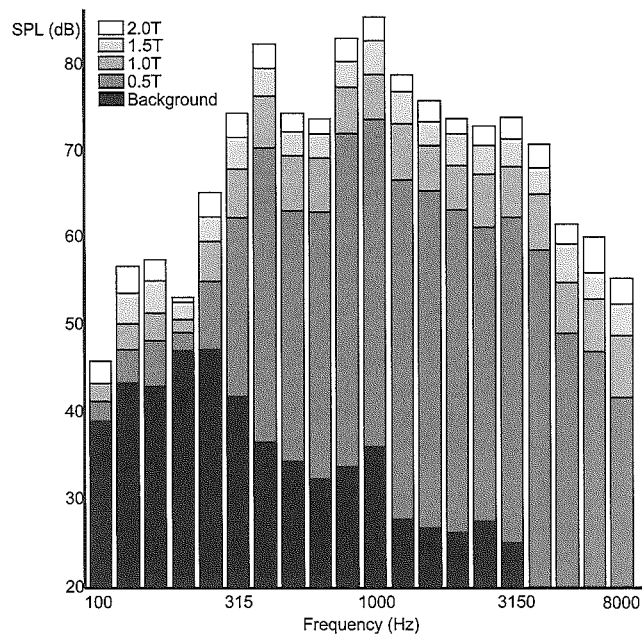


**Fig. 3** Continuous-equivalent SPLs at 1/3-octave band frequencies for all pulse sequences tested (averaged). SPL differences are equal for magnetic field strength changes of 0.5–1.0 Tesla and 1.0–2.0 Tesla. Note the considerable contribution of ambient background acoustic noise to the SPL at 100 and 250 Hz.

eme movements of the gradient coils, probably caused by the elastic properties of the gradient coil encasings. However, we could not substantiate this hypothesis.

The frequency distribution of the pulse sequences tested was similar to that of previous reports [8, 9, 11, 12, 18]. Alterations of the frequency distribution were not expected a priori because of unchanged gradient current pulses and acoustic transfer function [15].

It is of note that the magnitude of the Lorentz forces, producing the acoustic noise, is not dictated by the magnetic field strength solely. It can be appreciated from Eq. 1 that the gradient coil current  $I$  is equally important. In high-field MR systems, the gradient coil systems may encompass stronger gradients in order to circumvent, e.g. chemical shift and susceptibility artifacts. Like the magnetic field strength, a two-fold increase of the gradient strength may elevate SPL by 6 dB(L). Also, simultaneous doubling of both magnetic field strength and gradient strength would result in a 12-dB(L) increase of SPL (Eq. 2). In conclusion, our results may be used for extrapolation of acoustic noise levels for more adequate comparison of MR systems at various magnetic field strengths.

---

## References

1. Brummett RE, Talbot JM, Charuhas P (1988) Potential hearing loss resulting from MR imaging. *Radiology* 169:539-540
2. Hurwitz R, Lane SR, Bell RA, Brant-Zawadzki MN (1989) Acoustic analysis of gradient-coil noise in MR imaging. *Radiology* 173:545-548
3. Shellock FG, Ziarati M, Atkinson D, Chen DY (1998) Determination of gradient magnetic field-induced acoustic noise associated with the use of echo planar and three-dimensional, fast spin echo techniques. *J Magn Reson Imaging* 8:1154-1157
4. Moelker A, Maas RA, Lethimonnier F, Pattynama PMT (2002) Interventional MR Imaging at 1.5 T: quantification of sound exposure. *Radiol* 224:889-895
5. Elliott MR, Bowtell RW, Morris PG (1999) The effect of scanner sound in visual, motor, and auditory functional MRI. *Magn Reson Med* 41:1230-1235
6. Shellock FG, Morisoli SM, Ziarati M (1994) Measurement of acoustic noise during MR imaging: evaluation of six "worst-case" pulse sequences. *Radiology* 191:91-93
7. McJury M, Blug A, Joerger C, Condon B, Wyper D (1994) Short communication: acoustic noise levels during magnetic resonance imaging scanning at 1.5 T. *Br J Radiol* 67:413-415
8. Counter SA, Olofsson A, Grahn HF, Borg E (1997) MRI acoustic noise: sound pressure and frequency analysis. *J Magn Reson Imaging* 7:606-611
9. Cho ZH, Park SH, Kim JH, Chung SC, Chung ST, Chung JY, Moon CW, Yi JH, Sin CH, Wong EK (1997) Analysis of acoustic noise in MRI. *Magn Reson Imaging* 15:815-822
10. Miyati T, Banno T, Fujita H, Mase M, Narita H, Imazawa M, Sanada S, Koshida K, Kasuga T (2001) Characteristics of acoustic noise in echo-planar imaging. *Front Med Biol Eng* 10(4):345-356
11. Ravicz ME, Melcher JR, Kiang NY (2000) Acoustic noise during functional magnetic resonance imaging. *J Acoust Soc Am* 108:1683-1696
12. Foster JR, Hall DA, Summerfield AQ, Palmer AR, Bowtell RW (2000) Sound-level measurements and calculations of safe noise dosage during EPI at 3 T. *J Magn Reson Imaging* 12:157-163
13. Price DL, De Wilde JP, Papadaki AM, Curran JS, Kitney RI (2001) Investigation of acoustic noise on 15 MRI scanners from 0.2 T to 3 T. *J Magn Reson Imaging* 13:288-293
14. Mansfield P, Glover PM, Beaumont J (1998) Sound generation in gradient coil structures for MRI. *Magn Reson Med* 39:539-550
15. Hedeem RA, Edelstein WA (1997) Characterization and prediction of gradient acoustic noise in MR imagers. *Magn Reson Med* 37:7-10
16. American National Standard (1995) S1.13-1995. Measurement of sound pressure levels in air. Acoustical Society of America
17. Beranek L, Istvan L (1992) Noise and vibration control engineering: principles and applications, 2nd edn. Wiley-Interscience, New York
18. Miyati T, Banno T, Fujita H, Mase M, Narita H, Imazawa M, Ohba S (1999) Acoustic noise analysis in echo planar imaging: multicenter trial and comparison with other pulse sequences. *IEEE Trans Med Imaging* 18:733-736

## Technical Note

# Efficacy of Passive Acoustic Screening: Implications for the Design of Imager and MR-Suite

Adriaan Moelker, MD,\* Mika W. Vogel, MSc, and Peter M. T. Pattynama, MD

**Purpose:** To investigate the efficacy of passive acoustic screening in the magnetic resonance (MR) environment by reducing direct and indirect MR-related acoustic noise, both from the patient's and health worker's perspective.

**Materials and Methods:** Direct acoustic noise refers to sound originating from the inner and outer shrouds of the MR imager, and indirect noise to acoustic reflections from the walls of the MR suite. Sound measurements were obtained inside the magnet bore (patient position) and at the entrance of the MR imager (health worker position). Inner and outer shrouds and walls were lined with thick layers of sound insulation to eliminate the direct and indirect acoustic pathways. Sound pressure levels (SPLs) and octave band frequencies were acquired during various MR imaging sequences at 1.5 T.

**Results:** Inside the magnet bore, direct acoustic noise radiating from the inner shroud was most relevant, with substantial reductions of up to 18.8 dB when using passive screening of the magnetic bore. At the magnet bore entrance, blocking acoustic noise from the outer shroud and reflections showed significant reductions of 4.5 and 2.8 dB, respectively, and 9.4 dB when simultaneously applied. Inner shroud coverage contributed minimally to the overall SPL reduction.

**Conclusion:** Maximum noise reduction by passive acoustic screening can be achieved by reducing direct sound conduction through the inner and outer shrouds. Additional measures to optimize the acoustic properties of the MR suite have only little effect.

**Key Words:** magnetic resonance imaging; acoustic noise; acoustic noise reduction; passive noise reduction; safety  
**J. Magn. Reson. Imaging 2003;17:270–275.**  
© 2003 Wiley-Liss, Inc.

ACOUSTIC NOISE CAUSED BY magnetic resonance (MR) imaging has long been recognized as an important issue for patients and health workers alike (1). Its negative effects include, among others, temporary hearing disability, interference with verbal communication, and, potentially, with the use of new high-power gradients at higher field MR systems, permanent hearing loss (2–4).

Various techniques of acoustic noise reduction have been proposed and implemented, e.g., redesigning the gradient coil systems and reshaping pulse sequences (5–8). In most analyses, the MR imager has been treated as an isolated acoustic source, radiating its acoustic energy directly, i.e., from its inner and outer shrouds, to the patient, and the in-room health worker. However, the efficacy of applying acoustic insulators at both these levels has not been studied previously. Also, the contribution of indirect acoustic noise, originating from reverberations in the MR room (reflections resulting from the generally hard and reflective walls of the MR suite and from other objects), has hitherto been largely neglected. To our knowledge, only two investigators have emphasized that indirect acoustic noise may substantially contribute to the sound levels to which patients and health workers are exposed (9,10). Therefore, noise levels are likely to decrease when limiting these reflections of acoustic noise, e.g., by applying passive sound absorbing blankets to the boundaries of the MR suite. Because passive absorbance of acoustic noise is related to frequency (11), damping by passive means may also result in lower frequencies of MR-related acoustic noise. This is beneficial, as human hearing is most susceptible to higher frequencies >1 kHz (12). Likewise, speech is distorted by the reflective and reverberant characteristics of the room as speech understanding is inversely related to the extent of reverberation (13). Limiting the reverberant characteristics might, therefore, significantly improve speech intelligibility.

The purpose of our study was to quantify the efficacy of passive acoustic screening in the MR environment. More specifically, the research questions were to study 1) the extent of sound reduction that can potentially be achieved by blocking direct noise at the level of the inner and outer shrouds of the MR scanner, and indirect noise originating at the sound-reflecting walls of the MR suite, and 2) the contribution of these noise radiating sources to the overall sound level. This was studied from both the perspective of the patient inside the magnet bore, and the health worker, in particular, the interventional radiologist working near the entrance of the magnet bore during an

Erasmus MC, University Medical Center Rotterdam, Department of Radiology, Rotterdam, The Netherlands.

Presented at the 10th annual ISMRM meeting, 2002.

\*Address reprint requests to: A.M., Erasmus MC, University Medical Center Rotterdam, Department of Radiology, 50 Dr. Molewaterplein, 3015 GE Rotterdam, The Netherlands.  
E-mail: a.moelker@erasmusmc.nl

Received June 24, 2002; Accepted October 11, 2002.  
DOI 10.1002/jmri.10251  
Published online in Wiley InterScience (www.interscience.wiley.com).

© 2003 Wiley-Liss, Inc.



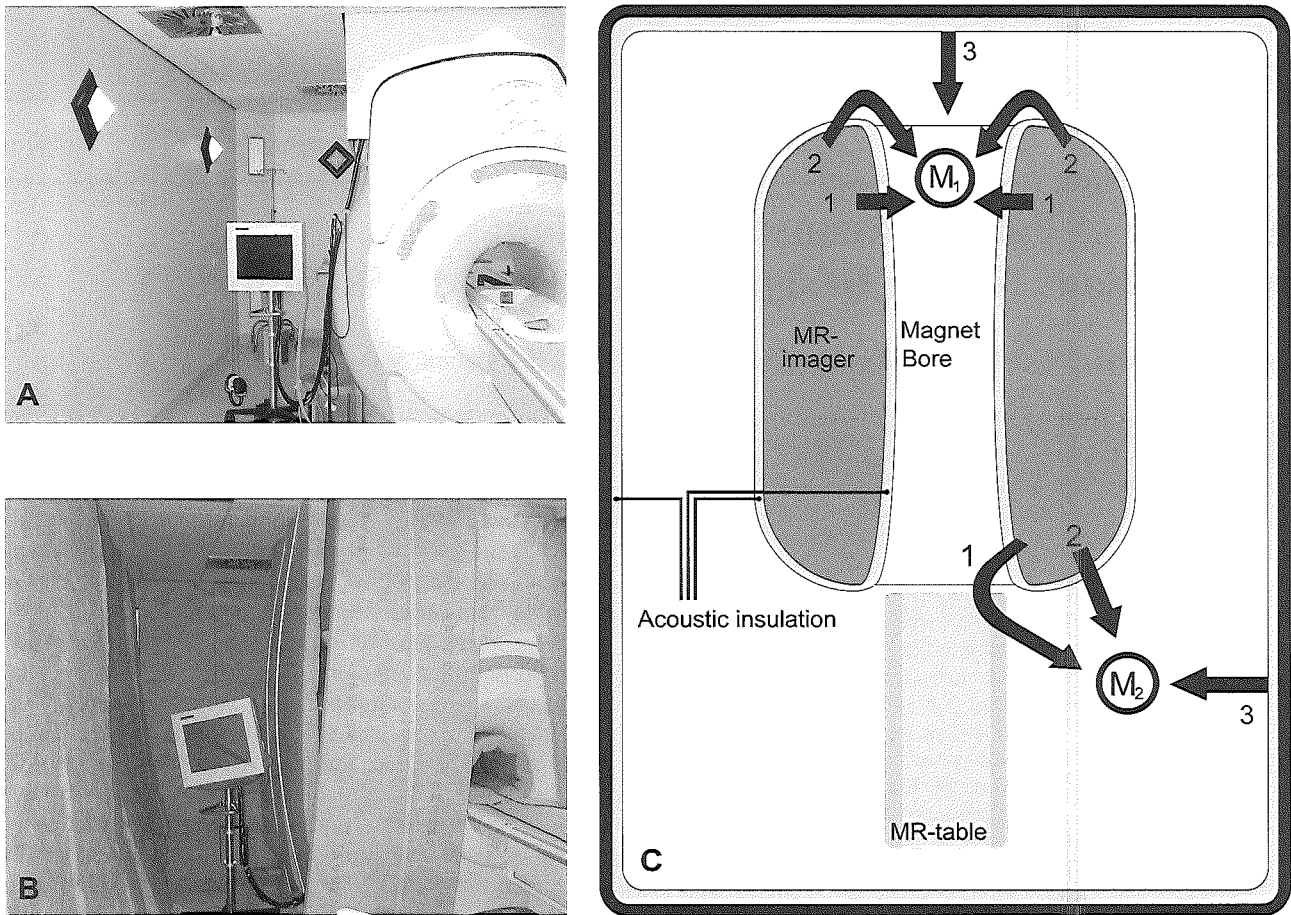


**Figure 1.** MR scanner and MR suite without (A) and with (B) passive acoustic screening. Schematic design of experimental set-up (C) of noise measurements at patient position ( $M_1$ ) and health worker position ( $M_2$ ) using noise-attenuating fiberglass (acoustic insulation) covering direct and indirect source pathways, i.e., hypothesized acoustic noise radiation directly from the inner (1) and the outer shroud (2), and indirectly from reflections (3).

interventional procedure.

## MATERIALS AND METHODS

### Study Design

Acoustic noise originates directly from the MR imager's inner and outer shrouds (including the end bells), and indirectly from reflections in the MR suite (Fig. 1). The relative contributions of direct and indirect acoustic noise to the overall sound pressure level (SPL) were quantified by virtually completely eliminating their sources and pathways by using thick layers of passive sound absorbing fiberglass (Saint-Gobain Isover Benelux B.V., Etten-Leur, The Netherlands, absorption coefficient > 0.95 at 1 kHz, 7.5-cm thickness). Acoustic isolation of the sources and pathways was done both separately and in various combinations. SPLs were recorded during various imaging pulse sequences (see below). Additionally, spectral noise profiles were recorded for calculating octave and 1/3-octave band frequencies, as the extent of reduction by the passive absorbing barrier material is known to be related to the frequency content of acoustic noise (11).

### Sound Measurements

The experimental set-up was in compliance with ANSI

protocol S1.13-1995 of the Acoustical Society of America (14). This led us to position the microphone vertically in the experimental set-up, as the acoustic MR environment was known to be diffuse (its sound levels decreased < 3 dB when doubling the distance to the acoustic noise source). Recordings were done both at a distance of 0.8 m from the MR imager at a height of 1.7 m, which is a plausible location of the health worker's ear (Fig. 1), and inside the magnet bore, i.e., at the location of the patient. Noise measurements were made with a 0.5-inch (1.27-cm) pre-polarized free-field condenser microphone (type 4189, Brüel & Kjær, DK-2850, Nærum, Denmark) mounted on a tripod and via a 10-m extension cable (AO-0442, Brüel & Kjær) connected to a type 1 digital sound level analyzer (Investigator 2260, Brüel & Kjær) positioned in the adjacent MR control room. SPLs were measured and time-averaged over a 30-second period, i.e., the equivalent-continuous SPL ( $L_{eq}$ ), and recorded on both linear (dB[L]) and A-weighted (dB[A]) scales; the latter adjusts for the frequency response of human hearing (15). The acoustic noise profiles were recorded for a 15-second period using a PC with shielded soundcard (ES1688, ESS Technology, Fremont, CA), coupled to the sound analyzer (16,17). Octave band frequencies and data analyses were performed using Matlab R12 software (The MathWorks, Inc., Novi, MI).



**Table 1**  
Results Measured Inside the Magnet Bore for Various Damping Configurations

Sequence	Frequency	Without damping (dB)		Damping (dB, reduction)		
		L(L) <sub>eq</sub>	L(A) <sub>eq</sub>	Bore	Shroud and bore	Bore, shroud and walls
Ambient	100 Hz	83.6	62.9			
EPI	2000 Hz	94.9	95.4	9.8	9.2	9.3
FGRET	2000 Hz	102.5	103.2	14.0	13.7	13.4
FSPGR	2000 Hz	108.5	109.5	19.3	18.6	18.8
FSE	2000 Hz	94.6	94.9	9.4	8.8	8.6
Spiral	1000 Hz	103.5	103.7	13.5	13.8	13.8
Average		100.7	101.3	13.2	12.8	12.8

L(L)<sub>eq</sub> = linear equivalent-continuous SPL; L(A)<sub>eq</sub> = A-weighted equivalent-continuous SPL.

Radiofrequency (RF) pulses exhibited relatively insignificant effects on the monitored acoustic noise profiles. This insensitivity to RF was similar to previous reports (2,9). Also, despite the presence of some amount of ferromagnetic material, the static 1.5-T magnetic field did not interfere with the sensitivity of the microphone (4). Nevertheless, calibration of the experiment set-up was tested at regular intervals.

The sound analyzer, checked by an appropriate sound source, had an accuracy of better than 0.1 dB. The PC-soundcard setup was analyzed using simultaneous recordings by PC and sound analyzer, and showed excellent agreement at all relevant octave band frequencies. The SD of the SPL values (equivalent-continuous linear SPL unless stated otherwise), as measured by the sound analyzer, and of the 1/3-octave band frequencies, as measured by the PC, were, for identical MR-sequences, < 0.35 dB and < 0.5 dB, respectively. As a comparison: an SPL reduction/increase of 1 dB is barely audible, whereas a 3-dB reduction/increase is considered audiophysically relevant, as it halves/doubles the potential health risks of acoustic noise (for SPLs between 80 and 140 dB[A]) (18).

#### MR Equipment and Pulse Sequences

Acoustic data were obtained from a Signa CV/i 1.5-T MR scanner (General Electric, Milwaukee, WI) with gradient hardware delivering a maximum of 40 mT/m gradients and with 150 T/m/second slew rates, using an integrated

quadrature-driven transceiver RF body coil. The MRI sequences used were: fast spin-echo (FSE, TR/TE = 500/17 msec), fast spoiled gradient recalled-echo (FSPGR, TR/TE = 7.2/2 msec), spiral trajectory k-space sampling sequence (TR/TE = 35/3 msec), echo planar imaging (EPI, TR/TE = 600/100 msec), and fast gradient recalled echo train (FGRET, hybrid EPI/FSPGR sequence, TR/TE = 34/3 msec). Of these, especially the FSPGR and FGRET sequences, using the highest gradient amplitudes and slew rates, seem suitable for real-time interventional MRI. The pulse sequence itself and the imaging parameters in a given pulse sequence were kept equal during the various acoustic damping experiments.

## RESULTS

### Patient's Perspective

Tables 1 and 2 show the equivalent-continuous linear and A-weighted SPLs, frequency distributions, and linear SPL reductions for various noise damping schemes, recorded during identical imaging sequences. Whenever measured inside an acoustically unshielded MR imager, i.e., at the position of the patient, the linear and A-weighted SPLs ranged from 94 dB up to 110 dB, with the most intense frequency 1/3-octave band at 2 kHz (Table 1).

Lining the magnet bore with acoustic insulation material resulted in a large, 9.4 dB(L) to 19.3 dB(L) attenuation of the MR-related acoustic noise levels. This extent of noise reduction was related to the SPL, i.e., higher reduc-

**Table 2**  
Results Measured at a Distance of 80 cm from the MR-Imager at 1.70m Height for Various Damping Configurations

Sequence	Frequency	Without damping (dB)		Damping (dB, reduction)					
		L(L) <sub>eq</sub>	L(A) <sub>eq</sub>	Bore	Shroud	Walls	Shroud and bore	Shroud and walls	Bore, shroud and walls
Ambient	100 Hz	67.9	52.2						
EPI	1250 Hz	82.2	82.3	1.5	4.4	3.2	7.6	6.9	10.5
FGRET	300-400 Hz 1250-2000 Hz	90.5	89.8	3.0	2.7	3.0	7.3	6.3	10.7
FSPGR	1000 Hz	90.8	90.6	0.2	3.9	2.0	7.7	7.0	11.6
FSE	1250 Hz	82.5	82.5	1.6	4.5	2.4	7.0	7.5	10.1
Spiral	800 Hz	98.3	98.2	0.1	7.0	3.5	8.3	9.5	12.2
Average		88.9	88.7	1.3	4.5	2.8	7.6	7.4	11.0

L(L)<sub>eq</sub> linear equivalent-continuous SPL, L(A)<sub>eq</sub> A-weighted equivalent-continuous SPL.

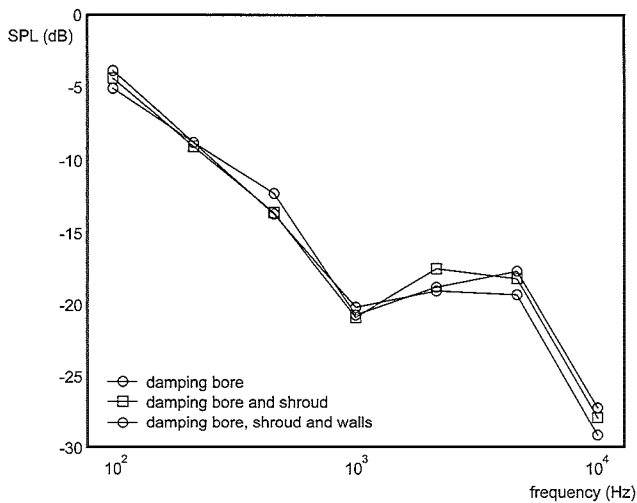


**Figure 2.** Linear SPL reductions vs. octave band frequencies measured at the patient location. SPLs are given for damping the inner bore; the inner bore and outer shroud; and the inner bore, outer shroud, and walls.

tions for noisier pulse sequences. Additional blocking of sounds radiated from the outer shroud and reflected by the MR suite walls did not significantly further reduce noise levels in any of the pulse sequences. Figure 2 demonstrates the proportional relation of sound reduction and frequency, with prominent reductions of up to 29 dB(L) at 4 kHz. This profile corresponded with the absorbance properties of the acoustic insulation material (better isolation at higher frequencies). Thus, acoustic noise radiated by the inner bore as perceived by the patient completely accounted for the overall SPL.

### Health Worker's Perspective

At a distance of 80 cm from the MR imager, near the entrance of the magnet bore, i.e., at the location of the health worker, linear and A-weighted SPLs ranged from 82 dB(L) to 98 dB(L) during the unscreened experiments (Table 2). The frequency distribution of most sequences was between 1 and 2 kHz, except for the spiral-k sequence, which had most of its acoustic energy in the 800 Hz band.

When covering the outer shroud with the passive sound insulating material, a relatively large SPL decrease of 4.5 dB(L) on average was measured, indicating that most of the acoustic energy was radiated directly from the outer shroud to the health worker. This was in particular the case for spiral-k imaging (7 dB[L] decrease). Acoustic noise radiation indirectly from reverberations and directly from the inner bore proved to be of lesser influence and was reduced by 2.8 dB(L) and 1.3 dB(L), respectively. However, the latter source pathway gained in its extent of contribution to the overall SPL when simultaneously covering the outer shroud. This was appreciated from the larger attenuation whenever both inner and outer shrouds were insulated, than the summed attenuation of these source pathways measured separately (e.g., 7.6 dB[L] vs. 5.8 dB[L], Table 2).

It was of interest that frequencies > 1250 Hz were predominantly originating from the inner shroud, whereas

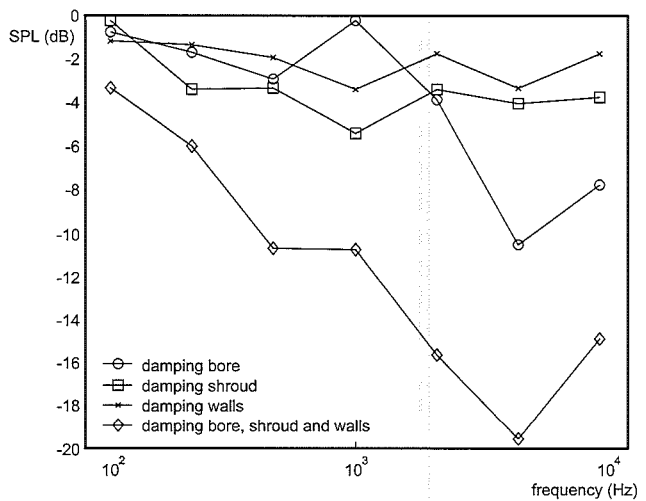


**Figure 3.** Linear SPL reductions vs. octave band frequencies measured at a distance of 80 cm from the MR imager at a height of 1.70 m. SPLs are given for damping the inner bore, outer shroud and walls, and in combination.

lower frequencies predominantly originated from the outer shroud (Fig. 3). Most likely, frequencies < 1250 Hz are largely conducted from the gradient coil supporting structures, through the main magnet towards the outer shroud. The extent of contribution to the overall SPL of the indirect source pathway was, conversely, uniformly distributed over the entire frequency range.

### DISCUSSION

Our study shows that substantial reductions in MR generated noise levels can be gained if appropriate care is given to eliminate noise sources and pathways directed to both the patient and in-room health worker. These acoustic noise sources and pathways in the MR environment can basically be assumed to radiate directly from inner and outer shrouds and indirectly from reverberations in the MR suite (i.e., sound waves are reflected by the poorly sound-absorbing walls of the room). The SPL reduction by blocking the sources and pathways elucidates their relevance to the overall sound level.

For a patient, direct acoustic noise radiation from the inner shroud is most relevant, as was demonstrated by the substantial reductions of up to 18.8 dB when eliminating this source pathway. This is, from an audiophysical perspective, a tremendous reduction in the potential health risks of acoustic noise, in particular the risk of hearing loss. This result corroborates earlier findings (9,11). Our experiments indicate that additional damping of outer shroud and room boundaries appears ineffective. This is, however, in contrast to the experiments of Mechefske, et al (11), who reported a reduction of 5 dB whenever applying fiberglass end-caps (to the bore entrance and exit), thereby blocking the sound waves (re-) entering the magnet bore. This discrepancy may be due to our use of thick layers of insulation in the magnet bore, which partially blocked acoustic noise (re-) entering the magnet bore. Another explanation may be in the relatively high background SPLs, masking the sounds of the outer shroud and in-room reflections (a loud noise masks a quieter one).

From the health worker's perspective, our experiments

showed that sound coming from the outer shroud radiation and from indirect reflections account for most of the acoustic energy when recording close to the entrance of the MR imager. The simultaneous isolation of both source pathways, resulting in an acoustic noise attenuation of 7.4 dB(L) on average, provides a relevant SPL reduction from the audiophysical perspective.

It is of note that the contributions of the direct acoustic noise source pathways to the overall SPL (at health worker's location) are interrelated because of masking. Therefore, concurrent elimination of the acoustic radiation from both inner and outer shroud seems especially effective. By contrast, the indirect source pathway is less interrelated with the direct source pathways, appreciated from the similar SPL reductions when applying acoustic insulation separately (results summed) and simultaneously (7.3 dB[L] and 7.4 dB[L], respectively). Differences are solely contributable to changes in the frequency spectrum.

At both the patient's and health worker's position, our results showed a relation between noise reduction by passive screening and frequency, with reductions of up to, respectively, 29 dB and 19 dB (Figs. 2 and 3). This seems beneficial, as human hearing is most sensitive to frequencies around 4 kHz (12). The SPLs of the imaging pulse sequences in this frequency area are, however, relatively small, because most of the acoustic energy is in the 1 to 2 kHz range (Tables 1 and 2). Despite this substantial noise reduction, the impact on overall SPLs is, therefore, low.

This study was conducted on a 1.5-T MR imager encompassing a gradient system with up to 150 T/m/second slew rates. The need for better resolution and signal-to-noise ratio, however, pushes MR imaging towards higher field strengths and gradient system power with steeper slew rates. The more powerful 3-T MR systems produce more intense SPLs at higher frequencies (19). Consequently, the use of passive acoustic screening may have even more impact in these newer MR systems than in systems at 1.5 T.

Our study showed that the application of acoustic insulation to the inner and outer shroud may be beneficial for both the patient and health worker. Presently, MR systems are not fully exploiting the advantages of such substantial acoustic noise reductions using passive insulators lining the magnet bore, probably because of their generally bulky dimensions. However, some systems have recently become available using a combination of acoustic insulators with a vacuum-enclosed gradient system (Excelart, Toshiba Corporation, Tochigi, Japan, and Signa Twinspeed, General Electric, Milwaukee, WI). Likewise, no commercial MR systems, to our knowledge, encompass acoustic insulators blocking sound propagation through the outer shroud toward the MR room.

Another potential solution may be in the application of active noise control; that is, the reduction of MR-generated acoustic noise by superposition of an exactly inversed sound (20). Currently, we are investigating the application of an analogous technique called "active structural acoustic control." This technique makes use of thin panels with actuators and vibro-acoustic sensors that allow for a high level of acoustic noise reduction. Such active panels, combined with passive noise-reducing materials, might replace

the currently used inner and outer shroud materials of the MR imager, thereby providing SPL reductions over a large frequency range at both patient and health worker locations.

## REFERENCES

1. Brummett RE, Talbot JM, Charuhas P. Potential hearing loss resulting from MR imaging. *Radiology* 1988;169:539-540.
2. Hurwitz R, Lane SR, Bell RA, Brant-Zawadzki MN. Acoustic analysis of gradient-coil noise in MR imaging. *Radiology* 1989;173:545-548.
3. Shellock FG, Ziarati M, Atkinson D, Chen DY. Determination of gradient magnetic field-induced acoustic noise associated with the use of echo planar and three-dimensional, fast spin echo techniques. *J Magn Reson Imaging* 1998;8:1154-1157.
4. Moelker A, Maas RA, Lethimonnier F, Pattynama PM. Interventional MR imaging at 1.5 T: quantification of sound exposure. *Radiology* 2002;224:889-895.
5. Bowtell R, Peters A. Analytic approach to the design of transverse gradient coils with co-axial return paths. *Magn Reson Med* 1999;41:600-608.
6. Mansfield P, Haywood B. Principles of active acoustic control in gradient coil design. *MAGMA* 2000;10:147-151.
7. Hennel F, Girard F, Loenneker T. "Silent" MRI with soft gradient pulses. *Magn Reson Med* 1999;42:6-10.
8. Loenneker T, Hennel F, Ludwig U, Hennig J. Silent BOLD imaging. *MAGMA* 2001;13:76-81.
9. Ravicz ME, Melcher JR, Kiang NY. Acoustic noise during functional magnetic resonance imaging. *J Acoust Soc Am* 2000;108:1683-1696.
10. Foster JR, Hall DA, Summerfield AQ, Palmer AR, Bowtell RW. Sound-level measurements and calculations of safe noise dosage during EPI at 3 T. *J Magn Reson Imaging* 2000;12:157-163.
11. Mechefske CK, Geris R, Gati JS, Rutt BK. Acoustic noise reduction in a 4 T MRI scanner. *MAGMA* 2002;13:172-176.
12. McJury M, Shellock FG. Auditory noise associated with MR procedures: a review. *J Magn Reson Imaging* 2000;12:37-45.
13. Houtgast T, Steeneken HJM. A review of the MTF concept in room acoustics and its use for estimating speech intelligibility in auditoria. *J Acoust Soc Am* 1985;77:1069-1077.
14. Measurement of sound pressure levels in air. American National Standard S1.13-1995. Melville, New York: Acoustical Society of America; 1995.
15. Determination of occupational noise exposure and estimation of noise-induced hearing impairment. American National Standard S3.44-1996. Melville, New York: Acoustical Society of America; 1996.
16. Cho ZH, Park SH, Kim JH, et al. Analysis of acoustic noise in MRI. *Magn Reson Imaging* 1997;15:815-822.
17. Counter SA, Olofsson A, Borg E, Bjelke B, Haggstrom A, Grahn HF. Analysis of magnetic resonance imaging acoustic noise generated by a 4.7 T experimental system. *Acta Otolaryngol* 2000;120:739-743.
18. Criteria for a recommended standard: occupational noise exposure - revised criteria 1998. Publication no. 98-126. Cincinnati, Ohio: National Institute for Occupational Safety and Health; 1998.
19. Hedeon RA, Edelstein WA. Characterization and prediction of gradient acoustic noise in MR imagers. *Magn Reson Med* 1997;37:7-10.
20. Chambers J, Akeroyd MA, Summerfield AQ, Palmer AR. Active control of the volume acquisition noise in functional magnetic resonance imaging: method and psychoacoustical evaluation. *J Acoust Soc Am* 2001;110:3041-3054.



## Chapter 8

Adriaan Moelker, MD  
Ronald A.J.J. Maas, PhD  
Mika W. Vogel, Msc  
Mohamed Ouhlous, MD  
Peter M.T. Pattynama, MD

### Index terms:

Magnetic resonance (MR), biological effects  
Magnetic resonance (MR), technology  
Magnetic resonance (MR), safety  
Radiology and radiologists

### Abbreviations:

SPL = sound pressure level  
MIRE = microphone-in-real-ear

Departments of Radiology (A.M., M.W.V., M.O., P.M.T.P.) and Audiophysics (R.A.J.J.M.), Erasmus Medical Center Rotterdam, 50 Dr. Molewaterplein, P.O. Box 1738, 3000 DR Rotterdam, The Netherlands

### Submitted to:

Investigative Radiology (May 2004)

Address Correspondence to A.M.  
(e-mail: a.moelker@erasmusmc.nl)

### Author contributions:

Guarantors of integrity of entire study, A.M., R.A.J.J.M., P.M.T.P.; study concepts and design, A.M., R.A.J.J.M., P.M.T.P.; literature research, A.M., R.A.J.J.M.; experimental studies, A.M., M.W.V., M.O.; data acquisition, A.M., M.W.V., M.O.; data analysis/ interpretation, A.M., P.M.T.P.; statistical analysis, A.M.; manuscript preparation, A.M., P.M.T.P.; definition of intellectual content, editing, revision/review, and final version approval, A.M., R.A.J.J.M., P.M.T.P., M.W.V., M.O.

# Importance of Bone Conducted Sound Transmission on Patient Hearing in the MR Scanner

**Introduction:** Acoustic noise is an unwanted side effect of magnetic resonance imaging (MRI) that is commonly tackled with passive hearing protection devices. In an MR scanner, however, with the patient completely surrounded by the MR sound source and in close contact with the vibrating MR table and gantry, bone-conduction may increase subjective sound levels restricting the efficacy of passive protection that reduces air-conducted noise only. It was therefore our aim to evaluate the influence of bone-conduction in the MR environment compared to a standardized acoustic environment.

**Materials and Methods:** Ten volunteers were subjected to MR tones, covering the frequency range relevant for hearing and at 60 dB, generated through the MR system's gradient coils. A masking method was adapted and used for evaluating bone-conduction. Bone-conduction was determined for various passive damping conditions in an MR scanner and was compared to that acquired in an acoustically calibrated environment. The contribution of mechanical vibrations to bone-conduction in the MR tunnel was determined. Also, with a microphone in the ear canal, the objective efficacy of the passive protection measures was determined.

**Results:** We found no difference between the bone-conduction experiments executed inside the imager and in the acoustically controlled environment. Elimination of bone-conduction hearing through the mechanically vibrating parts of the MR imager did not influence subjective hearing levels. The overall insertion loss of the passive hearing protectors was over 20 dB with strongest effects at 0.4 kHz and 2.5 kHz.

**Conclusion:** Bone-conduction is not more pronounced inside the MR scanner than outside. Therefore, the previous reports on the subjective evaluation of protection devices in MRI hold their validity.

A well recognized drawback of magnetic resonance imaging (MRI) is in the acoustic noise that is produced during the imaging process (1,2). Patients are routinely subjected to high sound pressure levels (SPLs), averaging around 95 to 105 decibels (dB), for some MR pulse sequences increasing up to 130 dB, with peak SPLs going much higher (3). These SPL values are well above generally accepted safety rules (4,5). Indeed, discrete changes in cochlear function could be demonstrated in subjects following MR noise exposure even when wearing ear protection (6). MR-generated acoustic noise negatively affects communication between the patient and the MR operator, and MR noise is also a limiting factor in functional MR experiments, especially those targeted at the auditory cortex (7,8). The problem of MR noise will likely increase given the current trend towards more powerful MR systems operating at ever higher field strengths and with faster gradient switching (9,10).

The most effective and currently most widely used method for MRI noise reduction is passive noise control - the application of earplugs and earmuffs (11). However, passive hearing devices only reduce air-conducted sound transmission, leaving bone-conduction, i.e. the noise radiated to head and body and directly transmitted to the inner ear, unaffected (12). Under normal audiometric circumstances (outside the MR scanner), bone-conduction is much

less effective than air-conduction with resultant perceived noise levels of approximately 40 dB less (11). However, when passively attenuated air-conducted sounds fall below the bone-conduction limits, it is the bone-conducted sound that determines the overall cochlear input. Additional passive measures will then be ineffective in further lowering the perceived noise level.

In fact, the MR scanner is not a "normal" audiometric environment. The MR scanner, from the audiometric point of view, is different in that a subject situated in the MR tunnel is completely surrounded by the source of sound, which will result in more intense direct radiation of sounds to the patient's head and body. Moreover, subjects inside the MR bore are directly exposed to mechanical vibrations conveyed from the gradient coil assembly to the MR table and to the shroud (13,14). Contact of the subject's head and body with the MR table and shroud will introduce an additional bone-conducted vibro-acoustic sound pathway along which MR-related acoustic noise transmits to the subject's inner ear. Overall, one might therefore argue, bone-conduction may be a more effective route of sound transmission inside the MR scanner than outside, and this may directly impair the efficiency of passive noise reduction methods, thereby altering optimal strategies to reduce overall MR noise perception.

This was the rationale to (1) evaluate whether bone-conduction is more effective inside than outside the MR scanner, (2) differentiate subjective hearing through mechanical vibrations from conventional bone-conduction in the MR-imager, and (3) determine the objective efficacy of passive isolation by means of protectors that are commonly applied in MRI.

## Materials and methods

### Subjects and study design

Our analysis was based on measurements in 10 healthy volunteers without hearing impairment, as evidenced by a normal pure-tone audiogram. First, we compared the efficiency of bone-conduction hearing of MR sounds inside an MR scanner with that outside the MR-imager. Quantification of bone conduction, in

**TABLE 1**  
Sound Insulation Conditions Assessed in the Experiments

Separate conditions	Combined conditions
Earmuff	Subject support and foam lining MR bore
Earplug	Earmuff and earplug
Foam lining MR bore	Earplug and subject support
Subject support (mattress)	Earmuff and earplug and subject support

general, requires that the air-conducted sound intensity is reduced to a level below that of bone conduction (15). For this, we used earplugs (E-A-R Classic, Aearo Ltd, Poynton, United Kingdom) and earmuffs (Viking, Bilsom, Hampshire, United Kingdom). The volunteers were positioned inside the MR scanner and subjected to calibrated sounds directly produced by the MR scanner. The MR sounds of this part of the experiment were recorded with a microphone (type 4189, Brüel & Kær, Nærum, Denmark) close to the subject's ears. The subjects were then examined outside the imager in an acoustically controlled anechoic audiometric booth (Industrial Acoustic Company, Inc., Bronx, NY) and were exposed to the recorded MR sounds, now played out by a loudspeaker at exactly the same sound level. We also studied whether and how effectively vibro-acoustic bone conduction in the MR bore could be lowered by means of (foam) cushioning. The subject was protected from direct contact with the MR by several mattresses (polyurethane): a small cushion with a thickness of 10 cm under the subject's head, a 7 cm-thick mattress on the MR table, and additional pieces of foam where the subject touched the MR tunnel (Table 1).

### MR equipment

Experiments were done on a 1.5T scanner (Signa Cv/i, General Electric, Milwaukee, WI, USA) operating under LX9.1 software and by using the x-gradient coil (Fig 1). A fast gradient recalled echo MR pulse sequence was modified to continuously play out a sinusoidal sound. Control of the MR sounds produced by the gradient pulse was obtained by using custom-made software that set up a software server running on the MR host computer. This server handled reques-

ts for adjustment of the period and the gradient amplitudes over the existing TCP/IP interface. To communicate with the daemon, we implemented a client on a computer equipped with Matlab (R12, The MathWorks, Inc., Novi, MI), which calculated the required period and amplitudes. The MR gradients were fed the sinusoidal input currents at frequencies of 230, 463, 1.157, 1.736, 2.315, 2.976 and 4.167 Hz. These frequencies had been selected on the basis of two criteria: (1) the frequencies had to be in the range applied in standard audiometric testing (250, 500, 1.000, 2.000, 4.000 Hz) and (2) they had to be resonant frequencies of the MR system, at which vibrations of the MR table and gantry are most likely to occur (16). The chosen tonal stimuli were not perfectly sinusoidal, primarily because the waveform was digitally generated in discrete steps and exhibited soft harmonics (16,17). During the experiments, the SPL of the MR sounds was set to 60 dB as measured at the subjects' ears inside the MR imager by using a feedback loop with the Matlab client and the MR hardware.

### Measurement of objective SPLs

Objective sound levels (air-conducted) were assessed by measuring the SPL at the subject's eardrum (see appendix for a more detailed description on objective and subjective hearing), using the microphone-in-real-ear (MIRE) method (12). This method makes use of a small flexible tube inside the external auditory canal that transmits air-conducted acoustic noise from the auditory canal to a small copper shielded microphone (EK-3024, Knowles Electronics Holdings, Ill, USA) positioned behind the ear. Using the MIRE method, the effectiveness of blocking air-conducted sound transmission (insertion loss)

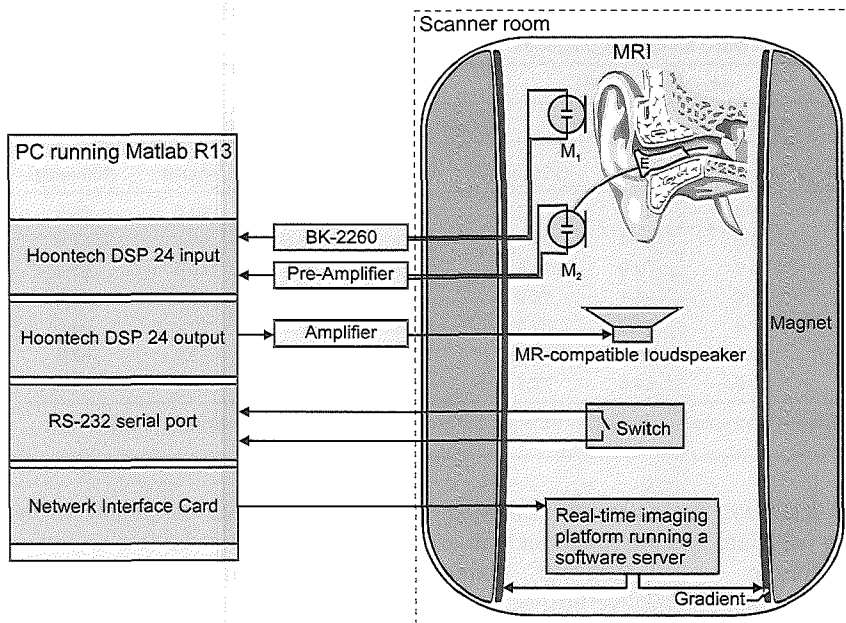


**Figure 1.** Cross-section of the MR imager (bore, gradient coils and magnet) with a schematic overview of the microphone type 4189 ( $M_1$ ) connected to the sound-level meter (BK-2260), the microphone type EK-3024 ( $M_2$ ) connected to a small tube (E) that penetrated an earplug receiving acoustic signals from within the external ear canal, and the experiment setup of the PC and MR imager's real-time platform. The switch was used by the subject to respond to the task during the experiments.

could be monitored. The insertion loss equals the difference between the reference and the insulation condition (18).

#### Measurement of subjective SPLs

We assessed the subjective hearing level of MR sounds by using a previously validated masking method (12), both inside the MR system as well as in the audiometric booth (see Appendix). Basically, the masking method relies on the minimal SPL of a masking noise required to obscure the MR sound. The effectiveness of bone-conduction inside the MR bore and in the audiometric booth could be directly compared by taking the minimal masking SPLs in these two conditions. In the MR scanner, masking noise was played out over an MR-compatible modified loudspeaker inside the MR tunnel facing the subject's head, using a method adopted from previous bone-conduction experiments (11). In the audiometric booth, an unmodified but otherwise identical loudspeaker was positioned at exactly the same location and orientation relative to the subject's head. Masking noise played out by the loudspeaker point source will cause perception of noise through both air- and bone-conduction. If one assumes

that MR sounds transmit more efficiently by bone conduction inside than outside of the MR scanner, then it follows that a higher SPL of masking noise is required inside the MR scanner. Thus, the absolute difference in masking SPLs between the two measurement conditions is a direct measure of the difference in efficacy of bone-conduction.

White masking noise was produced for a period of 6 seconds, during which the MR scanner produced the gradient sound for 2 seconds. Subjects were asked to indicate that they could hear the MR noise within the white noise by pressing a switch. The initial level of white masking noise was chosen well above the level of the MR sounds and was decreased in 3-dB steps every six seconds until the subject responded. The average of 3 cycles was taken as the masking level for a given MR sound frequency. The frequencies were presented randomly.

Finally, the vibro-acoustic pathway, as a separate entity within bone-conduction, was further assessed by comparing masking experiments with and without the head and body supports (MR environment only). By comparing the minimal masking level for these conditions,

the contribution of the vibro-acoustic pathway to bone-conduction in the MR environment was quantified.

#### Audio equipment

We made use of two microphones in the experiments: a type 4189 microphone measured SPLs in the MR bore close to the subject's ear and a MIRE microphone (EK-3024) measured SPLs in the external ear canal. The type 4189 microphone was connected to a sound analyzer (Investigator 2260, Brüel & Kjær) and put through to a PCI audiocard (Audio DSP24, Hoontech, Bucheon City, Korea) and was used for calibrating the complete experiment setup (19). The MIRE microphone was pre-amplified with 30 dB before capture, using a custom-built high performance JFET input operational pre-amplifier located outside the MR room. The response of the EK-3024 microphone setup was checked in the anechoic environment. The personal computer, equipped with the audiocard and Matlab software, was used for (1) generating and recording the masking noise and MR sounds, (2) calibrations and calculations, and (3) controlling the MR acoustic noise. A custom-built graphical user interface integrated and handled these operations automatically. For presenting the masking noise, an MR-compatible loudspeaker was made based on the idea of Baumgart et al. (20): the cone of a Sony audio speaker (XS-HA172-6) was disposed of its magnet and assembled to a wooden board, an aluminium cradle and a copper lattice grid protected the loudspeaker from damage. The speaker was placed perpendicular to the magnetic field, in front of the subject's head, and was driven by a solid state amplifier (HY 60, ILP Electronics Ltd, Kent, UK).

#### Analyses

Calculation of the insertion losses for the various insulation conditions was executed in Matlab software. One-third octave bands were determined for the recorded waveforms in compliance with ANSI-protocol S1.11-1986 of the Acoustical Society of America using 3rd order filters and band-center frequencies recommended in ANSI-protocol S1.6-1984 (21,22). The subjective data were



**TABLE 2**  
Average Masking Levels for the MR Tone Frequencies and Tested Damping Conditions

Frequency (Hz)	Masking level (dB)									
	No damping			Coverage of MR bore		Earplug		Earplug and earmuff		
	Present	Absent	Reference	Present	Absent	Present	Absent	Present	Absent	Reference
230	85.1	89.4	85.5	86.4	88.6	105.1	103.5	89.1	91.0	86.8
463	93.6	90.6	87.0*	83.5	86.4	89.4	88.3	93.8	98.4	87.6
1.157	80.2	82.3	80.8	79.7	79.9	76.5	75.9	78.7	79.3	85.4*
1.736	79.9	79.5	83.7	82.6	84.1	78.2	77.4	78.4	78.4	83.6
2.315	84.2	83.3	79.9	81.4	86.4	83.1	81.5	80.7	80.2	81.6
2.976	78.8	78.5	77.7	82.2	85.9	80.2	75.1	79.2	79.1	82.6
4.167	77.8	78.8	79.2	79.6	81.5	77.7	75.1	82.3	76.4	79.6

\*p-value < 0.05; in the MR imager, the vibro-acoustic pathway was present (present) or eliminated (absent). Reference = data measured in calibrated acoustic environment. See also Figure 2.

compared with the reference conditions and statistically tested for significance (for each frequency and insulation condition). To this end, student's t-tests were performed using SPSS version 12 for Windows (SPSS Inc., Chicago, USA); a p-value of .05 was considered statistically significant. To test the hypothesis that bone-conduction was similar in both the MR-environment and in the anechoic booth, a nonparametric Sign-test procedure was performed in Microsoft Excel version 10.0 (Microsoft Corporation, Redmond, WA, USA) with Analyse-It version 7.1 add-in software (Analyse-it Software Ltd, Leeds, UK). The differences between the two variables for all subjects were computed and classified as either positive or negative and the distribution was tested against a probability of .5. All statistical inferences were adjusted for multiple testing by using Bonferroni correction.

### Results

The experiment outcomes discussed in this section are arranged into subjective and objective measurements. The first provide the results of the bone-conduction experiments executed in the MR-environment and the audiometric booth. The latter report on the acoustic properties of the passive noise control devices that were applied in the masking experiments.

#### Subjective measurements

In table 2 the mean SPLs of the masking noise required to completely mask the MR tones are presented for the various damping conditions with and without blocking the vibro-acous-

tic pathway. The reference condition (no isolation) and the condition with a maximum contribution of bone-conduction to subjective hearing were repeated in the anechoic booth and compared to those acquired in the MR imager. The sign-test showed no significant difference between the masking experiments executed inside and outside the imager, except for the reference condition and earplug and earmuff combination, at 463 Hz and 1157 Hz, respectively. Adjusting the statistical inferences for multiple testing resulted in insignificant differences in subjective masking levels between both environments. It was therefore concluded that bone-conduction in a MR imager is virtually equal to bone-conduction in an acoustically calibrated environment.

Furthermore, the minimum SPLs for masking the MR tones in the circumstances that eliminated the vibro-acoustic pathway were all of similar intensity (except at 463 Hz). In other words, even in conditions with maximum contribution of conduction hearing, the noise levels required for masking the MR sounds did not alter. This indicated, again, that bone-conduction in the MR scanner that surrounds the patient is equal to bone-conduction in normal conditions, outside of the MR scanner.

The effect of obstructing the vibro-acoustic pathway is depicted in figure 2 with the insulation circumstances arranged according to the degree of insertion loss. Despite the usage of thick materials that supported both the head and body concurrently with air-conduction isolation, the effect of vibrations of MR table and gantry appeared trivial. An increase in

masking intensities was found for the 230 Hz MR tone in the first condition (-4.3 dB), i.e. without isolation, and for the 2.315 Hz stimulus when insulating the magnet bore (-5.3 dB); the masking level decreased at 2.976 Hz and 4.167 Hz with approximately 6 dB when wearing earplugs and the combination of ear defenders. Adjusting for multiple testing, however, resulted in insignificant contributions of vibrational bone-conduction to subjectively perceived MR tones in all isolation conditions. Thus, the mechanical vibrations of the MR scanner did not contribute significantly to bone-conduction in the MRI.

#### Objective measurements

The attenuation characteristics of the various damping conditions were determined inside the MR scanner using the objective MIRE method and illustrated in figure 3 (means and standard errors for 1/3-octave bands). The head and body support of the subjects resulted in an average insertion loss in the external ear canal of 1.8 dB. The insulating polyurethane foam that covered the MR tunnel gave a modest reduction of the SPL, in particular for frequencies neighboring 1 and 6 kHz. Polymer foam earplugs, by contrast, reduced the overall sound level in the external ear canal by 20 dB with relatively strong attenuation in the lower frequency ranges < 1 kHz. Largest effects were found at the 0.4 kHz and the 2.5 kHz 1/3-octave band. Similar data were recorded for the Bilsom headset with somewhat lesser low frequency attenuation but superior damping above 1 kHz. Evidently, the addition of head and



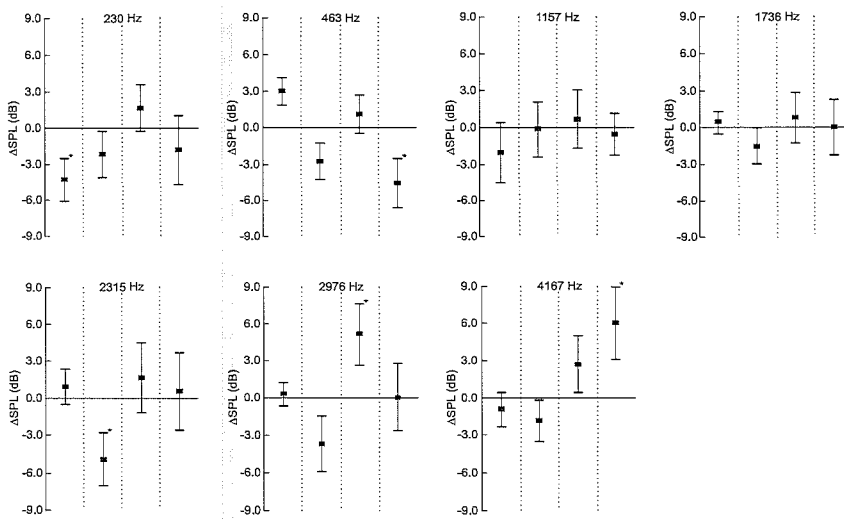


**Figure 2.** Mean differences and standard errors ( $n=10$ ) for the vibro-acoustic pathway measurements (present minus absent). The effect of the vibro-acoustic pathway is given for the damping conditions (none, coverage of MR tunnel, earplug and combination of earplug and earmuff) as tested for all MR frequencies. \* $p$ -value  $< .05$ .

body support did not substantially alter the attenuating characteristics of the objective MIRE results for the combined ear defenders.

Because the frequency transfer of the sound generating path was calibrated and, consequently, truly white noise was produced at 80 dB, the MIRE recording of the reference condition provided the filter characteristics of the external ear canal (Fig. 4). The ear canal acted as a filter that reduced low frequencies, acted as a resonator enhancing mid frequencies between 1 and 7 kHz and reduced higher frequencies. This distribution is in agreement with the findings of previous reports (23). Differences between subjects were modest with an average standard error of 2.2 dB, likely caused by differences in the physical dimensions of the head and external ear. It is of note that SPLs in higher 1/3-octave bands appear higher; however these cover a larger frequency range resulting in a higher sound level within that octave band (approximately 1 dB per octave band). Also, the transfer function of the external ear canal was relevant for neither the objective nor the subjective tests. The first was based on the difference between reference condition and damping condition, both experiencing the same external ear transfer function. Likewise, in the masking experiments both MR stimuli and masking noise were affected equally.

## Discussion

Our study shows that bone-conduction in the MR environment is of no more importance than that in a calibrated anechoic room. Moreover, bone-conduction through mechanical vibrations proved not of influence on the bone conduction hearing inside a real MR imager, even not with virtually complete blockage of the air-conducted route. In this respect, the MR table and inner shroud are apparently sufficiently decoupled from the vibrating gradient assembly. To our knowledge, bone-conduction has hitherto largely been neglected in the MR environment: the emphases of both passive and active noise reduction techniques have been on their objective performance (insertion loss) (24) and/or on the subjective efficacy in other than MR environments (11, 17). Because in our analysis bone conduction was similar inside and outside the MR scanner, the results previously described by other researchers based on experiments performed in other environments than a real MR imager can be safely interpolated to real MRI conditions.

The measured insertion losses of earplugs and earmuffs are in agreement with the values found by other researchers (11,18,25). For earmuffs, as an example, Ravicz et al. (11) found moderate reductions at low frequencies, approximately 10 dB  $< 500$  Hz, and excellent reductions of about 30 dB at 2 kHz (in our data 10 and 25

dB, respectively). Likewise, our experiments demonstrate that objective sound levels in the external auditory canal are not confined to air-conduction alone (11). This can be appreciated from the inferior insertion loss of the earplug/earmuff combination set against the sum of their separate objective attenuations, i.e. they do not add-up linearly. Thus, the generally held assumption that the objective MIRE measure is strictly representing air-conducted MR-sounds does not hold true. This effect has been described elsewhere as “the external ear component“ of bone-conduction (26) and is predominantly the effect of osseo-tympanic motion (radiation of sound in the external ear canal itself) generating a sound field in the external ear canal (27).

The noise level required to mask the 230 Hz MR stimulus in the earplug condition was seriously intense, 105.1 dB, and dropped to 89.1 dB in combination with the earmuffs. The vibro-acoustic route accounted for only 1.6 dB (Table 2) and is therefore not a likely cause. A more relevant factor may be the so-called occlusion effect. Normally, sound waves can escape from the open ear canal. If the canal is blocked by hearing protection, additional sound pressure at particularly low frequencies is generated in the closed ear canal and transmitted to the cochlea (27). The external ear canal filter becomes flatter with an increase in sound level of over 20 dB at 100 Hz that falls off at about -6 dB per octave band (27). As a consequence, the 230 Hz stimulus became relatively louder in contrast to the masking noise level.

In conclusion, our experiments demonstrate that bone-conduction in the MR environment, specifically in the magnet bore, is equal to bone-conduction in calibrated environments. Although conduction hearing is a prominent limiting factor to sound protectors, their efficacy is not further restricted by the MR environment. Therefore, previous reports on the subjective evaluation of the passive and active hearing devices applied in MRI hold their validity, whether they were obtained outside the MR environment, in imager mock-ups, or in a real MR system.

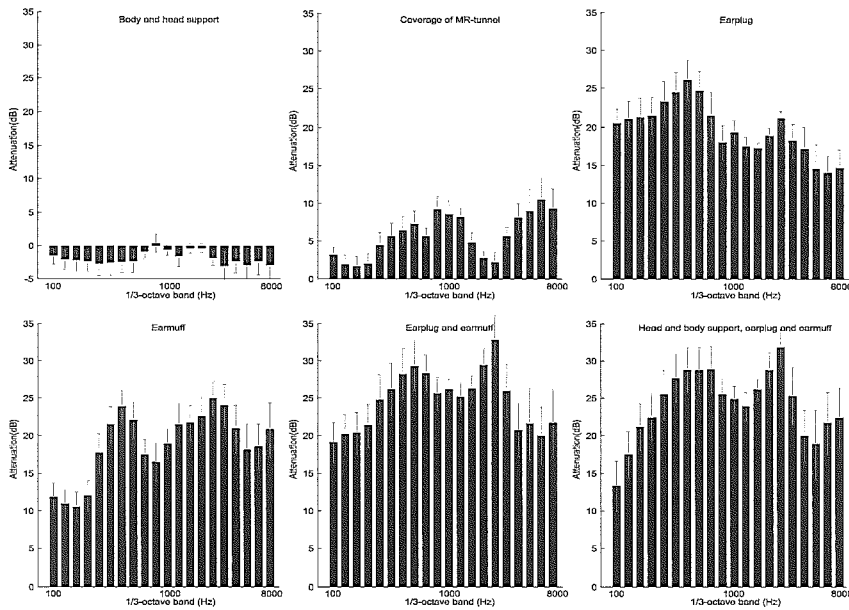


**Figure 3.** Objective attenuation of the various test conditions. The bars are the mean 1/3-octave band frequency levels and the whiskers indicate the standard error (n=10). These values are measured with the MIRE method.

## Appendix

A subject in the magnet bore experiences MR acoustic noise that reaches the subject's cochlea through multiple routes. These routes encompass those through air, directly towards the external auditory canal and the eardrum (air-conduction), and those through the bony tissues of the subject (bone-conduction). In the latter, the head and body experience a vibration, in fact strictly originating from air-conducted sound waves, that is transmitted to the inner ear. The cochlea is then stimulated through

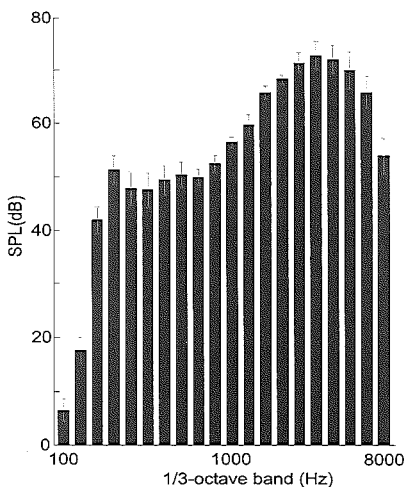


**Figure 4.** Filter characteristic of the external ear canal. Demonstrated are the 1/3-octave band frequency levels for white noise at a level of 80 dB, measured using the MIRE method, and the whiskers indicate the standard error (n=10). The ear canal's attenuation represents a high-pass filter.

movements of the ossicles in the middle ear, by compression and distortion of the bony labyrinth and by osseotympanic motion, i.e. the radiation of sound in the ear canal itself (27,28). The objective sound level is the SPL as measured in the external ear canal (with a microphone-in-real-air, MIRE) and represents the air-conducted sound pathway only. By contrast, the subjective sound level is the SPL of a sound as experienced by a subject and, therefore, comprises both sound conduction through air and tissues. If air-conducted sounds are (substantially) louder than bone-conducted sounds, then the subjective SPL equals the objective SPL. But, if air-conducted sounds are softer than bone-conducted sounds, the subjective SPL is higher than the objective SPL. It is particularly in MRI that bone-conduction may become a relevant issue, because of usage of passive hearing protection (obliged in MRI if sound levels are > 99 dBA) which reduces air-conduction, but leaves bone-conduction unaffected (11,25). In the MR imager, an additional bone-conduction pathway may add to the subjective sound levels, i.e. through the mechanical vibrations conveyed from the gradient system to the MR table and subsequently to the subject.

The standard audiometric method for quantifying the subjective efficacy

of acoustic isolators, defined as the difference in experienced sound levels with versus without acoustic isolation, is the determination of hearing thresholds (12). In the MR tunnel, however, this is impractical because of high ambient sound levels that mask the tonal stimuli. Loudness matching, as an alternate method, is less sensitive to background noise. This technique has previously been employed for determining the efficacy of an active noise cancellation system for MRI (17). There are reports, however, that indicate that the variable sound (controlled by the subject) is adjusted towards the comfortable level (12,29) causing underestimation of the subjective level. Thirdly, subjective loudness estimation can also be measured by the masking method. This method has proven a valid technique for attenuation measurements in noisy environments (12) and was therefore adapted for use in our experiment.

## References

1. Hurwitz R, Lane SR, Bell RA, Brant-Zawadzki MN. Acoustic analysis of gradient-coil noise in MR imaging. *Radiology* 1989; 173:545-548.
2. Langkowski JH, Thiele F, Maas R, Kooijman H. Measurement of noise levels in MR tomography at 1.5 Tesla. *Rofo Fortschr Geb Röntgenstr Neuen Bildgeb Verfahr* 1989; 151:483-486.
3. Moelker A, Wielopolski PA, Pattynama PM. Acoustic noise and related safety considerations in magnetic resonance imaging environments. *RSNA 87th scientific assembly & annual meeting 2001 - Categorical Course Practical MR safety considerations 2001*.
4. The Council of European Communities. Council Directive of 12 may 1986 on the protection of workers from the risks related to exposure to noise at work. 1986; 86/188/EEC.
5. National Institute for Occupational Safety and Health (NIOSH). Criteria for a recommended standard, Occupational Noise Exposure, Revised criteria 1998. 1998; Publication No. 98-126.
6. Radomskij P, Schmidt MA, Heron CW, Prasher D. Effect of MRI noise on cochlear function. *Lancet* 2002; 359:1485.
7. Moelker A, Pattynama PM. Acoustic noise concerns in functional magnetic resonance imaging. *Hum Brain Mapp* 2003; 20:123-141.
8. Amaro E, Jr., Williams SC, Shergill SS, et al. Acoustic noise and functional magnetic resonance imaging: Current strategies and future prospects. *J Magn Reson Imaging* 2002; 16:497-510.
9. Moelker A, Wielopolski PA, Pattynama PM. Relationship between magnetic field strength and magnetic-resonance-related

- acoustic noise levels. *Magma* 2003; - 16:52-55.
10. Mansfield P, Glover PM, Beaumont J. Sound generation in gradient coil structures for MRI. *Magn Reson Med* 1998; 39:539-550.
  11. Ravicz ME, Melcher JR. Isolating the auditory system from acoustic noise during functional magnetic resonance imaging: examination of noise conduction through the ear canal, head, and body. *J Acoust Soc Am* 2001; 109:216-231.
  12. Berger EH. Methods of measuring the attenuation of hearing protection devices. *J Acoust Soc Am* 1986; 79:1655-1687.
  13. Edelstein WA, Hedeem RA, Mallozzi RP, El-Hamamsy SA, Ackermann RA, Havens TJ. Making MRI quieter. *Magn Reson Imaging* 2002; 20:155-163.
  14. Katsunuma A, Takamori H, Sakakura Y, Hamamura Y, Ogo Y, Katayama R. Quiet MRI with novel acoustic noise reduction. *Magma* 2002; 13:139-144.
  15. Berger EH. Is real-ear attenuation at threshold a function of hearing level? *J Acoust Soc Am* 1985; 78:1588-1595.
  16. Tomasi DG, Ernst T. Echo planar imaging at 4 Tesla with minimum acoustic noise. *J Magn Reson Imaging* 2003; 18:128-130.
  17. Chambers J, Akeroyd MA, Summerfield AQ, Palmer AR. Active control of the volume acquisition noise in functional magnetic resonance imaging: method and psychoacoustical evaluation. *J Acoust Soc Am* 2001; 110:3041-3054.
  18. Toivonen M, Paakkonen R, Savolainen S, Lehtomaki K. Noise attenuation and proper insertion of earplugs into ear canals. *Ann Occup Hyg* 2002; 46:527-530.
  19. Counter SA, Olofsson A, Borg E, Bjelke B, Haggstrom A, Grahn HF. Analysis of magnetic resonance imaging acoustic noise generated by a 4.7 T experimental system. *Acta Otolaryngol* 2000; 120:739-743.
  20. Baumgart F, Kaulisch T, Tempelmann C, et al. Electrodynamical headphones and woofers for application in magnetic resonance imaging scanners. *Med Phys* 1998; 25:2068-2070.
  21. American National Standard S1.11-1986. Specification for Octave-Band and Fractional-Octave-Band Analog and Digital Filters. Acoustical Society of America. 1986.
  22. American National Standard S1.6-1984. Preferred frequencies, frequency levels, and band numbers for acoustical measurements. Acoustical Society of America. 1986.
  23. Ballachanda BB. Theoretical and applied external ear acoustics. *J Am Acad Audiol* 1997; 8:411-420.
  24. Moelker A, Vogel MW, Pattynama PM. Efficacy of passive acoustic screening: implications for the design of imager and MR-suite. *J Magn Reson Imaging* 2003; 17:270-275.
  25. Guidance for the Submission Of Pre-market Notifications for Magnetic Resonance Diagnostic Devices. Washington DC: U.S. Department Of Health and Human Services, Food and Drug Administration, Center for Devices and Radiological Health 1998.
  26. Khanna SM, Tonndorf J, Queller JE. Mechanical parameters of hearing by bone conduction. *J Acoust Soc Am* 1976; 60:139-154.
  27. Stenfelt S, Wild T, Hato N, Goode RL. Factors contributing to bone conduction: the outer ear. *J Acoust Soc Am* 2003; 113:902-913.
  28. Stenfelt S, Hato N, Goode RL. Factors contributing to bone conduction: the middle ear. *J Acoust Soc Am* 2002; 111:947-959.
  29. Stenfelt S, Hakansson B. Air versus bone conduction: an equal loudness investigation. *Hear Res* 2002; 167:1-12.



# Real-Time Modulation of Acoustic Gradient Noise in Interventional MRI

ADRIAAN MOELKER, MIKA W. VOGEL, PETER M.T. PATTYNAMA

*Department of Radiology, Erasmus Medical Center Rotterdam, 50 Dr. Molewaterplein, P.O. Box 1738, 3000 DR Rotterdam, The Netherlands*

**ABSTRACT:** Acoustic noise is inherent to magnetic resonance imaging (MRI) and poses safety risks to patients and interventional radiologists. Although a spectrum of noise reduction techniques has been implemented, new developments further increase sound levels. Silent pulse sequences based on derating gradient currents have been proposed but are limited to slow pulse sequences not suitable for interventional MRI (iMRI). However, iMRI does not continuously require fast imaging with high image update rates. Therefore, the aim of this study was to develop a tool that could remotely derate the gradient currents in real time, operated by the interventionalist. The duration of the derated gradients is increased to retain image resolution [this extends imaging time and echo time (TE)]. The experiment setup consisted of a custom-built remote controller located in the interventional MR room. A fast spoiled gradient recalled echo (FSPGR) sequence was tested and acoustic recordings were made with a microphone in the magnet bore. An optical link sent data from the remote controller to a computer that was connected to a 1.5-T cardiovascular MR scanner over ethernet. A software server installed on the MR system received the requests and passed these on to the integrated pulse generator in order to control the real-time imaging. Slew rate adjustments were accomplished by calculating instruction period changes and adjusted waveform amplitudes accordingly. The experimental setup reduced the slew rate up to 16-fold, which resulted in a considerable acoustic noise reduction of 21.1 dBA. The remote controller performed well and image quality showed no substantial qualitative changes. We made use of the previously described idea of silent pulse sequence designing. Although derating is at the expense of the image refresh rate, our real-time slew rate reduction is compatible with the fact that iMRI procedures do not continuously require fast image update rates. © 2004 Wiley Periodicals, Inc. *Concepts Magn Reson Part B (Magn Reson Engineering)* 20B: 34-39, 2004

**KEY WORDS:** magnetic resonance (MR); magnetic resonance guidance; magnetic resonance safety; magnetic resonance acoustic noise; acoustic noise reduction

## INTRODUCTION

Acoustic noise is an unwanted side effect of magnetic resonance imaging (MRI) (1). Its effects are of concern particularly in interventional MRI

Received 16 June 2003; revised 23 August 2003; accepted 26 August 2003

Correspondence to: Adriaan Moelker; E-mail: a.moelker@erasmusmc.nl

Concepts in Magnetic Resonance Part B (Magnetic Resonance Engineering), Vol. 20B(1) 34-39 (2004)

Published online in Wiley InterScience  
(www.interscience.wiley.com). DOI 10.1002/cmrb.20004

© 2004 Wiley Periodicals, Inc.

(iMRI) in which both patient and interventionalist are subjected to hazardous acoustic noise levels for a substantial amount of time (2, 3). The potential risk is in the development of temporary and permanent hearing damage (4, 5). In addition, the current advent of iMRI requires faster scanning techniques for real-time imaging with better resolution and signal-to-noise ratios. These are provided by recent improvements in gradient performance and magnetic field strengths but at the expense of acoustic noise production.

Various techniques for reducing MR-related acoustic noise have been proposed and tested in the MR environment, among others, magnetic force balanced gradient coils and the application of heavy acoustic insulators in the scanner (6-8).

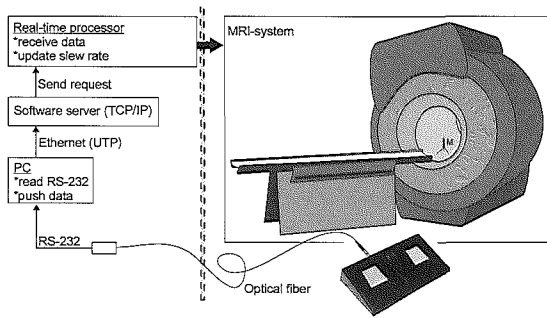


**Figure 1** Experiment setup. Acoustic noise measurements were performed at the isocenter of the MR scanner.

A promising development is in the acoustic optimization of the gradient currents (pulses) that are fed to the coils during the imaging process, i.e., the so-called silent pulse sequences (9). Basically, such gradient pulses are low-pass filtered, which effectively removes higher-order frequency components in the generated acoustic output (10). To this end, the gradient currents are shaped sinusoidal rather than square. Also, the number of gradient ramps is minimized by merging pulses, thereby lowering the fundamental excitation frequency (human hearing becomes less sensitive at low frequencies).

Unfortunately, silent pulse sequences have reduced performance with slower imaging refresh rates and consequently are less suitable for real-time iMRI with high refresh rates (11). On the other hand, interventional procedures do not continuously require full system capabilities and may allow for intervals with less demanding gradient pulses. Therefore, the aim of this study was to develop a tool that hooks up with the MR system and remotely modifies the shape of the gradient pulses in real time. Slew rates and gradient amplitudes are reduced while gradient pulse durations are increased to retain image resolution at constant gradient coil power dissipation [this extends imaging time and echo time (TE)].

## MATERIALS AND METHODS

### Study Design

The experiment setup consisted of a custom-built remote controller device inside the MR room that was linked optically to an RS-232 port of a personal computer (PC) in the operator room (Fig. 1). The RS-232 data were captured using custom-written software in Matlab R13 (The Mathworks, Inc., Novi, MI) and passed on to a software server on a 1.5-T cardiovascular MR system (Signa CV/i; General Electric, Milwaukee, WI) using transmission control protocol/internet protocol (TCP/IP). The software server handled real-time waveform modification requests over an ethernet connection. Using this setup, slew rates of the gradient pulses could be remotely controlled.

### Remote Controller

The remote controller was designed as a foot pedal with up and down switches so that it could be operated easily by the interventionalist (Fig. 1). The foot switch to fiber interface (Fig. 2) was a digital potentiometer (DS1669, Dallas Semiconductor, Sunnyvale, CA) and provided discrete tap points over a 10-k $\Omega$ -resistive range used for opening a transistor driving a light-emitting device (LED, infrared). The switches (S1 and S2) were mechanical-type contact closure switches that caused the digital wiper to go up and down depending on the switch used. Switch inputs that lasted longer than 1 s caused the wiper to move one position every 100 ms, resulting in a total time to transcend the complete resistive range in  $\sim 7$  s. For feedback to the MR interventionalist, a two-digit display was used that indicated the device's output within 40 steps. The power supply was supported by lithium ion batteries or alternating current (AC).

The infrared source was attached to a sub miniature assembly (SMA) optical connector (LF-SMA; Laser Components, Olching, Germany) for

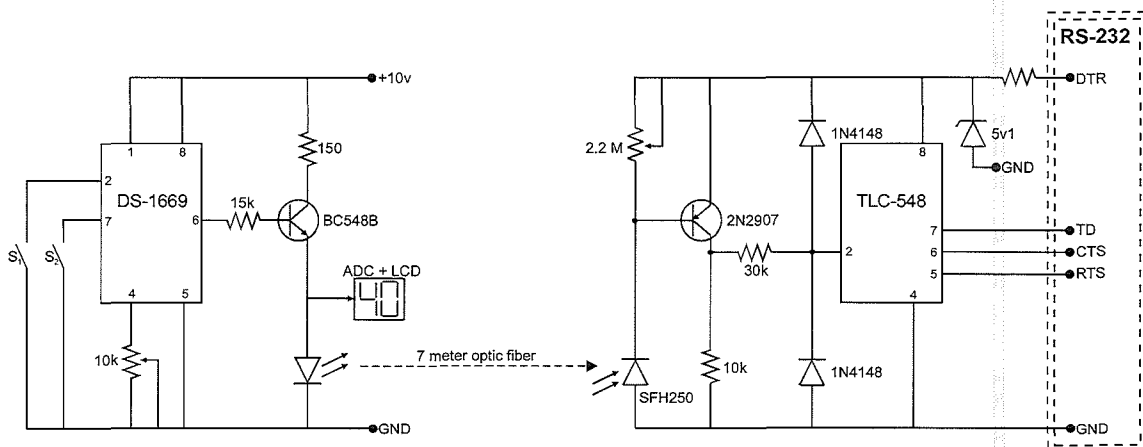


**Figure 2** Schematic diagram of remote controller with fiber optic coupling. DTR, data terminal ready; GND, ground.

```

s = serial(COM1,'baudrate',115200);           % make serial port object
fopen(s);                                     % open serial port

s.DataTerminalReady = 'on';                  % set DTR to one (power supply TLC-548 on)

s.RequestToSend = 'off';                     % set RTS to zero (clock select TLC-548)

for i = 1:8;                                  % loop for capturing 8-bit binary data
    readdata = s.PinStatus;                   % read status CTS (dataline TLC-548)
    readdata = readdata.ClearToSend;
    if readdata(1:2) == 'on';                 % fill in binary value
        data(i) = 1;
    else
        data(i) = 0;
    end
    fwrite(s,0);                               % set TD to one (set I/O clock, uses parity-bit)
end

s.RequestToSend = 'on';                       % set RTS to one (clock select TLC-548)
s.DataTerminalReady = 'off';                 % set DTR to zero (power supply TLC-548 off)

fclose(s);                                    % close serial port

```

**Figure 3** Matlab code for capturing 8-bit data from the remote controller device. Readout is done on a serial bit-by-bit basis at a 115-kbps bit rate. Note that the I/O clock runs by writing parity bits, because error checking is enabled by default in Matlab serial port communication.

transmitting light through a 600-micron optical fiber (HCP-M0600T; Laser Components) to the operator room. This was deemed necessary for not risking any damage to the PC due to radio frequency (RF) leakage. Subsequently, the infrared light was picked up by a photosensitive diode (SFH250; Siemens, Nuremberg, Germany) and was used for driving an 8-bit analogue-to-digital converter (ADC) with integrated serial communication (TLC-548; Texas Instruments, Inc., Dallas, TX). The readout of the ADC was controlled by locally written software on a PC (Fig. 3). First, a serial port object was created with a 115-kbps connection speed and its data transmit line (DTS) was set to *on* for supplying ~10 V to the ADC. Next, the clockselect line of the ADC was set to *off* using the request-to-send (RTS) line for allowing an 8-bit serial conversion. The first bit was read subsequently from the clear-to-send (CTS) line. An input/output (I/O) clock cycle forced a shift to the second bit, driven by the *fwrite* command that wrote to the transmit data (TD) line. Because the parity bit, typically used for error checking, interfered with the I/O clock and could not be deactivated, the parity bit itself was used for the bit shift. After capturing a complete byte of data, the I/O clock was set to *off* (RTS control line) causing a reset condition. Finally, the 8-bit word was converted to a percentage by dividing by 256. In the experiments, time averaging was used over 0.5 s for increasing numeric stability.

## MR Equipment and Acoustic Noise Measurements

Imaging was performed using the manufacturer's real-time imaging platform (CNV 3 software, General Electric, Milwaukee, WI). Real-time control of the pulse sequence was obtained using in-house developed software that set up a software server running in a background process on the MR-host computer. This server handled requests for adjustment of slew rates, gradient amplitudes, and timings over the existing TCP/IP interface. Up to 10 requests/s could be handled. To communicate with the demon, we implemented a client in Matlab, which calculated scaling factors for predefined gradient waveforms of the realtime pulse sequence database, based on the input of the remote controller device. Then, these values were sent over to the server.

To control the real-time imaging, the server connected to the integrated pulse generator, which consisted of six logic cell array-based sequencers. One master sequencer synchronized the waveforms, of which three controlled the digital waveform generation of gradient pulses. Both gradient waveform and instruction memory could be modified in real time. Slew rate adjustments were accomplished by calculating instruction period changes and adjusted waveform amplitudes accordingly. Reducing the slew rates and amplitudes resulted in the extension of repetition time (TR) and TE and, consequently, in a reduction of the imaging refresh rate.

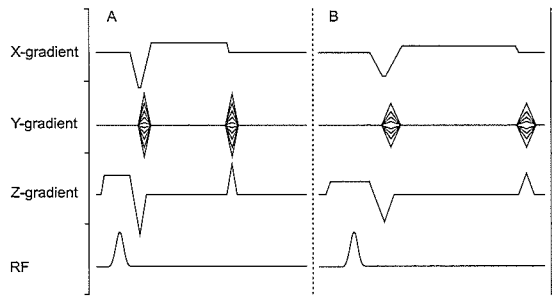


**Figure 4** Reference PSD and low acoustic noise PSD with lower slew rate, lower amplitudes, and extended duration (not scaled). Both TR (not appreciable from the figure) and TE are extended by the technique.

The adjustments were discrete as dictated by the gradient sequencer update capacity, which was as low as 4  $\mu$ s in our MR system.

Using this setup, we were able to remotely control the behavior of the real-time pulse sequence diagram (PSD). The amplitude and period modifications were programmed such that all low-order moments were identical (Fig. 4). However, total magnetization by the gradient coil may have been reduced slightly because of the polynomial behavior of root-mean-square (RMS) driver currents ( $I_{\text{RMS}}$ ) according to the calculation of RMS integral-of-gradient current  $I_g$  over time ( $t$ ):

$$I_{\text{RMS}} = \sqrt{\frac{1}{\text{TR}} \int_0^{\text{TR}} [I_g(t)]^2 dt.}$$

### Acoustic Measurements

Acoustic data were measured for slew rates that ranged from a maximum of 150  $\text{Tm}^{-1}\cdot\text{s}^{-1}$  to a minimum of 9.4  $\text{Tm}^{-1}\cdot\text{s}^{-1}$  (16 times lower), using an integrated quadrature driven transceiver RF body coil. The slew rates of various kinds of pulse sequences could be modified with this experiment setup, but the pulse sequence tested was fast spoiled gradient recalled echo [FSPGR; TR/TE = 20 ms/4.2 ms; field of view (FOV), 480 mm; matrix 256\*128; slice thickness, 5 mm; flip angle, 20°] because it is suitable for real-time imaging and, therefore, relevant to iMRI. A pre polarized-free field condenser microphone (type 4189; Bruël & Kjær, Nærum, Denmark) was positioned in the scanner's isocenter and via a 10-m extension cable (AO-0442; Bruël & Kjær) connected to a type 1 digital sound level analyzer (Investigator 2260; Bruël & Kjær). The equivalent-continuous A-filtered sound pressure level (SPL) was considered the preferred measure because it reflected the overall (time-averaged) SPL over a 15-s measurement period. In addition, an A-filter accounted for the decreased sensitivity of the human hearing for

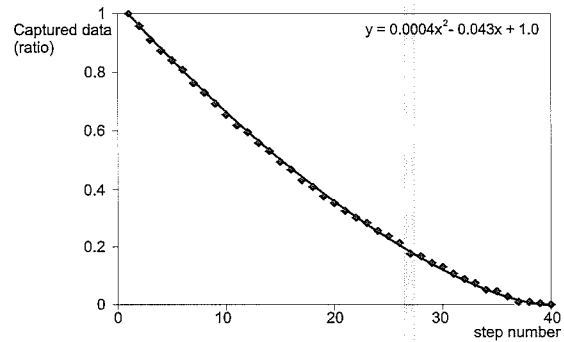


**Figure 5** Data captured by Matlab with respect to the step number on the remote controller. The data strongly correlated with the given equation ( $y$ =captured data and  $x$ =step number).

frequencies below 1kHz and over 6 kHz (12). The amplitude- and frequency-dependent effects of the main magnetic field and the switching gradient fields on the calibration of the sound measurement setup have been tested previously and were negligible (2, 13). The effect on image quality was visually evaluated using a copper sulphate phantom and human brain images.

### RESULTS

Figure 5 shows that the data captured from the remote controller was slightly nonlinear regarding the number of switch taps. The data could be fitted nicely with a second-order polynomial (correlation coefficient, 0.99). The SD of the non time-averaged readouts was smaller than 2%. Because of time averaging over 0.5 s (~10 readout periods for a TR of 20 ms), deviation of the requests to the real-time imaging platform was even smaller (<1%).

The acoustic noise attenuation that could be achieved depended on the slew rate used (Fig. 6) and was up to 21.1 dBA (16 times reduction). For larger slew rate reductions, the sound levels of the MR-generated noise were approximating those of the ambient background levels and, therefore, the advantageous effect of noise attenuation became less. The unfiltered linear-equivalent continuous SPL showed less reduction (15.2 dB, not shown), indicating that some of the acoustic noise attenua-

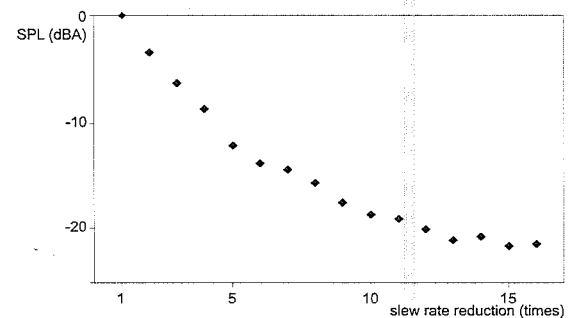


**Figure 6** Relative acoustic noise reduction on A-weighted scale for reductions of the slew rate (and amplitude) ranging from 1 to 16 times.



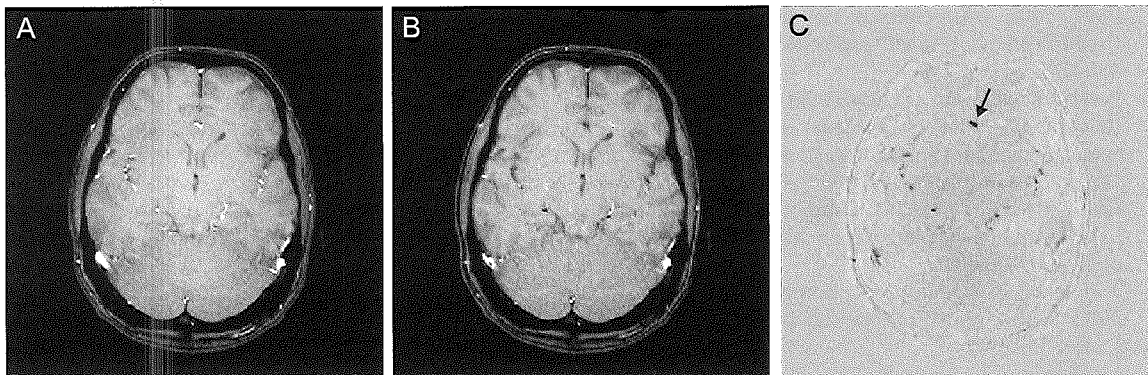


**Figure 7** Brain images using (A) a reference scan and (B) a scan with 16 times reduced slew rate and amplitude. (C) Except from blood inflow phase changes due to the longer TE (arrow), no substantial differences could be appreciated in the difference image.

tion was a result of a lower-frequency distribution of the MR noise.

The total magnetization by of the gradient pulses was kept equal, i.e., the amplitude decreased concurrent with lengthening the gradient pulse period. As expected, no visual changes in image quality could be appreciated from brain images (Fig. 7). The small phase changes in blood vessels were caused by the longer TE (inflow of unexcited blood). Note that extending the gradient pulses evidently reduced the refresh rate of the real-time imaging protocol.

## DISCUSSION

We have shown an adaptive method of acoustic noise reduction using a remote controller situated in the MR room. The prototype performed adequately and could vary the gradient pulse amplitude and period over a large range. Although the optical connection was analogue, the data transmission was only slightly nonlinear. In future controller designs, data transmission should be digital, making additional features such as real-time modification of other imaging parameters easier to implement.

The pulse sequences commonly used in iMRI typically generate intense acoustic noise levels (2). In our study, levels were up to 96 dBA, using less-demanding imaging parameters (TR of 20 s). Nevertheless, this SPL substantially exceeds the safety limits of 85 dBA as supposed by federal governments in the United States (14). Our experiments showed a noise attenuation of 21.1 dB on an A-weighted scale and a lower but still considerable reduction of 15.2 dB on a linear scale. From a safety perspective, such acoustic noise reduction holds that the risk of hearing damage is reduced by a factor of 128 (15).

Numerous studies have been published on how to limit acoustic noise during MRI and various successful techniques have been proposed, developed, and implemented in MR systems. These are based on primarily passive methods such as heavy

acoustic insulators, vacuum packing of the gradient system, and better gradient- and RF-coil designs (8, 16, 17). However, continuous improvements in imaging techniques and MR hardware counteract these techniques. As an example, the gradient and magnet field strengths are related with the acoustic output; doubling either of these results in a 6-dB gain of SPL (18). In addition, novel imaging techniques, such as balanced steady-state-free precession, completely exploit the gradient system of the MR scanner with evidently excessive acoustic noise production.

The adaptive method we tested is based on the work of previous investigators who showed the acoustic benefit of derating gradient currents (10). In addition, we lowered the gradient period causing the fundamental frequency of the pulse sequence to decrease. The net effect is a larger acoustic noise reduction than expected based on derating alone, because of the filter characteristics of the A-filtering (high pass). Extending the period of the gradient current, as a relative drawback, is at the expense of the refresh rate. However, because slew rates could be modified in real-time, our method can take advantage of the fact that iMRI procedures do not continuously require fast image update rates.

Finally, MR-generated acoustic noise largely hampers speech understanding between interventionalists (1), especially during worst-case pulse sequences, i.e., those commonly applied in iMRI. Therefore, an additional benefit of our adaptive imaging method is in its potential to quickly improve verbal communication whenever required. A reduction of 21 dBA equalizes an appreciable lowering of one's voice from, e.g., extreme shouting to a normal conversational level.

## REFERENCES

1. McJury M, Shellock FG. 2000. Auditory noise associated with MR procedures: A review. *J Magn Reson Imaging* 12:37-45.
2. Moelker A, Maas RA, Lethimonnier F, Pattynama

- PMT. 2002. Interventional MR Imaging at 1.5 T: Quantification of sound exposure. *Radiology* 224: 889-895.
3. Foster JR, Hall DA, Summerfield AQ, Palmer AR, Bowtell RW. 2000. Sound-level measurements and calculations of safe noise dosage during EPI at 3 T. *J Magn Reson Imaging* 12:157-163.
  4. Brummett RE, Talbot JM, Charuhas P. 1988. Potential hearing loss resulting from MR imaging. *Radiology* 169:539-540.
  5. Radomskij P, Schmidt MA, Heron CW, Prasher D. 2002. Effect of MRI noise on cochlear function. *Lancet* 359:1485.
  6. Mechefske CK, Geris R, Gati JS, Rutt BK. 2002. Acoustic noise reduction in a 4 T MRI scanner. *Magma* 13:172-176.
  7. Mansfield P, Haywood B, Coxon R. 2001. Active acoustic control in gradient coils for MRI. *Magn Reson Med* 46:807-818.
  8. Katsunuma A, Takamori H, Sakakura Y, Hamamura Y, Ogo Y, Katayama R. 2002. Quiet MRI with novel acoustic noise reduction. *MAGMA* 13:139-144.
  9. De Zwart JA, Van Gelderen P, Kellman P, Duyn JH. 2002. Reduction of gradient acoustic noise in MRI using SENSE-EPI. *Neuroimage* 16:1151-1155.
  10. Hennel F, Girard F, Loenneker T. 1999. "Silent" MRI with soft gradient pulses. *Magn Reson Med* 42:6-10.
  11. Hennel F. 2001. Fast spin echo and fast gradient echo MRI with low acoustic noise. *J Magn Reson Imaging* 13:960-966.
  12. Acoustical Society of America. American National Standard S1.13-1995. Measurement of sound pressure levels in air. Melville, NY: Acoustical Society of America.
  13. Price DL, De Wilde JP, Papadaki AM, Curran JS, Kitney RI. 2001. Investigation of acoustic noise on 15 MRI scanners from 0.2 T to 3 T. *J Magn Reson Imaging* 13:288-293.
  14. Occupational Safety and Health Administration (OSHA). OSHA FR-1910.95, 61 Federal Regulations 9227. 1996. Occupational noise exposure (Occupational Health and Environmental Control). Washington DC: US Department of Labor, Occupational Safety and Health Administration.
  15. Acoustical Society of America. American National Standard S3.44-1996. Determination of occupational noise exposure and estimation of noise-induced hearing impairment. Melville, NY: Acoustical Society of America.
  16. Moelker A, Vogel MW, Pattynama PMT. 2003. Efficacy of passive acoustic screening: Implications for the design of imager and MR suite. *J Magn Reson Imaging* 17:270-275.
  17. Edelstein WA, Hedeem RA, Mallozzi RP, El-Hamamsy SA, Ackermann RA, Havens TJ. 2002. Making MRI quieter. *Magn Reson Imaging* 20:155-163.
  18. Moelker A, Wielopolski PA, Pattynama PMT. 2003. Relationship between magnetic field strength and magnetic-resonance related acoustic noise levels. *MAGMA* 16:52-55.

## Summary and prospects

Magnetic resonance imaging (MRI) is a technique in which strong static and dynamic magnetic fields are used to create virtual slices of the human body. The process of MR imaging is associated with several health and safety issues which may negatively affect patient and radiological health workers. Potentially hazardous are biological effects of both the static and dynamic magnetic fields, the torques of the magnetic fields acting on ferromagnetic objects, thermal effects, and the negative effects of high acoustic sound pressures. The subject of this dissertation is the evaluation and modification of acoustic noise generated during MRI.

**Chapter 2** presents an overview of the current knowledge on acoustics and MRI, starting with a description of the various sources of MR-related acoustic noise. The gradient coil produces most of the acoustic noise. During the process of imaging, the gradient coil induces an alternating magnetic field that counteracts the strong static magnetic field. The gradient coil therefore starts acting as a large loudspeaker producing sounds that are within the range of audible frequencies. Average sound levels of up to 130 dB with peak levels over 140 dB have been demonstrated for MR imagers at 3 Tesla. These quantitative and qualitative characteristics are determined by the imaging parameters, specifically repetition time, echo time, field of view and slice thickness. Furthermore, this chapter discusses the negative effects of the magnetic gradient field, main magnetic field and radio frequency pulses on sound measurements in the MR environment. It also provides a guide on adequately performing sound measurements in MRI. Finally, an overview of the current acoustic-noise-reduction techniques in MRI and those under development is presented.

In chapters 3, 4 and 5, the problem of acoustic noise in MRI is assessed by experiments and discussed within the context of data from the literature.

Brummet et al. (1988) described the risk which MR acoustic noise

poses to hearing of patients inside the MR imager. Their findings have recently been corroborated by Radomski and colleagues who found a temporary decrease in otoacoustic emissions in 16 subjects, despite the use of protective devices. However, the exposure of engineers and health workers to MR noise has hitherto never been discussed. Exposure to acoustic noise is cumulative, and chronic exposure can induce the development of permanent hearing damage. The advent of interventional MRI, during which health workers are repeatedly exposed to MR noise for extended periods of time, may have therefore increased the risk of health workers to hearing damage. To quantify the risk of permanent hearing loss, sound levels during MR pulse sequences that are suitable for interventional imaging were measured. The results, presented in **Chapter 3**, indicate that MR noise indeed creates an occupational hazard to the interventional radiologist. The sound levels are substantially above the levels permitted by American and European guidelines, particularly for pulse sequences with high image-refresh rates. During an interventional procedure in which these rapid pulse sequences are employed, permanent hearing loss occurs within minutes. Therefore, adequate hearing protection should be required.

In **Chapter 4**, the effect of MR acoustic noise on speech recognition is investigated. Verbal communication is a prerequisite in several practical situations. First, speech intelligibility between interventionalists should be adequate and is essential for safely performing MR-guided interventional procedures. Second, in auditory functional MRI, the presentation of verbal stimuli to the subject should be uncontaminated and intelligible. In this study, speech intelligibility during MR noise has been determined, specifically for pulse sequences that are relevant to both interventional and functional MRI. In

addition, the effect of passive hearing protection on intelligibility was determined. To this end, 15 subjects listened to spoken text in the presence of MR noise and repeated this text as correctly as possible. The sound level of the presented text was modified in discrete steps towards a level at which half of the spoken text could be reproduced correctly. The results show that speech understanding suffers from MR acoustic noise, both from the perspective of the interventional radiologist placed beside the imager and from the perspective of the patient lying inside the imager. The interventionalist needs to speak loudly or, depending on the pulse sequence, even shout to be understood by either a colleague. The speech level required for adequate communication with the patient lying in the MR tunnel is even higher, because of the extreme sound intensity at the patient's location. Passive hearing protection has a positive effect on speech intelligibility; it halves the required vocal effort.

The negative effect of MR-related acoustic noise on functional MRI (fMRI) is the subject of **Chapter 5**. fMRI is based on quantifying the increase in cerebral blood flow as a response to activation of brain regions. fMRI plays an increasing role in pre-operative staging for brain surgery by delineating diseased from normal tissue and in research into neurodegenerative and psychiatric diseases. MR noise during fMRI causes a type of artifact in which brain activity appears to be absent. This can cause physicians to wrongly conclude that the tissue is diseased. MR-related acoustic noise interferes with functional MR acquisitions through the reduction in the dynamic range of the MR signal and by affecting the perception and processing of the stimulus of interest by a distracting effect. Functional MRI, specifically fMRI of the auditory cortex, may be further impaired by the imager noise due to its screening effects on stimuli and

due to the activation of the auditory cortex by the imager's noise itself, concurrently with the scarce resolution at which this cortical region can be imaged. Besides the acoustic noise reduction techniques mentioned in chapter 2, this current chapter discusses modifications in fMRI experimental set-ups, also called the silent imaging paradigms. Basically, these paradigms attempt to eliminate the intra- and inter-acquisition response of the brain to the imager's noise. The intra-acquisition response refers to a brain response induced by imager noise that interferes with the functional data to be acquired later on within the same image acquisition. As the response to scanner noise is slow, the intra-acquisition interference decreases when using very rapid volume acquisitions (< 3 seconds). The inter-acquisition response is generated when the acoustic noise cortical response persists during the next volume acquisition. By extending the time between the acquisitions, such that the next volume acquisition occurs only after the acoustic noise response has subsided, the inter-acquisition response can be completely avoided.

The need for better signal-to-noise ratios and resolution has pushed MRI towards the development and application of high-field MR scanners encompassing dedicated gradient assemblies. As an example, data from the European Magnetic Resonance Forum show an increase in the investment in high field MR systems since 2000. Specifically these factors, i.e. field and gradient strength, are theoretically related to acoustic noise levels. In **Chapter 6**, the relationship between sound level and static magnetic field strength has been validated experimentally. To this end, sound measurements were performed making use of a Siemens Magnetom Vision MRI scanner equipped with a Helicon rampable magnet. During various pulse sequences, acoustic data were acquired at field strengths increasing step-wise from 0.5 to 2.0 Tesla. The results of our experiments are in good agreement with what theory predicts: an increase of 6 dB when doubling the magnetic field strength.

Evidently, it is important to develop techniques that reduce the

acoustic noise experienced in MRI. In **Chapter 7**, the subject is the importance of passive noise reduction with respect to both the patient positioned inside the MR system and the radiologist located beside the MR system. A subdivision of acoustic source pathways into direct and indirect was made, i.e. originating at the inner and outer shrouds of the MR scanner and originating at the sound-reflecting walls of the MR suite, respectively. The relative contributions of direct and indirect acoustic noise to the overall sound level, as measured at both patient and radiologist locations, were quantified by blocking their pathways by using thick layers of passive sound absorbers. The experiments showed that, for a patient, direct acoustic noise radiation from the inner shroud of the MR scanner is most relevant. Substantial acoustic noise reduction of up to 19 dB(L) can be provided by adequate isolation of the MR tunnel. Sound coming from the outer shroud radiation and from indirect reflections accounts for most of the acoustic energy when recording close to the entrance of the MR imager at the location of the radiologist. The simultaneous isolation of both source pathways results in an acoustic noise attenuation of up to 9.5 dB(L).

Currently, the most widely used method to reduce MRI noise to a comfortable and safe level is passive noise control. The passive protectors used in MRI, however, only reduce air-conducted sound transmission, leaving bone-conduction, i.e. the noise radiated to head and body and directly transmitted to the inner ear, unaffected. In a normal environment, the efficacy of hearing protectors is reduced when bone-conduction contributes significantly to the subjective sound level. However, the MR scanner is not a normal audiometric environment, and bone-conduction may be a more effective route of sound transmission inside the MR scanner than in a normal environment, both because the patient is completely surrounded by the MR sound source (the gradient assembly) and because the patient is in close contact with the vibrating MR table and gantry. In **Chapter 8**, the aim was therefore to evaluate the influence of bone-conduction in the MR environment and to

differentiate subjective hearing through mechanical vibrations from conventional bone-conduction in the MR imager. The analysis was based on 10 volunteers with the subjects both inside the MR tunnel and in an anechoic room, and a masking method was adapted to determine the subjective sound levels to MR noise. The contribution of bone-conduction to the subjective MR sound levels was measured for various configurations of hearing protectors. The results demonstrated that bone-conduction is not more pronounced inside the MR scanner than outside, specifically not when using MR-compatible passive hearing protection. Therefore, the previous reports on the subjective evaluation of protection devices in MRI hold their validity.

The last study on noise reduction described in this thesis makes use of a recently developed technique in which the gradient coils are excited less aggressively. As these so-called silent pulse sequences are inherently restricted to slow image acquisition, silent pulse sequences are thought not to be suitable for real-time image formation, and therefore their application in interventional MRI has not been documented previously. However, **Chapter 9** demonstrates that interventional MRI with silent pulse sequences is feasible, provided that the image refresh rate – and subsequently the sound production – can be modified by the radiologist in real-time. Evidently, interventional MRI does not continuously require fast imaging with high image update rates. The experimental setup in this study consisted of a custom-built remote controller located in the interventional MR room and connected to a 1.5 T MR scanner through optical fiber and over ethernet. In real-time, the MR noise could be lowered with 21 dB(A) and the image refresh rate 16-fold. From a safety perspective, such acoustic noise reduction holds that the risk of hearing damage is reduced by a factor of 128.

### **Prospects for acoustic noise in the MR environment**

One can argue that acoustic noise production in MR imagers will increase with the development and production of high field MR systems

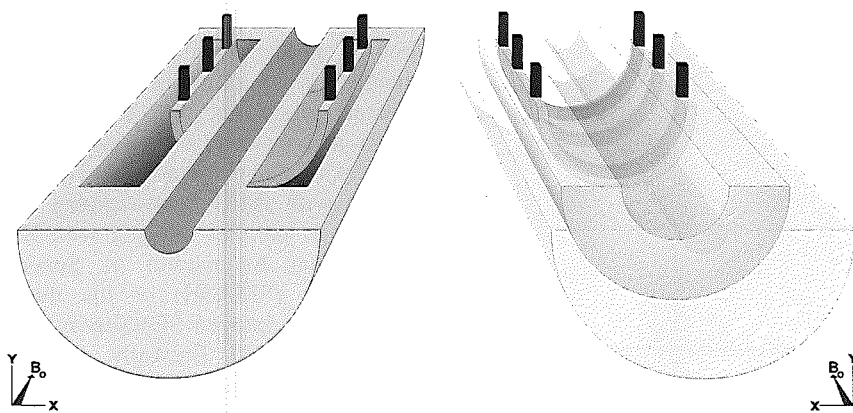


**Figure 1.** Novel MRI gradient structure for passive acoustic noise attenuation; the gradient coil is embedded in a cantilever.

with dedicated gradient assemblies. Currently, imagers available for human research have magnetic field strengths up to 9.4 Tesla (Center for Magnetic Resonance Research, Minneapolis, USA). In addition, several research centers are working on MR systems with field strengths of up to 11 Tesla (Commissariat à l'Énergie Atomique, Orsay, France), with which sound levels of over 160 dB have been recorded. A number of international organizations have created standards for medical devices in general and for diagnostic magnetic resonance devices in particular. The IEC 60601-2-33, a general safety guideline, is the most authoritative standard and is a basis for many other organizations, such as the North American Electrical Manufacturers Association (NEMA) and the Association for the Advancement of Medical Instrumentation (AAMI). The IEC guideline advises that maximum peak sound levels should be below 140 dB(A) and that time-averaged levels should be below 99 dB(A) for diagnostic magnetic resonance devices. It is of note that these sound levels pertain solely to diagnostic imaging. For research or experimental use, sometimes referred to as the second IEC level or mode, no guidelines are provided. This mode only requires approval of the local ethics committee, where applicable, and compliance with rules for occupational safety (e.g. European Directive 1986/86/188/EEC, sound exposure based on sound level and duration). MR devices purchased for clinical purposes, however, are frequently employed in research mode.

Moreover, devices not yet accepted for clinical use can be developed and tested experimentally. It is thus strongly advised that recommendations and guidelines for usage of MR devices under experimental conditions should be developed in order to protect the experimenter.

In chapters 2, 5, 7, 8 and 9, various sound reduction techniques that are implemented in magnetic resonance devices or are under development have been discussed. The majority of the implemented methods are based on passive noise reduction and the optimization of the geometry of the gradient coils and their encasings. However, in high field MR systems, these approaches do not sufficiently reduce acoustic noise towards sound levels that make these imagers suitable for clinical use. It is obvious that new noise reduction methods should be developed.

In a recent report of Bencsik et al., a gradient coil structure design for passive acoustic noise attenuation was proposed that can be readily implemented in longitudinal gradient coils. In the model, the gradient coil wire was held at the end of a thin epoxy resin cantilever that was held inside the coil structure (Fig 1). The interface between the cantilever and the main body of the gradient coil structure provides an excellent barrier to propagation of sound waves, and most of the acoustic energy is thus dissipated in the cantilever. The effects of this modification are substantial with reductions of 40 dB at an excitation frequency of 800 Hz. A potential problem in this novel gradient assembly is heat deposition,

which might be solved in the construction of hollow wires through which water circulates.

A second method of acoustic noise reduction, not yet investigated in the MR environment, is the application of active structural acoustic control (ASAC). ASAC is a technique analogous to active noise cancellation and makes use of panels with actuators and vibro-acoustic sensors that allow for a high level of acoustic noise reduction. Such active panels might replace the currently used inner and outer shroud materials of the MR imager, thereby providing an active isolation of the entire MR system. The efficacy of ASAC, however, is expected to be limited because of the extreme sound pressure levels and the frequency distribution of MR noise, predominantly >1 kHz. Hybrid isolation of vibration and sound waves by means of a combination of passive and active isolation is beneficial, with ASAC reducing sounds mainly below 1 kHz. Such a hybrid system may be further optimized by taking advantage of the repeatability of the MR sounds, which allows better prediction of the anti-vibrations in ASAC (Fig 3). Furthermore, the MR noise can, to a certain extent, be predicted based on the pulse sequence diagram.

Adequate communication in interventional MRI is problematic, despite the beneficial effect of passive noise reduction on speech intelligibility. In chapter 4, the use of a highly directional microphone located close to the speaker's mouth was recommended to improve speech understanding. The voice would then be played out through a headphone or loudspeaker. Recent developments in operating rooms are speech enhancement and speaker tracking. By placing arrays of directional and omni-directional microphones at the ceiling of the operating room coupled to a controller that analyses the signals, the position of a speaker can be estimated, and speech can be isolated from background acoustic noise. In MRI, speech enhancement and speaker tracking would be able to track the radiologist and to filter the radiologist's voice from the MR-related acoustic background noise. As in ASAC, optimisation can be achieved

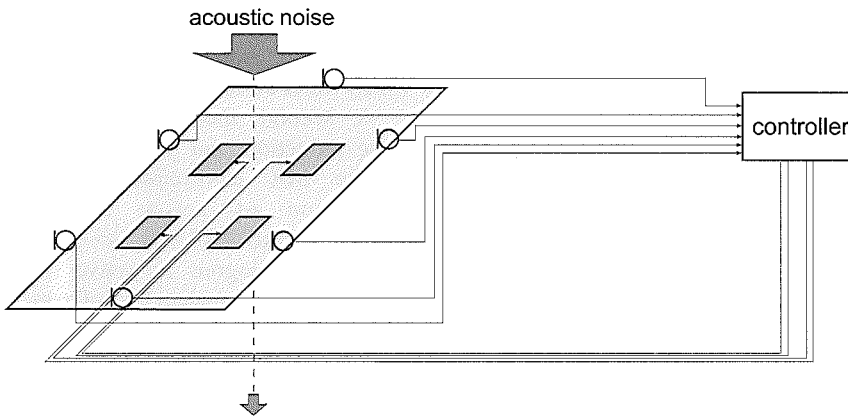


Figure 2. Basic setup of an active structural acoustic noise controller.

ved by processing the a-priori knowledge on MR noise. Finally, clear speech intelligibility in the MR environment is obtained when the filtered speech signals are amplified and presented.

In fMRI experiments, scanner noise interferes with stimulation, cognitive performance, and patient comfort. Passive insulation is not sufficient, due to bone-conduction, among other things. Several attempts have been made to produce silent pulse sequences suitable to fMRI (see chapter 5). One of these is based on the stimulation of MR signals by a burst of radiofrequency pulses, rather than noisy gradient pulses. Such a pulse sequence can be heard as only soft clicks with a sound intensity comparable to that of ambient noise. The sequence is intrinsically insensitive to certain artifacts, but is largely limited by its low signal-to-noise ratio (SNR)

and resolution. The SNR improves when making use of half-Fourier phase encoding, a technique in which only half of the data acquisition is

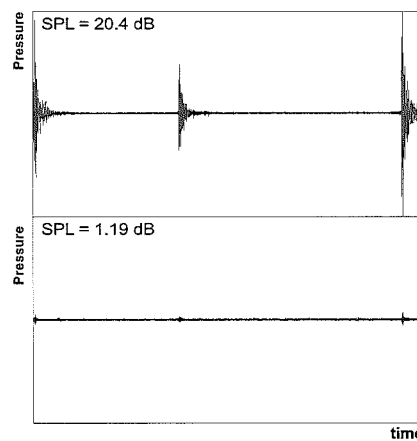


Figure 3. Subtraction of two successive TR periods demonstrates the repeatability of MR noise and provides a reduction of >19 dB.

performed. In a recent study, half-Fourier phase encoding was implemented in a burst imaging pulse sequence, albeit not one suitable for fMRI, and provided a 40% increase in SNR. A second technique that is compatible with fMRI burst-imaging sequences is parallel imaging with Simultaneous Acquisition of Spatial Harmonics (SMASH) or the more frequently employed SENSitivity Encoding (SENSE). Basically, parallel imaging makes use of antennae that capture MR signals from identical anatomic regions. Consequently, the number of phase encoding steps in data acquisition is reduced with a factor that equals the number of antennae. This technique speeds up image acquisition and improves both SNR and resolution. The combination of functional burst-imaging with the half-Fourier and parallel imaging techniques may provide a silent pulse sequence with good SNR and resolution that is suitable to fMRI.

The problem of acoustic noise in the MR environment will increase, but, fortunately, various techniques in sound reduction are under investigation and new developments can be elaborated. Improvements in speech intelligibility by speaker tracking and speech enhancement and further optimization of functional pulse sequences using half-Fourier and parallel imaging methods are valuable concepts for future research.

# Chapter 10

## Samenvatting en discussie

Magnetische resonantie (MR) beeldvorming is een beeldvormende techniek waarbij door middel van sterke vaste en wisselende magneetvelden doorsneden van het menselijke lichaam gemaakt worden. Het proces van beeldvorming met MRI is geassocieerd met verschillende veiligheidsproblemen die een negatief effect kunnen hebben op patiënten en radiologisch medewerkers. Tot de potentieel schadelijke oorzaken van MRI behoren onder andere de biologische effecten van de statische en dynamische magneetvelden, de mechanische krachten uitgeoefend op ferromagnetische voorwerpen, thermische effecten en het schadelijke effect van hoge geluidsdrukken. Het onderwerp van dit proefschrift is de evaluatie en modificatie van het geluid dat wordt geproduceerd tijdens MRI.

In **Hoofdstuk 2** wordt begonnen met een uiteenzetting van de verschillende geluidsbronnen in de MRI kamer. De belangrijkste geluidsverwekker is de gradiënt spoel. Tijdens de beeldvorming genereert de spoel een wisselend magneetveld dat tegengesteld is aan het sterke, statische magneetveld. Hierdoor functioneert de spoel als een grote luidspreker die geluid produceert waarvan de frequentie in het hoorbare gebied ligt. Geluidsniveaus tot 130 dB met nog hogere piekniveaus tot 140 dB zijn beschreven voor MRI scanners met een vast magneetveld van 3 Tesla. Deze kwantitatieve en kwalitatieve eigenschappen van gradiënt gerelateerd geluid zijn afhankelijk van de beeldvormingsparameters zoals repetitie tijd, echo tijd, beeldgrootte en sneed dikte. Het hoofdstuk presenteert verder een handreiking voor het adequaat verrichten van geluidsmetingen: naast standaarden ten behoeve van het meten van geluid, wordt de invloed van de MRI omgeving op de meetapparatuur besproken. Tenslotte volgt een beschrijving van de huidige geluidsreducerende technieken die in MRI worden toegepast of in ontwikkeling zijn.

In de hoofdstukken 3, 4, en 5 is de geluidsproblematiek geëvalueerd met

experimenten en aan de hand van literatuur onderzoek.

Het risico op gehoorsbeschadiging door blootstelling aan MRI geluid is reeds in 1988 beschreven door Brummet et al. en is recentelijk bevestigd door Radomski et al. die bij 16 patiënten een tijdelijke afname van otoacoustische emissies waarnamen, ondanks het gebruik van gehoorsbescherming. De blootstelling aan MRI geluid door technici en radiologisch personeel werd niet betrokken in de discussie. Bij chronische expositie treedt echter een cumulatief effect op en permanente schade aan het gehoor wordt op lange termijn zichtbaar. Door de opkomst van MRI geleide behandelingen, waarbij herhaaldelijk en gedurende lange tijd werkzaamheden worden verricht in de MRI ruimte, zal met name deze groep negatieve gevolgen ondervinden van chronische blootstelling aan MRI geluid. Om een schatting te maken van het risico op permanente gehoorsschade, zijn in de studie van **Hoofdstuk 3** geluidsdrukken gemeten tijdens puls sequenties die geschikt zijn voor interventie MRI (iMRI). Uit de resultaten blijkt dat MRI geluid in staat is gehoorsbeschadiging te veroorzaken. De gemeten geluidsdrukken zijn fors hoger dan toegestaan in Amerikaanse en Europese richtlijnen, in het bijzonder tijdens puls sequenties met een hoge beeldverversingssnelheid. Een interventie procedure met deze puls sequenties veroorzaakt al na enkele minuten permanente gehoorsschade. Adequate gehoorsbescherming is derhalve noodzakelijk.

In **Hoofdstuk 4** wordt het effect van MRI geluid op de spraakverstaanbaarheid beschreven. Er zijn een aantal praktische situaties waarin adequate verstaanbaarheid een vereiste is. Ten eerste is adequate verstaanbaarheid tussen interventie radioloog en ondersteunend personeel een vereiste voor het veilig uitvoeren van een procedure. Ten tweede behoren

bij de auditieve functionele MRI (fMRI) experimenten aangeboden verbale stimuli goed verstaan te worden. In deze studie is het effect van MRI geluid op de spraakverstaanbaarheid bepaald voor de puls sequenties die gebruikt worden in iMRI en fMRI. Tevens werd het effect van passieve gehoorsbescherming op de spraakverstaanbaarheid gemeten. Hiertoe luisterden vijftien vrijwilligers naar tekst fragmenten in aanwezigheid van MRI geluid en herhaalden de tekst zo correct mogelijk. Het geluidsniveau van de tekst werd in een aantal stappen aangepast naar een geluidsniveau waarop de helft van de tekst fragmenten kon worden verstaan. De resultaten laten zien dat zowel de interventie radioloog, naast de MRI scanner, als de patiënt, in de MRI scanner, worden belemmerd in verstaanbaarheid. De interventie radioloog moet hard praten en, afhankelijk van de puls sequentie, roepen om verstaan te kunnen worden. Voor de patiënt is fors meer stemvolume nodig, omdat de intensiteit van het MRI geluid in de tunnel hoger is dan naast de MRI scanner. Passieve geluidsbescherming heeft een positief effect op de verstaanbaarheid: het halveert het benodigde stemvolume.

De versturende invloed van MRI geluid op fMRI is het onderwerp van discussie in **Hoofdstuk 5**. fMRI is een techniek die cognitieve taken correleert aan hersenactiviteit door het detecteren van veranderingen van de cerebrale doorbloeding. In toenemende mate wordt fMRI gebruikt bij preoperatieve planning om normaal van ziek weefsel te kunnen afgrenzen, en bij onderzoek naar neurodegeneratieve en psychiatrische aandoeningen. Verstoring van het functionele experiment door MRI gerelateerd geluid leidt echter tot onjuiste gegevens en daarmee tot een verkeerde beoordeling van de functie van het onderzochte hersengebied. De belangrijkste oorzaken van verstoring door



MRI geluid zijn de beperking van het dynamisch bereik van het MRI signaal en de negatieve invloed op de concentratie van de patiënt. fMRI van het gehoor wordt verder beperkt door de lage resolutie waarmee de auditieve hersenschors afgebeeld kan worden, de maskering van auditieve stimuli door MRI geluid en, in het bijzonder, doordat MRI geluid zelf activiteit in de hersenschors induceert. Naast de in hoofdstuk 2 beschreven technieken van geluids-reductie, richt dit hoofdstuk zich voornamelijk op de geluids-arme experimentopzet, ook wel silent imaging paradigms genoemd. Deze paradigma's zijn gebaseerd op het vermijden van de intra-acquisitie en inter-acquisitie response van de hersenschors op het MRI geluid. De eerste response is de ongewenste corticale activatie geïnduceerd door MRI geluid tijdens een beeld acquisitie en gemeten binnen diezelfde acquisitie. Omdat de corticale response relatief traag is, wordt deze vermeden door de beeldacquisitie kort te houden (< 3 seconden). De corticale response op MRI geluid tijdens een acquisitie die gemeten wordt in een volgende beeld acquisitie is de inter-acquisitie response. Deze wordt voorkomen door de volgende beeld acquisitie uit te stellen totdat de response op het MRI geluid niet meer detecteerbaar is, een paradigma modificatie die ook wel sparse temporal sampling genoemd wordt.

Met name de behoefte aan grotere signaalsterkte en hogere resolutie leidt tot de ontwikkeling en het gebruik van MRI scanners met hoge veldsterktes en sterke gradiënt velden. Onderzoek van het EMRF (European Magnetic Resonance Forum) laat een toename sinds 2000 zien in de aanschaf van MRI systemen met hoge veldsterkte. Het zijn theoretisch juist deze twee factoren, de veld- en gradiëntsterkte, die het geluidsniveau tijdens MRI bepalen. In **Hoofdstuk 6** is de relatie tussen de veldsterkte en het geluidsniveau experimenteel gevalideerd. Hiertoe zijn geluidsmetingen verricht op een Siemens Magnetom Vision MRI scanner uitgerust met een van veldsterkte te veranderen Helicon magneet. Voor een reeks van puls sequenties zijn geluidsdrukken gemeten op verschillende veldsterktes oplopend van 0.5 tot 2.0 Tesla. De resulta-

ten waren overeenkomstig de theorie, namelijk een toename van de geluidsdruk met 6 dB met elke verdubbeling van de veldsterkte.

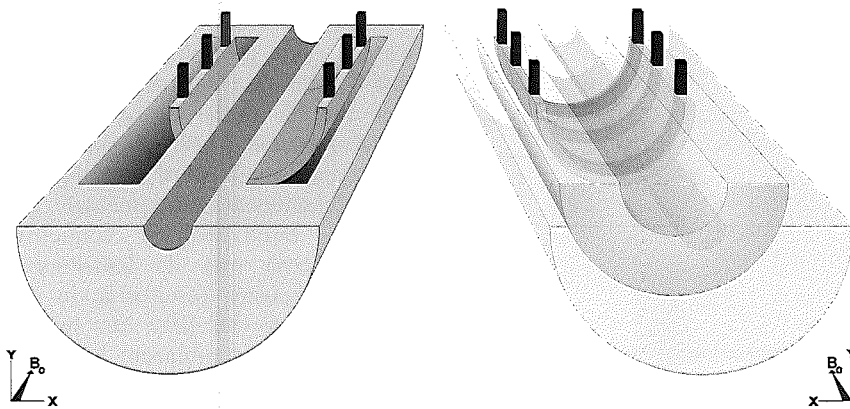
Het is dus belangrijk technieken te ontwikkelen die de geluidsproductie door MRI scanners beperken. In **Hoofdstuk 7** wordt ingegaan op het belang van passieve geluidsreductie voor de patiënt in de MRI tunnel en voor het radiologisch personeel naast het MRI systeem. Er is een indeling gemaakt in direct geluid, afgestraald door de binnen -en buitenzijde van het systeem, en indirect geluid via reflecties in de MRI ruimte. De relatieve bijdragen van de directe en indirecte geluidspaden aan de geluidsdruk zoals waargenomen naast en in de MRI scanner zijn vastgesteld door afzonderlijke isolatie van deze geluidspaden. De resultaten tonen aan dat de geluidsbelasting voor de patiënt volledig veroorzaakt wordt door geluidsafstraling van de binnenzijde van de MRI. Substantiële demping tot ruim 19 dB wordt bereikt met adequate isolatie van de tunnel. De geluidsdruk naast de MRI scanner, op de plaats van de interventie radioloog, wordt voornamelijk bepaald door directe geluidsafstraling van de buitenzijde van het MRI systeem en door reflecties in de MRI kamer. Gelijktijdige isolatie van deze geluidspaden levert een geluids-reductie op tot 9.5 dB.

De meest toegepaste methode om geluid naar een comfortabel en veilig niveau te brengen is het gebruik van passieve gehoorsbescherming. Passieve gehoorsbeschermers, zoals oordoppen en oorkappen, beperken de luchtgeleide voortplanting van geluid, maar laten de geluidstrillingen die via de benige structuren van het hoofd en lichaam het binnenoor bereiken ongemoeid. Omgekeerd kan worden gesteld dat de effectiviteit van passieve gehoorsbeschermers lager wordt naarmate de bijdrage van botgeleiding aan de subjectieve geluidsdruk toeneemt. De MRI tunnel is geen gewone audiometrische omgeving en botgeleiding speelt mogelijk een grote rol: ten eerste is de patiënt in de MRI tunnel volledig omgeven door de geluidsbron, het gradiënt systeem, en, ten tweede, ligt de patiënt op een tafel die mechanisch in contact staat met de vibrerende geluidsbron. Het doel

van de studie beschreven in **Hoofdstuk 8** is dan ook de bepaling van de mate van beengleiding in de MRI omgeving in vergelijking met een akoestisch optimale omgeving en de differentiatie tussen conventionele beengleiding en beengleiding door mechanische vibraties. Bij 10 vrijwilligers is de subjectieve gehoorsdrempel voor MRI geluid bepaald met een maskeringmethode, zowel in de MRI tunnel als in een anechoïsche omgeving. De bijdrage van beengleiding aan de subjectieve geluidsdruk van MRI geluid werd gemeten voor verschillende combinaties van gehoorsbescherming. De resultaten toonden dat de mate van beengleiding niet wordt beïnvloed door de MRI omgeving, in het bijzonder niet wanneer oordoppen en/of oorkappen worden gebruikt. Met andere woorden, de effectiviteit van gehoorsbeschermers in de MRI omgeving is gelijk aan de effectiviteit zoals die in de literatuur wordt beschreven.

In de laatste studie naar geluidsreductie wordt gebruik gemaakt van een recent beschreven techniek waarbij de puls sequentie de gradiëntspoel minder agressief exciteert. Door een belangrijke beperking van deze "stille" puls sequenties, namelijk de verlenging van de beeld acquisitie duur, zijn deze sequenties minder aantrekkelijk voor snelle beeldvorming en is de toepassing in iMRI derhalve niet beschreven. **Hoofdstuk 9** toont aan dat iMRI met een stille sequentie mogelijk is, mits de beeldverversingsfrequentie, en daarmee de geluidsdruk, door de radioloog in real-time aangepast kan worden. Het is immers niet noodzakelijk de volledige capaciteit van het MRI systeem met maximale beeldverversingsfrequentie te benutten gedurende de gehele interventie procedure. De experimentopstelling in deze studie bestond uit een zich in de MRI kamer bevindende regelaar die middels glasvezel en netwerk gekoppeld werd aan een 1.5 Tesla MRI scanner. Stapsgewijs kon de MRI geluidsproductie in real-time worden verlaagd met ruim 21 dB(A) en de beeldverversingsfrequentie met een factor 16. Vanuit het oogpunt van veiligheid geeft deze geluidsreductie een 128 maal lager risico op gehoorschade.





**Figuur 1.** MRI gradiënt constructie voor passieve geluidsreductie; de spoel is ingebed in een vrij dragende vleugel.

### Perspectief van geluid in de MR omgeving

Het ligt in de lijn der verwachting dat de geluidsproductie door MRI scanners toe zal nemen gezien de productie van systemen met hogere veldsterktes en sterkere gradiënten. MRI scanners met een veldsterkte tot 9.4 Tesla zijn beschikbaar voor experimenteel gebruik (Center for Magnetic Resonance Research, Minneapolis, USA). In verschillende centra wordt reeds gewerkt aan systemen met veldsterktes tot 11 Tesla (Commissariat à l'Energie Atomique, Orsay, Frankrijk) waarbij geluidsniveaus van 160 dB worden gemeten. Er bestaan verschillende internationale richtlijnen voor het accepteren van medisch elektrische apparatuur voor diagnostiek bij patiënten. De IEC 60601-2-33, een algemene veiligheidsstandaard, is de belangrijkste en wordt als leidraad genomen door diverse nationale en internationale organisaties, waaronder de North American Electrical Manufacturers Association (NEMA) en de Association for the Advancement of Medical Instrumentation (AAMI). De IEC richtlijn adviseert een piek geluidsniveau van 140 dB(A) en een gemiddeld geluidsniveau van 99 dB(A) als maximaal toelaatbaar voor MRI apparatuur voor klinisch gebruik. Het is opmerkelijk dat de richtlijnen zich voornamelijk beperken tot diagnostisch gebruik van MRI apparatuur. Voor experimenteel gebruik, in de IEC standaard aangeduid als het tweede niveau, is echter geen duidelijk omschreven richtlijn beschikbaar, maar wordt consultatie van de aan het onderzoeksinstituut verbonden medisch ethische commissie geadviseerd.

Diagnostische MRI apparatuur wordt echter gebruikt onder experimentele condities, vaak zonder toestemming van een medisch ethische commissie. Tevens kan MRI apparatuur experimenteel worden ontwikkeld zonder acceptatie voor klinisch gebruik. Vanzelfsprekend zijn richtlijnen op basis van arbeidshygiëne (b.v. Europese norm 1986; 86/188/EEC, toegestane blootstelling aan geluid op basis van dosis en tijdsduur) van toepassing. Het is echter zeer aanbevelenswaardig aanvullende adviezen en voorschriften te ontwikkelen voor experimenteel gebruik van MRI apparatuur ter bescherming van de onderzoeker.

In de hoofdstukken 2, 5, 7, 8, en 9 is een aantal geluidsreducerende technieken de revue gepasseerd die reeds geïmplementeerd of nog in staat van ontwikkeling zijn. Toegepaste technieken in de huidige MRI apparatuur zijn voornamelijk gebaseerd op passieve geluidsreductie en het zo optimaal mogelijk modelleren van de geometrie van de gradiëntspoel en zijn behuizing. Deze technieken zijn echter niet in staat om voldoende geluidsreductie te bewerkstelligen in MRI systemen met hoge veldsterktes, zodanig dat deze systemen voor klinisch gebruik aanvaardbaar zijn. Er is kennelijk behoefte aan ontwikkeling van nieuwe geluidsreducerende methoden.

Bencsik et al. beschreven recentelijk een modificatie van het gradiënt systeem waardoor op passieve wijze geluid wordt gereduceerd. Het model is eenvoudig te implementeren in longitudinale gradiënt spoelen. De gemodificeerde constructie bestaat uit

een aantal windingen ingebed in een dunne laag epoxy hars, hetgeen vervolgens in een tweede laag ingebed wordt (Fig 1). De binnenste laag is slechts met een dunne basis aan de buitenste laag bevestigd. Deze vrij dragende vleugel vormt een grote barrière tegen geleiding van vibraties, waardoor het merendeel van de akoestische energie in de binnenste laag wordt opgevangen. De beschreven effecten van deze modificatie zijn substantieel: een reductie van 40 dB bij een excitatie frequentie van 800 Hz. Een potentieel probleem bij deze nog experimentele constructie is de warmte afgifte door de spoelen bij de gebruikte excitatie frequenties en amperages.

Een tweede, nog niet nader onderzochte geluidsreducerende methode is de toepassing van actieve structurele geluidsreductie, ook bekend als active structural acoustic control (ASAC). ASAC werkt volgens het principe van het reduceren van de amplitude waarmee een structuur vibreert: de distributie van vibraties in het materiaal wordt zodanig veranderd dat vibraties in het materiaal destructief met elkaar interfereren (Fig 2). Door de gehele ombouw van het MRI systeem uit te rusten met ASAC wordt een actieve isolatie van het MRI systeem bereikt. Er kleven echter een aantal beperkingen aan het toepassen van ASAC in de MRI omgeving, onder andere veroorzaakt door de hoge geluidsdrukken en frequenties van het MRI geluid. Hybride isolatie van vibraties en geluid door middel van een combinatie van passieve en actieve demping is een ideale combinatie, waarbij ASAC zich voornamelijk beperkt tot frequenties lager dan 1 kHz. Een dergelijk hybride systeem zou verder geoptimaliseerd kunnen worden door de herhaalbaarheid van het geluid te gebruiken voor het voorspellen van de benodigde antivibraties in ASAC (Fig 3). Tevens is met a-priori kennis van de voorgeprogrammeerde gradiënt pulsen het MRI geluidsspectrum te schatten.

Adequate communicatie tijdens interventies is problematisch, ondanks het gunstige effect van passieve gehoorsbescherming op de spraakverstaanbaarheid. In de discussie van hoofdstuk 4 wordt de aanbeveling

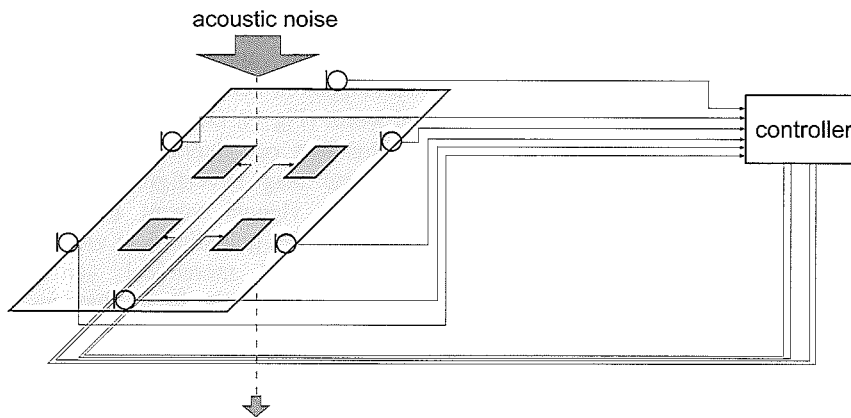


Figure 2. Principe van een actieve structurele geluidscontroller

gedaan de verstaanbaarheid te verbeteren door het gebruik van een directionele microfoon en een koptelefoon. Recente ontwikkelingen in operatie kamers zijn speech enhancement en speaker tracking. Door het plaatsen van directionele en omni-directionele microfoons tegen de plafonning van de operatie ruimte gekoppeld aan een controller die de signalen analyseert, is het mogelijk de positie van de spreker te bepalen en spraak te isoleren van achtergrond ruis. Toegepast in MRI zullen speech enhancement en speaker tracking de radioloog in de MRI ruimte kunnen lokaliseren en zijn spraak uit het MRI geluid filteren. Verdere optimalisatie is mogelijk op basis van voorkennis omtrent het MRI geluid. Door vervolgens de geïsoleerde spraak versterkt aan te bieden aan het radiologisch personeel is het probleem van slechte verstaanbaarheid opgelost.

In fMRI experimenten heeft scanner geluid een negatief effect op de auditieve stimulatie, het uitvoeren van cognitieve taken en het comfort van de patiënt. Passieve gehoorsbescherming is beperkt afdoende, o.a. door beengleiding. Derhalve zijn verschillende pogingen ondernomen om puls

sequenties minder luid te maken (zie hoofdstuk 5). Een van deze technieken is gebaseerd op stimulatie van MRI signalen door radiofrequentie pulsen (burst-imaging) in plaats van door luidruchtige gradiënten. De puls sequentie is slechts hoorbaar als zachte kliks vergelijkbaar met het niveau van achtergrond ruis. Als relatief voordeel heeft deze sequentie een intrinsieke ongevoeligheid voor bepaalde artefacten, maar nadelig zijn de lage signaal-ruis-verhouding (SNR)

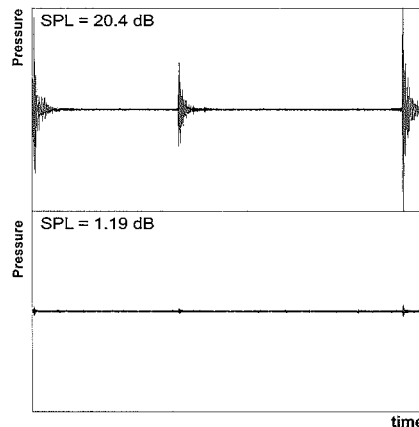


Figure 3. Het verschil van twee opeenvolgende TR perioden demonstreert de herhaalbaarheid van MRI geluid en geeft een reductie van >19 dB

en resolutie. De SNR kan verbeterd worden door gebruik te maken van half-Fourier fase codering, een techniek waarbij slechts de helft van de beeldinformatie wordt verzameld. In een recente studie werd een, nog niet voor functionele experimenten geschikte, burst-imaging sequentie gecombineerd met de half-Fourier techniek, hetgeen resulteerde in een SNR toename van 40%. Een tweede techniek die gecombineerd kan worden met voor fMRI geschikte burst-imaging sequenties is parallele beeldvorming met Simultaneous Acquisition of Spatial Harmonics (SMASH) of de meer gebruikte Sensitivity Encoding (SENSE). Parallele beeldvorming is gebaseerd op het gebruik van antennes voor het ontvangen van de MRI signalen afkomstig van dezelfde anatomische regio. Het aantal fase stappen voor data acquisitie wordt hiermee gereduceerd met een factor gelijk aan het aantal elementen. De parallele techniek versnelt de beeldvorming en verbeterd de resolutie en SNR. De combinatie van functionele burst-imaging met de half-Fourier en parallele techniek resulteert uiteindelijk in een stille sequentie met aantrekkelijke SNR en resolutie die geschikt is voor fMRI.

Het geluidsprobleem in MRI zal toe nemen, maar er zijn nog verschillende ontwikkelingen gaande en nieuwe ontwikkelingen te entameren. De verbetering van de spraakverstaanbaarheid met speaker tracking en speech enhancement en de verdere optimalisatie van functionele puls sequenties met half-Fourier en parallele beeldvorming zijn waardevolle ideeën voor vervolg onderzoek.

# Dankwoord

Het dankwoord, het laatste hoofdstuk in dit proefschrift en het laatste hoofdstuk dat ik schrijf op mijn inmiddels verouderde computer. Het geeft mij kort de gelegenheid iedereen te bedanken die heeft bijgedragen aan het tot stand komen van dit boekje.

Om te beginnen met mijn promotor, Professor Pattynama. Zo om de paar weken een gesprek over de gang van zaken is voor mij telkens weer een moment geweest om even op adem te komen, om vervolgens met frisse ideeën verder te gaan. U hebt mij de vele facetten van het onderzoek geleerd, van vraagstelling tot publicatie. Hartelijk dank!

Andries Zwamborn, beste collega. Jouw connecties binnen de universiteit hebben hun dienst bewezen. Altijd wist je wel iets te regelen; was het niet materiaal van de centraal instrumentele dienst, dan was het wel een financieel achterdeurtje om op korte termijn ergens aan te komen. Daar stond natuurlijk wel tegenover dat mijn tijd als afdeling-contact-persoon van de computerondersteuning voor negentig procent door jou werd gebruikt. Tenslotte wil ik je bedanken voor de vele uurtjes die je overdag en 's avonds hebt gespendeerd aan dit boekje. Een puik stukje werk.

Mohamed Ouhlous, studiegenoot, collega en paranimf. Naast de drie collegezalen en vijf kamers die we in de tussentijd gedeeld hebben, kan ik ook wel zeggen dat we een gemeenschappelijke woordenschat opgebouwd hebben, chardez. Ik zal ze niet alle noemen ;). Nog een paar maanden en dan zal jou ook het vuur aan de schenen gelegd worden. Sterkte met de voorbereidingen, bonne chance.

Mika, hé dude, jouw tomeloze inzet voor onderzoek en je kritische opmerkingen en adviezen hebben aan dit boekje bijgedragen. Je bent op vele markten thuis, maar ik kan natuurlijk niet nalaten dit compliment in perspectief te bekijken. Organisatie is niet je sterkste kant. Ooit ben ik van plan geweest je een agenda kado te doen. Maar bij nader inzien zou deze zeker op je bureau, of beter gezegd, ergens op je bureau verloren zijn geraakt. Jij ook veel succes toegewenst met de voorbereiding van je promotie.

Al is het niet van het eerste uur, Marc, met jou had ik een mindere collega kunnen treffen. Bedankt voor je statistische adviezen en hulp bij SPSS en Excel. Naast je serieuze instelling en onze gedeelde interesse in compu-zaken, ben je altijd in voor een grap. Eigenlijk...het ideale doelwit voor een goede grap. De wielklem houd je van mij tegoed! Het verbaast mij altijd weer hoe jij op een vaak voor mij niet te achterhalen manier aan sleutels kan komen, van kasten en kamers tot die van het (...) archief toe. Als je geen baan had als onderzoeker of arts-assistent, dan was je zeker slotenmaker geworden.

Ronald Maas, collega van de KNO, zonder jouw hulp was het mij niet gelukt. Ik ben je zeer dankbaar voor al de adviezen en ideeën op audiologisch gebied. Hugo Romijn, man van TNO en tevens schoonvader, als ik zeg "handige jongens, die Romijnen" dan is dat vast voldoende. Alle collega's van de Experimentele Radiologie, Thomas de Weert, Marion van Vliet, Zhouli Zhang, Karin ten Wolde en natuurlijk niet te vergeten Teun Rijdsdijk, bedankt voor de gezelligheid op de afdeling. Piotr Wielopolski, het was even wennen, die eerste keer, toen ik op de DdHK kwam voor enkele metingen op jouw MRI systeem. Met een waterval aan woorden probeerde je duidelijk te maken dat ik beter wat anders kon gaan doen... gelukkig eindigt zo'n waterval altijd met "fine". Ik wil je bedanken ... voor alle tijd die je hebt besteed aan het lezen van mijn stukken. En ... natuurlijk voor de uurtjes stoeien met tekenpakketten en discussieren over divx-spelers en videoprojectoren. Vermoedelijk is het volgende discussie onderwerp al in zicht ... hoe kunnen we het maximale halen uit WiFi. Linda Everse, Tom Williams, John Joyce and Willem Moelker, I would like to thank you all for your willingness to improve my English writing style that made the manuscripts as they currently are.

De belangrijkste heb ik tot het laatste bewaard. Pa en ma, jullie hebben mij de ruimte en middelen gegeven om te studeren. Het heeft veel voor mij betekend en ik hoop het later ook aan mijn eigen kroost te kunnen geven. Christel, mijn lieve vrouw, jouw steun en geduld zijn onbeschrijfbaar en hebben we zeker nodig voor de nieuwe op komst zijnde uitdaging ...



# List of publications

## Publications

- 2001 A. Moelker, P.A. Wielopolski, P.M.T. Pattynama.  
Categorical Course Practical MR safety considerations: Acoustic noise and related safety considerations.  
RSNA 87th scientific assembly & annual meeting.
- 2002 A. Moelker, A.J.J. Maas, F. Lethimonnier, P.M.T. Pattynama.  
Interventional MR imaging at 1.5 T: quantification of sound exposure.  
Radiology: 224;889-895.
- 2002 A. Moelker, P.A. Wielopolski, P.M.T. Pattynama.  
Categorical Course Practical MR safety considerations: Acoustic noise and related safety considerations.  
RSNA 88th scientific assembly & annual meeting.
- 2003 A. Moelker, M.W. Vogel, P.M.T. Pattynama.  
Efficacy of passive acoustic screening: implications for the design of imager and MR-suite.  
Journal of Magnetic Resonance Imaging: 17;270-275.
- 2003 A. Moelker, P.A. Wielopolski, P.M.T. Pattynama.  
Relationship between magnetic field strength and magnetic-resonance-related acoustic noise levels.  
MAGMA: 16;52-55.
- 2003 A. Moelker, P.M.T. Pattynama.  
Acoustic noise concerns in functional magnetic resonance imaging.  
Human Brain Mapping: 20;123-141.
- 2004 A. Moelker, M.W. Vogel, P.M.T. Pattynama.  
Real-Time Modulation of Acoustic Gradient Noise in Interventional MR Imaging. Concepts in Magnetic Resonance Part B - Engineering: 20B;34-39.
- 2004 A. Moelker, A.J.J. Maas, P.M.T. Pattynama.  
Verbal communication in MR environments: effect of MR system acoustic noise on speech understanding.  
Accepted by Radiology (publication in July 2004).

## Lectures

- 2001 A. Moelker and P.A. Wielopolski.  
Categorical Course Practical MR safety considerations: Acoustic safety concerns in MR environments.  
RSNA 87th scientific assembly & annual meeting.
- 2002 A. Moelker.  
Categorical Course Practical MR safety considerations: Acoustic safety concerns in MR environments.  
RSNA 88th scientific assembly & annual meeting.

## Abstracts

- 2000 M.W. Vogel, A. Moelker, N.A. Matheijssen, P.M.T. Pattynama  
Double echo phase thermometry (DEPTH): A novel concept for water proton resonance frequency-based MR thermometry.  
RSNA 86th scientific assembly & annual meeting.
- 2001 A. Moelker, M. Vogel, M. Ouhous, F. Lethimonnier, P.M.T. Pattynama.  
Operator Exposure to Acoustic Noise in Interventional MRI.  
Proceedings of the 9th Annual Meeting of the International Society of Magnetic Resonance in Medicine: p2180.
- 2002 M.W. Vogel, A. Moelker, N.A.A. Matheijssen, P.M.T. Pattynama.  
Double Echo Phase THERmometry (DEPTH): een nieuw concept voor magnetische resonantie thermometrie op basis van de water proton resonantie frequentie verschuiving.  
Nederlands Tijdschrift voor Geneeskunde 2002, p1110.
- 2002 A. Moelker, M.W. Vogel, M. Ouhous, P.M.T. Pattynama.  
Acoustic Noise Reverberation in the MR environment.  
Proceedings of the 10th Annual Meeting of the International Society of Magnetic Resonance in Medicine: p826.

- 2002 A. Moelker, M.W. Vogel, M. Ouhlous, P.M.T. Pattynama.  
Acoustic Noise Reduction in the Interventional MR suite.  
Proceedings of the 10th Annual Meeting of the International Society of Magnetic Resonance in Medicine: p847.
- 2002 M. Ouhlous, A. Moelker, M.W. Vogel, P.M.T. Pattynama, A. Van Der Lugt.  
Dedicated Phased-Array Coils for High Resolution MRI of the Carotid Artery.  
Proceedings of the 10th Annual Meeting of the International Society of Magnetic Resonance in Medicine: p866.
- 2002 M.W. Vogel, A. Moelker, M. Ouhlous, P.M.T. Pattynama.  
Movement Registration for PRF Based MR Thermometry.  
Proceedings of the 10th Annual Meeting of the International Society of Magnetic Resonance in Medicine: p2214.
- 2002 A. Moelker, M.W. Vogel, P.M.T. Pattynama.  
Acoustic noise reduction by passive screening materials in the MR scanner and room.  
Proceedings of the 19th Annual Meeting of the ESMRMB: p236.
- 2002 A. Moelker, P.A. Wielopolski, P.M.T. Pattynama.  
The relationship of magnetic field strength and MR-related acoustic noise levels.  
Proceedings of the 19th Annual Meeting of the ESMRMB: p236.

# Curriculum Vitae

De auteur van dit proefschrift werd geboren te Leiden op 19 februari 1975.

In 1993 behaalde hij zijn diploma van het Voorbereidend Wetenschappelijk Onderwijs aan het Christelijk Lyceum te Gouda en begon aansluitend aan zijn studie Geneeskunde aan de Erasmus Universiteit te Rotterdam. In 1994 behaalde hij zijn Propedeuse met Lof en studeerde vier jaar later af op de afdeling Intensive Care Research en Optische Spectroscopie aan het Erasmus Medisch Centrum te Rotterdam. In 2000 behaalde hij zijn artsexamen.

Na zijn opleiding Geneeskunde trad hij als Assistent in Opleiding in dienst van de afdeling Radiologie aan het ErasmusMC. In samenwerking met en onder supervisie van Prof. dr. P.M.T. Pattynama heeft hij het promotieonderzoek "*Evaluation of acoustic noise in the MR environment*" opgezet. Ten tijde van zijn promotieonderzoek heeft hij gewerkt aan het Interuniversitair Cardiologisch Instituut Nederland project "*Ramanspectroscopy of the arterial wall*" op de afdeling Intensive Care Research en Optische Spectroscopie.

Sinds januari 2004 werkt hij in het kader van de opleiding Radiologie als art-assistent op de afdeling Radiologie van het ErasmusMC.

